Leptogenesis in the superstring inspired E_6 model

Dissertation

zur Erlangung des Grades eines

Doktors der Naturwissenschaften

der Abteilung Physik

der Universität Dortmund

vorgelegt von

Alexander Kartavtsev

Februar 2007

Zusammenfassung

Die beobachtete Baryonasymmetrie des Universums findet eine elegante Erklärung im Rahmen des Szenarios der Leptogenese. Wir analysieren verschiedene Aspekte dieses Szenarios, wobei wir den Einfluss von Störungen der Energiedichte und der Metrik der Raum–Zeit auf die Erzeugung der Lepton- und Baryonasymmetrie mit einbeziehen. Wir betrachten ferner die Umwandlung der Leptonasymmetrie in eine Baryonasymmetrie und untersuchen die Effekte, die damit zusammenhängen, dass die Leptonasymmetrie von Null verschiedene chemische Potentiale der anderen Teilchensorten induziert. Es wird eine Abschätzung für die obere Grenze der Leptonasymmetrie im Standardmodell und im durch die Superstring–Theorie inspirierten E_6–Modell gemacht, und die für die Leptogenese relevanten Eigenschaften dieses Modells werden im Detail diskutiert. Das Szenario der Leptogenese sagt von Null verschiedene Massen der Neutrinos vorher, die in Oszillations–Experimenten gemessen worden sind. Wir berechnen die für die Interpretation der experimentellen Resultate relevanten Wirkungsquerschnitte für die kohärente Pionerzeugung durch Neutrinostreuung an Kernen mittels geladener und neutraler Ströme.

Abstract

The observed baryon asymmetry of the Universe is elegantly explained in the framework of the baryogenesis via leptogenesis scenario. We analyze various aspects of this scenario including the influence of perturbations of the energy density and space–time metric perturbations on the generation of the lepton and baryon asymmetries. We also consider conversion of the lepton asymmetry into the baryon asymmetry and investigate the effects associated with the fact, that the lepton asymmetry induces nonzero chemical potentials of the other species. We estimate upper bound on the asymmetry in the Standard Model and in the superstring inspired E_6 model. Properties of this model relevant for leptogenesis are discussed in detail. The baryogenesis via leptogenesis scenario predicts nonzero masses of the neutrinos, measured in the oscillation experiments. We calculate cross sections of the charged and neutral current coherent pion production by neutrino scattering off nuclei relevant for the interpretation of the experimental results.

Contents

Introduction

The observed baryon asymmetry of the Universe is one of the most intriguing problems of particle physics and cosmology. The baryon–to–photon ratio Y_B has been recently measured by the Wilkinson Microwave Anisotropy Probe (WMAP) satellite to unprecedented precision. The reported value for Y_B is [1]

$$Y_B = \frac{n_B}{n_\gamma} = 6.5^{+0.4}_{-0.3} \cdot 10^{-10}$$

where $n_B = n_b - n_{\bar{b}}$ and n_γ are the number densities for the net baryon number B and for photons at the present epoch, respectively.

As is commonly accepted, the early Universe passed through a phase of accelerating expansion (the inflationary epoch) that was driven by a negative–pressure vacuum energy density [2, 3]. Any preexisting baryon number asymmetry was diluted to an unobservable small value during inflation [4]. Consequently the observed asymmetry has been generated dynamically after the inflation.

The cosmological baryon excess can be generated dynamically, provided that the three Sakharov conditions [5] are fulfilled:

– baryon (or baryon minus lepton) number non–conservation;

– C and CP violation;

– and deviation from thermal equilibrium.

A number of scenarios based on various models has been considered in the past. The Standard Model itself could in principle be a good candidate, as it contains all the necessary ingredients. However, both CP violation in the quark sector and deviation from thermal equilibrium during the electroweak phase transition are insufficient to reproduce the observed baryon asymmetry. In the supersymmetric extensions of the Standard Model baryon asymmetry can in principle be generated by the Affleck–Dine mechanism [6]. In this scenario the baryon asymmetry is generated due to coherent oscillations of flat directions around the minimum of the potential, provided that the former ones are made of scalar quarks and carry baryon number. However,

it is still not clear under which conditions this mechanism can generate a baryon asymmetry of the requested magnitude.

The discovery of anomalous electroweak processes [7, 8], violating baryon (B) and lepton (L) numbers but conserving the difference $B-L$, led to the widely adopted scenario of baryogenesis via leptogenesis. According to the scenario of leptogenesis suggested by M. Fukugita and T. Yanagida [9], lepton number asymmetry is generated at a GUT scale in the decay of heavy Majorana neutrinos. Since the Majorana mass term violates lepton number by two units, the first Sakharov condition is fulfilled already at classical level. Baryon number is violated at quantum level by the anomalous electroweak processes, which are sufficiently fast at high temperature and convert the lepton asymmetry into the baryon asymmetry. Complex couplings of the heavy Majorana neutrino to the conventional neutrinos and the Higgs ensure, that the second Sakharov condition is fulfilled. Technically the CP asymmetry arises due to interference of tree–level and one–loop–vertex [9] and tree–level and one–loop–self–energy [10] diagrams. At temperatures of the order of the Majorana neutrino mass, $T \sim M \sim 10^9 - 10^{11}$, GeV the Universe expands rapidly, so that the slowly decaying heavy neutrinos are out of kinetic equilibrium. Thus, the third Sakharov condition is also fulfilled in the scenario under consideration.

In this thesis several aspects of the Fukugita–Yanagida scenario are studied. In chapter 1, the influence of the effects of general relativity on the generation of lepton and baryon asymmetries is investigated. In particular, we investigate how the energy density carried by the heavy decaying particles affects the expansion rate of the Universe and, in turn, the generation of a baryon asymmetry. As the early Universe was to a very good approximation homogeneous and isotropic, it became a common practice to completely neglect the primeval perturbations of energy density and metric created by quantum fluctuations in the inflaton field. These primeval perturbations, however, were of utmost importance for the subsequent formation of large scale structure. The quantitative parameter which determines the degree of deviation from thermal equilibrium is the ratio of the heavy neutrino decay width to the expansion rate of the Universe. Since the expansion rate in regions of higher or smaller energy density differs from that of the homogeneous background, lepton and baryon asymmetries become functions of space coordinates – an interesting effect that has been ignored altogether in the previous calculations. In the regions of higher energy density the generation of lepton and baryon asymmetries has been slightly more efficient than in the regions of lower energy density. Thus, even before structure formation has started at a temperature $T \sim 3 \cdot 10^4$ K, the seeds of the future galaxies and other large scale structures contained higher–than–average number of baryons and leptons.

Sphaleron transitions, which are in thermal equilibrium in a wide range of temperatures, convert the lepton asymmetry, generated in decay of the heavy neutrinos, into baryon asymmetry

in such a way, that the sum $3B+L$ is zero for left–handed fermions. Together with the sphaleron processes fast decay, inverse decay and scattering processes ensure, that all particle species carry an asymmetry, which is proportional to the lepton asymmetry with the coefficients of proportionality being determined by the particle content of the model. This usually neglected effect leads to a modification of coefficients of individual terms in the Boltzmann equations. The rapidness of the sphaleron transitions also implies, that the Boltzmann equations describe evolution of the lepton number, not evolution of the $B-L$, as has been tacitly assumed by some of the researches in this field.

We also solve the system of Boltzmann equations for the lepton asymmetry in the Standard Model supplemented by three generations of heavy Majorana neutrinos and compare the numerical estimates with the experimental observations.

The Standard Model is very likely to be a part of a more fundamental theory. The exotic interactions, which are strongly suppressed at low energies, will certainly affect the generation of the lepton and baryon asymmetries at the scales of order of 10^{10} GeV. It is therefore of interest to consider leptogenesis in the superstring inspired E_6 model, which is discussed in chapter 2. At present, the superstring theory and its latest formulation, M–theory, is the most promising candidate for a truly unified theory of fundamental interactions. Apart from the fact that the model naturally follows from breaking of the superstring $E_8 \otimes E_8$, it has also several features relevant for low–energy phenomenology. In particular the model allows chiral representations, global gauge anomalies are automatically cancelled, and its fundamental representation contains the fifteen known fermions along with two Higgs–like doublet and a right–handed neutrino [11, 12, 13, 14]. We discuss in detail the particle content of the model along with possible charge assignments, as well as constraints coming from the proton stability and the requirement of dynamical breaking of $B-L$ symmetry, which is a gauge symmetry in this model.

In chapter 3 we consider leptogenesis in the superstring inspired E_6 model. We develop a system of Boltzmann equations for the heavy Majorana (s)neutrinos and (s)leptons and solve the equations numerically. Supersymmetric leptogenesis has already been considered by several authors [15, 16]. The difference from the previous calculations arises primarily from the extended particle content of the model under consideration. In particular, the E_6 model contains three generations of Higgs doublets and new quarks coupled to the Majorana neutrinos.

An exciting feature of baryogenesis via leptogenesis scenario is that it predicts a nonzero mass of the conventional neutrino. After breaking of the electroweak symmetry the neutrino receives a small Majorana mass through the see–saw mechanism. Recent SuperKamiokande [17, 18] and SNO [19, 20, 21, 22, 23] experiments confirmed, that the conventional neutrinos indeed have nonzero masses. High precision measurements of neutrino masses and mixing angles in the

forthcoming experiments require good understanding of interactions of the neutrino beam with the target material. Recent measurements of the K2K collaboration [24] revealed a discrepancy between the theoretical predictions for the cross section of coherent scattering of low energy neutrinos and the experimental results. Chapter 4 is devoted to a discussion of coherent pion production by neutrinos and the calculation of the corresponding cross section using PCAC [25]. It is shown, that a reliable calculation of the cross section is possible provided that specific kinematic cuts are introduced. The obtained results are in agreement with the experimental measurements.

In appendix A several standard formulas for one–loop integrals are summarized. In appendix B we introduce spinor notation and compare properties of Weyl, Dirac and Majorana neutrinos. In appendix C we collect general formulas useful for calculation of reduced cross sections and reaction densities of decay as well as of $2 \leftrightarrow 2$ and $2 \leftrightarrow 3$ scattering processes. Finally, appendix E contains the kinematics of $2 \to 3$ scattering with the mass of the final lepton taken into account, which is relevant for the calculation of coherent neutrino–nucleus scattering cross section.

Chapter 1

Leptogenesis in nonuniform Universe

According to the third Sakharov condition a successful generation of lepton and baryon asymmetries requires a deviation from thermal equilibrium. One of the quantities parametrizing the degree of deviation from thermal equilibrium is the ratio of the Majorana neutrino decay width to the expansion rate of the Universe. Whereas the former is determined by the field theoretical model used, the latter one is determined by the equations of general relativity.

As the early Universe was to a very good approximation homogeneous and isotropic, it became a common practice to completely neglect the primeval perturbations of energy density and metric created by quantum fluctuations in the inflaton field. These primeval perturbations, however, were of utmost importance for the subsequent formation of large scale structure. In this chapter we analyze the influence of the associated effects of general relativity on the generation of lepton and baryon asymmetries.

In section 1.1 we review in some detail general features of the baryogenesis via leptogenesis mechanism suggested by M. Fukugita and T. Yanagida [9] and specify the model. The analysis presented in this chapter relies only on general relativity and can therefore be applied to a wide range of models. To be specific, however, we illustrate our results using the Standard Model supplemented by three heavy Majorana neutrinos with non–degenerate masses.

The Boltzmann equation in the inhomogeneous Universe with linear perturbations of the space–time metric taken into account is derived in section 1.2.

In section 1.3 we derive an explicit form of the collision terms, which contribute to generation and washout of the lepton asymmetry in the Standard Model.

The energy density carried by the heavy decaying particles affects the expansion rate of the Universe and the time development of the scale factor, thus affecting the generation of lepton and baryon asymmetries. The role of the associated effects in the homogeneous Universe is considered in section 1.4. Results of this section prove to be useful for the analysis of leptogenesis in the inhomogeneous Universe.

Since the expansion rate of the Universe in regions of higher or smaller energy density differs from that of the homogeneous background, lepton and baryon asymmetries become functions of space coordinates. As is argued in section 1.5, in the regions of higher energy density the generation of lepton and baryon asymmetries has been slightly more efficient than in the regions of smaller energy density. Consequently, even before the structure formation began after the onset of the matter–dominated epoch, seeds of the future galaxies and other large scale structures contained higher–than–average numbers of baryons and leptons.

Finally, in section (1.6) we review conversion of the lepton asymmetry into the baryon asymmetry by sphalerons, express chemical potentials of the Standard Model species through the chemical potential of the leptons and give numerical estimates for the theoretical upper bound on the baryon asymmetry of the Universe.

1.1 The baryogenesis via leptogenesis scenario

In the original paper "Baryogenesis Without Grand Unification" M. Fukugita and T. Yanagida [9] suggested a simple and elegant scenario of baryogenesis via leptogenesis reviewed in this section.

One difficulty which arises whenever one tries to explain the observed baryon asymmetry within the Standard Model is associated with the fact, that all the SM species apart from the neutrino are electrically charged. A direct violation of baryon number would inevitable lead to nonzero electric charge of the Universe in direct opposition to results of observational cosmology. Even the neutrino cannot be used for the generation of the asymmetry: although its electric charge is zero, the second component of the $SU_L(2)$ doublet it belongs to – the electron – is a charged particle. Thus, despite its tremendous success in explaining results of numerous low energy experiments, the Standard Model should be extended.

The Standard Model neutrino is a massless Weyl fermion, whereas the phenomenon of neutrino oscillation recently confirmed by the SNO collaboration [20] points out, that neutrinos have small but nonzero masses. The generation of the neutrino mass through renormalizable interactions requires an extension of the Standard Model by a right–handed neutrino – a gauge singlet coupled to the known particles (leptons and the Higgs) only via Yukawa interactions. If one also introduces a Majorana mass term for the right–handed neutrino, then after the spontaneous breaking of the electroweak symmetry the see–saw mechanism generates naturally small Majorana masses of the conventional neutrinos. The Lagrangian of the model reads

$$\mathcal{L} = \mathcal{L}_{SM} + N(\bar{L}\hat{\lambda}^{\dagger}\tilde{H}) - \frac{1}{2}\bar{N}\hat{M}N^{c} + \text{h.c.} \tag{1.1}$$

where L stands for the lepton doublets, $\tilde{H} = i\sigma_2 H^{\dagger}$ is the charge conjugate Higgs doublet, and

N are components of the physical Majorana neutrino $\Psi = \frac{1}{\sqrt{2}}(N + N^c)$ in the four–component notation. Without loss of generality the right–handed neutrino mass matrix $\hat{M}$ can be chosen to be real and diagonal. The Yukawa coupling matrix $\hat{\lambda}$ has off–diagonal complex entries.

Now that the model is specified, let us discuss in some detail fulfillment of the three Sakharov conditions and generation of the lepton and baryon asymmetries in this model. A Majorana fermion is a truly neutral particle[1], so that its lepton number is equal to zero. Therefore lepton number is violated (by one unit) in decay of the right–handed neutrino into leptons and the Higgs already at tree level, and the first Sakharov condition is automatically fulfilled. The

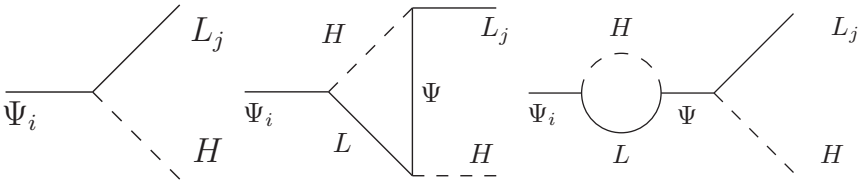

Figure 1.1: Tree–level and one–loop–level diagrams of the right–handed neutrino decay.

interference of tree–level and one–loop–vertex [9] and tree–level and one–loop–self–energy [10] diagrams leads to generation of *CP* asymmetry, so that the second Sakharov condition is fulfilled as well. Due to violation of *CP* rate of decay into leptons differs from the rate of decay into antileptons, so that a nonzero net lepton number is generated. Lepton number is also violated by

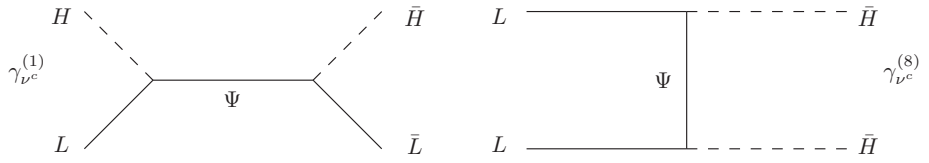

Figure 1.2: Scattering processes violating lepton number by two units.

two units in two–body scattering processes mediated by the right–handed neutrino and by one

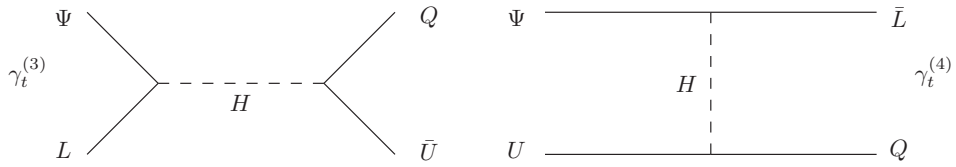

Figure 1.3: Scattering processes violating lepton number by one unit.

unit by the Higgs mediated scattering processes. The two–body scattering processes violating lepton number tend to washout the lepton asymmetry generated in decays of the right–handed neutrino, and in thermal equilibrium the asymmetry would be washed out completely. However,

[1]This means in particular, that a bare Majorana mass term can be introduced for none of the Standard Model species as those transform nontrivially under the $SU_C(3) \otimes SU_L(2) \otimes U_Y(1)$ gauge group.

at temperatures of the order of the right–handed neutrino mass the Universe expands very fast, so that the slowly decaying heavy neutrinos are out of kinetic equilibrium, and the third Sakharov condition is fulfilled as well.

From the discussion so far, the following picture emerges. After inflation is over and the Universe reheats, all the species[2] are in equilibrium and the net lepton number is equal to zero. As the temperature decreases, the right–handed neutrinos of the heaviest generation decay and produce an asymmetry, which is immediately washed out by scattering processes mediated by the right–handed neutrinos of all three generations. As the temperature drops below the mass of the lightest right–handed neutrino, the asymmetry produced in its decay is no longer completely washed out, because the scattering processes are suppressed at low temperature. By the time the temperature drops well below the lightest right–handed neutrino mass, almost all the heavy particles have decayed, so that no new asymmetry is generated, and the scattering processes are strongly suppressed, so that the asymmetry is not washed out. Thus the lepton number in comoving volume reaches an asymptotic value.

Of course we still need a mechanism able to convert the generated lepton asymmetry into baryon asymmetry. Although all the perturbative Standard Model processes are known to conserve lepton and baryon numbers, these are only "accidental" symmetries of the model and are violated by nonperturbative anomalous electroweak processes [7]. As the anomalous processes are induced by the nontrivial structure of the $SU_L(2)$ vacuum and do not violate the gauge symmetry of the Standard Model, the electric charge is automatically conserved. The anomalous electroweak processes are rapid at sufficiently high temperatures. Theoretical estimates [26] show, that in the standard Big Bang scenario their rate exceeds the rate of expansion of the Universe at temperatures 10^2 GeV $\leq T \leq 10^{12}$ GeV, i.e. down to the electroweak phase transition. After the phase transition the Standard Model species acquire masses. As the temperature further decreases, fermions of the third and second generation decay and the asymmetry is transferred to the electrons and light baryons. Part of the asymmetry is carried by the light neutrinos of all three generations. As these neutrinos are low energetic, they are very difficult to observe.

1.2 Boltzmann equation in the early Universe

Strictly speaking, a self–consistent calculation of the lepton number asymmetry generated in the decay of the heavy Majorana requires use of the Kadanoff–Baym equation [27]. In practice, however, solving the Kadanoff–Baym equation for a realistic system is hardly possible due to the complexity of the task. The common approach in this situation is to approximate the

[2]This statement is true provided that the reheating temperature is higher than the Majorana mass. Otherwise the right–handed neutrinos are out of equilibrium after the reheating.

Kadanoff–Baym equation by the Boltzmann equation. This is achieved by employing a Wigner transformation, a gradient expansion, the Kadanoff–Baym ansatz and by using the quasi–particle approximation [28]. These approximations are motivated by equilibrium considerations, and therefore one can safely apply the Boltzmann equations only to systems which are sufficiently close to thermal equilibrium.

The general form of the Boltzmann equation reads [29, 30]

$$\frac{\mathrm{d}f}{\mathrm{d}\lambda} = \hat{C}[f] \tag{1.2}$$

where λ is the affine parameter along a geodesic, and $\hat{C}$ the collision operator acting on the one–particle phase space distribution function f. As the Boltzmann equation treats particles as on–shell states, f is a function of space–time coordinates x^α and three components of the particle momentum p_i, or, alternatively, the particle kinetic energy E and the unit vector of the momentum direction $\hat{\mathrm{p}}_i$. Thus we can rewrite the left–hand side of (1.2) using the chain rule

$$\frac{\partial f}{\partial x^0} + \frac{\partial f}{\partial x^i}\frac{P^i}{P^0} + \frac{\partial f}{\partial E}\frac{1}{P^0}\frac{dE}{d\lambda} + \frac{\partial f}{\partial \hat{\mathrm{p}}_i}\frac{1}{P^0}\frac{d\hat{\mathrm{p}}_i}{d\lambda} = \frac{\hat{C}[f]}{P^0}, \tag{1.3}$$

where the definition $P^\mu = \frac{\mathrm{d}x^\mu}{\mathrm{d}\lambda}$ has been used. The dynamics of the contra– and covariant components of the four–momentum is determined by the geodesic equations [31]

$$\frac{\mathrm{d}P^\mu}{\mathrm{d}\lambda} + \Gamma^\mu_{\alpha\beta}P^\alpha P^\beta = 0, \quad \frac{\mathrm{d}P_\mu}{\mathrm{d}\lambda} - \frac{1}{2}\frac{\partial g_{\beta\gamma}}{\partial x^\mu}P^\beta P^\gamma = 0 \tag{1.4}$$

Experimental observations indicate, that the early Universe was to a very good approximation homogeneous and isotropic with an amplitude of density perturbations of order of $10^{-4}-10^{-5}$ [4]. The metric for a space–time with a homogeneous and isotropic spatial section is the maximally–symmetric Friedman–Robertson–Walker metric, which in a flat Universe can be written in the form

$$g^0_{\mu\nu} = \mathrm{diag}(1, -R^2, -R^2, -R^2), \tag{1.5}$$

where R is the cosmic scale factor. It depends only on time and is independent of the spatial coordinates.

Perturbations of the metric can be decomposed into tensor, vector and scalar components. The latter are most important because they exhibit gravitational instability and may lead to the formation of structure in the Universe. Scalar perturbations are characterized by four scalar functions [32] ϕ, ψ, B and $\mathcal{E}$

$$\delta g_{\mu\nu} = \begin{pmatrix} 2\phi & -B_{;i} \\ -B_{;i} & 2R^2\left(\psi\delta_{ij} - \mathcal{E}_{;ij}\right) \end{pmatrix} \tag{1.6}$$

where $\sum_i \mathcal{E}_{;ii} = 0$. To make a comparison with the existing literature easier we will also use the $h_{ij} \equiv \delta g_{ij}$ notation in what follows. A nonzero shift function $B_{;i}$ means, that comoving

worldlines and worldlines orthogonal to hypersurfaces of constant time are not collinear and we are dealing with a locally nonorthogonal coordinate system [30]. This complication is avoided here by setting $g_{0i} = B_{;i} = 0$.

In this case the square of the particle kinetic energy is given by $E^2 = P^0 P_0$, and the time co– and contravariant components of four–momentum are related to energy by $P_0 = E\sqrt{g_{00}}$ and $P^0 = E/\sqrt{g_{00}}$. Using the equations of geodesics and the expression for the Christoffel symbols in terms of the metric coefficients [31] we find for the derivative of energy

$$\frac{1}{P^0}\frac{dE}{d\lambda} = \frac{\partial g_{mn}}{\partial x^0}\frac{P^m P^n}{2E} - \frac{\partial\sqrt{g_{00}}}{\partial x^n}P^n \tag{1.7}$$

where summation over the indices m and n is assumed.

Let us now consider the derivative of the unit momentum vector

$$\frac{1}{P^0}\frac{d\hat{\mathrm{p}}_i}{d\lambda} = \frac{1}{P^0}\frac{d}{d\lambda}\left(\frac{\mathrm{p}_i}{\mathrm{p}}\right) = \frac{1}{P^0}\frac{\hat{\mathrm{p}}_i}{2\mathrm{p}^2}\left(\frac{1}{\hat{\mathrm{p}}_i^2}\frac{d\mathrm{p}_i^2}{d\lambda} - \frac{d\mathrm{p}^2}{d\lambda}\right), \tag{1.8}$$

where p_i and p are the components and the absolute value of the physical momentum respectively. In the case under consideration the components of physical momentum are related to spatial components of four–momentum by $\mathrm{p}_i^2 = -P^i P_i$ (no summation over i). Using the geodesic equations (1.4) once again we find

$$\begin{aligned}\frac{1}{P^0}\frac{d\mathrm{p}_i^2}{d\lambda} =& -\frac{1}{2}\left(\frac{\partial g_{00}}{\partial x^i}P^i P^0 + \frac{\partial g_{00}}{\partial x^m}g^{im}P_i P^0 - 2\frac{\partial g_{mn}}{\partial x^0}g^{im}P_i P^n\right)\\ &-\frac{1}{2P^0}\left(\frac{\partial g_{kn}}{\partial x^i}P^i P^k P^n + \frac{\partial g_{kn}}{\partial x^m}g^{im}P_i P^k P^n - 2\frac{\partial g_{mn}}{\partial x^k}g^{im}P_i P^k P^n\right)\end{aligned} \tag{1.9}$$

where the summation over m, n and k is assumed. The derivative of the particle momentum squared p^2 is obtained from (1.9) by summation over i. After the summation, the last three terms in (1.9) drop out, and the first two terms become equal. Since $E^2 = \mathrm{p}^2 + m^2$, the resulting expression differs from (1.7) only in an overall factor $2E$.

Before substituting (1.7) and (1.8) into the Boltzmann equation (1.3) one has to express components of four–momentum in terms of energy and momentum direction vector. As can be easily checked, to leading order in small perturbations the contravariant components of momentum P^α are related to the physical components of the momentum p_i and energy E by [33]

$$P^0 = E(1-\phi), \quad P^i = \frac{1}{R}\left(\delta_{im} + \frac{\delta g_{im}}{2R^2}\right)\mathrm{p}_m \tag{1.10}$$

Substituting (1.10) into (1.7) and expanding components of metric we obtain

$$\frac{1}{P^0}\frac{dE}{d\lambda} = -\left(\phi_{,n}\frac{\mathrm{p}\hat{\mathrm{p}}_n}{R} + \frac{\mathrm{p}^2}{E}\left[H - \dot{\psi} + \dot{\mathcal{E}}_{;nn}\hat{\mathrm{p}}_n^2\right]\right), \tag{1.11}$$

where $H \equiv \dot{R}/R$ is the Hubble parameter, $\dot{\psi} \equiv \partial\psi/\partial x^0$ and $\phi_{,n} \equiv \partial\phi/\partial x^n$.

Substituting (1.10) into the expressions for the derivatives of p_i^2 and p^2 and collecting all the terms, we obtain for the derivative of the momentum unit vector

$$\frac{1}{P^0}\frac{d\hat{\mathrm{p}}_i}{d\lambda} = \sum_n \frac{E^2\phi_{,n} + k^2\psi_{,n}}{RkE}(\hat{\mathrm{p}}_n\hat{\mathrm{p}}_i - \delta_{in}) - \hat{\mathrm{p}}_i(\dot{\mathcal{E}}_{;ii} - \dot{\mathcal{E}}_{;nn}\hat{\mathrm{p}}_n^2) \tag{1.12}$$

It is straightforward to check that this expression is consistent with the $\sum_i \hat{\mathrm{p}}_i \frac{d\hat{\mathrm{p}}_i}{d\lambda} = 0$ condition.

The isotropy and homogeneity of space–time in the FRW model of the Universe implies, that the zero–order phase space distribution functions are independent of spatial coordinates and the direction of momentum vector, so that $\frac{\partial f}{\partial x^i}$ and $\frac{\partial f}{\partial \hat{\mathrm{p}}_i}$ are first order quantities. Since the derivative of the momentum direction vector (1.12) is also of first order, the last term in (1.3) can be omitted. For the same reason we can neglect first order corrections to the $\frac{P^i}{P^0}$ factor in the second term of (1.3).

So far, we have specified only one gauge fixing condition, namely $B = 0$, so that the above analysis is valid for a wide class of gauges including the widely used *longitudinal* and *synchronous* gauges. The latter one is obtained by setting $\phi = 0$. In this gauge the Boltzmann equation takes the form[3]

$$\frac{\partial f}{\partial \tau} + \frac{\partial f}{\partial x^i}\frac{\mathrm{p}\hat{\mathrm{p}}_i}{E} - \frac{\partial f}{\partial E}\frac{\mathrm{p}^2}{E}\left(H - \dot{\psi} + \dot{\mathcal{E}}_{;ii}\hat{\mathrm{p}}_i^2\right) = \frac{\hat{C}[f]}{E} \tag{1.13}$$

For the reasons given above, in the FRW Universe equation (1.13) simplifies to

$$\frac{\partial f}{\partial \tau} - H\frac{\mathrm{p}^2}{E}\frac{\partial f}{\partial E} = \frac{\hat{C}[f]}{E} \tag{1.14}$$

As we are interested only in the total number of particles, it is convenient to integrate the Boltzmann equation (1.14) over the phase space. The integration of the first term gives the time derivative of the particle number density

$$n = \frac{g}{(2\pi)^3}\int f d\Omega_{\mathrm{p}} \tag{1.15}$$

where g is the number of spin degrees of freedom. The integration of the second term yields

$$\frac{g}{(2\pi)^3}\int \frac{\mathrm{p}^2}{E}\frac{\partial f}{\partial E}d^3\mathrm{p} = \frac{g}{2\pi^2}\int \frac{\partial f}{\partial(\mathrm{p}^2)}\mathrm{p}^4 d\mathrm{p} = -3n \tag{1.16}$$

As can easily be verified, the sum of the two terms reads

$$\frac{1}{\sqrt{-g_3}}\frac{\partial}{\partial \tau}(n\sqrt{-g_3}) = \int \frac{C[f]}{E}d\Omega_{\mathrm{p}} \tag{1.17}$$

where g_3 is the determinant of the spatial part of the metric (1.5), $\sqrt{-g_3} = R^3$. From equation (1.17) it follows, that in the absence of interactions the particle number in a comoving volume $Y \equiv n\sqrt{-g_3}$, where n stands either for number density of leptons or Majoranas, remains constant.

[3]Let us also note, that in the longitudinal gauge, which is obtained by setting $\mathcal{E}$ to zero, in the absence of anisotropic stress $\psi = \phi$ [32], and the Boltzmann equation reverts to that derived in [29].

Although the integrand on the right–hand side of the Boltzmann equation for the lepton asymmetry contains collision terms corresponding to all possible decay and scattering processes, it is clear that after integration over the phase space only processes changing lepton number remain. The dynamical explanation is as follows. Consider a small volume dV. In the FRW Universe, the macroscopic gas velocity is zero and consequently only processes which take place inside this volume can change the number of leptons in dV. All perturbative SM reactions are known to conserve lepton number. Therefore these processes are only capable of changing the phase space distribution of the SM species. At temperatures of the order of the Majorana neutrino mass the rate of the Standard Model interactions is higher than the expansion rate of the Universe, so that all the SM species are in kinetic equilibrium at this stage. This implies in particular, that their dynamics is sufficiently well described by equations of hydrodynamics. As is known, for an equilibrium system in an external static field left– and right–hand sides of Boltzmann equations vanish. Although in the expanding Universe the right–hand side of the Boltzmann equation does not vanish exactly, for species sufficiently close to equilibrium, as it is the case for the SM states, the deviation from zero is negligibly small. In other words, if we substitute the (equilibrium) distribution function determined by the fast interactions into the right–hand side of the Boltzmann equations with all possible SM processes taken into account, it will vanish after integration over the phase space. Due to the smallness of the Yukawa couplings the heavy neutrino decay rate is smaller (or at least not much bigger) than the expansion rate of the Universe. Therefore the collision terms corresponding to processes violating lepton number by one (the decay and the Higgs mediated scattering) or two units, with the Majorana neutrino in initial or intermediate state, do not vanish after integration over the phase space.

A similar argumentation is also valid for the Boltzmann equation for the Majorana neutrino number density. In this case the shape of the distribution function is determined by relatively fast elastic scattering processes of Majorana neutrinos off leptons and the Higgs. The commonly used *ansatz* for the Majorana neutrino distribution function is

$$f_\Psi(\tau, E, T) = g(\tau) f_\Psi^{eq}(E, T), \tag{1.18}$$

where τ is time, T is the temperature[4], and E is the particle energy. After integration over the phase space, collision terms corresponding to the fastest processes determining the phase space distribution function vanish and only terms corresponding to relatively slow decay and scattering processes changing number of Majoranas remain.

[4]It is important to note, that the introduction of macroscopic parameters like temperature and gas velocity is possible because the Standard Model species, which carry most of the energy density of the Universe, are in thermal equilibrium. This implies in particular, that phase space distribution of the leptons, quarks and the Higgs is described by the corresponding equilibrium distribution functions. Note also, that the third Sakharov condition requires time scale of variation of the macroscopic parameters to be smaller than the Majorana lifetime.

In the nonuniform Universe the situation is more complicated. In particular, due to the nonzero macroscopic particle flow, characterized by a macroscopic gas velocity $\vec{u}_1$, the lepton number asymmetry in a volume element dV is no longer conserved even if the lepton number violating reactions are frozen. The nonzero gas velocity also implies, that the single particle distribution function f is not isotropic in the phase–space. In addition, the gravitational field induces an anisotropy of the single particle distribution function in the coordinate space[5]. Let us discuss influence of these effects on the form of the integrated Boltzmann equation. Consider the second term on the left–hand side of (1.13). Deviation of $\frac{\partial f}{\partial x^i}$ from zero is induced by the nonzero gravitational field, and therefore this term, which is expected to be proportional to $\frac{\partial \psi}{\partial x^i}$, is a first order quantity. The integral of $f\frac{\mathrm{p}\hat{\mathrm{p}}_i}{E}$ over the phase space, which is proportional to $\vec{u}_1$, is also of first order. Consequently the resulting product, which is proportional to $(\vec{u}_1\vec{\nabla}\psi)$, is of second order and can be neglected[6]. Analogously, since $\mathcal{E}$ is of first order, any higher order corrections to the integral of the last term in the brackets in (1.13) over the phase space can be neglected, and it vanishes (recall that the zero–order distribution function is isotropic and that $\sum_i \mathcal{E}_{;ii} = 0$). Collecting the remaining (the first, the third and the fourth) terms we conclude that the form of the integrated Boltzmann equation in the inhomogeneous Universe coincides with (1.17) with the determinant of the spatial part of the space–time metric now given (to leading order) by $\sqrt{-g_3} = R^3(1 - 3\psi)$.

Turning from differentiation with respect to τ to differentiation with respect to $x \equiv M_1/T$, where M_1 is mass of the lightest Majorana, and using the definition of the particle number density in the comoving volume, we rewrite the Boltzmann equation (1.17) in a compact form, applicable both in the homogeneous and inhomogeneous models of the Universe, which will be used in what follows:

$$\frac{\partial Y}{\partial x} = \frac{\sqrt{-g_3}}{\dot{x}} \int \frac{C[f]}{E} d\Omega_{\mathrm{p}}. \tag{1.19}$$

Boltzmann equations for the lepton asymmetry and the Majorana neutrino number density should be coupled with the Einstein equations, which determine time dependence of the components of the metric and thermodynamic quantities. In the homogeneous Universe these reduce to one equation for time dependence of the temperature and one equation for the development of the scale factor, which are discussed in section 1.4. In the inhomogeneous Universe one has to solve complete set of the Einstein equations for small perturbations of the space–time metric, temperature and the macroscopic gas velocity, which are discussed in section 1.5.

[5] A well–known example of such a modification is the distribution of the atmosphere in the Earth's gravitational field.

[6] In the FRW Universe the distribution function is isotropic in both the coordinate and the phase spaces, so that both $\frac{\partial f}{\partial x^i}$ and the integral of $f\frac{\mathrm{p}\hat{\mathrm{p}}_i}{E}$ over the phase space identically vanish. It is clear that in the inhomogeneous Universe these terms can be at most of first order in perturbations of space–time metric and the gas velocity.

1.3 Collision terms

The set of the decay and scattering processes contributing to the generation and washout of the lepton asymmetry in the Standard Model is presented in figures 1.1, 1.2 and 1.3. In the Friedman–Robertson–Walker Universe the integral on the right–hand side of the Boltzmann equation (1.19) can be expressed through amplitudes $\mathcal{M}$ of these processes [4] in the following way:

$$-\int d\Pi_a d\Pi_b \dots d\Pi_i d\Pi_j (2\pi)^4 \delta^4(P_f - P_i) \left[|\mathcal{M}|^2_{a+b+\dots\to i+j+\dots} f_a f_b \dots (1 \pm f_i)(1 \pm f_j) \dots \right.$$
$$\left. - |\mathcal{M}|^2_{i+j+\dots\to a+b+\dots} f_i f_j \dots (1 \pm f_a)(1 \pm f_b) \dots \right], \quad (1.20)$$

where $d\Pi = \frac{d^3\mathrm{p}}{(2\pi)^3} \frac{g}{2E}$ is the Lorentz–invariant element of phase space, $\vec{\mathrm{p}}$ and E are physical momentum and energy respectively, and g is number of spin degrees of freedom. In the absence of Bose condensation or Fermi degeneracy the blocking and stimulated emission factors can be ignored, so that $1 \pm f \simeq 1$.

Since the collision terms in the Standard Model have been discussed in detail by a number of researches [34, 35, 36], we will only sketch the derivation here.

Let us first consider the *CP* violating decay and inverse decay of the Majorana neutrino depicted in figure 1.1. For the change of the lepton number we obtain

$$-\int d\Pi_\Psi d\Pi_L d\Pi_H (2\pi)^4 \delta^4(p_\Psi - p_L - p_H) \times \left[f_\Psi |\mathcal{M}|^2_{\Psi\to L\,H} - f_L f_H |\mathcal{M}|^2_{L\,H\to\Psi} \right.$$
$$\left. - f_\Psi |\mathcal{M}|^2_{\Psi\to \bar{L}\,\bar{H}} + f_{\bar{L}} f_{\bar{H}} |\mathcal{M}|^2_{\bar{L}\,\bar{H}\to\Psi} \right] \quad (1.21)$$

The one–loop vertex and self–energy diagrams induce small corrections to the tree–level decay amplitude (denoted by $\mathcal{M}_0$) $|\mathcal{M}|^2 = |\mathcal{M}_0|^2 \frac{(1\pm\varepsilon)}{2}$, where the plus sign corresponds to the $\Psi \to LH$ and $\bar{L}\bar{H} \to \Psi$ processes, whereas the minus sign to the $\Psi \to \bar{L}\bar{H}$ and $LH \to \Psi$ processes. The factor of one half arises because the Majorana neutirino can decay into both the LH and $\bar{L}\bar{H}$ pairs. Since interaction rates of the Standard Model species are bigger than the expansion rate of the Universe, they are in equilibrium at the stage under consideration. Consequently, the out–of–equilibrium decay of the Majorana neutrino only induces nonzero chemical potentials of the leptons (chemical potential of the left–handed leptons is denoted by μ_L), of the Higgs (denoted by μ_H), and of the left– and right–handed quarks (denoted by μ_Q and μ_U respectively). Chemical potential of the Majorana neutrino is equal to zero[7]. At high temperatures it is safe to use the Maxwell–Boltzmann distribution for both the bosonic and the fermionic species, so that

[7] As the Majorana neutrino is a truly neutral fermion, in thermal equilibrium its chemical potential is zero. However, due to CP violation, the decay rate of the Majorana neutrino with left helicity differs from decay rate of the Majorana neutrino with right helicity, so that if there is a deviation from thermal equilibrium, an effective chemical potential of the Majorana neutrino can be introduced [37]. This small effect is neglected here.

the equilibrium distribution function reads $f = \exp\left[-(E-\mu)/T\right]$. Taking into account that due to conservation of energy $E_\Psi = E_L + E_H$ (see also discussion in [4]), using the ansatz (1.18), and keeping the terms linear in the chemical potentials we finally rewrite (1.21) in the form

$$\gamma^\Psi_{LH}\left[\varepsilon\left(1+\frac{n_\Psi}{n^{eq}_\Psi}\right) - c_{\ell h}\frac{\mu_L}{T}\right] \tag{1.22}$$

where $c_{\ell h}\mu_L \equiv \mu_L + \mu_H$ is a sum of the chemical potentials of the leptons and the Higgs. The decay reaction density γ^Ψ_{LH}, which is defined in (C.1), can be expressed in terms of the tree–level decay width Γ_{Ψ_1} of the lightest Majorana and its equilibrium number density $n^{eq}_{\Psi_1}$ as

$$\gamma^\Psi_{LH} = n^{eq}_{\Psi_1}\Gamma_{\Psi_1}\frac{K_1(x)}{K_2(x)}, \quad \Gamma_{\Psi_1} = \frac{(\lambda\lambda^\dagger)_{11}}{8\pi}M_1, \tag{1.23}$$

where $K_1(x)$ and $K_2(x)$ are the modified Bessel functions.

Integrating the Maxwell–Boltzmann distribution function over the phase space we obtain for the equilibrium number density of the lightest Majoranas

$$n^{eq}_{\Psi_1} = \frac{g}{2\pi^2}T^3x^2K_2(x), \quad g = 2 \tag{1.24}$$

One can also easily calculate the sum (denoted by n^{eq}_L) and the difference (denoted by n_L) of the number of leptons and antileptons. Up to terms linear in the chemical potential μ_L

$$n_L = 2N\left(\frac{T^3}{\pi^2}\frac{2\mu_L}{T}\right), \quad n^{eq}_L = 2N\left(\frac{2T^3}{\pi^2}\right), \quad \frac{\mu_L}{T} = \frac{n_L}{n^{eq}_L}, \tag{1.25}$$

where the factor of $2N$ is the total number of the left–handed leptons in the model (N generations of two–component doublets), which arises because the asymmetry is carried by leptons of all the three generations.

Contribution of the decay and inverse decay processes into change of the number of the heavy neutrinos is obtained from (1.21) by an interchange of the last two signs, which yields

$$\gamma^\Psi_{LH}\left(1-\frac{n_\Psi}{n^{eq}_\Psi}\right) \tag{1.26}$$

Consider now the first of the two scattering processes depicted in figure 1.2. Since lepton number is violated by two units in this process, the corresponding contribution into change of the lepton number reads

$$-2\int d\Pi_L d\Pi_H d\Pi_{\bar{L}} d\Pi_{\bar{H}}(2\pi)^4\delta(P_f - P_i)\times\left[f_L f_H|\mathcal{M}'|^2_{LH\to\bar{L}\bar{H}} - f_{\bar{L}}f_{\bar{H}}|\mathcal{M}'|^2_{\bar{L}\bar{H}\to LH}\right] \tag{1.27}$$

where $|\mathcal{M}'|^2 = |\mathcal{M}|^2 - |\mathcal{M}_{RIS}|^2$ stands for the Real Intermediate State subtracted scattering amplitude. Contribution of real intermediate Majorana neutrino, which has already been accounted for by the decay and inverse decay processes, is subtracted in order to avoid double counting in

the Boltzmann equation for the lepton number asymmetry. Expanding the distribution functions and keeping only the terms linear in the chemical potentials we obtain

$$-2\int d\Pi_L d\Pi_H d\Pi_{\bar{L}} d\Pi_{\bar{H}} (2\pi)^4 \delta(P_f - P_i) \times f_L^0 f_H^0 [\left(|\mathcal{M}|^2_{LH\to\bar{L}\bar{H}} - |\mathcal{M}|^2_{\bar{L}\bar{H}\to LH}\right)$$
$$-\left(|\mathcal{M}_{RIS}|^2_{LH\to\bar{L}\bar{H}} - |\mathcal{M}_{RIS}|^2_{\bar{L}\bar{H}\to LH}\right) + c_{\ell h}\frac{\mu_L}{T}(|\mathcal{M}^{'}|^2_{LH\to\bar{L}\bar{H}} + |\mathcal{M}^{'}|^2_{\bar{L}\bar{H}\to LH})] \qquad (1.28)$$

where $f^0 \equiv \exp(-E/T)$. The unitarity implies [38], that the difference $|\mathcal{M}|^2_{LH\to\bar{L}\bar{H}} - |\mathcal{M}|^2_{\bar{L}\bar{H}\to LH}$ vanishes after summation over all initial and final states. Since the $\frac{\mu_L}{T}$ ratio is a first order quantity, we can neglect higher–order contributions to the RIS subtracted scattering amplitudes in (1.28), so that $|\mathcal{M}^{'}|^2_{LH\to\bar{L}\bar{H}} + |\mathcal{M}^{'}|^2_{\bar{L}\bar{H}\to LH} \approx 2|\mathcal{M}^{'}_0|^2$, where $\mathcal{M}^{'}_0$ stands for the tree–level scattering amplitude. From physical considerations it is clear, that a scattering mediated by real intermediate state can be considered as an inverse decay followed by a decay. As has been discussed above, contributions of the decay and inverse decay processes are proportional to γ^{Ψ}_{LH}. Contribution of the $\bar{L}\bar{H} \to \Psi \to LH$ process is proportional to $\frac{(1+\varepsilon)^2}{4}$, whereas contribution of the $LH \to \Psi \to \bar{L}\bar{H}$ process to $\frac{(1-\varepsilon)^2}{4}$ (see the discussion below equation (1.21)), so that the difference of the third and the fourth terms in (1.28), integrated over the phase space and multiplied by the factor of two, is given by $-2\varepsilon\gamma^{\Psi}_{LH}$. A careful calculation [34] confirms this qualitative result. Therefore (1.27) can be rewritten in the form

$$-4c_{\ell h}\frac{\mu_L}{T}\gamma^{'LH}_{\bar{L}\bar{H}} - 2\varepsilon\gamma^{\Psi}_{LH}. \qquad (1.29)$$

$\gamma^{'LH}_{\bar{L}\bar{H}}$ denotes the tree–level reaction density corresponding to the RIS subtracted reduced cross section (see equations (C.9), (C.18), (D.3) and (D.5))

$$\hat{\sigma}^{'LH}_{\bar{L}\bar{H}} = \sum_{ij}\frac{\sqrt{a_i a_j}}{4\pi z}(\lambda\lambda^{\dagger})^2_{ij}\left[\frac{z^2}{\mathcal{D}_{ij}(z)} + \frac{1}{P_i(z)}\left\{z - (z+a_j)\ln\left(\frac{z+a_j}{a_j}\right)\right\}\right. \qquad (1.30)$$
$$\left. + \frac{1}{P^*_j(z)}\left\{z - (z+a_i)\ln\left(\frac{z+a_i}{a_i}\right)\right\} + 2\frac{z+a_j}{a_i - a_j}\ln\left(\frac{z+a_j}{a_j}\right) + 2\frac{z+a_i}{a_j - a_i}\ln\left(\frac{z+a_i}{a_i}\right)\right],$$

where $a_i = \left(\frac{M_i}{M_1}\right)^2$ and $c_i = \left(\frac{\Gamma_i}{M_1}\right)^2$ are dimensionless Majorana neutrino mass and decay width squared respectively, and $z = \frac{s}{M_1^2}$ is square of dimensionless center of mass energy of the colliding particles.

Consider now the second of the depicted in figure 1.2 processes violating lepton number by two units. Proceeding as above we find for the contribution into change of the lepton number

$$2\int d\Pi_L d\Pi_L d\Pi_H d\Pi_H (2\pi)^4 \delta(P_f - P_i) \times [-f_L f_L |\mathcal{M}|^2_{LL\to\bar{H}\bar{H}} + f_{\bar{L}} f_{\bar{L}} |\mathcal{M}|^2_{\bar{L}\bar{L}\to HH}$$
$$- f_H f_H |\mathcal{M}|^2_{HH\to\bar{L}\bar{L}} + f_{\bar{L}} f_{\bar{L}} |\mathcal{M}|^2_{\bar{H}\bar{H}\to LL}] \qquad (1.31)$$

Taking into account that this process is to one–loop order *CP* conserving (so that the four scattering amplitudes are equal to leading order), expanding the distribution functions and

keeping only the terms linear in the chemical potentials we rewrite (1.31) in the form

$$-8c_{\ell h}\frac{\mu_L}{T}\gamma^{LL}_{\bar{H}\bar{H}} \tag{1.32}$$

where $\gamma^{LL}_{\bar{H}\bar{H}}$ is the tree–level reaction density corresponding to the reduced cross section

$$\hat{\sigma}^{LL}_{\bar{H}\bar{H}} = \sum_{ij}\frac{\sqrt{a_i a_j}}{4\pi}(\lambda\lambda^\dagger)^2_{ij}\left[\frac{2}{a_i-a_j}\ln\left(\frac{a_i(z+a_j)}{a_j(z+a_i)}\right)+\frac{1}{z+a_i+a_j}\ln\left(\frac{(z+a_j)(z+a_i)}{a_i a_j}\right)\right] \tag{1.33}$$

Consider now the depicted in figure 1.3 processes violating lepton number by one unit. These processes are also to leading order CP conserving, so that it is sufficient to consider only the tree–level diagrams, whose amplitudes are denoted by $\mathcal{M}_0$ in what follows. Contribution of the $\Psi L \to Q\bar{U}$ process into change of the number of the leptons is given by

$$-\int d\Pi_\Psi d\Pi_L d\Pi_Q d\Pi_U (2\pi)^4\delta(P_f-P_i)|\mathcal{M}_0|^2\left[f_\Psi f_L - f_Q f_{\bar{U}} - f_\Psi f_{\bar{L}} + f_{\bar{Q}} f_U\right] \tag{1.34}$$

The fast Standard Model process $H^0 \to u_R + \bar{u}_L$ ensures, that $\mu_H = \mu_U - \mu_Q$. Expanding the distribution functions and keeping only the terms linear in the chemical potentials, we rewrite (3.7) in the form

$$-2\frac{\mu_L}{T}\left(\frac{n_\Psi}{n^{eq}_\Psi}+c_H\right)\gamma^{\Psi L}_{Q\bar{U}}, \tag{1.35}$$

where $c_H \equiv \frac{\mu_H}{\mu_L}$ has been introduced.

The contribution into change of the number of the lightest Majoranas is obtained from (1.34) by an interchange of the two last signs, which yields

$$2\left(1-\frac{n_\Psi}{n^{eq}_\Psi}\right)\gamma^{\Psi L}_{Q\bar{U}}, \tag{1.36}$$

where $\gamma^{\Psi L}_{Q\bar{U}}$ is the tree–level reaction density corresponding to the reduced cross section ($a_1 = 1$)

$$\hat{\sigma}^{\Psi L}_{Q\bar{U}} = 3(\lambda\lambda^\dagger)_{11}\frac{\mathrm{Tr}(\lambda_u\lambda_u^\dagger)}{4\pi}\frac{(z-a_1)^2}{(z-a_h)^2}, \quad a_h = \left(\frac{m_h}{M_1}\right)^2 \tag{1.37}$$

The trace over the product of the quark Yukawa couplings is dominated by the top–quark coupling, and consequently it can be expressed through the top–quark mass $\frac{\mathrm{Tr}(\lambda_u\lambda_u^\dagger)}{4\pi} \simeq \frac{\alpha_w m_t^2}{2M_W^2}$, where α_w is related to the fine structure constant by $\alpha_w = \frac{\alpha}{\sin^2\Theta_W}$.

Contribution of the $\Psi Q \to LU$ process into change of the Majorana neutrino number reads

$$-\int d\Pi_\Psi d\Pi_Q d\Pi_L d\Pi_U (2\pi)^4\delta(P_f-P_i)|\mathcal{M}_0|^2\left[f_\Psi f_Q - f_L f_U + f_\Psi f_{\bar{Q}} - f_{\bar{L}} f_{\bar{U}}\right] \tag{1.38}$$

Using the ansatz (1.18), expanding the distribution functions and keeping only the terms linear in the chemical potentials we rewrite (1.38) in the form

$$2\left(1-\frac{n_\Psi}{n^{eq}_\Psi}\right)\gamma^{\Psi Q}_{LU} \tag{1.39}$$

Contribution of this process into change of the lepton number is obtained from (1.38) by an interchange of the last two signs, which yields

$$-2\frac{\mu_L}{T}\left(1+c_u-c_Q\frac{n_\Psi}{n_\Psi^{eq}}\right)\gamma_{LU}^{\Psi Q}, \tag{1.40}$$

where $\gamma_{LU}^{\Psi Q}$ is the tree–level reaction density corresponding to the reduced cross section

$$\hat{\sigma}_{LU}^{\Psi Q}=3(\lambda\lambda^\dagger)_{11}\,\frac{\mathrm{Tr}(\lambda_u\lambda_u^\dagger)}{4\pi}\,\frac{z-a_1}{z}\left[\frac{z-2a_1+2a_h}{z-a_1+a_h}+\frac{a_1-2a_h}{z-a_1}\ln\left(\frac{z-a_1+a_h}{a_h}\right)\right], \tag{1.41}$$

and c_u and c_Q are defined analogously to c_H.

Finally, the contribution of the $\Psi\bar{U}\to L\bar{Q}$ process into change of the heavy neutrino number coincides with (1.39), whereas contribution of this process into change of the lepton number is obtained from (1.40) by the $c_u\leftrightarrow -c_Q$ interchange. The tree–level reduced cross section $\hat{\sigma}_{L\bar{Q}}^{\Psi\bar{U}}$ is given by the same expression as the $\hat{\sigma}_{LU}^{\Psi Q}$.

Collecting all the terms and using relations (1.25) and the definition of particle number density in the comoving volume we obtain a system of Boltzmann equations for the Majorana and the lepton number densities in the FRW Universe

$$\frac{\partial Y_\Psi}{\partial x}=\frac{\sqrt{-g_3}}{\dot{x}}\left\{\left(1-\frac{Y_\Psi}{Y_\Psi^{eq}}\right)\left[\gamma_{LH}^{\Psi}+2\gamma_{Q\bar{U}}^{\Psi L}+2\gamma_{LU}^{\Psi Q}+2\gamma_{L\bar{Q}}^{\Psi\bar{U}}\right]\right\} \tag{1.42a}$$

$$\begin{aligned}\frac{\partial Y_L}{\partial x}=\frac{\sqrt{-g_3}}{\dot{x}}\Bigg\{&-\varepsilon\gamma_{LH}^{\Psi}\left(1-\frac{Y_\Psi}{Y_\Psi^{eq}}\right)-\frac{Y_L}{Y_L^{eq}}\frac{Y_\psi}{Y_\psi^{eq}}\left[2\gamma_{Q\bar{U}}^{\Psi L}-2c_q\gamma_{LU}^{\Psi Q}+2c_u\gamma_{L\bar{Q}}^{\Psi\bar{U}}\right] \\ &-\frac{Y_L}{Y_L^{eq}}\left[c_{\ell h}\gamma_{LH}^{\Psi}+4c_{\ell h}\gamma_{L\bar{H}}^{\prime LH}+8c_{\ell h}\gamma_{H\bar{H}}^{LL}+2c_h\gamma_{Q\bar{U}}^{\Psi L}+2(1+c_u)\gamma_{LU}^{\Psi Q}+2(1-c_q)\gamma_{L\bar{Q}}^{\Psi\bar{U}}\right]\Bigg\}\end{aligned} \tag{1.42b}$$

Equations (1.42) are similar to those discussed in the literature [34, 35, 36] and differ mainly in the chemical potentials of the quarks and the Higgs being taken into account. Values of the coefficients $c_{\ell h}$, c_h, c_q and c_u in the Standard Model above the electroweak phase transition are given by (1.110).

The reaction densities on the right–hand side of (1.42) depend on four real dimensional (the Majorana neutrino masses and the effective mass of the Higgs) and nine complex dimensionless (the neutrino Yukawa couplings) parameters. Reaction densities of the decay and the Higgs mediated scattering processes can be parametrized in terms of the lightest Majorana neutrino mass, the effective Higgs mass and the so–called effective neutrino mass

$$\tilde{m}_1\equiv(\lambda\lambda^\dagger)_{11}\frac{v^2}{M_1}, \tag{1.43}$$

where $v=174$ GeV is the Higgs expectation value at zero temperature. Reaction densities of the Majorana mediate processes depend on all the Majorana masses and the Yukawa couplings.

The effective neutrino mass should not be confused with the physical ones. In the scenario under consideration the conventional neutrinos acquire small masses via the see–saw mechanism.

The mass eigenstates are obtained by a unitary transformation of the neutrino mass matrix $\hat{m}$

$$\hat{m}_{ij} \approx -\sum_k \lambda_{ki} \frac{v^2}{M_k} \lambda_{kj} \ , \quad U^\dagger \hat{m}\, U^* = -\mathrm{diag}(m_1, m_2, m_3). \tag{1.44}$$

Contributions of the decay and the Higgs mediated processes are proportional to number of on–shell Majoranas, and rapidly fall off with decrease of temperature. On the contrary, the Majorana–mediated scattering processes are not strongly suppressed at low temperatures and play an important role in washout of the lepton number asymmetry. From equation (C.24) it follows, that at low temperatures (i.e. at large x) the leading contribution to the corresponding reaction densities comes from the small–z region. Expanding (1.30) and (1.33) around $z = 0$, substituting them into (C.24), and using the expression for the physical neutrino masses (1.44) we find, that contributions of these processes at low temperatures are mainly determined by the lightest Majorana mass M_1 and mean square of the physical neutrino masses $3\bar{m}^2 = m_1^2 + m_2^2 + m_3^2$, whereas influence of the other parameters is sub–dominant (see [36] for detailes). Values of the neutrino masses suggested by the results of the oscillation experiments $(\Delta m^2_{sol})^{\frac{1}{2}} \simeq 8 \cdot 10^{-3}$ eV and $(\Delta m^2_{atm})^{\frac{1}{2}} \simeq 5 \cdot 10^{-2}$ eV.

Summarizing the above we conclude, that to a first approximation the reaction densities on the right–hand side of (1.42) are determined by only four parameters: the lightest Majorana neutrino mass M_1, the effective neutrino mass $\tilde{m}_1$ (or, alternatively, by the κ), the mean square of the physical neutrino masses $\bar{m}$ and the parameter of CP violation ε. As is argued in [36], for the hierarchical neutrinos (that is, if $m_3 \simeq (\Delta m^2_{atm})^{\frac{1}{2}} \gg m_2 \simeq (\Delta m^2_{sol})^{\frac{1}{2}} \gg m_1$) an upper bound for the latter one reads

$$|\varepsilon| \lesssim \frac{3}{16\pi} \frac{M_1 (\Delta m^2_{atm})^{\frac{1}{2}}}{v^2} \simeq \frac{3\sqrt{3}}{16\pi} \frac{M_1 \bar{m}}{v^2}, \tag{1.45}$$

where we have taken into account, that for hierarchical neutrinos leading contribution to $\bar{m}$ is due to neutrino of the heaviest generation. For $M_1 = 10^9$ GeV and $\sqrt{3}\bar{m} = 5 \cdot 10^{-2}$ eV the upper bound on ε reaches the value $\sim 10^{-7}$. For a natural set of parameters the effective neutrino mass is expected [36] to be in the range $m_1 \leqslant \tilde{m}_1 \leqslant m_3$, which for the hierarchical neutrinos implies, that $\tilde{m}_1 \leqslant \sqrt{3}\bar{m}$.

Let us now turn to discussion of the right–hand side of (1.19) in a nonuniform model of the Universe. We assume here, that the decay and scattering amplitudes $\mathcal{M}$ are not affected by perturbations of the metric; more precisely, we assume, that expressed in terms of physical energy and momentum the decay and scattering amplitudes keep the same form as in the homogeneous and isotropic Universe. Under this assumption any variation from the homogeneous case may only appear after integration over the phase space. Expressed in terms of physical momentum and energy the invariant element of the phase space [33] $d\Pi = (-g_4)^{-\frac{1}{2}} \frac{dP_1 dP_2 dP_3}{(2\pi)^3} \frac{g}{2P^0}$, where g_4

is determinant of the metric, takes its conventional form $d\Pi = \frac{d^3\mathrm{p}}{(2\pi)^3}\frac{g}{2E}$. As has been argued in section 1.2, perturbations of the space–time metric induce a nonzero gradient of the phase space distribution function in the coordinate space and a nonzero macroscopic gas velocity $\vec{u}_1$. In the absence of the gradient in the coordinate space the modification of the reaction densities should be independent of direction of $\vec{u}_1$. Consequently, as can be checked by a direct calculation in some simple cases, the expansion of the reaction densities around $\vec{u}_1 = 0$ should contain only even powers of $\vec{u}_1$, i.e. terms of second and higher orders, which can be neglected. Modification of the phase space distribution functions and the reaction densities in the gravitational field requires a further investigation, and the associated effects are neglected here. In this approximation the right–hand side of (1.42) keeps its form. Thus, to the same approximation, the system of Boltzmann equations (1.42) is suitable for investigation of the generation of the lepton asymmetry in both the homogeneous and inhomogeneous models of the Universe.

Equations (1.42) give the lepton asymmetry as a function of the inverse temperature x. If one wants to compare the *time* development of the asymmetry in the two models of the Universe, one has to take into account, that time dependence of the temperature in the nonuniform Universe differs from that in the homogeneous one. We will return to this point in the next section.

1.4 Leptogenesis in the uniform Universe

Leptogenesis in the flat homogeneous and isotropic Universe has been analyzed by a number of researchers. We reconsider here their analysis taking into account the contribution of the Majorana neutrinos to the energy density of the Universe, which modifies the dependence of the expansion rate and the scale factor on temperature, thus affecting the generation of the lepton number asymmetry. Results of this section are useful for the analysis of the efficiency of leptogenesis in the nonuniform Universe.

The metric of the flat homogeneous and isotropic Universe is given by (1.5). To be consistent with the symmetry of the metric, the total momentum–energy tensor must be diagonal, and by isotropy the spatial components must be equal. The simplest realization of such a momentum–energy tensor is that of a perfect fluid characterized by energy density ρ and pressure p:

$$T^{\mu\nu} = \omega u^\mu u^\nu - p g^{\mu\nu}, \quad \omega \equiv \rho + p \tag{1.46}$$

The Einstein equations then reduce to two equations for the scale factor:

$$3\ddot{R} = -4\pi G R(\rho + 3p), \quad R\ddot{R} + 2\dot{R}^2 = 4\pi G R^2(\rho - p) \tag{1.47}$$

Eliminating $\ddot{R}$ we obtain the Friedman equation

$$3\dot{R}^2 = 8\pi G R^2 \rho \tag{1.48}$$

Conservation of the momentum–energy tensor, $T^{\mu\nu}{}_{;\nu} = 0$, gives the third equation relating the scale factor, energy density and pressure:

$$\dot{\rho} + 3H(\rho + p) = 0. \tag{1.49}$$

In the model we consider, energy density ρ and pressure p are sums of two terms. The first contribution is due to the massless[8] species of the Standard Model. As all the Standard Model processes, including the electroweak reactions, are fast at high temperatures, the SM species are in thermal equilibrium and are described by either Fermi–Dirac or Bose–Einstein distribution. Consequently,

$$\rho_{SM} = \frac{g_*\pi^2}{30}T^4, \quad p_{SM} = \frac{g_*\pi^2}{90}T^4 \tag{1.50}$$

In the Standard Model the effective number of massless degrees of freedom $g_* = 106.75$.

The second contribution is due to three generations of heavy Majorana neutrinos. The third Sakharov condition requires the heavy neutrinos to be out of equilibrium, so that in order to calculate their contribution to the total energy one has to solve a coupled system of the Einstein and the Boltzmann equations. However, if the deviation from thermal equilibrium is small, which in fact is the condition of applicability of the Boltzmann equation, then it is a sufficiently good approximation to neglect the deviation from thermal equilibrium in the Einstein equations. In this case

$$\rho_M = \frac{g_\star\pi^2}{30}T^4\sum_i r_\rho(x_i), \quad p_M = \frac{g_\star\pi^2}{90}T^4\sum_i r_p(x_i), \tag{1.51}$$

where $x_i \equiv \frac{M_i}{T}$ and $g_\star = 1.75$ is the effective number of "massless degrees of freedom" of a Majorana fermion. The functions $r_\rho(x)$ and $r_p(x)$ are integrals over the Fermi–Dirac distribution defined as

$$r_\rho(x) = \frac{120}{7\pi^4}\int_0^\infty \sqrt{z^2+x^2}\,\frac{z^2dz}{\exp(\sqrt{z^2+x^2})+1}, \tag{1.52a}$$

$$r_p(x) = \frac{120}{7\pi^4}\int_0^\infty \frac{z^2}{\sqrt{z^2+x^2}}\,\frac{z^2\,dz}{\exp(\sqrt{z^2+x^2})+1}, \tag{1.52b}$$

and tend to unity as x approaches zero. It is convenient to introduce

$$g_\rho = g_* + g_\star\sum_i r_\rho(x_i), \quad g_p = g_* + g_\star\sum_i r_p(x_i) \tag{1.53}$$

At temperatures higher than the mass of the heaviest Majorana neutrino (i.e. as $x \to 0$) all particles can effectively be considered as massless, and both g_ρ and g_p tend to the same limit

[8] Above the electroweak phase transition the vacuum expectation value of the Higgs is zero and the masses of all the fermions and gauge bosons are zero. Furthermore, we neglect the so–called effective thermal masses, as these are smaller than the temperature and can be safely neglected.

$g_\circ = g_* + 3g_\star = 112$. At temperatures lower than the mass of the lightest Majorana neutrino (i.e. as $x \to \infty$) both g_ρ and g_p tend to g_*.

Using equations (1.50), (1.51), (1.53) and relation $\frac{\partial}{\partial t} = \frac{\partial x}{\partial t}\frac{\partial}{\partial x}$ we find for the time derivative of the total energy density

$$\dot{\rho} = \dot{x}\rho\left(\frac{g_\rho^{'}}{g_\rho} - \frac{4}{x}\right) \tag{1.54}$$

where the prime denotes differentiation with respect to $x \equiv x_1$. Combining now equations (1.48), (1.49) and (1.54) we obtain an explicit expression for the time derivative of x:

$$\dot{x} = \frac{H(M_1)}{x} r_{\dot{x}}, \quad H(M_1) \equiv \frac{M_1^2}{M_{Pl}}\left(\frac{4\pi^3 g_*}{45}\right)^{\frac{1}{2}}, \quad r_{\dot{x}} = \sqrt{\frac{g_\rho}{g_*}}\frac{3 + g_p g_\rho^{-1}}{4 - x g_\rho^{'} g_\rho^{-1}} \tag{1.55}$$

By $H(M_1)$ we denote the value of the Hubble parameter at $T = M_1$ in the model with neglected contributions of the Majorana neutrinos to the energy density of the Universe. At temperatures lower than the mass of the lightest Majorana neutrino $r_{\dot{x}}$ tends to unity, and the expression for $\dot{x}$ takes its conventional form. A plot of the $r_{\dot{x}}$ is presented in figure 1.4.a. It is interesting to note

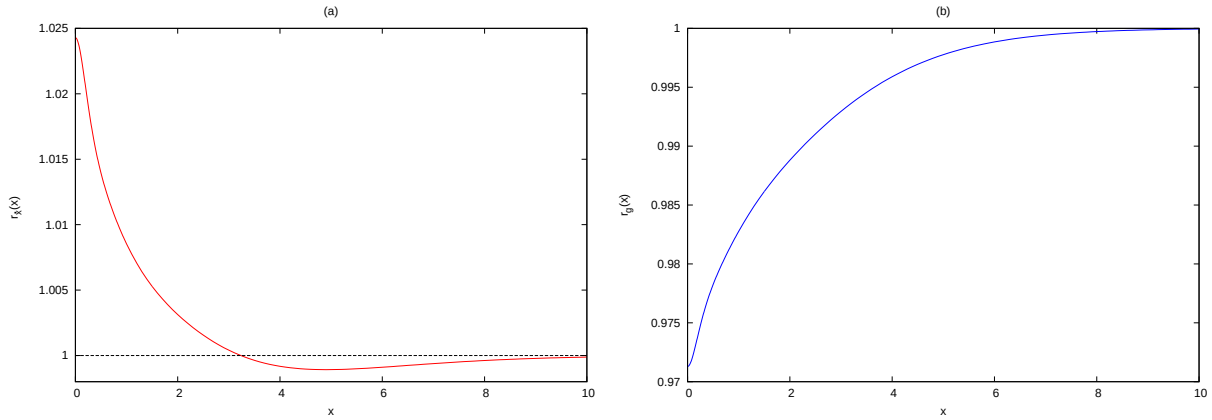

Figure 1.4: Ratios of $\dot{x}$ and $\sqrt{-g_3}$ in the model with three heavy Majorana neutrinos with masses $M_2 = \sqrt{10}M_1$ and $M_3 = 10M_1$ to those in the Standard Model.

that $r_{\dot{x}}$, which is bigger than unity at small x, crosses unity at a finite x and then asymptotically approaches unity from below as $x \to \infty$.

As follows from (1.50), at sufficiently high temperatures, when all the species can be considered as massless, $p = \frac{\rho}{3}$ and equation (1.49) simplifies to $\dot{\rho} = -4H\rho$ implying the well–known solution $R = \text{const} \cdot T^{-1}$. Therefore it is natural to represent the scale factor R as a product of T^{-1} and an unknown function $r_g(x)$:

$$R^3 = \text{const} \cdot T^{-3} \cdot r_g(x) \tag{1.56}$$

Substituting (1.56) into the Friedman equation (1.48) and using (1.55) we obtain a differential

equation for $r_g(x)$:

$$\frac{r_g^{'}(x)}{r_g(x)} = \frac{3}{x}\left[\frac{4 - x g_\rho^{'} g_\rho^{-1}}{3 + g_p g_\rho^{-1}} - 1\right] \tag{1.57}$$

Its solution satisfying the boundary condition $r_g(\infty) = 1$ is given by

$$r_g(x) = \exp\left(-3\int_x^\infty \left[\frac{4 - x g_\rho^{'} g_\rho^{-1}}{3 + g_p g_\rho^{-1}} - 1\right]\frac{dx}{x}\right) \tag{1.58}$$

and is presented in figure 1.4.b. Let us note, that, just like the function $r_{\dot{x}}$, the product $r_{\dot{x}} r_g^{-1}$ crosses unity from above at a finite x and then approaches unity from below as $x \to \infty$.

For computation it is convenient to rewrite the system of Boltzmann equations (1.42) in terms of dimensionless quantities. To this end we introduce a dimensionless Hubble parameter $\mathcal{H}(M_1) \equiv H(M_1)/M_1$ and dimensionless reaction densities $\hat{\gamma} \equiv \gamma/(M_1 T^3)$. Rewritten in terms of these quantities the system (1.42) takes the form:

$$\frac{\partial Y_\Psi}{\partial x} = \frac{r_g(x)}{r_{\dot{x}}(x)}\frac{x}{\mathcal{H}(M_1)}\left\{\left(1 - \frac{Y_\Psi}{Y_\Psi^{eq}}\right)\left[\hat{\gamma}_{LH}^{\Psi} + 2\hat{\gamma}_{Q\bar{U}}^{\Psi L} + 2\hat{\gamma}_{LU}^{\Psi Q} + 2\hat{\gamma}_{L\bar{Q}}^{\Psi \bar{U}}\right]\right\} \tag{1.59a}$$

$$\begin{aligned}\frac{\partial Y_L}{\partial x} = \frac{r_g(x)}{r_{\dot{x}}(x)}\frac{x}{\mathcal{H}(M_1)}\Bigg\{&-\varepsilon\hat{\gamma}_{LH}^{\Psi}\left(1 - \frac{Y_\Psi}{Y_\Psi^{eq}}\right) - \frac{Y_L}{Y_L^{eq}}\frac{Y_\psi}{Y_\psi^{eq}}\left[2\hat{\gamma}_{Q\bar{U}}^{\Psi L} - 2c_q\hat{\gamma}_{LU}^{\Psi Q} + 2c_u\hat{\gamma}_{L\bar{Q}}^{\Psi \bar{U}}\right] \\ &- \frac{Y_L}{Y_L^{eq}}\left[c_{\ell h}\hat{\gamma}_{LH}^{\Psi} + 4c_{\ell h}\hat{\gamma}_{\bar{L}\bar{H}}^{'LH} + 8c_{\ell h}\hat{\gamma}_{\bar{H}\bar{H}}^{LL} + 2c_h\hat{\gamma}_{Q\bar{U}}^{\Psi L} + 2(1+c_u)\hat{\gamma}_{LU}^{\Psi Q} + 2(1-c_q)\hat{\gamma}_{L\bar{Q}}^{\Psi \bar{U}}\right]\Bigg\}\end{aligned} \tag{1.59b}$$

In thermal equilibrium the final lepton asymmetry would be zero. The degree of deviation from thermal equilibrium is characterized by the ratios of reaction densities of the decay and scattering processes to the expansion rate of the Universe. In particular, if we neglect the contribution of the heavy neutrinos to the energy density, i.e. set $r_g = r_{\dot{x}} = 1$ in (1.59), then the degree of deviation from equilibrium in the *decay* of the Majorana neutrino is parametrized by the ratio

$$\kappa = \frac{\Gamma_{\Psi_1}}{H(M_1)} \equiv \frac{\tilde{m}_1}{m_*}, \quad m_* \equiv \frac{8\pi^{\frac{5}{2}}}{3\sqrt{5}} g_*^{\frac{1}{2}} \frac{v^2}{M_{Pl}} \simeq 10^{-3}\ \text{eV}, \tag{1.60}$$

As has been argued in [34], the smaller this ratio, i.e. the bigger the deviation from equilibrium is, the more efficient leptogenesis is. Consequently, an increase of $H(M_1)$ would lead to an increase of the efficiency. The nontrivial dependence of the $r_{\dot{x}} r_g^{-1}$ factor on x effectively modifies the Hubble parameter. Generalization of the above statement to the case under consideration would lead us then to the conclusion, that if $r_{\dot{x}} r_g^{-1}$ was bigger than unity for all x, the efficiency of leptogenesis would increase and vice versa. However, the nontrivial dependence of $r_{\dot{x}}$ and r_g on x results not only in the aforementioned effective modification of κ, but also in a modification of the equilibrium particle number densities in the comoving volume, $Y = r_g(nT^{-3})$. Results of a numerical analysis for various κ are presented in figure 1.5, where we have used $M_1 = 10^9$ GeV and $\sqrt{3}\bar{m} = 5 \cdot 10^{-2}$ eV for evaluation. As initial conditions we have used $Y_\Psi(x_0) = Y_\Psi^{eq}(x_0)$ and $Y_L(x_0) = 0$, where $x_0 = 10^{-3}$. It turns out, that for the chosen masses of the Majorana

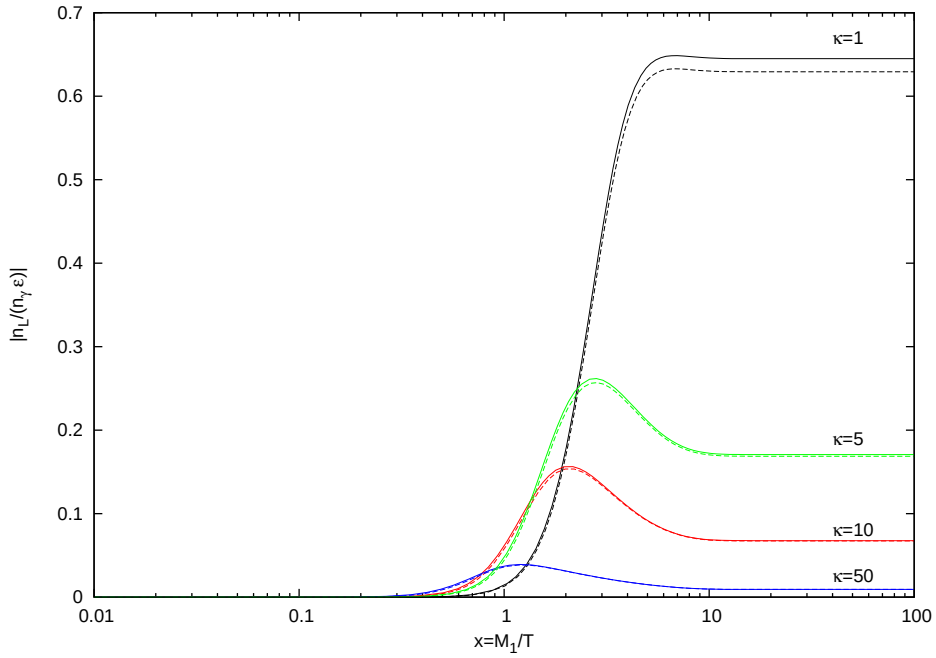

Figure 1.5: Efficiency of leptogenesis for various κ with (dashed lines) and without (solid lines) contribution of the heavy neutrinos to the energy density taken into account. Initial number density of the heavy neutrinos coincides with the equilibrium one.

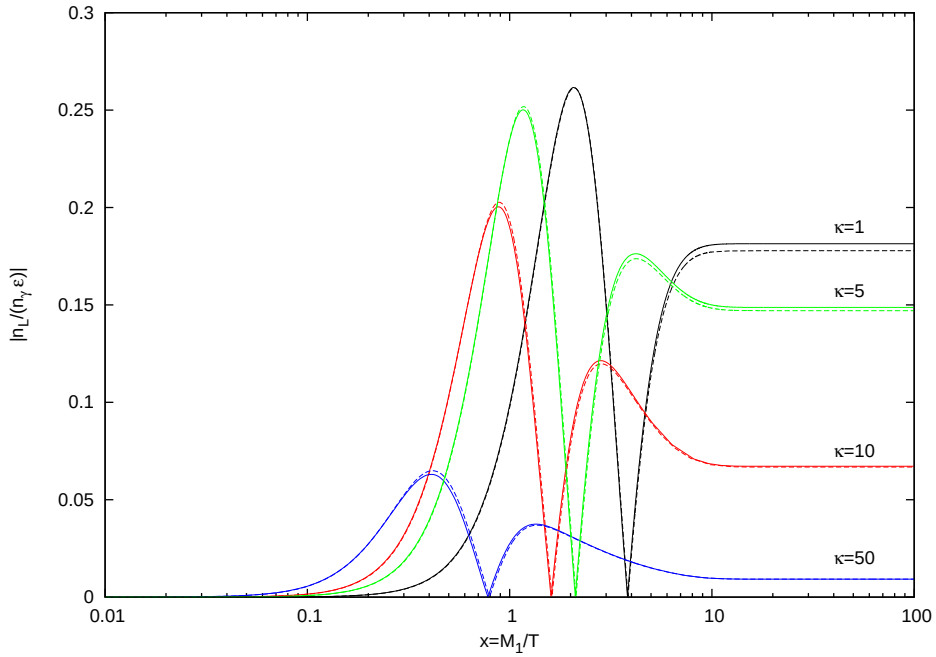

Figure 1.6: Efficiency of leptogenesis for various κ with (dashed lines) and without (solid lines) contributions of the heavy neutrinos to the energy density taken into account. Initial number density of the heavy neutrinos is taken to be zero.

neutrinos the change in the final asymmetry due to the deviation of $r_{\dot{x}}(x)$ from unity is negligibly small. On the contrary, the nontrivial dependence[9] of $r_g(x)$ on x results in a visible decrease of the final $\frac{n_L}{n_\gamma}$ ratio. The interpretation of this somewhat unexpected result is as follows. For all temperatures $r_g(x) \leqslant 1$ (see figure 1.4.b), and therefore the equilibrium particle number density in the comoving volume is always smaller than in the case of neglected contribution of the heavy neutrinos. Consequently, at a given x the same value of Y would correspond in the former case to a bigger degree of deviation from thermal equilibrium, which is characterized by the Y/Y^{eq} ratio. Since the washout processes tend to bring the system to equilibrium, the resulting $Y(x)$, as well as $Y(\infty)$, is smaller compared to the case of the neglected Majorana contributions.

Note, that absolute value of the lepton asymmetry in the two models is plotted in figure 1.5 as a function of the dimensionless inverse temperature x. Since contribution of the heavy neutrinos into the energy density changes the dependence of the temperature on time, the same x corresponds in the two models to two different values of time. Therefore, in order to compare the *time development* of the lepton asymmetry in the two models, one has to consider the inverse temperature as a function of time. As is clear from figure 1.5, already at moderate x the asymmetry reaches a constant asymptotic value, so that for comparison of *final* values of the asymmetry in the two models the time dependence of the inverse temperature is *irrelevant*.

One might argue, that the difference in the asymptotic value of the asymmetry in the cases with contribution of the Majorana neutrino to the energy density neglected and taken into account can be explained by the smaller initial value of $Y_\psi^0 = Y_\psi^{eq}$ in the latter case. It is therefore instructive to compute the asymmetry using the $Y_\Psi(x_0) = Y_L(x_0) = 0$ initial conditions. Population of the Majorana neutrinos is created in this case by the scattering and inverse decay processes. If the Yukawa interactions are weak (corresponds to small κ), they are unable to produce a thermal population of Majoranas, whereas if the Yukawa interactions are sufficiently strong (corresponds to large κ), the number of Majoranas almost reaches its equilibrium value. In the latter case the asymptotic value of the lepton asymmetry is expected to be independent of the initial conditions. The *CP* violating inverse decay processes produce an asymmetry, which obviously has a sign opposite to that in the decay. The lepton asymmetry generated by the decaying Majorana neutrinos compensates the asymmetry generated in the inverse decay at some point, so that $|Y_L|$ turns to zero and then starts to grow.

Results of a numerical analysis with the initial number of the Majoranas taken to be zero are presented in figure 1.6. Considerable smaller (compare, for instance, the solutions without contribution of the heavy neutrinos into the energy density taken into account) than in figure

[9] A multiplication of $r_g(x)$ by any constant factor corresponds to a redefinition of the scale factor normalization and leaves the $\frac{n_L}{n_\gamma}$ ratio unaltered.

1.5 value of the asymmetry for $\kappa = 1$ and $\kappa = 5$ is explained by the weakness of the Yukawa interactions, unable to produce a thermal population of the heavy Majoranas. Only for $\kappa = 10$ and $\kappa = 50$ the Yukawa interactions are sufficiently strong, and the asymptotic value of the asymmetry is the same as that in figure 1.5. For all the considered values of κ the asymmetry in the case of neglected Majorana contribution is bigger than with that taken into account (although for $\kappa = 10$ and $\kappa = 50$ the difference is hardly visible).

The above discussion can be summarized as follows. Consider two models of the early Universe. The first model is the FRW Universe with only the Standard Model species contributing to the energy density. The second model can be the homogeneous Universe with contributions of the Majorana neutrinos to the energy density taken into account or the inhomogeneous Universe considered in the next section. If (all other parameters and dependencies being equal) the ratio of $\dot{x}$ in the second model to that in the first one is bigger (smaller) than unity for all x, then the final lepton asymmetry in the second model is bigger (smaller) than in the first. Similarly, if (all other parameters and dependencies being equal) the ratio of $\sqrt{-g_3}$ in the second model to that in the first model is a monotonically growing (decaying) function, then the final lepton asymmetry in the second model is smaller (bigger) than in the second one.

In order to better understand the numerical results above it is instructive to obtain the analytical solution of the Boltzmann equations, which is possible in some limiting cases. We will consider the case of $\kappa \gg 1$. One of the reasons for that is that in the case of large κ the asymptotic asymmetry is independent of the initial conditions. To simplify the analysis we neglect the contribution of the Higgs–mediated scattering processes. Furthermore, for moderately large κ the scattering processes mediated by the Majorana neutrinos are sub–dominant in comparison to the inverse decay processes and are neglected as well. Equations (1.42) then simplify to

$$\frac{\partial \Delta}{\partial x} = -\frac{\partial Y_\Psi^{eq}}{\partial x} - \kappa x \gamma_D \Delta, \tag{1.61a}$$

$$\frac{\partial Y_L}{\partial x} = \varepsilon \kappa x \gamma_D \Delta - \kappa x \gamma_L Y_L, \tag{1.61b}$$

where the following notation has been introduced:

$$\Delta \equiv Y_\Psi - Y_\Psi^{eq}, \quad Y_\Psi^{eq} = r_g(x)\frac{x^2}{\pi^2}K_2(x), \quad \gamma_D = \frac{1}{r_{\dot{x}}}\frac{K_1(x)}{K_2(x)}, \quad \gamma_L = \frac{c_{\ell h}}{4N}\frac{x^2}{r_{\dot{x}}}K_1(x). \tag{1.62}$$

The solution of the system (1.61) corresponding to the initial conditions $\Delta(0) = Y_L(0) = 0$ reads

$$\Delta(x) = -\int_0^x Y_\Psi^{eq'}(x') \exp\left[-\int_{x'}^x x'' \kappa \gamma_D(x'') dx''\right] dx' \tag{1.63a}$$

$$Y_L = \varepsilon\kappa \int_0^x x' \Delta(x') \gamma_D(x') \exp\left[-\int_{x'}^x x'' \kappa \gamma_L(x'') dx''\right] dx' \tag{1.63b}$$

(see [4]). In the $\kappa \gg 1$ regime $\Delta' \simeq 0$, and it then follows from (1.61a), that $\kappa x \gamma_D \Delta \approx -Y_\Psi^{eq'}$. Furthermore, at $x \gg 1$ we obtain $Y_\Psi^{eq'}(x) \approx -[r_g(x) - r_g'(x)]\sqrt{\frac{x^3}{2\pi^3}}\exp(-x)$. Substitution into

(1.63b) yields

$$Y_L \approx \varepsilon \int_0^x [r_g(x') - r_g'(x')] \sqrt{\frac{x'^3}{2\pi^3}} \exp\left[-x' - \int_{x'}^x x'' \kappa \gamma_L(x'') dx''\right] dx' \tag{1.64}$$

For $x \to \infty$ the integral for Y_L can be evaluated using the method of steepest descent. Dividing the asymptotic value of the lepton asymmetry by the parameter of *CP* violation and the photon number density in the comoving volume, $Y_\gamma = \frac{2}{\pi^2} r_g$, we obtain

$$\eta \equiv \frac{n_L}{\varepsilon n_\gamma} = \frac{Y_L(x)}{\varepsilon Y_\gamma(x)} \approx \frac{\pi}{2} \frac{r_g(x_f) - r_g'(x_f)}{r_g(x)} \sqrt{\frac{x_f^3}{-(x''\kappa\gamma_L)'|_{x_f}}} \exp\left[-x_f - \int_{x_f}^x \kappa x'' \gamma_L(x'') dx''\right] \tag{1.65}$$

where x_f is determined by $\kappa x_f \gamma_L(x_f) = 1$. Large κ imply large x_f. In this case, approximately,

$$\tilde{\kappa}(x_f) x_f^{5/2} \exp(-x_f) \approx 1, \quad \tilde{\kappa} \equiv \frac{c_{\ell h}}{4N} \frac{\kappa}{r_{\dot{x}}} \tag{1.66}$$

If the contribution of the Majorana neutrinos to the energy density is neglected, then $r_g = r_{\dot{x}} = 1$. Let us assume for a moment, that $r_{\dot{x}} = 1$, whereas r_g is a nontrivial function of x. As follows from equation (1.66) and the definition of γ_L, the value of x_f remains unchanged, and the only difference from the case $r_g = r_{\dot{x}} = 1$ is the overall factor $r_g(x_f) - r_g'(x_f)$. If r_g is a monotonically growing function and reaches unity as $x \to \infty$, then $r_g < 1$ and $r_g'(x) > 0$ for any x_f. Therefore their difference is smaller than unity, and the efficiency decreases. Conversely, if r_g is a monotonically decaying function and reaches unity as $x \to \infty$, then $r_g > 1$ and $r_g'(x) < 0$ for any x_f. Consequently, the difference is bigger than unity, and the efficiency increases.

A deviation of $r_{\dot{x}}$ from unity effectively modifies κ and leads to a shift of x_f. For moderately large κ, the solution of (1.66) is given by [4] $x_f \simeq 4.2(\ln\tilde{\kappa})^{0.6}$. A simple calculation shows, that in the $x_f \gg 1$ limit $-(x\kappa\gamma_L)'|_{x_f} \simeq 1 + \frac{r_{\dot{x}}'(x_f)}{r_{\dot{x}}(x_f)}$, and $\int_{x_f}^\infty x\kappa\gamma_L dx \simeq 1 - \frac{r_{\dot{x}}'(x_f)}{r_{\dot{x}}(x_f)}$. In this approximation, substitution of x_f into (1.65) yields

$$\eta \simeq \frac{N}{2c_{\ell h}} \frac{1}{\kappa(\ln\tilde{\kappa})^{0.6}} \cdot \frac{r_g(x_f) - r_g'(x_f)}{r_g(\infty)} \cdot \frac{r_{\dot{x}}(x_f)}{\sqrt{1 + \frac{r_{\dot{x}}'(x_f)}{r_{\dot{x}}(x_f)}}} \exp\left(\frac{r_{\dot{x}}'(x_f)}{r_{\dot{x}}(x_f)}\right) \tag{1.67}$$

It is clear from (1.67), that the account of the nonzero chemical potential of the Higgs reduces the efficiency, and that the asymmetry is (approximately) inversely proportional to κ.

The numerical analysis shows (see figure 1.4), that for $x_f \gg 1$ the contribution of the terms proportional to $r_{\dot{x}}'(x_f)$ is small in comparison to the contribution of the terms proportional to $r_{\dot{x}}(x_f)$ and can be neglected. Since the deviation of $r_{\dot{x}}$ from unity is small, and $(\ln\tilde{\kappa})^{0.6}$ is a slowly varying function of $\tilde{\kappa}$, to a good approximation the ratio of the efficiency in the model with $r_g, r_{\dot{x}} \neq 0$ to that in the model with $r_g = r_{\dot{x}} = 1$ (and the same κ) is given by

$$r_\eta \simeq \frac{r_g(x_f) - r_g'(x_f)}{r_g(\infty)} \cdot \frac{r_{\dot{x}}(x_f)}{\sqrt{1 + \frac{r_{\dot{x}}'(x_f)}{r_{\dot{x}}(x_f)}}} \exp\left(\frac{r_{\dot{x}}'(x_f)}{r_{\dot{x}}(x_f)}\right) \overset{x_f \gg 1}{\simeq} \frac{r_g(x_f) - r_g'(x_f)}{r_g(\infty)} \cdot r_{\dot{x}}(x_f) \tag{1.68}$$

In the model with the contribution of the heavy neutrinos to the energy density taken into account r_g is a monotonically growing function, which asymptotically reaches unity, and $r_{\dot{x}} < 1$ at large x. Consequently, both of the factors in (1.68) are smaller than unity, and the efficiency is smaller than in the model with neglected contribution of the heavy neutrinos.

It may seem at first sight, that the ratio of the efficiencies is independent of κ. However, as follows from (1.66), an increase of κ leads to an increase of x_f. As both r_g and $r_{\dot{x}}$ asymptotically approach unity as $x \to \infty$ (see figure 1.4), the ratio (1.68) also tends to unity. This conclusion is in perfect agreement with the results of numerical analysis, see figure 1.5.

1.5 Leptogenesis in nonuniform Universe

As is commonly accepted at present, small (of order of 10^{-5} – 10^{-4}) primeval inhomogeneities of the energy density induced by quantum fluctuations in the inflaton field have been created during inflation – a period of accelerated expansion of the Universe [2, 3].

The Hubble radius $R_H \equiv H^{-1}$ gives the typical size of causally connected regions of space. A perturbation whose wavelength surpasses the Hubble radius is not affected by microscopic physics. Since the Hubble parameter H is constant during inflation, all cosmologically interesting scales begin sub–horizon sized, cross outside the Hubble radius during inflation, and later again cross back inside the horizon. Larger scales cross the horizon first and reenter last. The Hubble radius at temperature $T = M_1$ is given by

$$R_{H_L} \equiv H^{-1}(M_1) \simeq \left(\frac{45}{4\pi^3 g_\rho}\right)^{\frac{1}{2}} \frac{M_{Pl}}{M_1^2} \sim 10^{-32} \text{ pc} \tag{1.69}$$

where we have set $M_1 = 10^9$ GeV for definiteness. Scales of size $\lambda \gg R_{H_L}$ reenter the horizon only after the generation of lepton asymmetry is over and are therefore "frozen" during inflation. Had the perturbations of a sub–horizon scale $\lambda < R_{H_L}$ not become non–linear, at present they would have the size

$$\lambda_{pres} \lesssim \frac{R(t_{pres})}{R(t_{lept})} R_{H_L} \tag{1.70}$$

In the radiation dominated Universe $R \propto T^{-1}$. Since the transition between radiation domination and matter domination at $T_{trans} \approx 3 \times 10^4$ K the cosmic scale factor R has grown by slightly more than a factor of ten thousand [4]. Consequently, the ratio of the scale factors at present to that at the time of leptogenesis is of the order of 10^{21}. Therefore, had the perturbations which were of sub–horizon size during leptogenesis not become non–linear, at present they would have size $\lambda_{pres} \lesssim 10^{-11}$ pc. Non–linear effects would make this number even smaller. This is many orders of magnitude smaller than the typical galaxy size ~ 30 kpc. In other words, all perturbations of physically interesting scale were of superhorizon size and "frozen" during the period of leptogenesis.

Assuming a momentum–energy tensor of the form (1.46), one obtains the following set of Einstein equations for small perturbations of the metric [39]:

$$\ddot{h}_{kk} - 2H\dot{h}_{kk} - 2\dot{H}h_{kk} = 8\pi GR^2(\rho_1 + 3p_1), \tag{1.71a}$$

$$\frac{\partial}{\partial t}\left[R^{-2}\left(h_{kk,i} - h_{ki,k}\right)\right] = -16\pi GR^2(\rho + p)u_{1,i}, \tag{1.71b}$$

$$\begin{aligned} &h_{ij,kk} - h_{kj,ik} - h_{ki,jk} + h_{kk,ij} - R^2\ddot{h}_{ij} + R\dot{R}(\dot{h}_{ij} - \dot{h}_{kk}\delta_{ij}) + 2\dot{R}^2(h_{kk}\delta_{ij} - 2h_{ij}) \\ &= 8\pi GR^4(\rho_1 - p_1)\delta_{ij} - 8\pi GR^2(\rho - p)h_{ij}, \end{aligned} \tag{1.71c}$$

where ρ_1, p_1 and u_1 are the perturbations of energy density, pressure and the spatial components of the four–velocity respectively, and h_{ij} are the perturbations of the spatial components of the space–time metric.

To analyze the equations (1.71) we will follow the approach developed in [40]. Equation (1.71a) can easily be rewritten in terms of $h_L \equiv \sum_i h_{ii}/(2R^2)$:

$$\ddot{h}_L + 2H\dot{h}_L = 4\pi G\left(p_1 + \frac{\rho_1}{3}\right) \tag{1.72}$$

We will also need the trace of the equation (1.71c). Summing over $i = j$ and using the zero–order Einstein equations (1.47) we obtain

$$\ddot{h}_L + 6H\dot{h}_L - \frac{1}{3R^4}(h_{ii,kk} - h_{ik,ik}) = 4\pi G(p_1 - \rho_1) \tag{1.73}$$

Next we write the scalar mode of h_{ij} as a Fourier integral and split it into longitudinal and transverse parts:

$$h_{ij}(\tau, \vec{x}) = 2R^2(\tau)\int d^3q\, e^{i\vec{q}\vec{x}}\left[\delta_{ij}h_L(\tau, \vec{q}) - (\hat{q}_i\hat{q}_j - \delta_{ij}/3)h_T(\tau, \vec{q})\right], \quad \vec{q} = q\hat{q} \tag{1.74}$$

Note that h_L and h_T are used to denote longitudinal and transverse parts of the metric in both the real space and the Fourier space.

Equation (1.72) rewritten in terms of Fourier components obviously retains the form

$$\ddot{h}_L + 2H\dot{h}_L = 4\pi G\left(p_1 + \frac{\rho_1}{3}\right) \tag{1.75}$$

where p_1 and ρ_1 denote now Fourier components of pressure and energy density. Substitution of (1.74) into (1.73) yields

$$\ddot{h}_L + 6H\dot{h}_L + \frac{4}{3}\frac{q^2}{R^2}\left(h_L + \frac{h_T}{3}\right) = 4\pi G(p_1 - \rho_1) \tag{1.76}$$

Considering equation (1.71c) with $i \neq j$ we obtain

$$\ddot{h}_T + 3H\dot{h}_T = \frac{q^2}{R^2}\left(h_L + \frac{h_T}{3}\right) \tag{1.77}$$

As can easily be verified by direct substitution, the solution of the system of equations (1.75), (1.76) and (1.77) in the radiation dominated Universe is given by [40]

$$\delta \equiv \frac{\rho_1}{\rho} = \alpha\left(\frac{2C_1}{y^2} + \frac{y^2}{4} - \frac{y^4}{36} + \cdots\right) + \beta\left(\frac{2C_2}{y^2} - \frac{y}{3} + \frac{y^3}{10} + \cdots\right) \tag{1.78a}$$

$$h_L = \alpha\left(\frac{C_1}{2y^2} - \frac{C_1}{2}\ln y + \frac{y^2}{16} - \frac{y^4}{576} + \cdots\right) + \beta\left(\frac{C_2}{2y^2} - \frac{C_2}{2}\ln y - \frac{y}{3} + \frac{y^3}{90} + \cdots\right) \tag{1.78b}$$

$$h_T = 3\alpha\left(\frac{C_1}{2}\ln y - \frac{1}{4} - \frac{y^2}{24} + \frac{y^4}{960} + \ldots\right) + 3\beta\left(\frac{C_2}{2}\ln y + \frac{1}{2y} + \frac{y}{4} - \frac{y^3}{144} + \cdots\right) \tag{1.78c}$$

$$\theta \equiv \frac{i\vec{q}\,\vec{u}_1}{H} = \alpha\left(-\frac{3}{2}C_1 + \frac{y^4}{16} + \cdots\right) + \beta\left(-\frac{3}{2}C_2 - \frac{3y}{4} - \frac{y^3}{8} + \cdots\right) \tag{1.78d}$$

where $y = q\sqrt{\tau}/\sqrt{3}$. The coefficients C_1 and C_2 are constants of integration representing the residual gauge freedom and are removed by the conventional choice $C_1 = C_2 = 0$. Let us discuss this point in more detail. If $C_1, C_2 \neq 0$ then in the limit $q \to 0$ the leading terms in (1.78) are those proportional to a linear combination $C \equiv \alpha C_1 + \beta C_2$ of C_1 and C_2, irrespective of the value of τ.

$$\frac{\rho_1}{\rho_0} = \frac{2C}{y^2}, \quad h_L = \frac{C}{2y^2}, \quad h_T = \frac{3C}{2}\ln y \tag{1.79}$$

Upon substitution into (1.76) we see, that the right–hand side and the first two terms on the left–hand side of (1.76) increase with decrease of q, whereas the third term remains constant. Consequently in the limit $q \to 0$ this term can be neglected and equation (1.76) takes the form[10]

$$\ddot{h}_L + 6H\dot{h}_L = 4\pi G(p_1 - \rho_1) \tag{1.80}$$

Equations (1.75) and (1.80) are precisely the two equations, which one obtains by introducing a perturbation of the FRW metric $R^2(\tau) \to R^2(\tau)(1 - 2h_L(\tau))$ and substituting it into equations (1.47). In the FRW Universe the metric of space–time is characterized by a single quantity – the scale factor, which depends only on time and is independent of the spatial coordinates. Its explicit time dependence is determined by the form of the momentum–energy tensor. Obviously, the scale factor $R^2(\tau)(1 - 2h_L(\tau))$ still corresponds to a homogeneous Universe, but with the momentum–energy tensor different from the one determining $R^2(\tau)$. For instance, one could have used equations (1.75) and (1.80), to treat contribution of the Majorana neutrinos to the energy density, considered in the previous section. We thus conclude, that the spurious solutions proportional to C_1 and C_2 describe the dynamics of the *homogeneous background*, not the dynamics of the scalar perturbations, and should be removed by setting C_1 and C_2 to zero.

It also instructive to compare the solutions (1.78) with those in the longitudinal gauge [41]. According to [33], the solutions of the Einstein equations for small perturbations in the longitu-

[10] Equivalently, after averaging over the volume of a large scale inhomogeneity, the third term on the left–hand side of (1.73) is smaller than the first two terms.

dinal gauge are related to those in the synchronous gauge by

$$\phi = \frac{1}{2q^2}\left(h^{''} + 6\eta^{''} + \frac{R^{'}}{R}[h^{'} + 6\eta^{'}]\right), \quad \psi = \eta - \frac{1}{2q^2}\frac{R^{'}}{R}(h^{'} + 6\eta^{'}) \tag{1.81}$$

where a prime stands for differentiation with respect to conformal time. Switching to proper time and using the relations $h = -6h_L$, $6\eta = 2h_T + 6h_L$, which follow from the decomposition (1.74) and comparison with the corresponding expressions in [33], we obtain

$$\phi = \frac{R^2}{q^2}\left(\ddot{h}_T + 2H\dot{h}_T\right), \quad \psi = \frac{1}{3}(h_T + 3h_L) - \frac{R^2}{q^2}\dot{h}_T \tag{1.82}$$

It is trivial to check that the terms proportional to C in (1.78) do not contribute to ϕ and ψ, which confirms that these are spurious solutions. Substituting terms proportional to α and β, we obtain for ϕ and ψ

$$\psi = \phi = -\frac{\alpha}{6} + \frac{\beta}{2}\left(\frac{\sqrt{3}}{2q\tau^{\frac{1}{2}}} + \frac{3\sqrt{3}}{q^3\tau^{\frac{3}{2}}}\right) = -\frac{\alpha}{6} + \frac{\beta}{2}\left(\frac{1}{2y} + \frac{1}{y^3}\right) \tag{1.83}$$

The solution for $\delta = \frac{\rho_1}{\rho_0}$ is related to that in the synchronous gauge by [33]

$$\delta_{long} = \delta_{syn} + \alpha\frac{\rho_0^{'}}{\rho_0}, \quad \alpha = \frac{h^{'} + 6\eta^{'}}{2q^2} \tag{1.84}$$

Expressed in terms of h_L and h_T, this transformation takes the form

$$\delta_{long} = \delta_{syn} + \frac{R^2}{q^2}\dot{h}_T\frac{\dot{\rho}_0}{\rho_0} \tag{1.85}$$

Using the zero–order solution $\rho = 3/(32\pi G\tau^2)$, the solutions (1.78) and neglecting terms proportional to q and q^2, we obtain

$$\delta_{long} = \frac{\alpha}{3} + \beta\left(-\frac{\sqrt{3}}{q\tau^{\frac{1}{2}}} + \frac{6\sqrt{3}}{q^3\tau^{\frac{3}{2}}}\right) = \frac{\alpha}{3} + \beta\left(-\frac{1}{y} + \frac{2}{y^3}\right) \tag{1.86}$$

It is straightforward to check, that the solutions (1.83) and (1.86) are the leading terms of the expansion of the solutions obtained in [41], (1.87) and (1.88), in the vicinity of $y = 0$.

$$\phi = \frac{1}{2y^2}\left[-\alpha\left(\frac{\sin y}{y} - \cos y\right) + \beta\left(\frac{\cos y}{y} + \sin y\right)\right] \tag{1.87}$$

$$\delta = -\alpha\left[\left(\frac{2-y^2}{y^2}\right)\left(\frac{\sin y}{y} - \cos y\right) - \frac{\sin y}{y}\right] + 2\beta\left[\left(\frac{1-y^2}{y^2}\right)\left(\frac{\cos y}{y} + \sin y\right) + \frac{\sin y}{2}\right] \tag{1.88}$$

Our goal is to compare the efficiency of leptogenesis in the inhomogeneous Universe to that in the homogeneous background. As has been argued in section 1.3, under certain assumptions the system of Boltzmann equations in the inhomogeneous Universe (1.42) has to a first approximation the same form as in the uniform Universe. The difference from the homogeneous case arises through a different than in the uniform Universe dependence of $\dot{x}$ and $\sqrt{-g_3}$ functions on the

dimensionless inverse temperature $x = \frac{M_1}{T}$, or, alternatively, through a nontrivial dependence of the $r_{\dot{x}}$ and r_g on x. Note, that in the inhomogeneous Universe the temperature T is related to the background temperature T_0 by $T = T_0(1 + \Theta)$, where Θ is small.

The generalization of the momentum–energy tensor of a relativistic gas to the case of a perturbed space–time metric is given by [33]

$$T^{\mu}_{\nu} = \int dP_1 dP_2 dP_3 (-g)^{-\frac{1}{2}} \frac{P^{\mu} P_{\nu}}{P^0} f(x^i, P_j, \tau) \tag{1.89}$$

where g is the determinant of the space–time metric. In the synchronous gauge it coincides with the determinant of the spatial components of the metric $\sqrt{-g_3}$. The invariant integration measure can be expressed in terms of the physical momentum and solid angle, $dP_1 dP_2 dP_3 (-g)^{-\frac{1}{2}} = p^2\, dp\, d\Omega$. In the synchronous gauge $P^0 = P_0 = E$. Furthermore, as has already been mentioned, we neglect possible modifications of the phase space distribution functions induced by the gravitational field. In this approximation the energy density $\rho = T^0_0$ does not contain contributions from the gravitational field. A direct calculation shows, that in the absence of a preferred direction the leading contribution to the change of the gas energy density due to a small nonzero macroscopic velocity $\vec{u}_1$ is proportional to $\vec{u}_1^{\,2}$, i.e. is of second order, and can be neglected. Thus, to a first approximation the energy density of a relativistic gas in the nonuniform Universe is proportional to T^4. Consequently, there is a simple relation between perturbations of the energy density and the temperature, namely $\delta = 4\Theta$.

The determinant of the spatial components of the perturbed space–time metric is given by $\sqrt{-g_3} = R^3(1 - 3h_L)$. Note that the left–hand side of this expression corresponds to the temperature T, whereas R^3 on the right–hand side is calculated at T_0. Taking into account that in the homogeneous Universe $R^3 = T_0^{-3}$ and using the definition $r_g = T^3\sqrt{-g_3}$ we obtain

$$r_g = (1 + \Theta)^3(1 - 3h_L) \approx 1 + 3\Theta - 3h_L \tag{1.90}$$

The second quantity we are interested in is the time derivative of x. Taking into account that in the region of perturbation $x = x_0(1 + \Theta)^{-1}$, where x_0 is the background value of x, and that the Hubble parameter in the FRW Universe is given by $H = \dot{x}_0 x_0^{-1}$, we obtain

$$\dot{x} = \frac{\dot{x}_0}{1 + \Theta}\left(1 - \frac{1}{H}\frac{\dot{\Theta}}{1 + \Theta}\right), \tag{1.91}$$

where $\dot{x}_0$ is calculated in the homogeneous Universe at temperature T_0. Taking additionally into account that $\dot{x}_0(x) \propto x^{-1}$, we find for $r_{\dot{x}}$

$$r_{\dot{x}} \equiv \frac{\dot{x}(x)}{\dot{x}_0(x)} = \frac{1}{(1 + \Theta)^2}\left(1 - \frac{1}{H}\frac{\dot{\Theta}}{1 + \Theta}\right) \approx 1 - 2\Theta - \dot{\Theta}H^{-1} \tag{1.92}$$

Let us return to the spurious solutions of the Einstein equations at this point. From equations (1.79) it follows that $h_L = \frac{\delta}{4} = \Theta$, so that $r_g = 1$. Using the relation $\dot{\Theta} = \dot{y}\Theta'_y = Hy\Theta'_y$ we

obtain from (1.79) $\dot{\Theta} = -2H\Theta$, which yields $r_{\dot{x}} = 1$ just like in the homogeneous case (recall, that we negelect the contribution of the right–handed neutrinos to the energy density in this section). This analysis supports the assertion, that the spurious solutions describe the dynamics of the homogeneous background. It also demonstrates, that relating h_L to δ by comparison of coefficients of individual terms in the expansions is a reliable method.

At large y (i.e. for the late times or relatively small wavelengths) the leading terms in (1.78a) and (1.78b) are those quadratic in y, so that $h_L = \frac{\delta}{4} = \Theta$ and $\dot{\Theta} = 2H\Theta$ and we obtain

$$r_g = 1, \quad r_{\dot{x}} = 1 - 4\Theta \tag{1.93}$$

As follows from equation (1.68), in this case the efficiency of leptogenesis is smaller than in the homogeneous background.

However, at $T \sim M_1$ all physically relevant scales are of superhorizon size and have large wavelengths, i.e. correspond to very small q and y. At very small y, the leading terms in (1.78a) and (1.78b) are those linear in y, so that $h_L = \delta = 4\Theta$ and $\dot{\Theta} = H\Theta$ and we obtain

$$r_g = 1 - 9\Theta, \quad r_{\dot{x}} = 1 - 3\Theta \tag{1.94}$$

We are interested only in the perturbations growing with time, in which case Θ is positive and increases with time. In the radiation dominated Universe $\sqrt{\tau} \propto T^{-1} \propto x$, and we conclude that $\Theta \propto y = \alpha x$, where α is a small positive number. Since Θ is positive, $r_{\dot{x}}$ is smaller than unity, which tends to decrease the efficiency. On the other hand, since Θ increases with time, r_g is a decaying function of x, which tends to increase the efficiency.

For very large scale perturbations, to which we limit ourselves here, the terms proportional to y^2 in (1.78) start to dominate over those proportional to y at a very late time, i.e. at a very large value of the inverse temperature $x_b \gg x_f$, where x_f is the inverse temperature of the freeze–out (introduced in section 1.4) . Substituting $r_g = 1 - 9\alpha x$ and $r_{\dot{x}} = 1 - 3\alpha x$ to (1.68) we obtain for the ratios of the efficiencies at the inverse temperature $x \sim x_b$

$$r_\eta(x_b) \approx 1 + 3\alpha(2.5 + 3x_b - 4x_f) \tag{1.95}$$

Provided that $x_b \gg x_f$, the ratio (1.95) is bigger than unity. We, thus, conclude, that the efficiency of leptogenesis *increases* in the regions of higher energy density, as one would expect. Numerical solutions of the Boltzmann equations (1.42) with r_g and $r_{\dot{x}}$ given by (1.94) reproduce this result for all the considered κ. By the time x reaches x_b all the washout processes are frozen and the baryon minus lepton number is effectively conserved, so that the further development of the Universe, which is described by (1.93), does not influence this value.

Finally, let us note, that the lepton asymmetry in the physical volume, which is proportional to the product of the efficiency and the photon number density, is also bigger than in the uniform Universe, because the photon number density is bigger in the regions of higher energy density.

1.6 Baryon number violation

The nontrivial vacuum structure of non–Abelian gauge theories [7, 8, 42, 43] leads in the $SU_L(2)$ theory to an anomalous non–conservation of baryon and lepton numbers. The vacuum is usually regarded as a classical field configuration corresponding to a minimum of potential energy. It is common to choose only one (trivial) configuration to represent the vacuum state. The trivial solution of the Yang–Mills equations is given (in the $A_0 = 0$ gauge) by $\vec{A} = 0$. A Yang–Mills field configuration phase space can be divided into gauge–equivalent subspaces, which can be transformed one into another by a continuous gauge transformation. There are infinitely many field configuration, which are gauge equivalent to the trivial one

$$\vec{A}\,(\vec{x}) = g^{-1}(\vec{x})\nabla g(\vec{x}) \tag{1.96}$$

where g is the unitary matrix of gauge transformations. If $g(\vec{x})$ can be joined to the identity through a one–parameter continuous family of transformations

$$g(\vec{x}, 1) = g(\vec{x}); \quad g(\vec{x}, 0) = I \tag{1.97}$$

then these vacuum configurations are also topologically equivalent to the trivial one. However, not all of the gauge equivalent subspaces are also topologically equivalent — in Yang–Mills theories there is a countable infinity of classical vacuum configurations which have different topologies. The topologically inequivalent vacua are separated by a *finite* potential barrier.

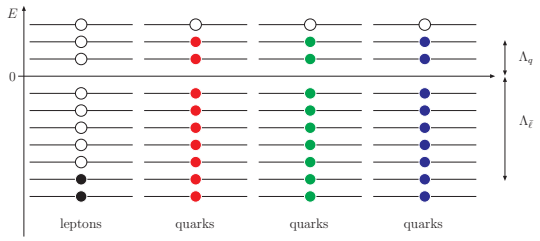

Figure 1.7: Illustration to the conversion of lepton asymmetry into baryon asymmetry.

Consequently, there is a finite amplitude for tunneling between topologically inequivalent vacua. In the course of a transition from one vacuum to a topologically inequivalent one, a fermion energy level is shifted upwards (downwards) and takes the position of its predecessor. In other words, new (anti)quarks and (anti)leptons are created out of the vacuum. Since all the left–handed Standard Model fermions have the same $SU_L(2)$ properties, a single transition leads to a creation of two left–handed leptons (an electron and a neutrino) and six left–handed quarks (up and down quarks of three colors) of each generation[11]. Since the baryon number of a quark

[11] Similar processes also take place in the $SU_C(3)$ theory. However, since the couplings of the gluons to quarks are vectorlike, the change of baryon number carried by left–handed quarks is exactly compensated by the change of baryon number carried by right–handed quarks.

is one third, whereas the lepton number of a lepton is unity, the difference $B - L$ is conserved.

At low temperatures the tunneling probability is exponentially small. At temperatures where the leptogenesis takes place, however, the electroweak symmetry is unbroken, and the exponential suppression of the baryon number non–conserving transitions, called sphaleron transitions [44], disappears. The power–counting estimate of the rate per unit time and unit volume in the unbroken phase is then [45, 46]

$$\Gamma_{sp} = \text{const} \cdot (\alpha_W T)^4. \tag{1.98}$$

The rate of the sphaleron transitions exceeds the expansion rate of the Universe in the standard Big–Bang scenario in the following interval of temperatures:

$$10^2 \text{ GeV} \leq T \leq 10^{12} \text{ GeV}. \tag{1.99}$$

In other words, the lepton asymmetry generated in the decay of the heavy neutrinos is instantly converted into the baryon asymmetry.

For a species in thermal equilibrium the excess of particles over antiparticles, i.e. the asymmetry, is parametrized in terms of its chemical potential. As the $SU_L(2)$ symmetry is unbroken at the stage under consideration, chemical potentials of upper and lower components of leptonic doublets, denoted by μ_i and μ_{i_L} respectively, are equal. This implies, that the chemical potentials of the W bosons are zero. The chemical potential of the B^0 gauge boson is zero because it is neutral. Note, that in the absence of rapid flavor–mixing interactions in the leptonic sector the chemical potentials of leptons of different generations are, generally speaking, not equal.

The unbroken $SU_L(2)$ symmetry also implies, that chemical potentials of top and bottom components of quark doublets, denoted by μ_{u_L} and μ_{d_L} respectively, are equal. Moreover, since the $SU_C(3)$ symmetry is exact at any temperature, the chemical potentials of the components of color triplets are equal as well. This implies in particular, that the chemical potential of the gluon fields is zero. In addition, rapid flavor–changing interactions assure that the chemical potentials of quarks of a given charge and chirality are the same, so that only three chemical potentials should be introduced: $\mu_{uL} = \mu_{dL}$ for left–handed and μ_{uR} and μ_{dR} for right–handed quarks of a given color.

Supersymmetric, as well as GUT, extensions of the Standard Model, one of which will be discussed in chapter 2, may contain more than one Higgs doublet. It is assumed here, that mixing between the Higgs doublets assures equality of their chemical potentials: μ_- for all charged scalars and μ_0 for the neutral ones.

The free–energy $\mathcal{F}$ of the left–handed fermions is expressed in terms of their chemical potentials and the temperature as

$$\mathcal{F} = 2 \sum_{i=1..3} \mathcal{F}(\mu_i) + 6N\mathcal{F}(\mu_{uL}) \propto 2T^2 \sum_{i=1..3} \mu_i^2 + 6T^2 N \mu_{uL}^2 \ , \tag{1.100}$$

Baryon and lepton number densities are obtained by differentiating the free energy with respect to μ_i and μ_{uL}:

$$L_L = \sum_i \frac{\partial \mathcal{F}}{\partial \mu_i} \propto 4T^2\mu, \quad B_L = \frac{1}{3}\frac{\partial \mathcal{F}}{\partial \mu_{uL}} \propto 4T^2 N \mu_{uL}, \tag{1.101}$$

where $\mu \equiv \sum_i \mu_i$ has been introduced. From the fact that the sphalerons conserve baryon minus lepton quantum number separately for each generation [26] it follows, that $d\mu_i = d\mu_{uL}$. Minimization of the free energy yields

$$\frac{d\mathcal{F}}{d\mu_{uL}} \propto 4T^2(3N\mu_{uL} + \mu) \propto 3B_L + L_L = 0 \tag{1.102}$$

In other words, if sphaleron processes are in equilibrium, the sum of the lepton and thrice the baryon number carried by the left–handed fermions is zero.

To illustrate this conclusion let us assume that the initial baryon number is zero and the total lepton number is negative. Number and energy densities of leptons and quarks read

$$n_{\bar{\ell}} \propto \Lambda_{\bar{\ell}}^3, \quad n_q \propto 3\Lambda_q^3, \quad E_{\bar{\ell}} \propto \Lambda_{\bar{\ell}}^4, \quad E_q \propto 3\Lambda_q^4, \tag{1.103}$$

where Λ_q ($\Lambda_{\bar{\ell}}$) is the energy of the highest filled (lowest unfilled) quark (lepton) level.

In the course of sphaleron transitions empty negative lepton levels and filled negative quark levels cross the zero energy level from below, so that the number of antileptons is decreased, whereas the number of baryons is increased (see figure 1.7). While both $\Lambda_{\bar{\ell}}$ and Λ_q change, the sum $\Lambda_{\bar{\ell}} + \Lambda_q$ remains constant, so that

$$\frac{dE}{d\Lambda_q} \propto 3\Lambda_q^3 - \Lambda_{\bar{\ell}}^3 \propto n_q - n_{\bar{\ell}} \propto 3B_L + L_L = 0. \tag{1.104}$$

The energy density of the system reaches its minimum when the total number of antileptons is equal to the *total* number of quarks, i.e. the baryon number is equal to minus one third of the lepton number.

Relation (1.102) can also be obtained using the fact, that for equilibrium reactions the sum of chemical potentials of the incoming particles is equal to that of the outgoing ones. The sphaleron processes correspond to the creation of $(u_{iL}d_{iL}e_{iL}\nu_{iL})$ states [26] out of the vacuum. Therefore, as long as the sphaleron processes are in thermal equilibrium, the following relation among the chemical potentials is enforced:

$$3N(\mu_{uL} + \mu_{dL}) + \sum_{i=1..3} (\mu_{iL} + \mu_i) = 0, \tag{1.105}$$

where the factor of three is due to the three color degrees of freedom, while the summation over generations takes into account that fermions of all the generations are created simultaneously. Taking into account that $\mu_{u_L} = \mu_{d_L}$ and $\mu_i = \mu_{i_L}$ we arrive again at equation (1.102).

The electroweak interactions, which are in thermal equilibrium down to about $T_{dec} \simeq 2$ MeV, imply additional relations between the chemical potentials [47]:

$$\mu_W = \mu_- + \mu_0 \quad (W^- \leftrightarrow H^- + H^0) \tag{1.106a}$$

$$\mu_{dL} = \mu_{uL} + \mu_W \quad (W^- \leftrightarrow \bar{u}_L + d_L) \tag{1.106b}$$

$$\mu_{iL} = \mu_i + \mu_W \quad (W^- \leftrightarrow \bar{\nu}_{iL} + e_{iL}) \tag{1.106c}$$

$$\mu_{uR} = \mu_{uL} + \mu_0 \quad (H^0 \leftrightarrow \bar{u}_L + u_R) \tag{1.106d}$$

$$\mu_{dR} = \mu_{uL} + \mu_W - \mu_0 \quad (H^0 \leftrightarrow d_L + \bar{d}_R) \tag{1.106e}$$

$$\mu_{iR} = \mu_i + \mu_W - \mu_0 \quad (H^0 \leftrightarrow e_{iL} + \bar{e}_{iR}) \tag{1.106f}$$

Assuming a thermal distribution, the number density of fermions (bosons) is given by the Fermi–Dirac (Bose–Einstein) distribution

$$n_\pm = \int \frac{\mathrm{d}\mathbf{p}}{(2\pi)^3} \frac{g}{\exp[(E_\mathbf{p} \mp \mu)/T] \pm 1}, \tag{1.107}$$

where μ is the particle chemical potential and g is the number of internal degrees of freedom ($g = 1$ for massless Weyl fermions and $g = 2$ for massless vector bosons). Assuming that ratio of the chemical potential to the temperature is small and neglecting the particle mass we find for the excess of particles over antiparticles

$$n_+ - n_- = \frac{gT^3}{6}\frac{\mu}{T} \ \text{(fermions)}, \quad n_+ - n_- = \frac{gT^3}{3}\frac{\mu}{T} \ \text{(bosons)}. \tag{1.108}$$

Relations (1.106) and (1.108) make it possible to express the baryon and the lepton numbers, as well as total electric charge, in terms of just three chemical potentials. Omitting a common overall coefficient we find

$$B = N(\mu_{uL} + \mu_{uR}) + N(\mu_{dL} + \mu_{dR}) = 4N\mu_{uL} \tag{1.109a}$$

$$L = \sum_{i=1..3} (\mu_i + \mu_{iL} + \mu_{iR}) = 3\mu - N\mu_0 \tag{1.109b}$$

$$Q = 2N\mu_{u_L} - 2\mu + (4N + 2n)\mu_0 \tag{1.109c}$$

where n is the number of Higgs doublets in the model. The requirement that the total electric charge must be zero implies an additional relation between the chemical potentials.

From equations (1.109) it follows, that nonzero chemical potential of the leptons μ induces nonzero chemical potentials of quarks and the Higgs. As has been argued in section 1.3, the fact that all matter fields carry a fraction of the asymmetry leads to a modification of the coefficients of individual terms in the Boltzmann equations. For practical applications we need the chemical potentials of quarks and the Higgs expressed in terms of the chemical potential of the leptons. Assuming for simplicity that chemical potentials of leptons of different generations are equal,

$\mu_L \equiv \mu_{iL} = \mu_i$, and using relations (1.106) and (1.109a), we obtain in the case of the Standard Model

$$\mu_Q \equiv \mu_{dL} = \mu_{uL} = -\frac{\mu_\ell}{3} \equiv c_Q \mu_L \tag{1.110a}$$

$$\mu_H \equiv \mu_0 = -\mu_- = \frac{4}{3}\frac{N\mu_\ell}{2N+1} = \frac{4\mu_\ell}{7} \equiv c_H \mu_L \tag{1.110b}$$

$$\mu_u \equiv \mu_{uR} = \frac{2N-1}{2N+1}\frac{\mu_\ell}{3} = \frac{5\mu_\ell}{21} \equiv c_u \mu_L \tag{1.110c}$$

$$\mu_d \equiv \mu_{dR} = -\frac{6N+1}{2N+1}\frac{\mu_\ell}{3} = -\frac{19\mu_\ell}{21} \equiv c_d \mu_L \tag{1.110d}$$

$$\mu_e \equiv \mu_{iR} = \frac{2N+3}{2N+1}\frac{\mu_\ell}{3} = \frac{3\mu_\ell}{7} \equiv c_e \mu_L \tag{1.110e}$$

We are now in a position to relate the baryon and lepton numbers to $B-L$, which is conserved by the Standard Model processes. Making use of (1.109) we obtain [47, 48]

$$B = \frac{8N+4n}{22N+13n}(B-L) \approx 0.35\,(B-L), \tag{1.111a}$$

$$L = -\frac{14N+9n}{22N+13n}(B-L) \approx -0.65\,(B-L), \tag{1.111b}$$

where for the numerical evaluation we have used $n = 1$.

If the baryon number violating process were frozen at the epoch of leptogenesis, the lepton asymmetry generated in the *CP*–violating decay of the heavy neutrino would coincide (up to a sign) with $B - L$. However, since the lepton asymmetry is instantly converted into the baryon asymmetry, this equality does not hold. Consequently, what we need is not the relation between B and $B - L$, but a relation between B and L, which reads

$$B = -\frac{8N+4n}{14N+9n}\,L \approx -0.54\,L \tag{1.112}$$

According to the estimates performed in section 1.4, for $M_1 = 10^9$ GeV, $\sqrt{3}\bar{m} = 5 \cdot 10^{-2}$ eV and $\tilde{m}_1 = 10^{-2}$ eV (corresponds to $\kappa = 10$) the efficiency of leptogenesis $|n_L/(n_\gamma \varepsilon)| = 6.7 \cdot 10^{-2}$. For the same values of the parameters the upper bound on the *CP* asymmetry is given by $|\varepsilon| \lesssim 10^{-7}$. Combining these estimates with (1.112) we obtain an upper bound on the baryon asymmetry of the Universe in the Standard Model supplemented by three heavy right–handed Majorana neutrinos

$$Y_B = \frac{n_B}{n_\gamma} \lesssim 3.6 \cdot 10^{-9} \tag{1.113}$$

which is consistent with the experimental value $Y_B = 6.5^{+0.4}_{-0.3} \cdot 10^{-10}$. The factor of five difference from the experimental value can accounted for by a smaller value of the *CP* asymmetry in the decay or by a bigger value of the effective neutrino mass, or by both of these factors.

1.7 Conclusions

In this chapter the generation of the lepton and baryon asymmetries in the nonuniform Universe has been investigated.

We have derived a simple and compact form of the Boltzmann equation suitable for computation of the lepton asymmetry in both the FRW and the inhomogeneous models of the Universe. Effects associated with a nonzero macroscopic gas velocity and particle flow have been shown to be of the second order and therefore negligible.

To understand how a modification of the Universe expansion rate and the scale factor dependencies on the temperature influences the generation of the lepton asymmetry we have considered leptogenesis in the Universe with contribution of the heavy Majorana neutrinos to the total energy density taken into account. It has turned out, that in this case the asymptotic value of the asymmetry is smaller than that in the case of the neglected Majorana contribution. We have also found, that if the ratio of time derivative of the dimensionless inverse temperature $x = M_1/T$ to that in the FRW Universe is bigger than unity, then the efficiency of leptogenesis increases and vice versa. Analogously, if the ratio of the determinant of spatial components of the space–time metric to that in the FRW Universe is a monotonically decaying function of x, the efficiency of leptogenesis increases and vice versa. These properties of the solutions are easily "read off" from the approximate analytical solution of the Boltzmann equations, which we have derived in the limit $\kappa \gg 1$. The computed theoretical upper bound on the baryon asymmetry of the Universe is consistent with the results of experimental observations.

These results have been applied to the analysis of leptogenesis in the nonuniform Universe in the synchronous gauge. We have related the perturbations of the space time–metric and the time derivative of the inverse temperature to perturbations of the temperature using the known solutions of the Einstein equations. It has been shown that for growing large scale perturbations, which constitute seeds of the future large scale structures, leptogenesis is more efficient than in the homogeneous background. Therefore, even before structure formation began shortly after the onset of the matter–dominated epoch, seeds of the future galaxies and other large scale structures contained a higher–than–average number of baryons and leptons.

Chapter 2

The superstring inspired E_6 model

The ultimate goal of modern physics is the formulation of a unified field theory, able to unite the two fundamental theories: quantum field theory and general relativity. At present, the most promising hope for a truly unified and finite description of these two fundamental theories is superstring theory and its latest formulation, M–theory [49, 50, 51, 52]. Superstrings possess by far the largest set of gauge symmetries ever found in physics. Superstring's symmetry includes not only the Einstein's theory of general relativity and the Yang–Mills theory, but also supergravity and the Grand Unified Theories as subsets.

The cancellation of anomalies places stringent constraints on which gauge groups may be allowed by the superstring theory [53]. It turns out, that the gauge group of a supersymmetric theory must contain exactly 496 generators, which restricts us to either $SO(32)$ or $E_8 \otimes E_8$ group. The latter one has received most attention as it leads to chiral fermions, similar to those in the SM, whereas $SO(32)$ does not. The ten–dimensional $E_8 \otimes E_8$ heterotic superstring theory compactifies to the $M_4 \otimes \Gamma$, where Γ is the Calabi–Yau manifold with $SU(3)$ holonomy, and yields a low–energy theory with $N = 1$ supersymmetry. If Γ is simply connected, then the $E_8 \otimes E_8$ gauge group breaks down to the $E_6 \otimes E_8$ subgroup

$$E_8 \otimes E_8 \supset SU(3) \otimes E_6 \otimes E_8.$$

The unbroken E_8 describes a "shadow world", which interacts with ordinary matter only gravitationally and which may, in principle, be responsible for the breaking of supersymmetry. For a multiply connected manifold Γ the initial gauge group breaks down to $G \otimes E_8$ where G is a subgroup of E_6 [54]. In this scheme, chiral superfields $N_f\mathbf{27} + \delta(\mathbf{27} + \bar{\mathbf{27}})$ (where for a wide class of models $\delta = 1$) and **78** vector superfields of E_6 emerge as the zero mode spectra. States in $\delta(\mathbf{27} + \bar{\mathbf{27}})$ are denoted here by χ and $\bar{\chi}$ respectively, whereas states in N_f **27** are denoted by ψ.

Apart from having its origins in the superstring $E_8 \otimes E_8$, the E_6 model also has several features relevant for low–energy phenomenology:

– the model allows chiral representations;

– its fundamental representation contains the fifteen known fermions along with a right–handed neutrino and two Higgs–like doublets;

– the model is automatically anomaly free.

In this chapter, I will present a detailed classification of states of the fundamental and adjoint representations of E_6 and its physically relevant subgroups using the Cartan–Weyl method, which is briefly reviewed in section 2.1.

The issue of possible charge assignments, i.e. the correspondence between the set of weights and physical states, is discussed in section 2.2. It is argued there, that the model allows six charge assignments compatible with the Standard Model. Charge conservation in the processes involving states of different generations requires that the same charge assignment be used for all generations.

Some of the fields in the adjoint representation may lead to a rapid proton decay. Constraints implied by the proton stability are discussed in section 2.3. In addition to the intermediate gauge groups listed in [55] the $SU(5)\otimes U(1)\otimes U(1)$ is allowed for two charge assignments. Nevertheless, the Yukawa interactions implied by the residual $SU(5)$ symmetry make the rapid proton decay, mediated by new bottom quarks, unavoidable unless if those are very heavy.

The dynamical breaking of $B-L$ symmetry is considered in section 2.4. An interesting feature of the model under consideration is the presence of additional $\delta(\mathbf{27}+\overline{\mathbf{27}})$ generations, which contain right–handed neutrinos. Scalar components of the right–handed neutrinos may be used now to break the $B-L$ symmetry spontaneously. The introduction of a simple discrete symmetry ensures, that $B-L$ is broken at a scale, which is sufficiently high for generating large masses for the right–handed neutrinos, and that the right–handed scalar neutrinos of the three known generations do not acquire a vacuum expectation value (VEV). The same symmetry also forbids Yukawa couplings which, if present, would induce large masses for the conventional neutrinos. The supersymmetric structure of the theory ensures, that large quantum corrections to masses of scalars, associated with the presence of heavy gauge fields, cancel out. After the $B-L$ breaking, the residual gauge group is $SU_C(3)\otimes SU_L(2)\otimes U(1)\otimes U(1)$.

Finally, in section 2.5 we derive an explicit form of the Lagrangian of the Yukawa interactions, expressed in terms of the component fields.

Since a motivation for this work has been the construction of a model for leptogenesis, the E_6 model will be used for computation of the lepton and baryon asymmetries. This is performed in chapter 3, where numerical estimates are also included. The difference of leptogenesis in the E_6 model from leptogenesis in the Standard Model arises mainly from its extended particle content.

2.1 The Cartan–Weyl method

The exceptional group E_6 has a rich spectrum of physically acceptable, i.e. those leading to the $SU_C(3) \otimes U_{em}(1)$ group, breaking chains [56]. The intermediate symmetry groups include those extensively discussed in the literature, for example the Pati–Salam group [57]. The breakdown to the Pati–Salam model can proceed, for instance, via $SO(10)$ [58]

$$E_6 \to SO(10) \otimes U(1) \to SU_C(4) \otimes SU_L(2) \otimes SU_R(2) \otimes U(1) \tag{2.1}$$

The $SO(10)$ model itself has also attracted a lot of attention, as it naturally contains the right–handed neutrino, whose existence is suggested by the results of neutrino oscillation experiments. If gauge symmetry is broken by the Higgs mechanism, then the intermediate $SO(10)$ can also be broken down to $SU(5)$, considered in [59], via

$$E_6 \to SO(10) \otimes U(1) \to SU(5) \otimes U(1) \otimes U(1) \tag{2.2}$$

where the $SU(5)$ contains the Standard Model gauge group. There is also an attractive possibility of breaking the E_6 to another of its maximal subgroups, a direct product of three $SU(3)$ groups, which further breaks down to the Standard Model gauge group supplemented by additional $U(1)$ or $SU(2)$ groups, thus implying the existence of at least one extra "low–energy" gauge boson [60]. For instance the breaking chain (2.3)

$$E_6 \to SU_C(3) \otimes SU_L(3) \otimes SU_R(3) \to SU_C(3) \otimes SU_L(2) \otimes U(1) \otimes U(1) \tag{2.3}$$

gives rise to a new neutral $Z^{'}$ boson, which is mixed with the Standard Model Z boson.

In order to determine which breaking chains are consistent with the long–lived proton and other low–energy constraints, we need to know the properties of the particle states under transformations of the intermediate symmetry groups, i.e. their quantum numbers with respect to these groups.

A systematic study of quantum numbers of states in fundamental and adjoint representations is conveniently performed using the Cartan–Weyl method [61, 56]. In this method, each state is represented by its weight – a vector in an l dimensional Euclidean space, where l is equal to the rank of the group. An important ingredient of this method is the Cartan matrix of the group – a matrix whose elements are the scalar products of simple roots of the algebra. Given the highest weight of the fundamental or adjoint representation, one can deduce the rest of the weights using the following algorithm:

– take the highest weight $w = (a_1, a_2 \dots a_n)$;

– define positions and values of all its positive elements a_i;

– derive new weights by sequential a_i–times subtraction of the i–th row α_i of the Cartan matrix from the weight w

– repeat the second and the third steps with all the obtained weights until the lowest weight of the representation (the weight with all nonzero elements negative) is reached.

Let us illustrate this algorithm with a simple example of a $SU(2)$ group. It has rank one and therefore its weight is just a single number. The highest weight of its fundamental representation is given by $w_1 = 1$. The Cartan matrix $\hat{\mathcal{C}}$ in this case also reduces to a single number $\hat{\mathcal{C}}_{SU(2)} = 2$. Subtracting the Cartan matrix from the highest weight, we obtain a weight $w_2 = \bar{1}$ (where $\bar{1} \equiv -1$ is introduced) which is negative and therefore is the lowest weight of the fundamental representation. In other words, the fundamental representation of $SU(2)$ has dimension **2**. Consider now the adjoint representation. Its highest weight is $w_1 = 2$. Subtracting the Cartan matrix, we obtain a weight $w_2 = 0$. Since the positive element of the highest weight $a_1 = 2$, according to the algorithm we should subtract the Cartan matrix once again, which yields the lowest weight of the representation $w_3 = \bar{1}$. In other words, the adjoint representation of $SU(2)$ has dimension **3**.

The analysis of fundamental and adjoint representations of $SU(3)$ is just slightly more complicated. This group has rank two and its weight is a two–dimensional vector. Correspondingly, the Cartan matrix of $SU(3)$ is a two–by–two matrix

$$\hat{\mathcal{C}}_{SU(3)} = \begin{pmatrix} 2 & \bar{1} \\ \bar{1} & 2 \end{pmatrix} \tag{2.4}$$

The highest weight of its fundamental representation is given by $w_1 = (10)$ and has only one positive entry $a_1 = 1$. The subtraction of the first row of the Cartan matrix $\alpha_1 = (2\ \bar{1})$ gives the second weight $w_2 = (\bar{1}1)$, which again has only one positive element $a_2 = 1$. The subtraction of the second row of the Cartan matrix $\alpha_2 = (\bar{1}\ 2)$ gives the third weight $(0\bar{1})$ which does not have positive entries and is therefore the lowest weight of the fundamental representation. Thus, the fundamental representation of $SU(3)$ has dimension **3**. The weights of the conjugate representation, whose highest weight is given by $w_1 = (01)$, are derived analogously.

level	**3**	$\bar{\mathbf{3}}$	**8**
4			(11)
2	(10)	(01)	($\bar{1}$2) (2$\bar{1}$)
0	($\bar{1}$1)	(1$\bar{1}$)	(00) (00)
-2	(0$\bar{1}$)	($\bar{1}$0)	(1$\bar{2}$) ($\bar{2}$1)
-4			($\bar{1}\bar{1}$)

Consider now the adjoint representation of $SU(3)$, whose highest weight is given by $w_1 = (11)$. Both of its elements $a_1 = a_2 = 1$ are positive, so that we have to subtract the first and the

second rows of the Cartan matrix which gives rise to two weights $w_2 = (\bar{1}2)$ and $w_3 = (2\bar{1})$. It is readily seen that these weights coincide with the rows of the Cartan matrix, so that the next subtraction gives two zero weights $w_4 = w_5 = (00)$. As the positive elements of w_2 and w_3 are equal to two, in complete analogy with the $SU(2)$ case we have to subtract the corresponding rows of the Cartan matrix once again which gives $w_6 = (1\bar{2})$ and $w_7 = (\bar{2}1)$, each of which has only one positive element. The subtraction of the corresponding rows of the Cartan matrix yields one and the same weight $w_8 = (\bar{1}\bar{1})$ with no positive elements. We thus obtained all the eight weights of the adjoint representation of $SU(3)$. Note that already in this simple case two degenerate weights, i.e. similar weights corresponding to different states, appear. In general, the number of degenerate weights coincides with rank of the group.

A $SU(N)$ group has rank N, which implies N degenerate weights in the adjoint representation. The Cartan matrix is tridiagonal with diagonal entries equal to 2 and off–diagonal to $\bar{1}$. In what follows we order weights according to their levels. Level of a weight is given by the scalar products of the weight and level vector of the group. The level vector of a $SU(N)$ group reads

$$R_{SU(N+1)} = (N, 2(N-1), 3(N-2), \ldots, (N-1)2, N). \tag{2.5}$$

Level vector of a $SU(3)$, for instance, is given by $R_{SU(3)} = (2, 2)$, whereas for a $SU(5)$ we obtain from (2.5) $R_{SU(5)} = (4, 6, 6, 4)$.

Applying the above to a $SU(5)$ group we obtain the system of weights of **5** (fundamental), **10** and **24** (adjoint) dimensional representations, presented in table 2.1.

level	**5**	**10**	**24**
8			(1001)
6		(0100)	($\bar{1}$101) (101$\bar{1}$)
4	(1000)	(1$\bar{1}$10)	(0$\bar{1}$11) ($\bar{1}$11$\bar{1}$) (11$\bar{1}$0)
2	($\bar{1}$100)	($\bar{1}$010) (10$\bar{1}$1)	(00$\bar{1}$2) (0$\bar{1}$2$\bar{1}$) ($\bar{1}$2$\bar{1}$0) (2$\bar{1}$00)
0	(0$\bar{1}$10)	($\bar{1}$1$\bar{1}$1) (100$\bar{1}$)	(0000) (0000) (0000) (0000)
-2	(00$\bar{1}$1)	(0$\bar{1}$01) ($\bar{1}$10$\bar{1}$)	(001$\bar{2}$) (01$\bar{2}$1) (1$\bar{2}$10) ($\bar{2}$100)
-4	(000$\bar{1}$)	(0$\bar{1}$1$\bar{1}$)	(01$\bar{1}\bar{1}$) (1$\bar{1}\bar{1}$1) ($\bar{1}\bar{1}$10)
-6		(00$\bar{1}$0)	(1$\bar{1}$0$\bar{1}$) ($\bar{1}$0$\bar{1}$1)
-8			($\bar{1}$00$\bar{1}$)

Table 2.1: Weights of **5** (fundamental), **10** and **24** (adjoint) dimensional representations of $SU(5)$. The level vector of $SU(5)$ is given by $R_{SU(5)} = (4, 6, 6, 4)$.

The weights of the conjugate representations $\bar{\mathbf{5}}$ and $\bar{\mathbf{10}}$ of $SU(5)$ are easily obtained from the weights of the **5** and **10** dimensional representations presented in table 2.1 by the transformation $(a_1a_2a_3a_4) \to (a_4a_3a_2a_1)$, which leaves the level vector and the adjoint representation invariant.

The Cartan matrix of the orthogonal group $SO(10)$ reads [56]

$$\hat{\mathcal{C}}_{SO(10)} = \begin{pmatrix} 2 & \bar{1} & 0 & 0 & 0 \\ \bar{1} & 2 & \bar{1} & 0 & 0 \\ 0 & \bar{1} & 2 & \bar{1} & \bar{1} \\ 0 & 0 & \bar{1} & 2 & 0 \\ 0 & 0 & \bar{1} & 0 & 2 \end{pmatrix} \tag{2.6}$$

Proceeding as above, we derive the weights of **10** (fundamental), **16** (spinor) and **45** (adjoint) dimensional representations of $SO(10)$ presented in table 2.2.

level	**10**	**16**	**45**
14			(01000)
12			(1$\bar{1}$100)
10		(00001)	($\bar{1}$0100) (10$\bar{1}$11)
8	(10000)	(0010$\bar{1}$)	($\bar{1}$1$\bar{1}$11) (100$\bar{1}$1) (1001$\bar{1}$)
6	($\bar{1}$1000)	(01$\bar{1}$10)	(0$\bar{1}$011) ($\bar{1}$10$\bar{1}$1) ($\bar{1}$101$\bar{1}$) (101$\bar{1}\bar{1}$)
4	(0$\bar{1}$100)	(1$\bar{1}$010) (010$\bar{1}$0)	(0$\bar{1}$1$\bar{1}$1) (0$\bar{1}$11$\bar{1}$) ($\bar{1}$11$\bar{1}\bar{1}$) (11$\bar{1}$00)
2	(00$\bar{1}$11)	($\bar{1}$0010) (1$\bar{1}$1$\bar{1}$0)	(00$\bar{1}$02) (0$\bar{1}$2$\bar{1}\bar{1}$) (00$\bar{1}$20) ($\bar{1}$2$\bar{1}$00) (2$\bar{1}$000)
0	(000$\bar{1}$1) (0001$\bar{1}$)	($\bar{1}$01$\bar{1}$0) (10$\bar{1}$01)	(00000) (00000) (00000) (00000) (00000)
-2	(001$\bar{1}\bar{1}$)	($\bar{1}$1$\bar{1}$01) (1000$\bar{1}$)	(0010$\bar{2}$) (01$\bar{2}$11) (001$\bar{2}$0) (1$\bar{2}$100) ($\bar{2}$1000)
-4	(01$\bar{1}$00)	(0$\bar{1}$001) ($\bar{1}$100$\bar{1}$)	(01$\bar{1}$1$\bar{1}$) (01$\bar{1}\bar{1}$1) (1$\bar{1}\bar{1}$11) ($\bar{1}\bar{1}$100)
-6	(1$\bar{1}$000)	(0$\bar{1}$10$\bar{1}$)	(010$\bar{1}\bar{1}$) (1$\bar{1}$01$\bar{1}$) (1$\bar{1}$0$\bar{1}$1) ($\bar{1}$0$\bar{1}$11)
-8	($\bar{1}$0000)	(00$\bar{1}$10)	(1$\bar{1}$1$\bar{1}\bar{1}$) ($\bar{1}$001$\bar{1}$) ($\bar{1}$00$\bar{1}$1)
-10		(000$\bar{1}$0)	(10$\bar{1}$00) ($\bar{1}$01$\bar{1}\bar{1}$)
-12			($\bar{1}$1$\bar{1}$00)
-14			(0$\bar{1}$000)

Table 2.2: Weights of **10** (fundamental), **16** (spinor) and **45** (adjoint) dimensional representations of $SO(10)$. Level vector of $SO(10)$ is given by $R_{SO(10)} = (8, 14, 18, 10, 10)$.

In what follows we will also need weights of states of the $\bar{\mathbf{16}}$ representation. From the structure of the level vector, which has only two equal entries, it is clear, that these are obtained from the weights of **16** by the transformation $(a_1a_2a_3a_4a_5) \to (a_1a_2a_3a_5a_4)$ which leaves both the level vector and the adjoint representation invariant.

The exceptional groups, especially the E series, have received considerable attention from model builders. One of the main motivations is that if one of the exceptional groups were part of a complete theory, then there might be a chance of going beyond the Yang–Mills construction and "explaining" why it is the correct choice of gauge group. E_6 has rank 6 and 78 generators, and is the only exceptional group with non–self conjugate irreps, so it is the only exceptional group for which flavor–chiral theory is possible. The Cartan matrix of the exceptional group E_6

is given by [56]

$$\hat{\mathcal{C}}_{E_6} = \begin{pmatrix} 2 & \bar{1} & 0 & 0 & 0 & 0 \\ \bar{1} & 2 & \bar{1} & 0 & 0 & 0 \\ 0 & \bar{1} & 2 & \bar{1} & 0 & \bar{1} \\ 0 & 0 & \bar{1} & 2 & \bar{1} & 0 \\ 0 & 0 & 0 & \bar{1} & 2 & 0 \\ 0 & 0 & \bar{1} & 0 & 0 & 2 \end{pmatrix} \tag{2.7}$$

Proceeding as above, we derive the weights of **27** (fundamental) and **78** (adjoint) dimensional representations of E_6, which are presented in table 2.3.

level	**27**	**78**
22		(000001)
20		(00100$\bar{1}$)
18		(01$\bar{1}$100)
16	(100000)	(1$\bar{1}$0100) (010$\bar{1}$10)
14	($\bar{1}$10000)	($\bar{1}$00100) (1$\bar{1}$1$\bar{1}$10) (0100$\bar{1}$0)
12	(0$\bar{1}$1000)	($\bar{1}$01$\bar{1}$10) (10$\bar{1}$011) (1$\bar{1}$10$\bar{1}$0)
10	(00$\bar{1}$101)	($\bar{1}$010$\bar{1}$0) ($\bar{1}$1$\bar{1}$011) (10001$\bar{1}$) (10$\bar{1}$1$\bar{1}$1)
8	(000$\bar{1}$11) (00010$\bar{1}$)	($\bar{1}$1$\bar{1}$1$\bar{1}$1) (0$\bar{1}$0011) ($\bar{1}$1001$\bar{1}$) (1001$\bar{1}\bar{1}$) (100$\bar{1}$01)
6	(0000$\bar{1}$1) (001$\bar{1}$1$\bar{1}$)	($\bar{1}$10$\bar{1}$01) (0$\bar{1}$01$\bar{1}$1) (0$\bar{1}$101$\bar{1}$) ($\bar{1}$101$\bar{1}\bar{1}$) (101$\bar{1}$0$\bar{1}$)
4	(00010$\bar{1}\bar{1}$) (01$\bar{1}$010)	($\bar{1}$11$\bar{1}$0$\bar{1}$) (0$\bar{1}$1$\bar{1}$01) (00$\bar{1}$110) (0$\bar{1}$11$\bar{1}\bar{1}$) (11$\bar{1}$000)
2	(01$\bar{1}$1$\bar{1}$010) (1$\bar{1}$0010)	(0$\bar{1}$2$\bar{1}$0$\bar{1}$) ($\bar{1}$2$\bar{1}$000) (00$\bar{1}$002) (000$\bar{1}$20) (00$\bar{1}$2$\bar{1}$0) (2$\bar{1}$0000)
0	(010$\bar{1}$00) (1$\bar{1}$01$\bar{1}$0) ($\bar{1}$00010)	(000000) (000000) (000000) (000000) (000000) (000000)
$\bar{2}$	(1$\bar{1}$1$\bar{1}$00) ($\bar{1}$001$\bar{1}$0)	(01$\bar{2}$101) (1$\bar{2}$1000) (001002$\bar{2}$) (0001$\bar{2}$0) (001$\bar{2}$10) ($\bar{2}$10000)
-4	(10$\bar{1}$001) ($\bar{1}$01$\bar{1}$00)	(1$\bar{1}\bar{1}$101) (01$\bar{1}$10$\bar{1}$) (001$\bar{1}\bar{1}$0) (01$\bar{1}\bar{1}$11) ($\bar{1}\bar{1}$1000)
-6	(10000$\bar{1}$) ($\bar{1}$1$\bar{1}$001)	(1$\bar{1}$0101$\bar{1}$) (010$\bar{1}$1$\bar{1}$) (01$\bar{1}$0$\bar{1}$1) (1$\bar{1}$0$\bar{1}$11) ($\bar{1}$0$\bar{1}$101)
-8	($\bar{1}$1000$\bar{1}$) (0$\bar{1}$0001)	($\bar{1}$00101$\bar{1}$) (1$\bar{1}$1$\bar{1}$1$\bar{1}$) (0100$\bar{1}\bar{1}$) (1$\bar{1}$00$\bar{1}$1) ($\bar{1}$00$\bar{1}$11)
-10	(0$\bar{1}$100$\bar{1}$)	($\bar{1}$01$\bar{1}$1$\bar{1}$) (10$\bar{1}$010) (1$\bar{1}$10$\bar{1}\bar{1}$) ($\bar{1}$000$\bar{1}$1)
-12	(00$\bar{1}$100)	($\bar{1}$1$\bar{1}$010) (10$\bar{1}$1$\bar{1}$0) ($\bar{1}$010$\bar{1}\bar{1}$)
-14	(000$\bar{1}$10)	(0$\bar{1}$0010) (100$\bar{1}$00) ($\bar{1}$1$\bar{1}$1$\bar{1}$0)
-16	(0000$\bar{1}$0)	(0$\bar{1}$01$\bar{1}$0) ($\bar{1}$10$\bar{1}$00)
-18		(0$\bar{1}$1$\bar{1}$00)
-20		(00$\bar{1}$001)
-22		(00000$\bar{1}$)

Table 2.3: Weights of **27** (fundamental) and **78** (adjoint) dimensional representations of E_6. The level vector of E_6 is given by $R_{E_6} = (16, 30, 42, 30, 16, 22)$.

From the structure of the level vector it is clear, that the weights of the states of the $\bar{\mathbf{27}}$ representation are obtained from the weights of the **27** by the transformation $(a_1a_2a_3a_4a_5a_6) \rightarrow (a_5a_4a_3a_2a_1a_6)$ which leaves both the level vector and the adjoint representation invariant.

Now that we have weights of all the groups we are interested in, we should deduce projection matrices which take the weights of E_6 to the weights of its subgroups. Let us first consider the $E_6 \to SO(10) \otimes U(1)$ breaking chain. The commonly used convention is that the highest weight of a representation of a group is projected onto the highest weight of its subgroup representation. For instance, the **27** dimensional fundamental representation of E_6 is mapped to the **16** dimensional fundamental representation of $SO(10)$ whereas $\bar{\mathbf{27}}$ of E_6 is mapped to $\bar{\mathbf{16}}$ of $SO(10)$. Likewise, the highest weight of the adjoint of E_6 is mapped to the highest weight of the adjoint of $SO(10)$. The resulting projection matrix is a six–by–six matrix. Its first five rows which project a six–dimensional weight of E_6 to the corresponding five–dimensional weight of $SO(10)$ are easily deduced from the table 2.4, where the branching rules of E_6 representations are given. The last row projects the weights of E_6 to the corresponding one–dimensional weights of the

Branching rule	E_6	$SO(10)$
$\mathbf{27} = \mathbf{1} + \mathbf{10} + \mathbf{16}$	(100000)	(00001)
$\bar{\mathbf{27}} = \mathbf{1} + \bar{\mathbf{10}} + \bar{\mathbf{16}}$	(000010)	(00010)
$\mathbf{78} = \mathbf{1} + \mathbf{45} + \mathbf{16} + \bar{\mathbf{16}}$	(000001)	(01000)
$\mathbf{351} = \mathbf{10} + \bar{\mathbf{16}} + \mathbf{16} + \mathbf{45} + \bar{\mathbf{120}} + \mathbf{144}$	(000100)	(10010)
$\bar{\mathbf{351}} = \bar{\mathbf{10}} + \mathbf{16} + \bar{\mathbf{16}} + \bar{\mathbf{45}} + \mathbf{120} + \bar{\mathbf{144}}$	(010000)	(10001)
$\mathbf{2925} = \mathbf{16} + \bar{\mathbf{16}} + \mathbf{45}_1 + \mathbf{45}_2 + \mathbf{120}_1 + \mathbf{120}_2 + \mathbf{144} + \mathbf{210} + \mathbf{560} + \mathbf{945}$	(001000)	(10100)

Table 2.4: Branching of E_6 representations.

$U(1)$ subgroup and is deduced up to an overall factor from the requirement, that all components of the $SO(10)$ subgroup have the same $U(1)$ charge. As can be easily checked using table 2.4, the explicit form of the projection matrix is

$$P_{E_6 \to SO(10)\otimes U(1)} = \begin{pmatrix} 0 & 1 & 1 & 1 & 0 & 0 \\ 0 & 0 & 0 & 0 & 0 & 1 \\ 0 & 0 & 1 & 0 & 0 & 0 \\ 0 & 0 & 0 & 1 & 1 & 0 \\ 1 & 1 & 0 & 0 & 0 & 0 \\ 1 & \bar{1} & 0 & 1 & \bar{1} & 0 \end{pmatrix} \tag{2.8}$$

Analogously, we deduce the $SO(10) \to SU(5) \otimes U(1)$ projection matrix. The branching rules of $SO(10)$ representations are presented in table 2.5. The first four rows of the resulting five–by–five projection matrix take five–dimensional weights of the $SO(10)$ representation to four–dimensional weights of its $SU(5)$ subgroup, whereas the fifth row projects weights of the $SO(10)$ to weights of its $U(1)$ subgroup.

Branching rule	$SO(10)$	$SU(5)$
$\mathbf{10}=\mathbf{5}+\bar{\mathbf{5}}$	(10000)	(1000)
$\mathbf{16}=\mathbf{1}+\bar{\mathbf{5}}+\mathbf{10}$	(00001)	(0100)
$\mathbf{45}=\mathbf{1}+\mathbf{10}+\bar{\mathbf{10}}+\mathbf{24}$	(01000)	(1001)
$\mathbf{120}=\mathbf{5}+\bar{\mathbf{5}}+\mathbf{10}+\bar{\mathbf{10}}+\mathbf{45}+\bar{\mathbf{45}}$	(00100)	(0101)
$\mathbf{144}=\mathbf{5}+\bar{\mathbf{5}}+\mathbf{10}+\mathbf{15}+\mathbf{24}+\mathbf{40}+\bar{\mathbf{45}}$	(10010)	(1010)

Table 2.5: Branching of $SO(10)$ representations.

As can be easily checked using table 2.5, the projection matrix reads

$$P_{SO(10)\to SU(5)\otimes U(1)} = \begin{pmatrix} 1 & 1 & 0 & 0 & 0 \\ 0 & 0 & 1 & 0 & 1 \\ 0 & 0 & 0 & 1 & 0 \\ 0 & 1 & 1 & 0 & 0 \\ 2 & 0 & 2 & 1 & \bar{1} \end{pmatrix} \tag{2.9}$$

Finally we have to derive the matrix projecting $SU(5)$ to the Standard Model gauge group. The branching rules of $SU(5)$ representations are given in table 2.6. The first two rows ot the

Branching rule	$SU(5)$	$SU(3)\otimes SU(2)$
$\mathbf{5}=(\mathbf{1},\mathbf{2})+(\mathbf{3},\mathbf{1})$	(1000)	(10)(0)
$\bar{\mathbf{5}}=(\mathbf{1},\mathbf{2})+(\mathbf{1},\bar{\mathbf{3}})$	(0001)	(01)(0)
$\mathbf{10}=(\mathbf{1},\mathbf{1})+(\mathbf{3},\mathbf{1})+(\mathbf{3},\mathbf{2})$	(0100)	(10)(1)
$\bar{\mathbf{10}}=(\mathbf{1},\mathbf{1})+(\bar{\mathbf{3}},\mathbf{1})+(\bar{\mathbf{3}},\mathbf{2})$	(0010)	(01)(1)

Table 2.6: Branching of $SU(5)$ representations.

four–by–four projection matrix take four–dimensional weights of $SU(5)$ representation to two–dimensional weights of its $SU(3)$ subgroup, the third row to one–dimensional weights of $SU(2)$ and the last row to weights of its $U(1)$ subgroup. Explicit form of the projection matrix:

$$P_{SU(5)\to SU(3)\otimes SU(2)\otimes U(1)} = \begin{pmatrix} 0 & 1 & 1 & 0 \\ 1 & 1 & 0 & 0 \\ 0 & 0 & 1 & 1 \\ \bar{2} & 1 & \bar{1} & 2 \end{pmatrix} \tag{2.10}$$

An embedding of the $SO(10)$, $SU(5)$ and the Standard Model gauge groups into the fundamental and the adjoint representations of E_6 is presented correspondingly in table 2.7 and table 2.8.

E_6	SO(10) $\otimes U(1)$	SU(5)$\otimes U(1)^2$	$SU(3) \otimes SU(2)$ $\otimes U(1)^3$	I	II	III	IV	V	VI	(Z, ρ)
27	**16**	**10**	**3,2**							
$[100000]$	$[00001]_1$	$[0100]_{1,\bar{1}}$	$[10][1]_{,1,\bar{1},1}$	u	u	u	u	u	u	$-\varepsilon$
$[1\bar{1}0010]$	$[\bar{1}0010]_1$	$[\bar{1}010]_{1,\bar{1}}$	$[\bar{1}1][1]_{,1,\bar{1},1}$	u	u	u	u	u	u	$-\varepsilon$
$[10000\bar{1}]$	$[0\bar{1}001]_1$	$[\bar{1}10\bar{1}]_{1,\bar{1}}$	$[0\bar{1}][1]_{,1,\bar{1},1}$	u	u	u	u	u	u	$-\varepsilon$
$[0000\bar{1}1]$	$[010\bar{1}0]_1$	$[10\bar{1}1]_{1,\bar{1}}$	$[10][\bar{1}]_{,1,\bar{1},1}$	d	d	d	d	d	d	$-\varepsilon$
$[0\bar{1}0001]$	$[\bar{1}100\bar{1}]_1$	$[0\bar{1}01]_{1,\bar{1}}$	$[\bar{1}1][\bar{1}]_{,1,\bar{1},1}$	d	d	d	d	d	d	$-\varepsilon$
$[0000\bar{1}0]$	$[000\bar{1}0]_1$	$[00\bar{1}0]_{1,\bar{1}}$	$[0\bar{1}][\bar{1}]_{,1,\bar{1},1}$	d	d	d	d	d	d	$-\varepsilon$
27	**16**	**10**	$\bar{\mathbf{3}}, \mathbf{1}$							
$[00\bar{1}101]$	$[01\bar{1}10]_1$	$[1\bar{1}10]_{1,\bar{1}}$	$[01][0]_{,1,\bar{1},\bar{4}}$	u^c	u^c	d^c	D^c	d^c	D^c	$\alpha - \varepsilon$
$[01\bar{1}1\bar{1}0]$	$[10\bar{1}01]_1$	$[100\bar{1}]_{1,\bar{1}}$	$[1\bar{1}][0]_{,1,\bar{1},\bar{4}}$	u^c	u^c	d^c	D^c	d^c	D^c	$\alpha - \varepsilon$
$[00\bar{1}100]$	$[00\bar{1}10]_1$	$[0\bar{1}1\bar{1}]_{1,\bar{1}}$	$[\bar{1}0][0]_{,1,\bar{1},\bar{4}}$	u^c	u^c	d^c	D^c	d^c	D^c	$\alpha - \varepsilon$
27	**16**	**10**	**1,1**							
$[1\bar{1}1\bar{1}00]$	$[\bar{1}01\bar{1}0]_1$	$[\bar{1}1\bar{1}1]_{1,\bar{1}}$	$[00][0]_{,1,\bar{1},6}$	e^c	e^c	ν^c	S	ν^c	S	$-\alpha - \varepsilon$
27	**16**	$\bar{\mathbf{5}}$	$\bar{\mathbf{3}}, \mathbf{1}$							
$[0\bar{1}1000]$	$[00101\bar{1}]_1$	$[0001]_{1,3}$	$[01][0]_{,1,3,2}$	d^c	D^c	u^c	u^c	D^c	d^c	$\beta - \varepsilon$
$[0010\bar{1}\bar{1}]$	$[1\bar{1}1\bar{1}0]_1$	$[01\bar{1}0]_{1,3}$	$[1\bar{1}][0]_{,1,3,2}$	d^c	D^c	u^c	u^c	D^c	d^c	$\beta - \varepsilon$
$[0\bar{1}100\bar{1}]$	$[0\bar{1}10\bar{1}]_1$	$[\bar{1}000]_{1,3}$	$[\bar{1}0][0]_{,1,3,2}$	d^c	D^c	u^c	u^c	D^c	d^c	$\beta - \varepsilon$
27	**16**	$\bar{\mathbf{5}}$	**1,2**							
$[00010\bar{1}]$	$[1\bar{1}010]_1$	$[001\bar{1}]_{1,3}$	$[00][1]_{,1,3,\bar{3}}$	ν	N	ν	N	E^c	E^c	$2\varepsilon - \gamma$
$[\bar{1}001\bar{1}0]$	$[1000\bar{1}]_1$	$[1\bar{1}00]_{1,3}$	$[00][\bar{1}]_{,1,3,\bar{3}}$	e	E	e	E	N^c	N^c	$2\varepsilon - \gamma$
27	**16**	**1**	**1,1**							
$[10\bar{1}001]$	$[\bar{1}1\bar{1}01]_1$	$[0000]_{1,\bar{5}}$	$[00][0]_{,1,\bar{5},0}$	ν^c	S	e^c	e^c	S	ν^c	$-\beta - \varepsilon$
27	**10**	**5**	**3,1**							
$[\bar{1}10000]$	$[10000]_{\bar{2}}$	$[1000]_{\bar{2},2}$	$[10][0]_{,\bar{2},2,\bar{2}}$	D	D	D	D	D	D	2ε
$[\bar{1}00010]$	$[0001\bar{1}]_{\bar{2}}$	$[0\bar{1}10]_{\bar{2},2}$	$[\bar{1}1][0]_{,\bar{2},2,\bar{2}}$	D	D	D	D	D	D	2ε
$[\bar{1}1000\bar{1}]$	$[1\bar{1}000]_{\bar{2}}$	$[000\bar{1}]_{\bar{2},2}$	$[0\bar{1}][0]_{,\bar{2},2,\bar{2}}$	D	D	D	D	D	D	2ε
27	**10**	**5**	**1,2**							
$[001\bar{1}1\bar{1}]$	$[0\bar{1}100]_{\bar{2}}$	$[\bar{1}100]_{\bar{2},2}$	$[00][1]_{,\bar{2},2,3}$	E^c	E^c	N	ν	N	ν	$2\varepsilon - \alpha$
$[\bar{1}01\bar{1}00]$	$[001\bar{1}\bar{1}]_{\bar{2}}$	$[00\bar{1}1]_{\bar{2},2}$	$[00][\bar{1}]_{,\bar{2},2,3}$	N^c	N^c	E	e	E	e	$2\varepsilon - \alpha$
27	**10**	$\bar{\mathbf{5}}$	$\bar{\mathbf{3}}, \mathbf{1}$							
$[000\bar{1}11]$	$[\bar{1}1000]_{\bar{2}}$	$[0001]_{\bar{2},\bar{2}}$	$[01][0]_{,\bar{2},\bar{2},2}$	D^c	d^c	D^c	d^c	u^c	u^c	$\gamma - \varepsilon$
$[010\bar{1}00]$	$[000\bar{1}1]_{\bar{2}}$	$[01\bar{1}0]_{\bar{2},\bar{2}}$	$[1\bar{1}][0]_{,\bar{2},\bar{2},2}$	D^c	d^c	D^c	d^c	u^c	u^c	$\gamma - \varepsilon$
$[000\bar{1}10]$	$[\bar{1}0000]_{\bar{2}}$	$[\bar{1}000]_{\bar{2},\bar{2}}$	$[\bar{1}0][0]_{,\bar{2},\bar{2},2}$	D^c	d^c	D^c	d^c	u^c	u^c	$\gamma - \varepsilon$
27	**10**	$\bar{\mathbf{5}}$	**1,2**							
$[01\bar{1}010]$	$[00\bar{1}11]_{\bar{2}}$	$[001\bar{1}]_{\bar{2},\bar{2}}$	$[00][1]_{,\bar{2},\bar{2},\bar{3}}$	N	ν	E^c	E^c	ν	N	$2\varepsilon - \beta$
$[\bar{1}1\bar{1}001]$	$[01\bar{1}00]_{\bar{2}}$	$[1\bar{1}00]_{\bar{2},\bar{2}}$	$[00][\bar{1}]_{,\bar{2},\bar{2},\bar{3}}$	E	e	N^c	N^c	e	E	$2\varepsilon - \beta$
27	**1**	**1**	**1,1**							
$[1\bar{1}01\bar{1}0]$	$[00000]_4$	$[0000]_{4,0}$	$[00][0]_{,4,0,0}$	S	ν^c	S	ν^c	e^c	e^c	$-\gamma - \varepsilon$

Table 2.7: Embedding of $SO(10)$ and $SU(5)$ into fundamental representation of E_6.

E_6	SO(10) $\times U(1)$	SU(5)$\times U(1)^2$	$SU(3)\times SU(2)\ \times U(1)^3$	I	II	III	IV	V	VI	(Z,ρ)
78	**16**	**1**	**1**,**1**							
$[01\bar{1}\bar{1}11]$	$[\bar{1}1\bar{1}01]_{\bar{3}}$	$[0000]_{\bar{3},\bar{5}}$	$[00][0]_{\bar{3},\bar{5},0}$	ν^c	$\bar{\nu^c}$	e^c	e_0^c	$\bar{e^c}$	$\bar{e}_0^c$	$\gamma-\beta$
78	**16**	**10**	$\bar{\mathbf{3}}$,**1**							
$[\bar{1}1\bar{1}010]$	$[00\bar{1}10]_{\bar{3}}$	$[0\bar{1}1\bar{1}]_{\bar{3},\bar{1}}$	$[\bar{1}0][0]_{\bar{3},\bar{1},\bar{4}}$	u^c	$u_{\bar{4}}^c$	d^c	d^c	$u_{\bar{4}}^c$	u^c	$\alpha+\gamma$
$[\bar{1}2\bar{1}000]$	$[10\bar{1}01]_{\bar{3}}$	$[100\bar{1}]_{\bar{3},\bar{1}}$	$[1\bar{1}][0]_{\bar{3},\bar{1},\bar{4}}$	u^c	$u_{\bar{4}}^c$	d^c	d^c	$u_{\bar{4}}^c$	u^c	$\alpha+\gamma$
$[\bar{1}1\bar{1}011]$	$[01\bar{1}10]_{\bar{3}}$	$[1\bar{1}10]_{\bar{3},\bar{1}}$	$[01][0]_{\bar{3},\bar{1},\bar{4}}$	u^c	$u_{\bar{4}}^c$	d^c	d^c	$u_{\bar{4}}^c$	u^c	$\alpha+\gamma$
78	**16**	**10**	**3**,**2**							
$[\bar{1}10\bar{1}00]$	$[000\bar{1}0]_{\bar{3}}$	$[00\bar{1}0]_{\bar{3},\bar{1}}$	$[0\bar{1}][\bar{1}]_{\bar{3},\bar{1},1}$	d	$d_{\bar{2}}$	d	$d_{\bar{2}}$	X	X	γ
$[\bar{1}00\bar{1}11]$	$[\bar{1}100\bar{1}]_{\bar{3}}$	$[0\bar{1}01]_{\bar{3},\bar{1}}$	$[\bar{1}1][\bar{1}]_{\bar{3},\bar{1},1}$	d	$d_{\bar{2}}$	d	$d_{\bar{2}}$	X	X	γ
$[\bar{1}10\bar{1}01]$	$[010\bar{1}0]_{\bar{3}}$	$[10\bar{1}1]_{\bar{3},\bar{1}}$	$[10][\bar{1}]_{\bar{3},\bar{1},1}$	d	$d_{\bar{2}}$	d	$d_{\bar{2}}$	X	X	γ
$[010\bar{1}1\bar{1}]$	$[0\bar{1}001]_{\bar{3}}$	$[\bar{1}10\bar{1}]_{\bar{3},\bar{1}}$	$[0\bar{1}][1]_{\bar{3},\bar{1},1}$	u	$u_{\bar{2}}$	u	$u_{\bar{2}}$	Y	Y	γ
$[000\bar{1}20]$	$[\bar{1}0010]_{\bar{3}}$	$[\bar{1}010]_{\bar{3},\bar{1}}$	$[\bar{1}1][1]_{\bar{3},\bar{1},1}$	u	$u_{\bar{2}}$	u	$u_{\bar{2}}$	Y	Y	γ
$[010\bar{1}10]$	$[00001]_{\bar{3}}$	$[0100]_{\bar{3},\bar{1}}$	$[10][1]_{\bar{3},\bar{1},1}$	u	$u_{\bar{2}}$	u	$u_{\bar{2}}$	Y	Y	γ
78	**16**	**10**	**1**,**1**							
$[001\bar{2}10]$	$[\bar{1}01\bar{1}0]_{\bar{3}}$	$[\bar{1}1\bar{1}1]_{\bar{3},\bar{1}}$	$[00][0]_{\bar{3},\bar{1},6}$	e^c	e_0^c	ν^c	$\bar{\nu^c}$	$\bar{e}_0^c$	$\bar{e^c}$	$\gamma-\alpha$
78	**16**	$\bar{\mathbf{5}}$	**1**,**2**							
$[\bar{2}10000]$	$[1000\bar{1}]_{\bar{3}}$	$[1\bar{1}00]_{\bar{3},3}$	$[00][\bar{1}]_{\bar{3},3,\bar{3}}$	e	e	e	e	e	e	3ε
$[\bar{1}1001\bar{1}]$	$[1\bar{1}010]_{\bar{3}}$	$[001\bar{1}]_{\bar{3},3}$	$[00][1]_{\bar{3},3,\bar{3}}$	ν	ν	ν	ν	ν	ν	3ε
78	**16**	$\bar{\mathbf{5}}$	$\bar{\mathbf{3}}$,**1**							
$[\bar{1}01\bar{1}1\bar{1}]$	$[0\bar{1}10\bar{1}]_{\bar{3}}$	$[\bar{1}000]_{\bar{3},3}$	$[\bar{1}0][0]_{\bar{3},3,2}$	d^c	d^c	u^c	$u_{\bar{4}}^c$	u^c	$u_{\bar{4}}^c$	$\beta+\gamma$
$[\bar{1}11\bar{1}0\bar{1}]$	$[1\bar{1}1\bar{1}0]_{\bar{3}}$	$[01\bar{1}0]_{\bar{3},3}$	$[1\bar{1}][0]_{\bar{3},3,2}$	d^c	d^c	u^c	$u_{\bar{4}}^c$	u^c	$u_{\bar{4}}^c$	$\beta+\gamma$
$[\bar{1}01\bar{1}10]$	$[0010\bar{1}]_{\bar{3}}$	$[0001]_{\bar{3},3}$	$[01][0]_{\bar{3},3,2}$	d^c	d^c	u^c	$u_{\bar{4}}^c$	u^c	$u_{\bar{4}}^c$	$\beta+\gamma$
78	**45**	$\bar{\mathbf{1}}\bar{\mathbf{0}}$	**1**,**1**							
$[01\bar{2}101]$	$[01\bar{2}11]_0$	$[1\bar{1}1\bar{1}]_{0,\bar{4}}$	$[00][0]_{0,\bar{4},\bar{6}}$	$\bar{e}_0^c$	$\bar{e^c}$	e_0^c	e^c	$\bar{\nu^c}$	ν^c	$\alpha-\beta$
78	**45**	$\bar{\mathbf{1}}\bar{\mathbf{0}}$	$\bar{\mathbf{3}}$,**2**							
$[00\bar{1}001]$	$[\bar{1}1\bar{1}00]_0$	$[0\bar{1}00]_{0,\bar{4}}$	$[\bar{1}0][\bar{1}]_{0,\bar{4},\bar{1}}$	$\bar{u}_{\bar{2}}$	$\bar{u}$	$\bar{Y}$	$\bar{Y}$	$\bar{u}$	$\bar{u}_{\bar{2}}$	$-\beta$
$[01\bar{1}0\bar{1}1]$	$[01\bar{1}\bar{1}1]_0$	$[10\bar{1}0]_{0,\bar{4}}$	$[1\bar{1}][\bar{1}]_{0,\bar{4},\bar{1}}$	$\bar{u}_{\bar{2}}$	$\bar{u}$	$\bar{Y}$	$\bar{Y}$	$\bar{u}$	$\bar{u}_{\bar{2}}$	$-\beta$
$[00\bar{1}002]$	$[\bar{1}2\bar{1}00]_0$	$[1\bar{1}01]_{0,\bar{4}}$	$[01][\bar{1}]_{0,\bar{4},\bar{1}}$	$\bar{u}_{\bar{2}}$	$\bar{u}$	$\bar{Y}$	$\bar{Y}$	$\bar{u}$	$\bar{u}_{\bar{2}}$	$-\beta$
$[10\bar{1}010]$	$[\bar{1}0\bar{1}11]_0$	$[\bar{1}01\bar{1}]_{0,\bar{4}}$	$[\bar{1}0][1]_{0,\bar{4},\bar{1}}$	$\bar{d}_{\bar{2}}$	$\bar{d}$	$\bar{X}$	$\bar{X}$	$\bar{d}$	$\bar{d}_{\bar{2}}$	$-\beta$
$[11\bar{1}000]$	$[00\bar{1}02]_0$	$[010\bar{1}]_{0,\bar{4}}$	$[1\bar{1}][1]_{0,\bar{4},\bar{1}}$	$\bar{d}_{\bar{2}}$	$\bar{d}$	$\bar{X}$	$\bar{X}$	$\bar{d}$	$\bar{d}_{\bar{2}}$	$-\beta$
$[10\bar{1}011]$	$[\bar{1}1\bar{1}11]_0$	$[0010]_{0,\bar{4}}$	$[01][1]_{0,\bar{4},\bar{1}}$	$\bar{d}_{\bar{2}}$	$\bar{d}$	$\bar{X}$	$\bar{X}$	$\bar{d}$	$\bar{d}_{\bar{2}}$	$-\beta$
78	**45**	$\bar{\mathbf{1}}\bar{\mathbf{0}}$	**3**,**1**							
$[100\bar{1}00]$	$[\bar{1}00\bar{1}1]_0$	$[\bar{1}1\bar{1}0]_{0,\bar{4}}$	$[0\bar{1}][0]_{0,\bar{4},4}$	$\bar{u}_{\bar{4}}^c$	$\bar{u}^c$	$\bar{u}_{\bar{4}}^c$	$\bar{u}^c$	$\bar{d}^c$	$\bar{d}^c$	$-\alpha-\beta$
$[1\bar{1}0\bar{1}11]$	$[\bar{2}1000]_0$	$[\bar{1}001]_{0,\bar{4}}$	$[\bar{1}1][0]_{0,\bar{4},4}$	$\bar{u}_{\bar{4}}^c$	$\bar{u}^c$	$\bar{u}_{\bar{4}}^c$	$\bar{u}^c$	$\bar{d}^c$	$\bar{d}^c$	$-\alpha-\beta$
$[100\bar{1}01]$	$[\bar{1}10\bar{1}1]_0$	$[01\bar{1}1]_{0,\bar{4}}$	$[10][0]_{0,\bar{4},4}$	$\bar{u}_{\bar{4}}^c$	$\bar{u}^c$	$\bar{u}_{\bar{4}}^c$	$\bar{u}^c$	$\bar{d}^c$	$\bar{d}^c$	$-\alpha-\beta$
78	**45**	**24**	**3**,**2**							
$[\bar{1}1\bar{1}1\bar{1}0]$	$[10\bar{1}00]_0$	$[1\bar{1}0\bar{1}]_{0,0}$	$[0\bar{1}][\bar{1}]_{0,0,\bar{5}}$	X	X	$d_{\bar{2}}$	d	$d_{\bar{2}}$	d	α
$[\bar{1}0\bar{1}101]$	$[01\bar{1}\bar{1}]_0$	$[1\bar{2}10]_{0,0}$	$[\bar{1}1][\bar{1}]_{0,0,\bar{5}}$	X	X	$d_{\bar{2}}$	d	$d_{\bar{2}}$	d	α

Table 2.8: Embedding of $SO(10)$ and $SU(5)$ into adjoint representation of E_6 (beginning).

E_6	SO(10) $\times U(1)$	SU(5)$\times U(1)^2$	$SU(3) \times SU(2)$ $\times U(1)^3$	I	II	III	IV	V	VI	(Z,ρ)
$[\bar{1}1\bar{1}1\bar{1}1]$	$[11\bar{1}00]_0$	$[2\bar{1}00]_{0,0}$	$[10][\bar{1}]_{0,0,\bar{5}}$	X	X	$d_{\bar{2}}$	d	$d_{\bar{2}}$	d	α
$[01\bar{1}10\bar{1}]$	$[1\bar{1}\bar{1}11]_0$	$[001\bar{2}]_{0,0}$	$[0\bar{1}][1]_{0,0,\bar{5}}$	Y	Y	$u_{\bar{2}}$	u	$u_{\bar{2}}$	u	α
$[00\bar{1}110]$	$[00\bar{1}20]_0$	$[0\bar{1}2\bar{1}]_{0,0}$	$[\bar{1}1][1]_{0,0,\bar{5}}$	Y	Y	$u_{\bar{2}}$	u	$u_{\bar{2}}$	u	α
$[01\bar{1}100]$	$[10\bar{1}11]_0$	$[101\bar{1}]_{0,0}$	$[10][1]_{0,0,\bar{5}}$	Y	Y	$u_{\bar{2}}$	u	$u_{\bar{2}}$	u	α
78	**1**	**1**	**1**,**1**							
[000000]	$[00000]_0$	$[0000]_{0,0}$	$[00][0]_{0,0,0}$	ψ^0	ψ^0	ψ^0	ψ^0	ψ^0	ψ^0	0
78	**45**	**1**	**1**,**1**							
[000000]	$[00000]_0$	$[0000]_{0,0}$	$[00][0]_{0,0,0}$	ϕ^0	ϕ^0	ϕ^0	ϕ^0	ϕ^0	ϕ^0	0
78	**45**	**24**	**1**,**1**							
[000000]	$[00000]_0$	$[0000]_{0,0}$	$[00][0]_{0,0,0}$	γ^0	γ^0	γ^0	γ^0	γ^0	γ^0	0
78	**45**	**24**	**8**,**1**							
$[00000\bar{1}]$	$[0\bar{1}000]_0$	$[\bar{1}00\bar{1}]_{0,0}$	$[\bar{1}\bar{1}][0]_{0,0,0}$	g	g	g	g	g	g	0
$[0100\bar{1}\bar{1}]$	$[1\bar{1}0\bar{1}1]_0$	$[01\bar{1}\bar{1}]_{0,0}$	$[1\bar{2}][0]_{0,0,0}$	g	g	g	g	g	g	0
$[0\bar{1}0010]$	$[\bar{1}001\bar{1}]_0$	$[\bar{1}\bar{1}10]_{0,0}$	$[\bar{2}1][0]_{0,0,0}$	g	g	g	g	g	g	0
[000000]	$[00000]_0$	$[0000]_{0,0}$	$[00][0]_{0,0,0}$	g	g	g	g	g	g	0
78	**45**	**24**	**8**,**1**							
[000000]	$[00000]_0$	$[0000]_{0,0}$	$[00][0]_{0,0,0}$	g	g	g	g	g	g	0
$[0100\bar{1}0]$	$[100\bar{1}1]_0$	$[11\bar{1}0]_{0,0}$	$[2\bar{1}][0]_{0,0,0}$	g	g	g	g	g	g	0
$[0\bar{1}0011]$	$[\bar{1}101\bar{1}]_0$	$[0\bar{1}11]_{0,0}$	$[\bar{1}2][0]_{0,0,0}$	g	g	g	g	g	g	0
[000001]	$[01000]_0$	$[1001]_{0,0}$	$[11][0]_{0,0,0}$	g	g	g	g	g	g	0
78	**45**	**24**	**1**,**3**							
$[\bar{1}000\bar{1}1]$	$[010\bar{1}\bar{1}]_0$	$[1\bar{1}\bar{1}1]_{0,0}$	$[00][\bar{2}]_{0,0,0}$	W^-	W^-	W^-	W^-	W^-	W^-	0
[000000]	$[00000]_0$	$[0000]_{0,0}$	$[00][0]_{0,0,0}$	W^0	W^0	W^0	W^0	W^0	W^0	0
$[10001\bar{1}]$	$[0\bar{1}011]_0$	$[\bar{1}11\bar{1}]_{0,0}$	$[00][2]_{0,0,0}$	W^+	W^+	W^+	W^+	W^+	W^+	0
78	**45**	**24**	$\bar{\mathbf{3}}$,**2**							
$[0\bar{1}1\bar{1}00]$	$[\bar{1}01\bar{1}\bar{1}]_0$	$[\bar{1}0\bar{1}1]_{0,0}$	$[\bar{1}0][\bar{1}]_{0,0,5}$	$\bar{Y}$	$\bar{Y}$	$\bar{u}_{\bar{2}}$	$\bar{u}$	$\bar{u}_{\bar{2}}$	$\bar{u}$	$-\alpha$
$[001\bar{1}\bar{1}0]$	$[001\bar{2}0]_0$	$[01\bar{2}1]_{0,0}$	$[1\bar{1}][\bar{1}]_{0,0,5}$	$\bar{Y}$	$\bar{Y}$	$\bar{u}_{\bar{2}}$	$\bar{u}$	$\bar{u}_{\bar{2}}$	$\bar{u}$	$-\alpha$
$[0\bar{1}1\bar{1}01]$	$[\bar{1}11\bar{1}\bar{1}]_0$	$[00\bar{1}2]_{0,0}$	$[01][\bar{1}]_{0,0,5}$	$\bar{Y}$	$\bar{Y}$	$\bar{u}_{\bar{2}}$	$\bar{u}$	$\bar{u}_{\bar{2}}$	$\bar{u}$	$-\alpha$
$[1\bar{1}1\bar{1}1\bar{1}]$	$[\bar{1}\bar{1}100]_0$	$[\bar{2}100]_{0,0}$	$[\bar{1}0][1]_{0,0,5}$	$\bar{X}$	$\bar{X}$	$\bar{d}_{\bar{2}}$	$\bar{d}$	$\bar{d}_{\bar{2}}$	$\bar{d}$	$-\alpha$
$[101\bar{1}0\bar{1}]$	$[0\bar{1}1\bar{1}1]_0$	$[\bar{1}2\bar{1}0]_{0,0}$	$[1\bar{1}][1]_{0,0,5}$	$\bar{X}$	$\bar{X}$	$\bar{d}_{\bar{2}}$	$\bar{d}$	$\bar{d}_{\bar{2}}$	$\bar{d}$	$-\alpha$
$[1\bar{1}1\bar{1}10]$	$[\bar{1}0100]_0$	$[\bar{1}101]_{0,0}$	$[01][1]_{0,0,5}$	$\bar{X}$	$\bar{X}$	$\bar{d}_{\bar{2}}$	$\bar{d}$	$\bar{d}_{\bar{2}}$	$\bar{d}$	$-\alpha$
78	**45**	**10**	$\bar{\mathbf{3}}$,**1**							
$[\bar{1}0010\bar{1}]$	$[1\bar{1}01\bar{1}]_0$	$[0\bar{1}1\bar{1}]_{0,4}$	$[\bar{1}0][0]_{0,4,\bar{4}}$	$u^c_{\bar{4}}$	u^c	$u^c_{\bar{4}}$	u^c	d^c	d^c	$\alpha+\beta$
$[\bar{1}101\bar{1}\bar{1}]$	$[2\bar{1}000]_0$	$[100\bar{1}]_{0,4}$	$[1\bar{1}][0]_{0,4,\bar{4}}$	$u^c_{\bar{4}}$	u^c	$u^c_{\bar{4}}$	u^c	d^c	d^c	$\alpha+\beta$
$[\bar{1}00100]$	$[1001\bar{1}]_0$	$[1\bar{1}10]_{0,4}$	$[01][0]_{0,4,\bar{4}}$	$u^c_{\bar{4}}$	u^c	$u^c_{\bar{4}}$	u^c	d^c	d^c	$\alpha+\beta$
78	**45**	**10**	**3**,**2**							
$[\bar{1}010\bar{1}\bar{1}]$	$[1\bar{1}1\bar{1}\bar{1}]_0$	$[00\bar{1}0]_{0,4}$	$[0\bar{1}][\bar{1}]_{0,4,1}$	$d_{\bar{2}}$	d	X	X	d	$d_{\bar{2}}$	β
$[\bar{1}\bar{1}1000]$	$[00102\bar{2}]_0$	$[0\bar{1}01]_{0,4}$	$[\bar{1}1][\bar{1}]_{0,4,1}$	$d_{\bar{2}}$	d	X	X	d	$d_{\bar{2}}$	β

Table 2.8: Embedding of $SO(10)$ and $SU(5)$ into adjoint representation of E_6 (continuation).

E_6	SO(10) $\times U(1)$	SU(5)$\times U(1)^2$	$SU(3) \times SU(2)$ $\times U(1)^3$	I	II	III	IV	V	VI	(Z,ρ)
$[\bar{1}010\bar{1}0]$	$[101\bar{1}\bar{1}]_0$	$[10\bar{1}1]_{0,4}$	$[10][\bar{1}]_{0,4,1}$	$d_{\bar{2}}$	d	X	X	d	$d_{\bar{2}}$	β
$[001002\bar{2}]$	$[1\bar{2}100]_0$	$[\bar{1}10\bar{1}]_{0,4}$	$[0\bar{1}][1]_{0,4,1}$	$u_{\bar{2}}$	u	Y	Y	u	$u_{\bar{2}}$	β
$[0\bar{1}101\bar{1}]$	$[0\bar{1}11\bar{1}]_0$	$[\bar{1}010]_{0,4}$	$[\bar{1}1][1]_{0,4,1}$	$u_{\bar{2}}$	u	Y	Y	u	$u_{\bar{2}}$	β
$[001001\bar{1}]$	$[1\bar{1}100]_0$	$[0100]_{0,4}$	$[10][1]_{0,4,1}$	$u_{\bar{2}}$	u	Y	Y	u	$u_{\bar{2}}$	β
78	**45**	**10**	**1**,**1**							
$[0\bar{1}2\bar{1}0\bar{1}]$	$[0\bar{1}2\bar{1}\bar{1}]_0$	$[\bar{1}1\bar{1}1]_{0,4}$	$[00][0]_{0,4,6}$	e_0^c	e^c	$\bar{e}_0^c$	$\bar{e^c}$	ν^c	$\bar{\nu^c}$	$\beta-\alpha$
78	**$\bar{16}$**	**5**	**3**,**1**							
$[10\bar{1}1\bar{1}0]$	$[00\bar{1}01]_3$	$[000\bar{1}]_{3,\bar{3}}$	$[0\bar{1}][0]_{3,\bar{3},\bar{2}}$	$\bar{d}^c$	$\bar{d}^c$	$\bar{u}^c$	$\bar{u}_{\bar{4}}^c$	$\bar{u}^c$	$\bar{u}_{\bar{4}}^c$	$-\beta-\gamma$
$[1\bar{1}\bar{1}101]$	$[\bar{1}1\bar{1}10]_3$	$[0\bar{1}10]_{3,\bar{3}}$	$[\bar{1}1][0]_{3,\bar{3},\bar{2}}$	$\bar{d}^c$	$\bar{d}^c$	$\bar{u}^c$	$\bar{u}_{\bar{4}}^c$	$\bar{u}^c$	$\bar{u}_{\bar{4}}^c$	$-\beta-\gamma$
$[10\bar{1}1\bar{1}1]$	$[01\bar{1}01]_3$	$[1000]_{3,\bar{3}}$	$[10][0]_{3,\bar{3},\bar{2}}$	$\bar{d}^c$	$\bar{d}^c$	$\bar{u}^c$	$\bar{u}_{\bar{4}}^c$	$\bar{u}^c$	$\bar{u}_{\bar{4}}^c$	$-\beta-\gamma$
78	**$\bar{16}$**	**5**	**1**,**2**							
$[1\bar{1}00\bar{1}1]$	$[\bar{1}10\bar{1}0]_3$	$[00\bar{1}1]_{3,\bar{3}}$	$[00][\bar{1}]_{3,\bar{3},3}$	$\bar{\nu}$	$\bar{\nu}$	$\bar{\nu}$	$\bar{\nu}$	$\bar{\nu}$	$\bar{\nu}$	-3ε
$[2\bar{1}0000]$	$[\bar{1}0001]_3$	$[\bar{1}100]_{3,\bar{3}}$	$[00][1]_{3,\bar{3},3}$	$\bar{e}$	$\bar{e}$	$\bar{e}$	$\bar{e}$	$\bar{e}$	$\bar{e}$	-3ε
78	**$\bar{16}$**	**10**	**1**,**1**							
$[00\bar{1}2\bar{1}0]$	$[10\bar{1}10]_3$	$[1\bar{1}1\bar{1}]_{3,1}$	$[00][0]_{3,1,\bar{6}}$	$\bar{e^c}$	$\bar{e}_0^c$	$\bar{\nu^c}$	ν^c	e_0^c	e^c	$\alpha-\gamma$
78	**$\bar{16}$**	**$\bar{10}$**	**$\bar{3}$**,**2**							
$[0\bar{1}01\bar{1}0]$	$[0000\bar{1}]_3$	$[0\bar{1}00]_{3,1}$	$[\bar{1}0][\bar{1}]_{3,1,\bar{1}}$	$\bar{u}$	$\bar{u}_{\bar{2}}$	$\bar{u}$	$\bar{u}_{\bar{2}}$	$\bar{Y}$	$\bar{Y}$	$-\gamma$
$[0001\bar{2}0]$	$[100\bar{1}0]_3$	$[10\bar{1}0]_{3,1}$	$[1\bar{1}][\bar{1}]_{3,1,\bar{1}}$	$\bar{u}$	$\bar{u}_{\bar{2}}$	$\bar{u}$	$\bar{u}_{\bar{2}}$	$\bar{Y}$	$\bar{Y}$	$-\gamma$
$[0\bar{1}01\bar{1}1]$	$[0100\bar{1}]_3$	$[1\bar{1}01]_{3,1}$	$[01][\bar{1}]_{3,1,\bar{1}}$	$\bar{u}$	$\bar{u}_{\bar{2}}$	$\bar{u}$	$\bar{u}_{\bar{2}}$	$\bar{Y}$	$\bar{Y}$	$-\gamma$
$[1\bar{1}010\bar{1}]$	$[0\bar{1}010]_3$	$[\bar{1}01\bar{1}]_{3,1}$	$[\bar{1}0][1]_{3,1,\bar{1}}$	$\bar{d}$	$\bar{d}_{\bar{2}}$	$\bar{d}$	$\bar{d}_{\bar{2}}$	$\bar{X}$	$\bar{X}$	$-\gamma$
$[1001\bar{1}\bar{1}]$	$[1\bar{1}001]_3$	$[010\bar{1}]_{3,1}$	$[1\bar{1}][1]_{3,1,\bar{1}}$	$\bar{d}$	$\bar{d}_{\bar{2}}$	$\bar{d}$	$\bar{d}_{\bar{2}}$	$\bar{X}$	$\bar{X}$	$-\gamma$
$[1\bar{1}0100]$	$[00010]_3$	$[0010]_{3,1}$	$[01][1]_{3,1,\bar{1}}$	$\bar{d}$	$\bar{d}_{\bar{2}}$	$\bar{d}$	$\bar{d}_{\bar{2}}$	$\bar{X}$	$\bar{X}$	$-\gamma$
78	**$\bar{16}$**	**$\bar{10}$**	**3**,**1**							
$[1\bar{1}10\bar{1}\bar{1}]$	$[0\bar{1}1\bar{1}0]_3$	$[\bar{1}1\bar{1}0]_{3,1}$	$[0\bar{1}][0]_{3,1,4}$	$\bar{u}^c$	$\bar{u}_{\bar{4}}^c$	$\bar{d}^c$	$\bar{d}^c$	$\bar{u}_{\bar{4}}^c$	$\bar{u}^c$	$-\alpha-\gamma$
$[1\bar{2}1000]$	$[\bar{1}010\bar{1}]_3$	$[\bar{1}001]_{3,1}$	$[\bar{1}1][0]_{3,1,4}$	$\bar{u}^c$	$\bar{u}_{\bar{4}}^c$	$\bar{d}^c$	$\bar{d}^c$	$\bar{u}_{\bar{4}}^c$	$\bar{u}^c$	$-\alpha-\gamma$
$[1\bar{1}10\bar{1}0]$	$[001\bar{1}0]_3$	$[01\bar{1}1]_{3,1}$	$[10][0]_{3,1,4}$	$\bar{u}^c$	$\bar{u}_{\bar{4}}^c$	$\bar{d}^c$	$\bar{d}^c$	$\bar{u}_{\bar{4}}^c$	$\bar{u}^c$	$-\alpha-\gamma$
78	**$\bar{16}$**	**1**	**1**,**1**							
$[0\bar{1}11\bar{1}\bar{1}]$	$[1\bar{1}10\bar{1}]_3$	$[0000]_{3,5}$	$[00][0]_{3,5,0}$	$\bar{\nu^c}$	ν^c	$\bar{e^c}$	$\bar{e}_0^c$	e^c	e_0^c	$\beta-\gamma$

Table 2.8: Embedding of $SO(10)$ and $SU(5)$ into adjoint representation of E_6 (continuation).

As is readily seen from table 2.7 along with one (**3**,**2**), two ($\bar{\mathbf{3}}$,**1**), one (**1**,**2**) and one (**1**,**1**) representations of $SU(3) \otimes SU(2)$ which contain respectively the left– and the right–handed Standard Model quarks, the leptonic doublet and the right–handed electron, the fundamental representation of E_6 also fits additional (**3**,**1**) and ($\bar{\mathbf{3}}$,**1**) representations which contain new quarks, two additional (**1**,**2**) representations, which contain new leptons, and two additional (**1**,**1**) representations containing the Standard Model singlets. Likewise, apart from the Standard Model gauge fields, the adjoint of E_6 contains a rich spectrum of new states including those mediating the proton decay. This issue will be discussed in more detail in section 2.3.

E_6	$SU(3)$			$SU(2)_{,Y}$				Assignments						(Z,ρ)
	C	L	R	L	R	$R^{'}$	$R^{''}$	I	II	III	IV	V	VI	
27	**3**	**3**	**1**	**2**										
$[100000]$	$[10]$	$[10]$	$[00]$	$[1]_{,1}$	$[0]_{,0}$	$[0]_{,0}$	$[0]_{,0}$	u	u	u	u	u	u	$-\varepsilon$
$[1\bar{1}0010]$	$[\bar{1}1]$	$[10]$	$[00]$	$[1]_{,1}$	$[0]_{,0}$	$[0]_{,0}$	$[0]_{,0}$	u	u	u	u	u	u	$-\varepsilon$
$[10000\bar{1}]$	$[0\bar{1}]$	$[10]$	$[00]$	$[1]_{,1}$	$[0]_{,0}$	$[0]_{,0}$	$[0]_{,0}$	u	u	u	u	u	u	$-\varepsilon$
$[0000\bar{1}1]$	$[10]$	$[\bar{1}1]$	$[00]$	$[\bar{1}]_{,1}$	$[0]_{,0}$	$[0]_{,0}$	$[0]_{,0}$	d	d	d	d	d	d	$-\varepsilon$
$[0\bar{1}0001]$	$[\bar{1}1]$	$[\bar{1}1]$	$[00]$	$[\bar{1}]_{,1}$	$[0]_{,0}$	$[0]_{,0}$	$[0]_{,0}$	d	d	d	d	d	d	$-\varepsilon$
$[0000\bar{1}0]$	$[0\bar{1}]$	$[\bar{1}1]$	$[00]$	$[\bar{1}]_{,1}$	$[0]_{,0}$	$[0]_{,0}$	$[0]_{,0}$	d	d	d	d	d	d	$-\varepsilon$
27	**3**	**3**	**1**	**1**										
$[\bar{1}10000]$	$[10]$	$[0\bar{1}]$	$[00]$	$[0]_{,\bar{2}}$	$[0]_{,0}$	$[0]_{,0}$	$[0]_{,0}$	D	D	D	D	D	D	2ε
$[\bar{1}00010]$	$[\bar{1}1]$	$[0\bar{1}]$	$[00]$	$[0]_{,\bar{2}}$	$[0]_{,0}$	$[0]_{,0}$	$[0]_{,0}$	D	D	D	D	D	D	2ε
$[\bar{1}1000\bar{1}]$	$[0\bar{1}]$	$[0\bar{1}]$	$[00]$	$[0]_{,\bar{2}}$	$[0]_{,0}$	$[0]_{,0}$	$[0]_{,0}$	D	D	D	D	D	D	2ε
27	$\bar{\mathbf{3}}$	**1**	$\bar{\mathbf{3}}$	**1**										
$[00\bar{1}101]$	$[01]$	$[00]$	$[\bar{1}0]$	$[0]_{,0}$	$[\bar{1}]_{,\bar{1}}$	$[\bar{1}]_{,\bar{1}}$	$[0]_{,2}$	u^c	u^c	d^c	D^c	d^c	D^c	$-\varepsilon+\alpha$
$[01\bar{1}1\bar{1}0]$	$[1\bar{1}]$	$[00]$	$[\bar{1}0]$	$[0]_{,0}$	$[\bar{1}]_{,\bar{1}}$	$[\bar{1}]_{,\bar{1}}$	$[0]_{,2}$	u^c	u^c	d^c	D^c	d^c	D^c	$-\varepsilon+\alpha$
$[00\bar{1}100]$	$[\bar{1}0]$	$[00]$	$[\bar{1}0]$	$[0]_{,0}$	$[\bar{1}]_{,\bar{1}}$	$[\bar{1}]_{,\bar{1}}$	$[0]_{,2}$	u^c	u^c	d^c	D^c	d^c	D^c	$-\varepsilon+\alpha$
$[000\bar{1}11]$	$[01]$	$[00]$	$[01]$	$[0]_{,0}$	$[0]_{,2}$	$[1]_{,\bar{1}}$	$[1]_{,\bar{1}}$	D^c	d^c	D^c	d^c	u^c	u^c	$-\varepsilon+\gamma$
$[010\bar{1}00]$	$[1\bar{1}]$	$[00]$	$[01]$	$[0]_{,0}$	$[0]_{,2}$	$[1]_{,\bar{1}}$	$[1]_{,\bar{1}}$	D^c	d^c	D^c	d^c	u^c	u^c	$-\varepsilon+\gamma$
$[000\bar{1}10]$	$[\bar{1}0]$	$[00]$	$[01]$	$[0]_{,0}$	$[0]_{,2}$	$[1]_{,\bar{1}}$	$[1]_{,\bar{1}}$	D^c	d^c	D^c	d^c	u^c	u^c	$-\varepsilon+\gamma$
$[0\bar{1}1000]$	$[01]$	$[00]$	$[1\bar{1}]$	$[0]_{,0}$	$[1]_{,\bar{1}}$	$[0]_{,2}$	$[\bar{1}]_{,\bar{1}}$	d^c	D^c	u^c	u^c	D^c	d^c	$-\varepsilon+\beta$
$[0010\bar{1}\bar{1}]$	$[1\bar{1}]$	$[00]$	$[1\bar{1}]$	$[0]_{,0}$	$[1]_{,\bar{1}}$	$[0]_{,2}$	$[\bar{1}]_{,\bar{1}}$	d^c	D^c	u^c	u^c	D^c	d^c	$-\varepsilon+\beta$
$[0\bar{1}100\bar{1}]$	$[\bar{1}0]$	$[00]$	$[1\bar{1}]$	$[0]_{,0}$	$[1]_{,\bar{1}}$	$[0]_{,2}$	$[\bar{1}]_{,\bar{1}}$	d^c	D^c	u^c	u^c	D^c	d^c	$-\varepsilon+\beta$
27	**1**	$\bar{\mathbf{3}}$	**3**	**2**										
$[001\bar{1}1\bar{1}]$	$[00]$	$[1\bar{1}]$	$[10]$	$[1]_{,\bar{1}}$	$[1]_{,1}$	$[1]_{,1}$	$[0]_{,\bar{2}}$	E^c	E^c	N	ν	N	ν	$2\varepsilon-\alpha$
$[\bar{1}01\bar{1}00]$	$[00]$	$[\bar{1}0]$	$[10]$	$[\bar{1}]_{,\bar{1}}$	$[1]_{,1}$	$[1]_{,1}$	$[0]_{,\bar{2}}$	N^c	N^c	E	e	E	e	$2\varepsilon-\alpha$
$[01\bar{1}010]$	$[00]$	$[1\bar{1}]$	$[\bar{1}1]$	$[1]_{,\bar{1}}$	$[\bar{1}]_{,1}$	$[0]_{,\bar{2}}$	$[1]_{,1}$	N	ν	E^c	E^c	ν	N	$2\varepsilon-\beta$
$[\bar{1}1\bar{1}001]$	$[00]$	$[\bar{1}0]$	$[\bar{1}1]$	$[\bar{1}]_{,\bar{1}}$	$[\bar{1}]_{,1}$	$[0]_{,\bar{2}}$	$[1]_{,1}$	E	e	N^c	N^c	e	E	$2\varepsilon-\beta$
$[00010\bar{1}]$	$[00]$	$[1\bar{1}]$	$[0\bar{1}]$	$[1]_{,\bar{1}}$	$[0]_{,\bar{2}}$	$[\bar{1}]_{,1}$	$[\bar{1}]_{,1}$	ν	N	ν	N	E^c	E^c	$2\varepsilon-\gamma$
$[\bar{1}001\bar{1}0]$	$[00]$	$[\bar{1}0]$	$[0\bar{1}]$	$[\bar{1}]_{,\bar{1}}$	$[0]_{,\bar{2}}$	$[\bar{1}]_{,1}$	$[\bar{1}]_{,1}$	e	E	e	E	N^c	N^c	$2\varepsilon-\gamma$
27	**1**	$\bar{\mathbf{3}}$	**3**	**1**										
$[1\bar{1}1\bar{1}00]$	$[00]$	$[01]$	$[10]$	$[0]_{,2}$	$[1]_{,1}$	$[1]_{,1}$	$[0]_{,\bar{2}}$	e^c	e^c	ν^c	S	ν^c	S	$-\varepsilon-\alpha$
$[10\bar{1}001]$	$[00]$	$[01]$	$[\bar{1}1]$	$[0]_{,2}$	$[\bar{1}]_{,1}$	$[0]_{,\bar{2}}$	$[1]_{,1}$	ν^c	S	e^c	e^c	S	ν^c	$-\varepsilon-\beta$
$[1\bar{1}01\bar{1}0]$	$[00]$	$[01]$	$[0\bar{1}]$	$[0]_{,2}$	$[0]_{,\bar{2}}$	$[\bar{1}]_{,1}$	$[\bar{1}]_{,1}$	S	ν^c	S	ν^c	e^c	e^c	$-\varepsilon-\gamma$

Table 2.9: Embedding of $SU(3)\otimes SU(3)\otimes SU(3)$ into fundamental representation of E_6. Here $\varepsilon=\frac{1}{3}(\alpha+\beta+\gamma)$, $\bar{x}\equiv -x$. The zero root breaking SM gauge group preserving direction is given by $Z=(-\varepsilon,\varepsilon,\beta,2\varepsilon-\gamma,\varepsilon,0)$.

E_6	$SU(3)$			$SU(2)_{,Y}$				Assignments						(Z,ρ)
	C	L	R	L	R	$R^{'}$	$R^{''}$	I	II	III	IV	V	VI	
78	**1**	**8**	**1**											
$[2\bar{1}0000]$	[00]	[11]	[00]	$[1]_{,3}$	$[0]_{,0}$	$[0]_{,0}$	$[0]_{,0}$	$\bar{e}$	$\bar{e}$	$\bar{e}$	$\bar{e}$	$\bar{e}$	$\bar{e}$	-3ε
$[1\bar{1}00\bar{1}1]$	[00]	$[\bar{1}2]$	[00]	$[\bar{1}]_{,3}$	$[0]_{,0}$	$[0]_{,0}$	$[0]_{,0}$	$\bar{\nu}$	$\bar{\nu}$	$\bar{\nu}$	$\bar{\nu}$	$\bar{\nu}$	$\bar{\nu}$	-3ε
$[10001\bar{1}]$	[00]	$[2\bar{1}]$	[00]	$[2]_{,0}$	$[0]_{,0}$	$[0]_{,0}$	$[0]_{,0}$	W^+	W^+	W^+	W^+	W^+	W^+	0
[000000]	[00]	[00]	[00]	$[0]_{,0}$	$[0]_{,0}$	$[0]_{,0}$	$[0]_{,0}$	W^0	W^0	W^0	W^0	W^0	W^0	0
$[\bar{1}000\bar{1}1]$	[00]	$[\bar{2}1]$	[00]	$[\bar{2}]_{,0}$	$[0]_{,0}$	$[0]_{,0}$	$[0]_{,0}$	W^-	W^-	W^-	W^-	W^-	W^-	0
$[\bar{1}1001\bar{1}]$	[00]	$[1\bar{2}]$	[00]	$[1]_{,\bar{3}}$	$[0]_{,0}$	$[0]_{,0}$	$[0]_{,0}$	ν	ν	ν	ν	ν	ν	3ε
$[\bar{2}10000]$	[00]	$[\bar{1}\bar{1}]$	[00]	$[\bar{1}]_{,\bar{3}}$	$[0]_{,0}$	$[0]_{,0}$	$[0]_{,0}$	e	e	e	e	e	e	3ε
[000000]	[00]	[00]	[00]	$[0]_{,0}$	$[0]_{,0}$	$[0]_{,0}$	$[0]_{,0}$	γ^0	γ^0	γ^0	γ^0	γ^0	γ^0	0
78	**1**	**1**	**8**											
$[001\bar{2}10]$	[00]	[00]	[11]	$[0]_{,0}$	$[1]_{,3}$	$[2]_{,0}$	$[1]_{,\bar{3}}$	e^c	e_0^c	ν^c	$\bar{\nu^c}$	$\bar{e}_0^c$	$\bar{e}^c$	$\gamma-\alpha$
$[01\bar{1}\bar{1}11]$	[00]	[00]	$[\bar{1}2]$	$[0]_{,0}$	$[\bar{1}]_{,3}$	$[1]_{,\bar{3}}$	$[2]_{,0}$	ν^c	$\bar{\nu^c}$	e^c	e_0^c	$\bar{e}^c$	$\bar{e}_0^c$	$\gamma-\beta$
$[0\bar{1}2\bar{1}0\bar{1}]$	[00]	[00]	$[2\bar{1}]$	$[0]_{,0}$	$[2]_{,0}$	$[1]_{,3}$	$[\bar{1}]_{,\bar{3}}$	e_0^c	e^c	$\bar{e}_0^c$	$\bar{e}^c$	ν^c	$\bar{\nu^c}$	$\beta-\alpha$
[000000]	[00]	[00]	[00]	$[0]_{,0}$	$[0]_{,0}$	$[0]_{,0}$	$[0]_{,0}$	ϕ^0	ϕ^0	ϕ^0	ϕ^0	ϕ^0	ϕ^0	0
$[01\bar{2}101]$	[00]	[00]	$[\bar{2}1]$	$[0]_{,0}$	$[\bar{2}]_{,0}$	$[\bar{1}]_{,\bar{3}}$	$[1]_{,3}$	$\bar{e}_0^c$	$\bar{e}^c$	e_0^c	e^c	$\bar{\nu^c}$	ν^c	$\alpha-\beta$
$[0\bar{1}11\bar{1}\bar{1}]$	[00]	[00]	$[1\bar{2}]$	$[0]_{,0}$	$[1]_{,\bar{3}}$	$[\bar{1}]_{,3}$	$[\bar{2}]_{,0}$	$\bar{\nu^c}$	ν^c	$\bar{e}^c$	$\bar{e}_0^c$	e^c	e_0^c	$\beta-\gamma$
$[00\bar{1}2\bar{1}0]$	[00]	[00]	$[\bar{1}\bar{1}]$	$[0]_{,0}$	$[\bar{1}]_{,\bar{3}}$	$[\bar{2}]_{,0}$	$[\bar{1}]_{,3}$	$\bar{e}^c$	$\bar{e}_0^c$	$\bar{\nu^c}$	ν^c	e_0^c	e^c	$\alpha-\gamma$
[000000]	[00]	[00]	[00]	$[0]_{,0}$	$[0]_{,0}$	$[0]_{,0}$	$[0]_{,0}$	ω^0	ω^0	ω^0	ω^0	ω^0	ω^0	0
78	**8**	**1**	**1**											
[000001]	[11]	[00]	[00]	$[0]_{,0}$	$[0]_{,0}$	$[0]_{,0}$	$[0]_{,0}$	g	g	g	g	g	g	0
$[0\bar{1}0011]$	$[\bar{1}2]$	[00]	[00]	$[0]_{,0}$	$[0]_{,0}$	$[0]_{,0}$	$[0]_{,0}$	g	g	g	g	g	g	0
$[0100\bar{1}0]$	$[2\bar{1}]$	[00]	[00]	$[0]_{,0}$	$[0]_{,0}$	$[0]_{,0}$	$[0]_{,0}$	g	g	g	g	g	g	0
[000000]	[00]	[00]	[00]	$[0]_{,0}$	$[0]_{,0}$	$[0]_{,0}$	$[0]_{,0}$	g	g	g	g	g	g	0
[000000]	[00]	[00]	[00]	$[0]_{,0}$	$[0]_{,0}$	$[0]_{,0}$	$[0]_{,0}$	g	g	g	g	g	g	0
$[0100\bar{1}\bar{1}]$	$[1\bar{2}]$	[00]	[00]	$[0]_{,0}$	$[0]_{,0}$	$[0]_{,0}$	$[0]_{,0}$	g	g	g	g	g	g	0
$[0\bar{1}0010]$	$[\bar{2}1]$	[00]	[00]	$[0]_{,0}$	$[0]_{,0}$	$[0]_{,0}$	$[0]_{,0}$	g	g	g	g	g	g	0
$[00000\bar{1}]$	$[\bar{1}\bar{1}]$	[00]	[00]	$[0]_{,0}$	$[0]_{,0}$	$[0]_{,0}$	$[0]_{,0}$	g	g	g	g	g	g	0
78	$\bar{\mathbf{3}}$	**3**	**3**											
$[1\bar{1}1\bar{1}10]$	[01]	[10]	[10]	$[1]_{,1}$	$[1]_{,1}$	$[1]_{,1}$	$[0]_{,\bar{2}}$	$\bar{X}$	$\bar{X}$	$\bar{d}_{\bar{2}}$	$\bar{d}$	$\bar{d}_{\bar{2}}$	$\bar{d}$	$-\alpha$
$[101\bar{1}0\bar{1}]$	$[1\bar{1}]$	[10]	[10]	$[1]_{,1}$	$[1]_{,1}$	$[1]_{,1}$	$[0]_{,\bar{2}}$	$\bar{X}$	$\bar{X}$	$\bar{d}_{\bar{2}}$	$\bar{d}$	$\bar{d}_{\bar{2}}$	$\bar{d}$	$-\alpha$
$[1\bar{1}1\bar{1}1\bar{1}]$	$[\bar{1}0]$	[10]	[10]	$[1]_{,1}$	$[1]_{,1}$	$[1]_{,1}$	$[0]_{,\bar{2}}$	$\bar{X}$	$\bar{X}$	$\bar{d}_{\bar{2}}$	$\bar{d}$	$\bar{d}_{\bar{2}}$	$\bar{d}$	$-\alpha$
$[10\bar{1}011]$	[01]	[10]	$[\bar{1}1]$	$[1]_{,1}$	$[\bar{1}]_{,1}$	$[0]_{,\bar{2}}$	$[1]_{,1}$	$\bar{d}_{\bar{2}}$	$\bar{d}$	$\bar{X}$	$\bar{X}$	$\bar{d}$	$\bar{d}_{\bar{2}}$	$-\beta$
$[11\bar{1}000]$	$[1\bar{1}]$	[10]	$[\bar{1}1]$	$[1]_{,1}$	$[\bar{1}]_{,1}$	$[0]_{,\bar{2}}$	$[1]_{,1}$	$\bar{d}_{\bar{2}}$	$\bar{d}$	$\bar{X}$	$\bar{X}$	$\bar{d}$	$\bar{d}_{\bar{2}}$	$-\beta$

Table 2.10: Embedding of $SU(3)\otimes SU(3)\otimes SU(3)$ into adjoint representation of E_6 (beginning). Color, isospin and hypercharge (as well as $B-L$, unless otherwise indicated) of the states designated like the SM states are the same as charges of their SM counterparts. If present, the subscript is thrice the $B-L$ charge. All charges of overlined states are opposite to those of non overlined ones. For example, for $\bar{d}_{\bar{2}}$: $I_3=\frac{1}{2}$, $Y=-\frac{1}{3}$, $B-L=\frac{2}{3}$.

E_6	$SU(3)$			$SU(2)_{,Y}$				Assignments						(Z,ρ)
	C	L	R	L	R	$R^{'}$	$R^{''}$	I	II	III	IV	V	VI	
78	$\bar{\mathbf{3}}$	**3**	**3**											
$[10\bar{1}010]$	$[\bar{1}0]$	$[10]$	$[\bar{1}1]$	$[1]_{,1}$	$[\bar{1}]_{,1}$	$[0]_{,\bar{2}}$	$[1]_{,1}$	$\bar{d}_{\bar{2}}$	$\bar{d}$	$\bar{X}$	$\bar{X}$	$\bar{d}$	$\bar{d}_{\bar{2}}$	$-\beta$
$[1\bar{1}0100]$	$[01]$	$[10]$	$[0\bar{1}]$	$[1]_{,1}$	$[0]_{,\bar{2}}$	$[\bar{1}]_{,1}$	$[\bar{1}]_{,1}$	$\bar{d}$	$\bar{d}_{\bar{2}}$	$\bar{d}$	$\bar{d}_{\bar{2}}$	$\bar{X}$	$\bar{X}$	$-\gamma$
$[1001\bar{1}\bar{1}]$	$[1\bar{1}]$	$[10]$	$[0\bar{1}]$	$[1]_{,1}$	$[0]_{,\bar{2}}$	$[\bar{1}]_{,1}$	$[\bar{1}]_{,1}$	$\bar{d}$	$\bar{d}_{\bar{2}}$	$\bar{d}$	$\bar{d}_{\bar{2}}$	$\bar{X}$	$\bar{X}$	$-\gamma$
$[1\bar{1}010\bar{1}]$	$[\bar{1}0]$	$[10]$	$[0\bar{1}]$	$[1]_{,1}$	$[0]_{,\bar{2}}$	$[\bar{1}]_{,1}$	$[\bar{1}]_{,1}$	$\bar{d}$	$\bar{d}_{\bar{2}}$	$\bar{d}$	$\bar{d}_{\bar{2}}$	$\bar{X}$	$\bar{X}$	$-\gamma$
$[0\bar{1}1\bar{1}01]$	$[01]$	$[\bar{1}1]$	$[10]$	$[\bar{1}]_{,1}$	$[1]_{,1}$	$[1]_{,1}$	$[0]_{,\bar{2}}$	$\bar{Y}$	$\bar{Y}$	$\bar{u}_{\bar{2}}$	$\bar{u}$	$\bar{u}_{\bar{2}}$	$\bar{u}$	$-\alpha$
$[001\bar{1}\bar{1}0]$	$[1\bar{1}]$	$[\bar{1}1]$	$[10]$	$[\bar{1}]_{,1}$	$[1]_{,1}$	$[1]_{,1}$	$[0]_{,\bar{2}}$	$\bar{Y}$	$\bar{Y}$	$\bar{u}_{\bar{2}}$	$\bar{u}$	$\bar{u}_{\bar{2}}$	$\bar{u}$	$-\alpha$
$[0\bar{1}1\bar{1}00]$	$[\bar{1}0]$	$[\bar{1}1]$	$[10]$	$[\bar{1}]_{,1}$	$[1]_{,1}$	$[1]_{,1}$	$[0]_{,\bar{2}}$	$\bar{Y}$	$\bar{Y}$	$\bar{u}_{\bar{2}}$	$\bar{u}$	$\bar{u}_{\bar{2}}$	$\bar{u}$	$-\alpha$
$[00\bar{1}002]$	$[01]$	$[\bar{1}1]$	$[\bar{1}1]$	$[\bar{1}]_{,1}$	$[\bar{1}]_{,1}$	$[0]_{,\bar{2}}$	$[1]_{,1}$	$\bar{u}_{\bar{2}}$	$\bar{u}$	$\bar{Y}$	$\bar{Y}$	$\bar{u}$	$\bar{u}_{\bar{2}}$	$-\beta$
$[01\bar{1}0\bar{1}1]$	$[1\bar{1}]$	$[\bar{1}1]$	$[\bar{1}1]$	$[\bar{1}]_{,1}$	$[\bar{1}]_{,1}$	$[0]_{,\bar{2}}$	$[1]_{,1}$	$\bar{u}_{\bar{2}}$	$\bar{u}$	$\bar{Y}$	$\bar{Y}$	$\bar{u}$	$\bar{u}_{\bar{2}}$	$-\beta$
$[00\bar{1}001]$	$[\bar{1}0]$	$[\bar{1}1]$	$[\bar{1}1]$	$[\bar{1}]_{,1}$	$[\bar{1}]_{,1}$	$[0]_{,\bar{2}}$	$[1]_{,1}$	$\bar{u}_{\bar{2}}$	$\bar{u}$	$\bar{Y}$	$\bar{Y}$	$\bar{u}$	$\bar{u}_{\bar{2}}$	$-\beta$
$[0\bar{1}01\bar{1}1]$	$[01]$	$[\bar{1}1]$	$[0\bar{1}]$	$[\bar{1}]_{,1}$	$[0]_{,\bar{2}}$	$[\bar{1}]_{,1}$	$[\bar{1}]_{,1}$	$\bar{u}$	$\bar{u}_{\bar{2}}$	$\bar{u}$	$\bar{u}_{\bar{2}}$	$\bar{Y}$	$\bar{Y}$	$-\gamma$
$[0001\bar{2}0]$	$[1\bar{1}]$	$[\bar{1}1]$	$[0\bar{1}]$	$[\bar{1}]_{,1}$	$[0]_{,\bar{2}}$	$[\bar{1}]_{,1}$	$[\bar{1}]_{,1}$	$\bar{u}$	$\bar{u}_{\bar{2}}$	$\bar{u}$	$\bar{u}_{\bar{2}}$	$\bar{Y}$	$\bar{Y}$	$-\gamma$
$[0\bar{1}01\bar{1}0]$	$[\bar{1}0]$	$[\bar{1}1]$	$[0\bar{1}]$	$[\bar{1}]_{,1}$	$[0]_{,\bar{2}}$	$[\bar{1}]_{,1}$	$[\bar{1}]_{,1}$	$\bar{u}$	$\bar{u}_{\bar{2}}$	$\bar{u}$	$\bar{u}_{\bar{2}}$	$\bar{Y}$	$\bar{Y}$	$-\gamma$
$[\bar{1}01\bar{1}10]$	$[01]$	$[0\bar{1}]$	$[10]$	$[0]_{,\bar{2}}$	$[1]_{,1}$	$[1]_{,1}$	$[0]_{,\bar{2}}$	d^c	d^c	u^c	$u^c_{\bar{4}}$	u^c	$u^c_{\bar{4}}$	$\beta+\gamma$
$[\bar{1}11\bar{1}0\bar{1}]$	$[1\bar{1}]$	$[0\bar{1}]$	$[10]$	$[0]_{,\bar{2}}$	$[1]_{,1}$	$[1]_{,1}$	$[0]_{,\bar{2}}$	d^c	d^c	u^c	$u^c_{\bar{4}}$	u^c	$u^c_{\bar{4}}$	$\beta+\gamma$
$[\bar{1}01\bar{1}1\bar{1}]$	$[\bar{1}0]$	$[0\bar{1}]$	$[10]$	$[0]_{,\bar{2}}$	$[1]_{,1}$	$[1]_{,1}$	$[0]_{,\bar{2}}$	d^c	d^c	u^c	$u^c_{\bar{4}}$	u^c	$u^c_{\bar{4}}$	$\beta+\gamma$
$[\bar{1}1\bar{1}011]$	$[01]$	$[0\bar{1}]$	$[\bar{1}1]$	$[0]_{,\bar{2}}$	$[\bar{1}]_{,1}$	$[0]_{,\bar{2}}$	$[1]_{,1}$	u^c	$u^c_{\bar{4}}$	d^c	d^c	$u^c_{\bar{4}}$	u^c	$\alpha+\gamma$
$[\bar{1}2\bar{1}000]$	$[1\bar{1}]$	$[0\bar{1}]$	$[\bar{1}1]$	$[0]_{,\bar{2}}$	$[\bar{1}]_{,1}$	$[0]_{,\bar{2}}$	$[1]_{,1}$	u^c	$u^c_{\bar{4}}$	d^c	d^c	$u^c_{\bar{4}}$	u^c	$\alpha+\gamma$
$[\bar{1}1\bar{1}010]$	$[\bar{1}0]$	$[0\bar{1}]$	$[\bar{1}1]$	$[0]_{,\bar{2}}$	$[\bar{1}]_{,1}$	$[0]_{,\bar{2}}$	$[1]_{,1}$	u^c	$u^c_{\bar{4}}$	d^c	d^c	$u^c_{\bar{4}}$	u^c	$\alpha+\gamma$
$[\bar{1}00100]$	$[01]$	$[0\bar{1}]$	$[0\bar{1}]$	$[0]_{,\bar{2}}$	$[0]_{,\bar{2}}$	$[\bar{1}]_{,1}$	$[\bar{1}]_{,1}$	$u^c_{\bar{4}}$	u^c	$u^c_{\bar{4}}$	u^c	d^c	d^c	$\alpha+\beta$
$[\bar{1}101\bar{1}\bar{1}]$	$[1\bar{1}]$	$[0\bar{1}]$	$[0\bar{1}]$	$[0]_{,\bar{2}}$	$[0]_{,\bar{2}}$	$[\bar{1}]_{,1}$	$[\bar{1}]_{,1}$	$u^c_{\bar{4}}$	u^c	$u^c_{\bar{4}}$	u^c	d^c	d^c	$\alpha+\beta$
$[\bar{1}0010\bar{1}]$	$[\bar{1}0]$	$[0\bar{1}]$	$[0\bar{1}]$	$[0]_{,\bar{2}}$	$[0]_{,\bar{2}}$	$[\bar{1}]_{,1}$	$[\bar{1}]_{,1}$	$u^c_{\bar{4}}$	u^c	$u^c_{\bar{4}}$	u^c	d^c	d^c	$\alpha+\beta$
78	**3**	$\bar{\mathbf{3}}$	$\bar{\mathbf{3}}$											
$[100\bar{1}01]$	$[10]$	$[01]$	$[01]$	$[0]_{,2}$	$[0]_{,2}$	$[1]_{,\bar{1}}$	$[1]_{,\bar{1}}$	$\bar{u}^c_{\bar{4}}$	$\bar{u}^c$	$\bar{u}^c_{\bar{4}}$	$\bar{u}^c$	$\bar{d}^c$	$\bar{d}^c$	$-\alpha-\beta$
$[1\bar{1}0\bar{1}11]$	$[\bar{1}1]$	$[01]$	$[01]$	$[0]_{,2}$	$[0]_{,2}$	$[1]_{,\bar{1}}$	$[1]_{,\bar{1}}$	$\bar{u}^c_{\bar{4}}$	$\bar{u}^c$	$\bar{u}^c_{\bar{4}}$	$\bar{u}^c$	$\bar{d}^c$	$\bar{d}^c$	$-\alpha-\beta$
$[100\bar{1}00]$	$[0\bar{1}]$	$[01]$	$[01]$	$[0]_{,2}$	$[0]_{,2}$	$[1]_{,\bar{1}}$	$[1]_{,\bar{1}}$	$\bar{u}^c_{\bar{4}}$	$\bar{u}^c$	$\bar{u}^c_{\bar{4}}$	$\bar{u}^c$	$\bar{d}^c$	$\bar{d}^c$	$-\alpha-\beta$
$[1\bar{1}10\bar{1}0]$	$[10]$	$[01]$	$[1\bar{1}]$	$[0]_{,2}$	$[1]_{,\bar{1}}$	$[0]_{,2}$	$[\bar{1}]_{,\bar{1}}$	$\bar{u}^c$	$\bar{u}^c_{\bar{4}}$	$\bar{d}^c$	$\bar{d}^c$	$\bar{u}^c_{\bar{4}}$	$\bar{u}^c$	$-\alpha-\gamma$
$[1\bar{2}1000]$	$[\bar{1}1]$	$[01]$	$[1\bar{1}]$	$[0]_{,2}$	$[1]_{,\bar{1}}$	$[0]_{,2}$	$[\bar{1}]_{,\bar{1}}$	$\bar{u}^c$	$\bar{u}^c_{\bar{4}}$	$\bar{d}^c$	$\bar{d}^c$	$\bar{u}^c_{\bar{4}}$	$\bar{u}^c$	$-\alpha-\gamma$
$[1\bar{1}10\bar{1}\bar{1}]$	$[0\bar{1}]$	$[01]$	$[1\bar{1}]$	$[0]_{,2}$	$[1]_{,\bar{1}}$	$[0]_{,2}$	$[\bar{1}]_{,\bar{1}}$	$\bar{u}^c$	$\bar{u}^c_{\bar{4}}$	$\bar{d}^c$	$\bar{d}^c$	$\bar{u}^c_{\bar{4}}$	$\bar{u}^c$	$-\alpha-\gamma$
$[10\bar{1}1\bar{1}1]$	$[10]$	$[01]$	$[\bar{1}0]$	$[0]_{,2}$	$[\bar{1}]_{,\bar{1}}$	$[\bar{1}]_{,\bar{1}}$	$[0]_{,2}$	$\bar{d}^c$	$\bar{d}^c$	$\bar{u}^c$	$\bar{u}^c_{\bar{4}}$	$\bar{u}^c$	$\bar{u}^c_{\bar{4}}$	$-\beta-\gamma$
$[1\bar{1}\bar{1}101]$	$[\bar{1}1]$	$[01]$	$[\bar{1}0]$	$[0]_{,2}$	$[\bar{1}]_{,\bar{1}}$	$[\bar{1}]_{,\bar{1}}$	$[0]_{,2}$	$\bar{d}^c$	$\bar{d}^c$	$\bar{u}^c$	$\bar{u}^c_{\bar{4}}$	$\bar{u}^c$	$\bar{u}^c_{\bar{4}}$	$-\beta-\gamma$
$[10\bar{1}1\bar{1}0]$	$[0\bar{1}]$	$[01]$	$[\bar{1}0]$	$[0]_{,2}$	$[\bar{1}]_{,\bar{1}}$	$[\bar{1}]_{,\bar{1}}$	$[0]_{,2}$	$\bar{d}^c$	$\bar{d}^c$	$\bar{u}^c$	$\bar{u}^c_{\bar{4}}$	$\bar{u}^c$	$\bar{u}^c_{\bar{4}}$	$-\beta-\gamma$
$[010\bar{1}10]$	$[10]$	$[1\bar{1}]$	$[01]$	$[1]_{,\bar{1}}$	$[0]_{,2}$	$[1]_{,\bar{1}}$	$[1]_{,\bar{1}}$	u	$u_{\bar{2}}$	u	$u_{\bar{2}}$	Y	Y	γ
$[000\bar{1}20]$	$[\bar{1}1]$	$[1\bar{1}]$	$[01]$	$[1]_{,\bar{1}}$	$[0]_{,2}$	$[1]_{,\bar{1}}$	$[1]_{,\bar{1}}$	u	$u_{\bar{2}}$	u	$u_{\bar{2}}$	Y	Y	γ
$[010\bar{1}1\bar{1}]$	$[0\bar{1}]$	$[1\bar{1}]$	$[01]$	$[1]_{,\bar{1}}$	$[0]_{,2}$	$[1]_{,\bar{1}}$	$[1]_{,\bar{1}}$	u	$u_{\bar{2}}$	u	$u_{\bar{2}}$	Y	Y	γ
$[00100\bar{1}]$	$[10]$	$[1\bar{1}]$	$[1\bar{1}]$	$[1]_{,\bar{1}}$	$[1]_{,\bar{1}}$	$[0]_{,2}$	$[\bar{1}]_{,\bar{1}}$	$u_{\bar{2}}$	u	Y	Y	u	$u_{\bar{2}}$	β

Table 2.10: Embedding of $SU(3)\otimes SU(3)\otimes SU(3)$ into adjoint representation of E_6 (continuation).

E_6	$SU(3)$			$SU(2)_{,Y}$				Assignments						(Z,ρ)
	C	L	R	L	R	$R^{'}$	$R^{''}$	I	II	III	IV	V	VI	
$[0\bar{1}101\bar{1}]$	$[\bar{1}1]$	$[1\bar{1}]$	$[1\bar{1}]$	$[1]_{,\bar{1}}$	$[1]_{,\bar{1}}$	$[0]_{,2}$	$[\bar{1}]_{,\bar{1}}$	$u_{\bar{2}}$	u	Y	Y	u	$u_{\bar{2}}$	β
$[001002\bar{2}]$	$[0\bar{1}]$	$[1\bar{1}]$	$[1\bar{1}]$	$[1]_{,\bar{1}}$	$[1]_{,\bar{1}}$	$[0]_{,2}$	$[\bar{1}]_{,\bar{1}}$	$u_{\bar{2}}$	u	Y	Y	u	$u_{\bar{2}}$	β
$[01\bar{1}100]$	$[10]$	$[1\bar{1}]$	$[\bar{1}0]$	$[1]_{,\bar{1}}$	$[\bar{1}]_{,\bar{1}}$	$[\bar{1}]_{,\bar{1}}$	$[0]_{,2}$	Y	Y	$u_{\bar{2}}$	u	$u_{\bar{2}}$	u	α
$[00\bar{1}110]$	$[\bar{1}1]$	$[1\bar{1}]$	$[\bar{1}0]$	$[1]_{,\bar{1}}$	$[\bar{1}]_{,\bar{1}}$	$[\bar{1}]_{,\bar{1}}$	$[0]_{,2}$	Y	Y	$u_{\bar{2}}$	u	$u_{\bar{2}}$	u	α
$[01\bar{1}10\bar{1}]$	$[0\bar{1}]$	$[1\bar{1}]$	$[\bar{1}0]$	$[1]_{,\bar{1}}$	$[\bar{1}]_{,\bar{1}}$	$[\bar{1}]_{,\bar{1}}$	$[0]_{,2}$	Y	Y	$u_{\bar{2}}$	u	$u_{\bar{2}}$	u	α
$[\bar{1}10\bar{1}01]$	$[10]$	$[\bar{1}0]$	$[01]$	$[\bar{1}]_{,\bar{1}}$	$[0]_{,2}$	$[1]_{,\bar{1}}$	$[1]_{,\bar{1}}$	d	$d_{\bar{2}}$	d	$d_{\bar{2}}$	X	X	γ
$[\bar{1}00\bar{1}11]$	$[\bar{1}1]$	$[\bar{1}0]$	$[01]$	$[\bar{1}]_{,\bar{1}}$	$[0]_{,2}$	$[1]_{,\bar{1}}$	$[1]_{,\bar{1}}$	d	$d_{\bar{2}}$	d	$d_{\bar{2}}$	X	X	γ
$[\bar{1}10\bar{1}00]$	$[0\bar{1}]$	$[\bar{1}0]$	$[01]$	$[\bar{1}]_{,\bar{1}}$	$[0]_{,2}$	$[1]_{,\bar{1}}$	$[1]_{,\bar{1}}$	d	$d_{\bar{2}}$	d	$d_{\bar{2}}$	X	X	γ
$[\bar{1}010\bar{1}0]$	$[10]$	$[\bar{1}0]$	$[1\bar{1}]$	$[\bar{1}]_{,\bar{1}}$	$[1]_{,\bar{1}}$	$[0]_{,2}$	$[\bar{1}]_{,\bar{1}}$	$d_{\bar{2}}$	d	X	X	d	$d_{\bar{2}}$	β
$[\bar{1}\bar{1}1000]$	$[\bar{1}1]$	$[\bar{1}0]$	$[1\bar{1}]$	$[\bar{1}]_{,\bar{1}}$	$[1]_{,\bar{1}}$	$[0]_{,2}$	$[\bar{1}]_{,\bar{1}}$	$d_{\bar{2}}$	d	X	X	d	$d_{\bar{2}}$	β
$[\bar{1}010\bar{1}\bar{1}]$	$[0\bar{1}]$	$[\bar{1}0]$	$[1\bar{1}]$	$[\bar{1}]_{,\bar{1}}$	$[1]_{,\bar{1}}$	$[0]_{,2}$	$[\bar{1}]_{,\bar{1}}$	$d_{\bar{2}}$	d	X	X	d	$d_{\bar{2}}$	β
$[\bar{1}\bar{1}\bar{1}\bar{1}1]$	$[10]$	$[\bar{1}0]$	$[\bar{1}0]$	$[\bar{1}]_{,\bar{1}}$	$[\bar{1}]_{,\bar{1}}$	$[\bar{1}]_{,\bar{1}}$	$[0]_{,2}$	X	X	$d_{\bar{2}}$	d	$d_{\bar{2}}$	d	α
$[\bar{1}0\bar{1}101]$	$[\bar{1}1]$	$[\bar{1}0]$	$[\bar{1}0]$	$[\bar{1}]_{,\bar{1}}$	$[\bar{1}]_{,\bar{1}}$	$[\bar{1}]_{,\bar{1}}$	$[0]_{,2}$	X	X	$d_{\bar{2}}$	d	$d_{\bar{2}}$	d	α
$[\bar{1}\bar{1}\bar{1}\bar{1}0]$	$[0\bar{1}]$	$[\bar{1}0]$	$[\bar{1}0]$	$[\bar{1}]_{,\bar{1}}$	$[\bar{1}]_{,\bar{1}}$	$[\bar{1}]_{,\bar{1}}$	$[0]_{,2}$	X	X	$d_{\bar{2}}$	d	$d_{\bar{2}}$	d	α

Table 2.10: Embedding of $SU(3)\otimes SU(3)\otimes SU(3)$ into adjoint representation of E_6 (continuation).

Let us now consider the $E_6 \to SU(3)\otimes SU(3)\otimes SU(3)$ breaking chain. As can be easily checked, the corresponding projection matrix is given by (2.11). The projection matrix maps the fundamental representation of E_6 into the fundamental representation of one of the $SU(3)$ subgroups (**1**,**1**,**3**), and the adjoint of E_6 into the adjoint of one of the $SU(3)$ subgroups (**1**,**1**,**8**). The embedding of $SU(3)\otimes SU(3)\otimes SU(3)$ representations into the fundamental and adjoint representations of E_6 is presented in tables 2.9 and 2.10 respectively.

$$P_{E_6\to SU(3)\otimes SU(3)\otimes SU(3)} = \begin{pmatrix} 1 & 1 & 1 & 1 & 1 & 0 \\ 0 & \bar{1} & \bar{1} & \bar{1} & \bar{1} & 0 \\ 0 & 0 & 1 & 0 & 0 & 0 \\ 0 & 0 & \bar{1} & \bar{1} & 0 & 0 \\ 1 & 2 & 2 & 1 & 0 & 1 \\ 0 & 0 & 1 & 1 & 1 & 1 \end{pmatrix} \tag{2.11}$$

One of the $SU(3)$ subgroups can be associated with the Standard Model $SU_C(3)$, whereas the other two are broken at low energies.

There is a three–fold ambiguity in projecting $SU(3)$ to $SU(2)\otimes U(1)$. The ambiguity is associated with the fact, that any of the three states of the fundamental representation of $SU(3)$ can be projected to a singlet of $SU(2)$. Since we have not yet specified the correspondence between weights of E_6 and states of the Standard Model, we are free to choose any of the three

possible projections, given by (2.12), to project one of the $SU(3)$ subgroups to $SU_L(2)$ of the Standard Model. The embedding presented in tables 2.9 and 2.10 corresponds to a choice of the $P_{_1SU(3)\to SU(2)}$ projection matrix.

$$P_{_1SU(3)\to SU(2)} = \begin{pmatrix} 1 & 0 \\ 1 & 2 \end{pmatrix},\ P_{_2SU(3)\to SU(2)} = \begin{pmatrix} 1 & 1 \\ 1 & \bar{1} \end{pmatrix},\ P_{_3SU(3)\to SU(2)} = \begin{pmatrix} 0 & 1 \\ \bar{2} & \bar{1} \end{pmatrix} \quad (2.12)$$

If the last of the $SU(3)$ groups is also broken down to $SU(2)$, then the aforementioned projection freedom leads to one left–right symmetric and two skew left–right symmetric models (see tables 2.9 and 2.10).

2.2 Particle content and charge assignments

As has already been mentioned, the fundamental representation of E_6 contains the fifteen known states of the Standard Model along with two Higgs doublets, a pair of new quarks and two SM singlets. The hypercharge Y of any state is given by a scalar product of the hypercharge operator $\hat{P}_Y$ and the weight of the state. Analogously the $B-L$ charge is given by a scalar product of the weight w of the state and the $B-L$ operator $\hat{P}_{B-L}$:

$$Y = (\hat{P}_Y \cdot w), \quad B-L = (\hat{P}_{B-L} \cdot w). \quad (2.13)$$

The left–handed Standard Model quarks, whose hypercharge and $B-L$ charge are known, belong to the ($\mathbf{3}$,$\mathbf{2}$) representation of the $SU_C(3) \otimes SU_L(2)$ subgroup of E_6 and correspond to the first six weights in the tables 2.7 and 2.9. The requirement that the hypercharge and the $B-L$ charge of these states be the same determines four out of six elements of each operator.

$$\hat{P}_Y = \frac{1}{3}(1,\ \bar{1},\ a_3,\ a_4,\ \bar{1},\ 0), \quad \hat{P}_{B-L} = \frac{1}{3}(1,\ \bar{1},\ b_3,\ b_4,\ \bar{1},\ 0) \quad (2.14)$$

The remaining elements can be determined from the embedding of the right–handed Standard Model quarks, which belong to ($\bar{\mathbf{3}}$,$\mathbf{1}$) of $SU_C(3) \otimes SU_L(2)$, into the fundamental representation of E_6. As the latter one contains three ($\bar{\mathbf{3}}$,$\mathbf{1}$) subgroups, there are three possible hypercharge:

$$\hat{P}_{Y_1} = \frac{1}{3}(1,\ \bar{1},\ 1,\ \bar{3},\ \bar{1},\ 0), \quad (2.15a)$$

$$\hat{P}_{Y_2} = \frac{1}{3}(1,\ \bar{1},\ \bar{5},\ \bar{3},\ \bar{1},\ 0), \quad (2.15b)$$

$$\hat{P}_{Y_3} = \frac{1}{3}(1,\ \bar{1},\ 1,\ 3,\ \bar{1},\ 0), \quad (2.15c)$$

and three possible $B-L$ operators:

$$\hat{P}_{B-L_1} = \frac{1}{3}(1,\ \bar{1},\ \bar{2},\ \bar{3},\ \bar{1},\ 0), \quad (2.16a)$$

$$\hat{P}_{B-L_2} = \frac{1}{3}(1,\ \bar{1},\ 1,\ 0,\ \bar{1},\ 0), \quad (2.16b)$$

$$\hat{P}_{B-L_3} = \frac{1}{3}(1,\ \bar{1},\ \bar{2},\ 0,\ \bar{1},\ 0). \quad (2.16c)$$

(or, alternatively, charge assignments) which reproduce the quantum numbers of the Standard Model states. The particle content of the model is of course independent of the particular choice

The Standard Model states						New states					
$B-L$	Y	I_3	Q_{em}	P		$B-L$	Y	I_3	Q_{em}	P	
1/3	1/3	1/2	2/3	u	$\}Q$	0	1	1/2	1	E^c	$\}H^u$
1/3	1/3	-1/2	-1/3	d		0	1	-1/2	0	N^c	
-1	-1	1/2	0	ν	$\}L$	0	-1	1/2	0	N	$\}H^d$
-1	-1	-1/2	-1	e		0	-1	-1/2	-1	E	
-1/3	-4/3	0	-2/3	u^c		-2/3	-2/3	0	-1/3	D	
-1/3	2/3	0	1/3	d^c		2/3	2/3	0	1/3	D^c	
1	2	0	1	e^c		1	0	0	0	ν^c	
						0	0	0	0	S	

Table 2.11: Particle content of E_6 – fundamental representation.

of the hypercharge and $B-L$ operators. The charges of states in the fundamental representation of E_6 are given in table 2.11. Note that the model contains two Higgs–like doublets H^u and H^d which are required in a supersymmetric model to give masses to the top and bottom components of the Standard Model doublets.

Different assignments correspond to different embeddings of states into subgroups of E_6. Out of nine $\hat{P}_{Y_i} \times \hat{P}_{B-L_j}$ combinations six are compatible with the SM:

$$\text{I}: \ (\hat{P}_{Y_1},\ \hat{P}_{B-L_1}), \qquad \text{II}: \ (\hat{P}_{Y_1},\ \hat{P}_{B-L_2}), \qquad \text{III}: \ (\hat{P}_{Y_2},\ \hat{P}_{B-L_1})$$
$$\text{IV}: \ (\hat{P}_{Y_2},\ \hat{P}_{B-L_3}), \qquad \text{V}: \ (\hat{P}_{Y_3},\ \hat{P}_{B-L_2}), \qquad \text{VI}: \ (\hat{P}_{Y_3},\ \hat{P}_{B-L_3})$$

The supersymmetric generalization of Yukawa interactions – the superpotential – is a holomorphic function of chiral superfields, i.e. it contains the chiral superfields, but not their complex conjugates. A renormalizable superpotential contains gauge–invariant quadratic (i.e. products of two chiral superfields) and cubic (i.e. products of three chiral superfields) terms. Since the weights of the fundamental representation are non–degenerate, one can easily construct the terms of the superpotential using the requirement that the weights of individual states add up to zero in each term. As follows from this simple criterion, terms bilinear in the chiral superfields are not allowed by gauge symmetry. Although all the trilinear terms can also be constructed using the criterion above, a somewhat more refined analysis [62, 63] is needed in order to determine

the relative signs of the individual terms of the superpotential. In the flavor basis

$$\begin{aligned} W = &-\lambda_1^{ijk} u_i^{\mathrm{c}} (Q_j H_k^{\mathrm{u}}) + \lambda_2^{ijk} d_i^{\mathrm{c}} (Q_j H_k^{\mathrm{d}}) + \lambda_3^{ijk} e_i^{\mathrm{c}} (L_j H_k^{\mathrm{d}}) + \lambda_4^{ijk} S_i (H_j^{\mathrm{u}} H_k^{\mathrm{d}}) + \lambda_5^{ijk} S_i D_j D_k^{\mathrm{c}} \\ &+ [-\lambda_6^{ijk} e_i^{\mathrm{c}} u_j^{\mathrm{c}} D_k + \lambda_7^{ijk} D_i^{\mathrm{c}} (Q_j L_k) + \lambda_8^{ijk} d_i^{\mathrm{c}} \nu_j^{\mathrm{c}} D_k] + [\lambda_9^{ijk} D_i (Q_j Q_k) + \lambda_{10}^{ijk} D_i^{\mathrm{c}} u_j^{\mathrm{c}} d_k^{\mathrm{c}}] \\ &- \lambda_{11}^{ijk} \nu_i^{\mathrm{c}} (L_j H_k^{\mathrm{u}}) \end{aligned} \tag{2.17}$$

In the limit of unification the coupling constants λ_n^{ijk} tend to the same value. Using table 2.7 or table 2.9 one can check that the corresponding weights add up to zero at each vertex.

The form of the superpotential is independent of the charge assignment in the sense that a change of the assignment will only result in a "permutation" of vertices. For example:

	$[10\bar{1}001]$	$[000010\bar{1}]$	$[\bar{1}01\bar{1}00]$	$[1\bar{1}01\bar{1}0]$	$[01\bar{1}010]$	$[101\bar{1}00]$
I	ν^c	ν	N^c	S	N	N^c
II	S	N	N^c	ν^c	ν	N^c
III	e^c	ν	E	S	E^c	E

Table 2.12: Permutation of vertices under change of charge assignment.

Along with the vertices with $i = j = k$ (i.e. states of the same generation) the superpotential (2.17) necessarily contains terms with states of different generations in one vertex. If the charge assignment for one of the generations differs from that for the other generations, then this will result in a vertex where the sum of the charges differs from zero. For instance, if in the example given above the assignment II is used for the first weight and the assignment I is used for the second and the third weights then

$$\begin{aligned} \nu^c \to S \Rightarrow \nu^c\,(\nu N^c) \to S\,(\nu N^c)\,, \quad \textstyle\sum B - L = -1 \\ S \to \nu^c \Rightarrow S\,(N N^c) \to \nu^c\,(N N^c)\,, \quad \textstyle\sum B - L = 1 \end{aligned}$$

If instead of the assignment II, the assignment III is used for the first weight, then it is a sum of electric charges, which is nonzero. Consequently, the same charge assignment must be used for all generations.

2.3 Gauge mediated proton decay

Since $SU(5)$ is a subgroup of E_6, the gauge sector of the model contains the X and Y bosons, which are known to mediate proton decay. In addition, there are also new gauge fields leading to a rapid proton decay (see table 2.13).

To assure that the proton is long–lived, these fields must be very heavy – of the order of 10^{15} GeV or more. If the only source of masses of those particles are VEVs of the neutral scalars,

then the masses of the $(u_{\bar{2}}, d_{\bar{2}})$ gauge bosons are determined by $\langle\tilde{\nu}^c\rangle$, mass of the Y boson is of the order of the EW symmetry breaking scale, and the X bosons remain massless even after all neutral scalars develop a nonzero VEV.

$B-L$	Y	I_3	Q_{em}	P	$B-L$	Y	I_3	Q_{em}	P
2/3	5/3	1/2	4/3	X	-2/3	1/3	1/2	2/3	$u_{\bar{2}}$
2/3	5/3	-1/2	1/3	Y	-2/3	1/3	-1/2	-1/3	$d_{\bar{2}}$

Table 2.13: Gauge fields which mediate proton decay.

Consequently, the gauge superfields which mediate proton decay have to become massive at the first stage of symmetry breaking. If the manifold Γ is multiply connected, then the effective Higgs mechanism [64, 65] breaks the symmetry at the compactification scale and induces large masses of the gauge fields.

From the discussion given above it follows that after the $E_8 \otimes E_8^{'}$ breaking, the gauge group of the model is not E_6 itself, but a subgroup G of E_6. A very elaborate analysis of many possible breaking chains has been performed in [55, 65]. It has been argued there that a gauge field receives a mass of the order of $O(10^{18})$ GeV if $(Z,\rho) \neq 0$. Here Z is the zero root breaking $SU_C(3) \otimes SU_L(2) \otimes U_Y(1)$ preserving direction, and ρ is the weight of the gauge field. Scalar products (Z,ρ) for fundamental and adjoint representations of E_6 are listed, respectively, in tables 2.7, 2.9 and 2.8, 2.10.

SU(5)	$SU(3) \otimes SU(2)_{,U(1)}$	I	II	III	IV	V	VI	(Z,ρ)
24	$(\mathbf{3},\mathbf{2})_{,\bar{5}}$	X	X	$d_{\bar{2}}$	d	$d_{\bar{2}}$	d	α
24	$(\mathbf{3},\mathbf{2})_{,\bar{5}}$	Y	Y	$u_{\bar{2}}$	u	$u_{\bar{2}}$	u	α

Table 2.14: (Z,ρ) products for $(\mathbf{3},\mathbf{2})_{\bar{5}}$ gauge fields.

The requirement of $(Z,\rho) \neq 0$ for the gauge fields which mediate proton decay does not allow $G = SO(10) \otimes U(1)$. The $(\mathbf{3},\mathbf{2})_{\bar{5}}$ states (and their charge conjugates) are the only states in the adjoint of $SU(5)$ which are not automatically massless. As seen from table 2.14, the requirement that these fields be massless (i.e. that $SU(5)$ is unbroken) does not lead to a rapid gauge mediated proton decay for the charge assignments IV and VI. In other words, in addition to the intermediate gauge groups listed in [55] as allowed, also $G = SU(5) \otimes U^2(1)$ is allowed for the charge assignments IV and VI. Nevertheless, in this case the residual $SU(5)$ symmetry implies that the couplings in (2.17) are related in the following way;

$$\lambda_1 = \lambda_2 = \lambda_4 = \lambda_{10}, \quad \lambda_5 = \lambda_7 = \lambda_9, \qquad \lambda_3 = \lambda_6, \quad \lambda_8 = \lambda_{11} \tag{2.18}$$

and the rapid proton decay mediated by heavy down–type quarks D and D^c is unavoidable.

Apart from scenarios with an extended color group there are only two options left:

$$G_{U(1)} = SU_C(3) \otimes SU_L(2) \otimes U(1) \otimes U(1) \otimes U(1), \tag{2.19}$$

$$G_{SU_R(2)} = SU_C(3) \otimes SU_L(2) \otimes SU_R(2) \otimes U(1) \otimes U(1). \tag{2.20}$$

If the intermediate scale symmetry group is given by (2.19), then the gauge sector of the SM is supplemented by two neutral states (the rest are superheavy), denoted by ϕ^0 and ω^0 (see table 2.10).

If the intermediate scale symmetry group is given by (2.20), then the gauge sector of the SM is supplemented by one $SU_R(2)$ singlet ω^0 and one $SU_R(2)$ triplet $(\phi^c, \phi^0, \bar{\phi}^c)$. There are three possible $SU_R(3) \to SU_R(2)_{,Y}$ projections which result in one left–right symmetric (R) and two skew left–right symmetric ($R^{'}$ and $R^{''}$) models. The $SU_R(2)$ counterparts of ϕ^0 for different choices of the projection and the charge assignment are given in table 2.15.

	Charge assignment					
	I	II	III	IV	V	VI
R	$e_0^c, \bar{e}_0^c$	$e^c, \bar{e}^c$	$e_0^c, \bar{e}_0^c$	$e^c, \bar{e}^c$	$\nu^c, \bar{\nu}^c$	$\nu^c, \bar{\nu}^c$
$R^{'}$	$e^c, \bar{e}^c$	$e_0^c, \bar{e}_0^c$	$\nu^c, \bar{\nu}^c$	$\nu^c, \bar{\nu}^c$	$e_0^c, \bar{e}_0^c$	$e^c, \bar{e}^c$
$R^{''}$	$\nu^c, \bar{\nu}^c$	$\nu^c, \bar{\nu}^c$	$e^c, \bar{e}^c$	$e_0^c, \bar{e}_0^c$	$e^c, \bar{e}^c$	$e_0^c, \bar{e}_0^c$

Table 2.15: $SU_R(2)$ counterparts of ϕ^0. Isospin and hypercharge (as well as $B-L$, unless otherwise indicated) of the states denoted in the same way as the SM states, are the same as the charges of their SM counterparts. If present, the subscript is thrice the $B-L$ charge.

While $SU_L(2)$ in (2.20) coincide with that of the Standard Model, U_{Y_L} is not the SM $U_Y(1)$. The hypercharge Y, as well as $B-L$, is a linear combination of Q_{Y_L}, Q_{Y_R} and I_{3R}. An explicit form of the gauge interactions $g_\alpha \Lambda_\alpha [\psi^+ T^\alpha \psi]$ for the first charge assignment and left–right symmetric model can be read off from table 2.9:

$$\begin{aligned}
&\frac{g_{Y_L}}{2} Y_L \left[\bar{Q}Q - 2\bar{D}D - (\bar{H}^u H^u + \bar{H}^d H^d) - \bar{L}L + 2(\bar{e^c}e^c + \bar{\nu^c}\nu^c) + 2\bar{S}S\right] \\
&+\frac{g_{Y_R}}{2} Y_R \left[-(\bar{d^c}d^c + \bar{u^c}u^c) + 2\bar{D^c}D^c + (\bar{H}^u H^u + \bar{H}^d H^d) - 2\bar{L}L + (\bar{e^c}e^c + \bar{\nu^c}\nu^c) - 2\bar{S}S\right] \\
&+\frac{g_{W_R}}{2} W_R^i \left[(d^c, u^c)^+ \tau_i (d^c, u^c) + (H^u, H^d)^+ \tau_i (H^u, H^d) + (e^c, \nu^c)^+ \tau_i (e^c, \nu^c)\right] + \ldots
\end{aligned} \tag{2.21}$$

At the unification scale the relation among the gauge couplings is as follows:

$$g_{W_R} = \sqrt{3}\, g_{Y_L} = \sqrt{3}\, g_{Y_R} = g_{E_6} \tag{2.22}$$

Instead of Y_L, Y_R and W_R^0 one can use their linear combination. For instance, in the limit (2.22) the linear combination $Y_{B-L} = \frac{1}{\sqrt{2}}(Y_L + Y_R)$ is a gauge field of $U_{B-L}(1)$. For later purposes it

is useful to choose linear combinations $\omega_0^{'}$, $\phi_0^{'}$, $\gamma_0^{'}$ in such a way, that only one of the new fields interacts with right–handed neutrinos and one of the fields interacts with neither of the SM singlets. After the Standard Model singlets develop VEVs, $\omega_0^{'}$ and $\phi_0^{'}$ acquire masses, while $\gamma_0^{'}$, which corresponds to $U_Y(1)$, remains massless. Rewritten in terms of these fields, (2.21) takes the form

$$g_{\gamma_0^{'}}\,\gamma_0^{'}\,\frac{1}{6}\left[\bar{Q}Q-4\bar{u^c}u^c+2\bar{d^c}d^c+2\bar{D^c}D^c-2\bar{D}D+3\bar{H^u}H^u-3\bar{H^d}H^d-3\bar{L}L+6\bar{e^c}e^c\right] \tag{2.23}$$
$$+g_{\phi_0^{'}}\,\phi_0^{'}\left[-\bar{Q}Q-\bar{u^c}u^c-2\bar{d^c}d^c+3\bar{D^c}D^c+2\bar{D}D+2\bar{H^u}H^u+3\bar{H^d}H^d-2\bar{L}L-\bar{e^c}e^c-5\bar{S}S\right]$$
$$+g_{\omega_0^{'}}\,\omega_0^{'}\left[\bar{Q}Q+\bar{u^c}u^c-2\bar{d^c}d^c+\bar{D^c}D^c-2\bar{D}D-2\bar{H^u}H^u+\bar{H^d}H^d-2\bar{L}L+\bar{e^c}e^c+4\bar{\nu^c}\nu^c+\bar{S}S\right]+..$$

At the unification scale the gauge couplings $g_{\gamma_0^{'}}$, $g_{\phi_0^{'}}$, $g_{\omega_0^{'}}$ are given by

$$g_{\gamma_0^{'}}=\sqrt{\frac{3}{5}}\,g_{E_6},\ g_{\phi_0^{'}}=\frac{g_{E_6}}{\sqrt{40}},\ g_{\omega_0^{'}}=\frac{g_{E_6}}{\sqrt{24}} \tag{2.24}$$

Reexpessed in terms of $\omega_0^{'}$, $\phi_0^{'}$, $\gamma_0^{'}$, the gauge interactions of neutral fields are obviously given by (2.23) irrespective of the intermediate scale symmetry group G, the charge assignment or the particular choice of the $SU_R(3)\to SU_R(2)_{\,Y}$ projection.

2.4 Breaking of the $B-L$ symmetry

Since $B-L$ is gauged, the Majorana mass of the right-handed neutrino, which is an essential ingredient of leptogenesis, is forbidden unless $B-L$ symmetry is broken down. Present data on neutrino masses as well as theoretical estimates of leptogenesis in other GUT models favor the 10^9-10^{11} GeV mass range [66, 67] for the right–handed neutrino.

There are two SM singlets whose scalar superpartners may be used to break the symmetry down to the SM: S and the right–handed neutrino.

The former one has zero $B-L$ charge, whereas the latter one has $B-L=1$. Therefore, it is the VEV of the scalar superpartner of the right-handed neutrino that breaks $B-L$ symmetry. S couples to Higgs doublets and its VEV $\langle\tilde{S}\rangle$ is the origin of the μ–term: $\mu=\lambda_4\langle\tilde{S}\rangle$.

If the right-handed sneutrino which develops the VEV couples to states of the three known generations, it induces huge Dirac masses for the components of L and H^u doublets via the last term in (2.17). Neglecting the possibility that one of the ν^c superfields decouples from the other states of the three known generations, one comes to the conclusion that all $\langle\tilde{\nu^c}\rangle=0$, and the $B-L$ symmetry is broken spontaneously by nonzero $\langle\tilde{\chi}_{\nu^c}\rangle$ and $\langle\tilde{\bar{\chi}}_{\nu^c}\rangle$ and, consequently, χ_{ν^c} and $\bar{\chi}_{\nu^c}$ are zero modes.

According to [65] chiral superfields in $\delta(\mathbf{27}+\bar{\mathbf{27}})$ can be massive through the Yukawa coupling $\mathbf{27}\cdot\bar{\mathbf{27}}\cdot\mathbf{78}$. If $(Z,\rho)\neq 0$ for a component of $\mathbf{27}$ or $\bar{\mathbf{27}}$ with weight ρ, the corresponding chiral superfield gets a compactification scale mass, while N_f $\mathbf{27}$ chiral superfields remain massless.

Table 2.9 shows, that for both discussed intermediate gauge groups $G_{U(1)}$ and $G_{SU_R(2)}$ and any charge assignment, it is possible to have massless χ_{ν^c} and $\bar{\chi}_{\nu^c}$. In the case of $G_{U(1)}$ right–handed neutrinos χ_{ν^c} and $\bar{\chi}_{\nu^c}$ are the only massless states in $\delta(\mathbf{27}+\bar{\mathbf{27}})$.

In the case of $G_{SU_R(2)}$ the number of zero modes in $\delta(\mathbf{27}+\bar{\mathbf{27}})$ depends on the charge assignment and the particular choice of the $SU_R(3)\to SU_R(2)$ projection (2.16).

	Charge assignment					
	I	II	III	IV	V	VI
R	(ν^c, e^c)	ν^c, (H^u, L)	(ν^c, e^c)	ν^c, (H^u, L)	(ν^c, S)	(ν^c, S)
$R^{'}$	ν^c, (H^u, L)	(ν^c, e^c)	(ν^c, S)	(ν^c, S)	(ν^c, e^c)	ν^c, (H^u, L)
$R^{''}$	(ν^c, S)	(ν^c, S)	ν^c, (H^u, L)	(ν^c, e^c)	ν^c, (H^u, L)	(ν^c, e^c)

Table 2.16: States in $\delta(\mathbf{27}+\bar{\mathbf{27}})$ which remain massless after the compactification. States of $\mathbf{27}$ and $\bar{\mathbf{27}}$ are labeled here by the same symbol. For instance, ν^c stands for both χ_{ν^c} and $\bar{\chi}_{\nu^c}$. Components of $SU_R(2)$ doublets are put into brackets.

If supersymmetry is exact, there are no negative mass squared terms needed to break $U_{B-L}(1)$ down spontaneously by the Higgs mechanism.

$$m_{\chi}^2|\tilde{\chi}_{\nu^c}|^2+m_{\bar{\chi}}^2|\tilde{\bar{\chi}}_{\nu^c}|^2-m_{\nu^c\,ij}^2\tilde{\nu}_i^{c*}\tilde{\nu}_j^c,\quad |m_{\bar{\chi}}^2|,|m_{\chi}^2|,|m_{\nu^c\,ij}^2|\sim m_{soft}^2 \tag{2.25}$$

These terms are assumed to come from the $E_8^{'}$ sector, where supersymmetry is considered to break down spontaneously. In the gravity-mediated supersymmetry breaking scenario the magnitude of the soft terms in the visible sector should be roughly of the order of $m_{soft}\sim\langle F\rangle/M_{Pl}$. For the commonly accepted value $m_{soft}\sim 10^3$ GeV the scale of supersymmetry breaking in the hidden sector $\langle F\rangle^{\frac{1}{2}}$ is about 10^{11} GeV. It is interesting to note that this value is of the same order as the desired mass scale of the right-handed neutrinos. One can consider this as a hint that at the stage when the right–handed neutrinos acquire masses, the temperature is still high enough to produce them thermally.

$\mathbf{SU_C(3)\otimes SU_L(2)\otimes U^3(1)}$ model. As is well known, the scalar potential consists of an F-term and D-term coming from the chiral superfield trilinear couplings and the gauge interactions respectively. The renormalizable superpotential (2.17) does not contain terms relevant for the symmetry breaking. The scalar potential coming from gauge interactions (2.23) and soft supersymmetry breaking is of the form

$$V=\frac{g_{\omega_0'}^2}{2}\left[\tilde{\psi}^*T_{\omega_0'}\tilde{\psi}+q_{\nu^c}\tilde{\chi}_{\nu^c}^*\tilde{\chi}_{\nu^c}-q_{\nu^c}\tilde{\bar{\chi}}_{\nu^c}^*\tilde{\bar{\chi}}_{\nu^c}\right]^2-\left[m_{\chi}^2|\tilde{\chi}_{\nu^c}|^2+m_{\bar{\chi}}^2|\tilde{\bar{\chi}}_{\nu^c}|^2\right]+m_{\nu^c\,ij}^2\tilde{\nu}_i^{c*}\tilde{\nu}_j^c \tag{2.26}$$

On the one hand, the VEVs of right-handed sneutrinos of $\delta(\mathbf{27}+\bar{\mathbf{27}})$ are expected to be at least of the same order as the masses of ν^c, i.e. $\langle\tilde{\chi}_{\nu^c}\rangle,\langle\tilde{\bar{\chi}}_{\nu^c}\rangle\geq 10^{11}$ GeV; on the other hand, such a

huge VEV should not generate large masses of scalar superpartners via the first term in (2.26). Consequently, the symmetry breaking should occur in the D–flat direction $\langle\tilde{\chi}_{\nu^c}\rangle = \langle\tilde{\bar{\chi}}_{\nu^c}\rangle$.

Combined with the requirement that all $\langle\tilde{\nu}^c\rangle$ be zero, this means that the contribution of the first term in (2.26) vanishes. To have symmetry breaking by the Higgs mechanism in this direction, the sum of the mass parameters in the second term should be positive:

$$m_{\chi}^2 + m_{\bar{\chi}}^2 > 0 \tag{2.27}$$

Non-renormalizable terms arise due to the interactions with exchange of superheavy fields, which correspond to excitations of internal degrees of freedom [68]. The general form of the non–renormalizable superpotential is

$$\begin{aligned} W = M_c^{-1} \Big[a_1^{ij}\, \nu_i^c \nu_j^c \bar{\chi}_{\nu^c} \bar{\chi}_{\nu^c} + a_2^i\, \nu_i^c \chi_{\nu^c} \bar{\chi}_{\nu^c} \bar{\chi}_{\nu^c} + a_3\, \chi_{\nu^c} \chi_{\nu^c} \bar{\chi}_{\nu^c} \bar{\chi}_{\nu^c} \Big] \\ + M_c^{-3} \Big[b_1\, \chi_{\nu^c} \chi_{\nu^c} \chi_{\nu^c} \bar{\chi}_{\nu^c} \bar{\chi}_{\nu^c} \bar{\chi}_{\nu^c} + b_2^i\, \nu_i^c \chi_{\nu^c} \chi_{\nu^c} \bar{\chi}_{\nu^c} \bar{\chi}_{\nu^c} \bar{\chi}_{\nu^c} \\ + b_3^{ij}\, \nu_i^c \nu_j^c \chi_{\nu^c} \bar{\chi}_{\nu^c} \bar{\chi}_{\nu^c} \bar{\chi}_{\nu^c} + b_4^{ijk}\, \nu_i^c \nu_j^c \nu_k^c \bar{\chi}_{\nu^c} \bar{\chi}_{\nu^c} \bar{\chi}_{\nu^c} \Big] + \dots \end{aligned} \tag{2.28}$$

Given that all $\langle\tilde{\nu}^c\rangle$ are zero, only $M_c^{3-2n}\,(\chi_{\nu^c}\bar{\chi}_{\nu^c})^n$ terms in (2.28) are relevant for the analysis of symmetry breaking. These terms are invariant with respect to $\chi_{\nu^c} \leftrightarrow \bar{\chi}_{\nu^c}$ transformation, whereas soft supersymmetry breaking terms in (2.26) are not, unless $m_{\chi}^2 = m_{\bar{\chi}}^2$. If this condition is not satisfied, then $\langle\tilde{\chi}_{\nu^c}\rangle$ cannot be equal to $\langle\tilde{\bar{\chi}}_{\nu^c}\rangle$. Nevertheless, since the gauge coupling g is of the order of unity, while m_{soft}/M_c is many orders of magnitude smaller than unity, the deviation from the D–flat direction $\langle\tilde{\chi}_{\nu^c}\rangle = \langle\tilde{\bar{\chi}}_{\nu^c}\rangle$ is very small. Considering $\langle\tilde{\bar{\chi}}_{\nu^c}\rangle - \langle\tilde{\chi}_{\nu^c}\rangle$ as a small perturbation in (2.31) one finds

$$\langle\tilde{\bar{\chi}}_{\nu^c}\rangle - \langle\tilde{\chi}_{\nu^c}\rangle \simeq \frac{m_{\bar{\chi}}^2 - m_{\chi}^2}{8\, g^2\, v_0} \tag{2.29}$$

This effect can be entirely neglected in the analysis of the non–renormalizable superpotential (2.28). As for gauge interactions, such a deviation from the D–flat direction will result in the generation of masses of scalars $\sim m_{\bar{\chi}}^2 - m_{\chi}^2$ via the first term in (2.26) which adds to the mass terms coming from the soft supersymmetry breaking. To simplify the analysis m_{χ}^2 and $m_{\bar{\chi}}^2$ are taken to be equal in what follows.

If the first non-vanishing terms in (2.28) are $M_c^{-1}(\nu^c\bar{\chi}_{\nu^c})^2 + M_c^{3-2n}(\chi_{\nu^c}\bar{\chi}_{\nu^c})^n$, then the generated VEV and the masses of right–handed neutrinos ν^c are

$$\langle\tilde{\chi}_{\nu^c}\rangle = \langle\tilde{\bar{\chi}}_{\nu^c}\rangle \sim (m_{soft}\, M_c^{2n-3})^{\frac{1}{2n-2}}, \quad M_{\nu^c} \sim (m_{soft}\, M_c^{n-2})^{\frac{1}{n-1}} \tag{2.30}$$

so that M_{ν^c} is of the order of 10^3 GeV for $n = 2$ and is of the order of 10^{11} GeV for $n = 3$.

Large masses of right–handed neutrinos suggest that $n = 3$ and, consequently, $a_3 = 0$ in (2.28). Moreover, a_2^i and b_2^i, as well as the coefficient c_2^i of the (not indicated) next similar term

in (2.28), are zero to avoid nonzero $\langle\tilde{\nu}^c\rangle$ and a Dirac–type mass for ν^c. The discrete symmetry of the compactified manifold possibly accomplishes these conditions [69] as well as the absence of bare mass terms $M\chi_{\nu^c}\bar{\chi}_{\nu^c}$ and $M\nu^c\bar{\chi}_{\nu^c}$ in the superpotential (2.17). There is no reason to expect the scale M to be below the compactification scale M_c so that presence of the first term would make spontaneous breaking of $B-L$ by χ_{ν^c} and $\bar{\chi}_{\nu^c}$ impossible, while the presence of the second one makes ν^c a component of the super heavy Dirac neutrino. Just as there are no $M\chi_{\nu^c}\bar{\chi}_{\nu^c}$ and $M\nu^c\bar{\chi}_{\nu^c}$ terms, there are no soft supersymmetry breaking terms $b_{\chi\bar{\chi}}\tilde{\chi}_{\nu^c}\tilde{\bar{\chi}}_{\nu^c}$ and $b_{\nu^c\bar{\chi}}\tilde{\nu^c}\tilde{\bar{\chi}}_{\nu^c}$ in (2.26). If present, the contributions of the b_3 and b_4 terms are small and will be neglected in the following discussion. Then the classical potential is of the form

$$\begin{aligned} V = {} & 4M_c^{-2}u^2\varrho_i\varrho_j\left[a_{li}a^*_{lj}u^2 + a_{ij}a^*_{nm}\varrho_n\varrho_m\right] + 9b_1b_1^*M_c^{-6}u^4v^4\left[u^2+v^2\right] \\ & + 6M_c^{-4}\left[b_1^*a_{ij}+b_1a^*_{ij}\right]\varrho_i\varrho_jv^3u^3 + \frac{g^2q^2_{\nu^c}}{2}\left[\varrho_i\varrho_i+v^2-u^2\right]^2 \\ & - \left[m_\chi^2v^2+m_{\bar{\chi}}^2u^2\right] + m^2_{\nu^c\,ij}\varrho_i\varrho_j \end{aligned} \tag{2.31}$$

with $\varrho_i=\langle\tilde{\nu}^c_i\rangle$, $v=\langle\tilde{\chi}_{\nu^c}\rangle$, $u=\langle\tilde{\bar{\chi}}_{\nu^c}\rangle$. For zero ϱ_i the D–flat direction is defined by $u^2=v^2$ and the minimum of the potential (2.31) corresponds to

$$v_0=\sqrt[8]{M_c^6(m_\chi^2+m_{\bar{\chi}}^2)/(90|b_1|^2)}, \qquad M^{ij}_{\nu_c}=2a_1^{ij}v_0^2M_c^{-1} \tag{2.32}$$

For nonzero ϱ_i the D–flat direction is defined by $u^2=v^2+\varrho_i\varrho_i$. The set of products $\varrho_i\varrho_j$ being considered as parameters, the minimizing of (2.31) with respect to v gives v as a function of $\varrho_i\varrho_j$. The true vacuum corresponds to the set $\varrho_i\varrho_j$ which minimizes $V(v(\varrho_i\varrho_j),\varrho_i\varrho_j)$. Expanding in powers of $\varrho_i\varrho_j$ in the vicinity of $\varrho_i\varrho_j=0$ and having in mind that the partial derivative with respect to v is zero:

$$\begin{aligned} V(v(\varrho_i\varrho_j),\varrho_i\varrho_j) \simeq {} & V(v_0,0) + \left(m^{2\,ij}_{\nu^c} - m^2_{\bar{\chi}}\,\delta^{ij}\right)\varrho_i\varrho_j \\ & + v_0^4M_c^{-2}\left[4a_1^{li}a_1^{*lj} + 6(b_1^*a_1^{ij}+b_1a_1^{*ij})v_0^2M_c^{-2} + 45b_1b_1^*v_0^4M_c^{-4}\delta^{ij}\right]\varrho_i\varrho_j \end{aligned} \tag{2.33}$$

Since the v_0/M_c ratio is small while v_0^2/M_c is large, the derivative (2.33) is dominated by the first term in square brackets which is positive definite. Therefore, $\varrho_i=0$ is at least a local minimum of the potential (2.31) for a wide range of parameters.

For large $\varrho_i\varrho_j$ it is sufficient to keep only the first term in (2.31), and an explicit calculation shows that $V(v(\varrho_i\varrho_j),\varrho_i\varrho_j)$ grows with growing $\varrho_i\varrho_j$, i.e. $\varrho_i\varrho_j=0$ is a global minimum of the classical potential:

$$V(v(\varrho_i\varrho_j),\varrho_i\varrho_j) = -M_c^2(m^2_{\tilde{\chi}_{\nu^c}}+m^2_{\tilde{\bar{\chi}}_{\nu^c}})^2(16a_1^{li}a_1^{*lj}\varrho_i\varrho_j)^{-1} + (m^2_{\tilde{\chi}_{\nu^c}}\delta^{ij}+m^{2\,ij}_{\nu^c})\varrho_i\varrho_j \tag{2.34}$$

A discrete symmetry which allows nonzero a_1^{ij}, b_1 and forbids nonzero a_2^i, a_3, b_2 couplings is essential for having large Majorana masses for right–handed neutrinos after symmetry breaking.

Suppose that right–handed neutrinos ν^c, χ_{ν^c}, $\bar{\chi}_{\nu^c}$ acquire additional phases under transformations of the discrete symmetry:

$$\nu^c \to \nu^c\, e^{i\alpha}, \quad \chi_{\nu^c} \to \chi_{\nu^c}\, e^{i\beta}, \quad \bar{\chi}_{\nu^c} \to \bar{\chi}_{\nu^c}\, e^{i\gamma} \tag{2.35}$$

Then from the requirement that a nonzero a_1^{ij} and b_1 are allowed while a_2^i, a_3, b_2^i, c_2^i are set to zero by the symmetry:

$$\begin{aligned} &\alpha+\gamma=\pi k, \quad \beta+\gamma=\frac{2\pi}{3}l, \quad (\alpha+\gamma)+(\beta+\gamma)\neq 2\pi m, \\ &\beta+\gamma\neq\pi n, \quad (\alpha+\gamma)+2(\beta+\gamma)\neq 2\pi q, \quad (\alpha+\gamma)+3(\beta+\gamma)\neq 2\pi p. \end{aligned} \tag{2.36}$$

Conditions (2.36) imply that $\frac{2}{3}l$ is not integer and, consequently, that $\alpha-\beta\neq 2\pi j$:

$$\alpha-\beta=(\alpha+\gamma)-(\beta+\gamma)=\pi(k-\frac{2}{3}l)\neq 2\pi j\neq 0 \tag{2.37}$$

In other words, ν^c and χ_{ν^c} have different transformation properties under the discrete symmetry. If the last term in (2.17) which is responsible for both small neutrino masses via the see-saw mechanism and leptogenesis is allowed by this symmetry, then the term $\chi_{\nu^c}(L_j H_k^u)$ is necessarily forbidden just as was assumed.

The bare mass term $M\chi_{\nu^c}\bar{\chi}_{\nu^c}$ is not invariant under transformations of the discrete symmetry and therefore is not allowed. From equations (2.36) it also follows that $\alpha+\gamma=\pi k$ with k – odd, so that the bare mass term $M\nu^c\bar{\chi}_{\nu^c}$ is forbidden as well. Finally, the coefficients b_3 and b_4 of the last two terms in (2.28) vanish for the same reasons.

After $\tilde{\chi}_{\nu^c}$ and $\tilde{\bar{\chi}}_{\nu^c}$ develop nonzero VEVs, the $U(1)$ symmetry, as well as the discrete symmetry (2.35), is broken down. The components of chiral (super)fields χ_{ν^c}, $\bar{\chi}_{\nu^c}$ and the gauge (super)field become massive. As $m_\chi^2=m_{\bar{\chi}}^2$ is assumed, the VEVs of $\tilde{\chi}_{\nu^c}$ and $\tilde{\bar{\chi}}_{\nu^c}$ are equal and it is natural to introduce new fields $h_1=(\chi-\bar{\chi})/\sqrt{2}$ and $h_2=(\chi+\bar{\chi})/\sqrt{2}$. The imaginary component of $\tilde{h}_1$ is 'eaten up' by the vector gauge field A, which acquires a large mass $M_A=M=gqv_0\sim 10^{14}$ GeV. The real component η of $\tilde{h}_1$ acquires the same mass $M_\eta=M$.

From the analysis of gauge interactions alone, it follows that two-component spinors λ (superpartner of A) and h_1 (superpartner of $\tilde{h}_1$) form a four–component Dirac spinor $M_f(h_1\lambda+\lambda^+h_1^+)$ with mass $M_f=M$. The non–renormalizable interactions induce a Majorana–type mass term $\sim m_{soft}(h_1h_1+c.c.)$. There is also a Majorana–type mass term $\sim m_{soft}(\lambda\lambda+c.c.)$ coming from the soft supersymmetry breaking, so that two linear combinations of h_1 and λ are Majorana fermions with large ($\sim M$) and close masses. The non–renormalizable interactions (2.28) also induce masses $\sim m_{soft}$ for the real component of $\tilde{h}_2$ and its fermionic superpartner h_2.

The gauge boson A, the fermion λ and the scalar η interact with other states in the fundamental representation of E_6 (in particular with Higgses) so that the self–energy of scalars

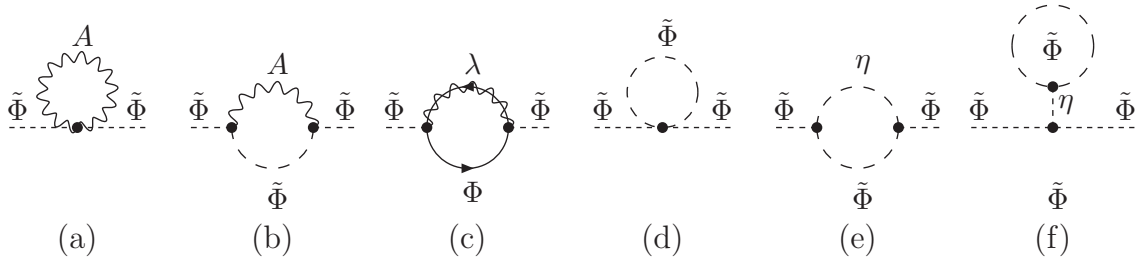

Figure 2.1: One–loop contributions to self–energy of scalars.

receives large contributions from diagrams with exchange of these heavy fields. For instance, see the case of one loop in figure 2.1.

As has already been mentioned in the introduction, the supersymmetric structure of the Lagrangian ensures that all large corrections, associated with the exchange of heavy fields, cancel out and only terms proportional to the soft supersymmetry breaking parameters remain:

$$\Pi^0(p^2) = 4\, g^2_{\omega_0'}\, q^2_{\tilde{\Phi}}\, m^2_{\tilde{\Phi}} B(m^2_{\tilde{\Phi}}, M^2), \qquad B(x,y) = \frac{(2\pi\mu)^{2\epsilon}}{\pi^2}\int \frac{d^{4-2\epsilon}k}{[k^2-x][(k-p)^2-y]} \tag{2.38}$$

$\mathbf{SU_C(3)\otimes SU_L(2)\otimes SU_R(2)\otimes U^2(1)}$ models. Tables 2.15 and 2.16 show, that it is sufficient to consider only the case of the first charge assignment and three $SU(3)_R \to SU_R(2)$ projections, the other cases being completely analogous.

In the case of the left–right symmetric (R) model, the zero modes in $\delta(\mathbf{27}+\bar{\mathbf{27}})$ are the $SU_R(2)$ doublets $\chi_R = (\chi_{e^c}, \chi_{\nu^c})$ and $\bar{\chi}_R = (\bar{\chi}_{\nu^c}, \bar{\chi}_{e^c})$. The scalar potential coming from the gauge interactions (2.21) and soft supersymmetry breaking is of the form

$$V = \frac{1}{8}\left(g^2_{Y_L} q^2_{Y_L} + g^2_{Y_R} q^2_{Y_R}\right)\left[(\tilde{\chi}^*_R \tilde{\chi}_R) - (\tilde{\bar{\chi}}^*_R \tilde{\bar{\chi}}_R)\right]^2 + \frac{g^2_{W_R}}{2}\left[\left(\tilde{\chi}^*_R \frac{\tau_i}{2}\tilde{\chi}_R\right) + \left(\tilde{\bar{\chi}}^*_R \frac{\tau_i}{2}\tilde{\bar{\chi}}_R\right)\right]^2 - \left[m^2_\chi\,(\tilde{\chi}^*_R\tilde{\chi}_R) + m^2_{\bar{\chi}}\,(\tilde{\bar{\chi}}^*_R\tilde{\bar{\chi}}_R)\right] \tag{2.39}$$

Let $v_1 \equiv \langle\tilde{\chi}_{\nu^c}\rangle$, $v_2 \equiv \langle\tilde{\chi}_{e^c}\rangle$ and $u_1 \equiv \langle\tilde{\bar{\chi}}_{\nu^c}\rangle$, $u_2 \equiv \langle\tilde{\bar{\chi}}_{e^c}\rangle$. The corresponding classical potential is

$$\begin{aligned} V = {} & \frac{1}{8}\left(g^2_{Y_L} q^2_{Y_L} + g^2_{Y_R} q^2_{Y_R}\right)\left[\left(|v_1|^2 + |v_2|^2\right) - \left(|u_1|^2 + |u_2|^2\right)\right] \\ & + \frac{1}{2} g^2_{W_R} |\left[v_2^* v_1 + u_1^* u_2\right]|^2 + \frac{1}{8} g^2_{W_R}\left[\left(|v_2|^2 - |v_1|^2\right) + \left(|u_1|^2 - |u_2|^2\right)\right] \\ & - \left[m^2_\chi\left(|v_1|^2 + |v_2|^2\right) + m^2_{\bar{\chi}}\left(|u_1|^2 + |u_2|^2\right)\right] \end{aligned} \tag{2.40}$$

There are symmetry breaking directions, which are D – flat. Vanishing of the first and the third terms in (2.40) requires that $|v_1| = |u_1|$ and $|v_2| = |u_2|$. With these conditions being satisfied, the second term in (2.40) vanishes if $v_1 = 0$ or $v_2 = 0$ or $arg(u_2) + arg(v_2) - arg(u_1) - arg(v_1) = \pi$.

The non-renormalizable superpotential, which bounds the classical potential from below, is similar to (2.28) with ν^c, χ_{ν^c} and $\bar{\chi}_{\nu^c}$ replaced with $SU_R(2)$ doublets $\psi_R = (e^c, \nu^c)$, $\chi_R =$

$(\chi_{e^c}, \chi_{\nu^c})$ and $\bar{\chi}_R = (\bar{\chi}_{\nu^c}, \bar{\chi}_{e^c})$. Its explicit form is

$$\begin{aligned} W = & M_c^{-1}\left[a_1^{ij}(\psi_R^i\bar{\chi}_R)(\psi_R^j\bar{\chi}_R) + a_2^i(\psi_R^i\bar{\chi}_R)(\psi_R^i\bar{\chi}_R) + a_3(\chi_R\bar{\chi}_R)(\chi_R\bar{\chi}_R)\right] \\ & + M_c^{-3}\left[(\chi_R\bar{\chi}_R)(\chi_R\bar{\chi}_R)(\chi_R\bar{\chi}_R) + b^i(\psi_R^i\bar{\chi}_R)(\chi_R\bar{\chi}_R)(\chi_R\bar{\chi}_R)\right. \\ & \left. + b_3^{ij}(\psi_R^i\bar{\chi}_R)(h^j\bar{\chi}_R)(\chi_R\bar{\chi}_R) + b_4^{ijk}(\psi_R^i\bar{\chi}_R)(\psi_R^j\bar{\chi}_R)(\psi_R^k\bar{\chi}_R)\right] + \ldots \end{aligned} \tag{2.41}$$

The freedom of $SU_R(2)$ gauge transformations allows to rotate away a possible VEV for one of the isospin components of one of the scalar fields, so one can take $u_2 = 0$ at the minimum of the potential. Since the classical potential under consideration reaches its minimum in one of the D – flat directions, v_2 is equal to zero as well. Then the following analysis is the same as in the case of the $SU_C(3) \otimes SU_L(2) \otimes U^3(1)$ model and furnishes the same result. The symmetry is broken down to $SU_C(3) \otimes SU_L(2) \otimes U^2(1)$.

The second skew left–right symmetric ($R^{''}$) model differs from the one above in S instead of e^c being an $SU_{R^{''}}(2)$ counterpart of the right–handed neutrino: $\chi_{R^{''}} = (\chi_{\nu^c}, \chi_S)$ and $\bar{\chi}_{R^{''}} = (\bar{\chi}_S, \bar{\chi}_{\nu^c})$. The symmetry is broken down to $SU_C(3) \otimes SU_L(2) \otimes U^2(1)$ as well.

In the case of the first skew left–right symmetric ($R^{'}$) model, the right–handed neutrino is an $SU_{R'}(2)$ singlet. Massless states in $\delta(27+\bar{27})$ are χ_{ν^c}, $\chi_{R'} = (\chi_{H^u}, \chi_L)$ and $\bar{\chi}_{\nu^c}$, $\bar{\chi}_{R'} = (\bar{\chi}_L, \bar{\chi}_{H^u})$. The classical potential coming from renormalizable and nonrenormalizable interactions is similar to (2.31) and yields the same results. The symmetry is broken down to $SU_C(3) \otimes SU_L(2) \otimes SU_{R'}(2) \otimes U(1)$.

Since the Higgs doublets (χ_{H^u}, χ_L) and $(\bar{\chi}_L, \bar{\chi}_{H^u})$ are contained in $\delta(\mathbf{27} + \bar{\mathbf{27}})$ as zero modes, there are directions in which the D-term potential vanishes for whatever large VEVs of these fields, i.e., there is a risk of breaking electroweak symmetry at a very high scale. To avoid it, the part of the classical potential which comes from the soft supersymmetry breaking should be positive in those directions, as is the case in the MSSM.

The coexistence of all the terms in the second row of (2.17) leads to the rapid proton decay, mediated by new D and D^c quarks, unless those are very heavy. The VEV of S which gives masses $\lambda_5^{ijk}\langle S_i\rangle$ to D and D^c is also the source of the μ–term $\lambda_4^{ijk}\langle S_i\rangle$. Although neither for $G_{U(1)}$ nor for $G_{SU_R(2)}$ the couplings λ_5^{ijk} and λ_5^{ijk} are related by symmetry, it is not natural to expect D and D^c to be much heavier than 1 TeV which is insufficient to suppress the proton decay. A solution to this problem may be provided by an appropriate discrete symmetry, which forbids some of the couplings in (2.17).

If this is a Z_2 symmetry, then there are only two models [70, 71] compatible with leptogenesis and nonzero neutrino masses. In the first model L and e^c, ν^c, D, D^c are odd, while the rest of the states are even, so that $\lambda_9 = \lambda_{10} = 0$. The second model differs from the first one in D and D^c being even, so that $\lambda_6 = \lambda_7 = \lambda_8 = 0$. Transformations of the discrete symmetry should

Model	R						$R^{'}$						$R^{''}$					
	d^c	u^c	H^u	H^d	e^c	ν^c	D^c	u^c	H^u	L	e^c	S	D^c	d^c	H^d	L	ν^c	S
1	+	+	+	+	-	-	-	+	+	-	-	+	-	+	+	-	-	+
2	+	+	+	+	-	-	+	+	+	-	-	+	+	+	+	-	-	+

Table 2.17: Transformation properties of components of $SU_R(2)$ doublets.

commute with transformations of the gauge symmetry. Table 2.17 shows, that this condition is satisfied only in the case of the left–right symmetric (R) model, while in both skew left–right symmetric models the components of $SU_R(2)$ doublets transform differently. Therefore, if proton stability is assured by such a discrete symmetry, the only allowed gauge group after breaking of G is $G^{'}_{U(1)} = SU_C(3) \otimes SU_L(2) \otimes U^2(1)$.

As is clear from the discussion above, only the difference $B-L$ (but not the lepton number L and the baryon number B separately) is gauged before the symmetry breaking. Moreover both B and L are violated at quantum level by the sphaleron processes. Consequently one can not unambiguously assign baryon and lepton numbers to the states of the model. However it can be done using the convention, that the Standard Model quarks have baryon number one third and zero lepton number and the Standard Model leptons have zero baryon number and lepton number equal to unity. Requiring that the total lepton and baryon charges of the term DQQ in the model with $\lambda_8 = 0$ be zero, we find that $B(D) = -\frac{2}{3}$ and $L(D) = 0$, so that D is a diquark in this model. Requiring that the total lepton and baryon charges of the term De^cu^c present in the model with $\lambda_8 \neq 0$ be zero, we find that $B(D) = \frac{1}{3}$ and $L(D) = 1$, so that D is a leptoquark in this model.

2.5 Superpotential and the Lagrange density

As has been argued above, after the breaking of the $B-L$ symmetry the residual gauge group is that of the Standard Model extended by one $U(1)$ group: $G^{'}_{U(1)} = SU_C(3) \otimes SU_L(2) \otimes U(1) \otimes U(1)$. After the symmetry breaking the right–handed neutrino acquires a large Majoran mass, so that the superpotential takes the form

$$\begin{aligned} W = & -\lambda_1^{ijk} u_i^{\mathrm{c}} (Q_j H_k^{\mathrm{u}}) + \lambda_2^{ijk} d_i^{\mathrm{c}} (Q_j H_k^{\mathrm{d}}) + \lambda_3^{ijk} e_i^{\mathrm{c}} (L_j H_k^{\mathrm{d}}) + \lambda_4^{ijk} S_i (H_j^{\mathrm{u}} H_k^{\mathrm{d}}) + \lambda_5^{ijk} S_i D_j D_k^{\mathrm{c}} \\ & + [-\lambda_6^{ijk} e_i^{\mathrm{c}} u_j^{\mathrm{c}} D_k + \lambda_7^{ijk} D_i^{\mathrm{c}} (Q_j L_k) + \lambda_8^{ijk} \nu_i^{\mathrm{c}} d_j^{\mathrm{c}} D_k] + [\lambda_9^{ijk} D_i (Q_j Q_k) + \lambda_{10}^{ijk} D_i^{\mathrm{c}} u_j^{\mathrm{c}} d_k^{\mathrm{c}}] \\ & - \lambda_{11}^{ijk} \nu_i^{\mathrm{c}} (L_j H_k^{\mathrm{u}}) + \frac{1}{2} \nu_i^c \hat{M}_{ij} \nu_j^c \end{aligned} \tag{2.42}$$

where either $\lambda_6 = \lambda_7 = \lambda_8 = 0$ or $\lambda_9 = \lambda_{10} = 0$ to ensure the proton stability. In the model with $\lambda_8 = 0$ the right–handed neutrino couples only to leptons and the Higgs, whereas in the model with $\lambda_8 \neq 0$ it also couples to the new singlet quarks, which introduces new decay channels.

In what follows we use the convention according to which the fermionic component of a chiral superfield is denoted by the same symbol as the superfield itself, the scalar component is denoted by the same symbol with tilde on top of it, and the auxiliary component is denoted by F with the corresponding superscript. For instance, in the y–basis (see appendix B) the right–handed neutrino chiral superfield is parametrized as

$$\nu^c(y,\theta) = \tilde{\nu}^c(y) + \sqrt{2}\theta\nu^c(y) + \theta^2 F_{\nu^c}(y) \tag{2.43}$$

In Feynman diagrams we will denote *all* scalars by dashed lines, whereas *all* fermions will be denoted by solid lines.

Excluding the auxiliary fields F, we obtain some terms of the Lagrange density $\mathcal{L} = \mathcal{L}_F + \mathcal{L}_S$ useful and relevant for the following analysis (we neglect the soft supersymmetry breaking terms).

$$\begin{aligned}\mathcal{L}_F &= \lambda_{11}^{ijk}\left[\tilde{\nu}_i^c L_j \epsilon H_k^u + \nu_i^c \tilde{L}_j \epsilon H_k^u + \nu_i^c L_j \epsilon \tilde{H}_k^u\right] - \lambda_8^{ijk}\left[\nu_i^c \tilde{d}_j^c D_k + \tilde{\nu}_i^c d_j^c D_k + \nu_i^c d_j^c \tilde{D}_k\right] \\ &\quad + \lambda_1^{ijk}\left[\tilde{u}_i^c Q_j \epsilon H_k^u + u_i^c \tilde{Q}_j \epsilon H_k^u + u_i^c Q_j \epsilon \tilde{H}_k^u\right] + \dots \qquad (2.44a) \\ \mathcal{L}_S &= \left[\lambda_{11}^{ijk}\lambda_{11}^{*mnk}\tilde{\nu}_i^c \tilde{L}_j \tilde{L}_n^\dagger \tilde{\nu}_m^{c\dagger} + \lambda_{11}^{ijk}\lambda_{11}^{*mjn}\tilde{\nu}_i^c \tilde{H}_k^u \tilde{H}_n^{u\dagger}\tilde{\nu}_m^{c\dagger} + M_i \lambda_{11}^{ijk}\tilde{\nu}_i^{c\dagger}(\tilde{L}_j \tilde{H}_k^u)\right] \\ &\quad + \left[\lambda_8^{ijk}\lambda_8^{*mnk}\tilde{\nu}_i^c \tilde{d}_j^c \tilde{d}_n^{c\dagger}\tilde{\nu}_m^{c\dagger} + \lambda_8^{ijk}\lambda_8^{*mjn}\tilde{\nu}_i^c \tilde{D}_k \tilde{D}_n^\dagger \tilde{\nu}_m^{c\dagger} + M_i \lambda_8^{ijk}\tilde{\nu}_i^{c\dagger}\tilde{d}_j^c \tilde{D}_k\right] \\ &\quad + \left[\lambda_{11}^{*ijk}\lambda_1^{mnk}\tilde{u}_m^c(\tilde{Q}_n \tilde{L}_j^\dagger)\tilde{\nu}_i^{c\dagger} + \lambda_{11}^{ijk}\lambda_1^{*mnk}\tilde{\nu}_i^c(\tilde{L}_j \tilde{Q}_n^\dagger)\tilde{u}_m^{c\dagger}\right] + \dots \qquad (2.44b)\end{aligned}$$

Since the vacuum expectation value of $\tilde{S}$ determines the value of the μ–term, which is expected to be of the order of 1 TeV, it is natural to assume, that the associated $U(1)$ symmetry is broken at a scale much below the Majorana neutrino mass scale $10^9 - 10^{11}$ GeV. The mass terms coming from soft–supersymmetry breaking are also expected to be of the order of 1 TeV, i.e. they are much smaller than the heavy neutrino mass as well. We also neglect the so–called thermal masses of all particles but the Higgses. For this reason, all the species but the Majorana neutrino are treated as massless in what follows.

2.6 Conclusions

In this chapter, a "low–energy" extension of the Standard Model compatible with the baryogenesis via leptogenesis scenario has been derived from the superstring inspired E_6 model.

The E_6 model allows six charge assignments compatible with the Standard Model. Charge conservation in processes involving states of different generations requires that the same charge assignment must be used for all generations.

The initial gauge symmetry is broken in a sequence of stages. The first stage is due to Calabi–Yau compactification and the effective Higgs mechanism. The condition that the proton is long-lived requires that the symmetry is broken either to $G_{U(1)}$ or $G_{SU_R(2)}$.

As the temperature drops, supersymmetry breaks down spontaneously in the hidden sector. The breaking of supersymmetry is mediated to the visible sector through gravity and manifests itself in the soft terms.

At the next stage right–handed scalar neutrinos of the two additional $(\mathbf{27} + \bar{\mathbf{27}})$ generations develop a nonzero VEV, breaking the $B - L$ symmetry. The introduction of a simple discrete symmetry ensures, that $B - L$ is broken at a scale, which is sufficiently high for generating large masses for the right-handed neutrinos, and that the right–handed scalar neutrinos of the three known generations do not acquire a VEV. The same symmetry also forbids Yukawa couplings which, if present, would induce large masses for the conventional neutrinos. The supersymmetric structure of the theory ensures that large quantum corrections to masses of the scalars, associated with the presence of heavy gauge fields, cancel out. Provided that a rapid proton decay mediated by the new quarks is forbidden by a Z_2 symmetry, the residual gauge symmetry after the breaking of the $B - L$ symmetry is given by $G'_{U(1)} = SU_C(3) \otimes SU_L(2) \otimes U(1) \otimes U(1)$.

Apart from the additional (compared to the SM) $U(1)$ symmetry, the characteristic feature of this "low–energy" model is its extended particle content. In addition to the known particles and right-handed neutrinos it contains a SM singlet S, new heavy quarks and three generations of Higgses, as well as their superpartners. Since both the new quarks and the Higgses couple to right-handed neutrinos, there are more $B - L$ violating decay channels than in the SM or its supersymmetric extension. At the same time there are more processes which washout the generated $B - L$ asymmetry.

The model is interesting not only from the viewpoint of successful leptogenesis, but also from the viewpoint of "low–energy" phenomenology. More specifically, mixing of the new fermions with the conventional ones and mixing of the additional "light" gauge boson with the Z–boson may have interesting consequences observable at the next generation of particle colliders.

Chapter 3

Leptogenesis in the E_6 model

In chapter 1 we have discussed the influence of the effects of general relativity on generation of the lepton and baryon asymmetries. These effects are to a large extent independent of the used quantum field model. It is clear however, that the asymptotic values of the lepton and baryon asymmetries strongly depend on the model we use for the calculation. In particular, new decay and scattering channels, which appear in the supersymmetric and GUT extensions of the Standard Model, may strongly influence the generation of the lepton asymmetry.

In this chapter we consider leptogenesis in the model discussed in the previous chapter. As far as leptogenesis is concerned, the main difference of this model, whose gauge group after the breaking of the $B-L$ symmetry is given by $SU_C(3)\otimes SU_L(2)\otimes U(1)\otimes U(1)$, from the SM is its extended particle content. Whereas in the Standard Model the right–handed neutrino can only decay into a lepton and the Higgs, in the model under consideration the right–handed neutrino can also decay into superpartners of the aforementioned species and, for certain values of the parameters, into new quarks. Thus, there are more processes which generate the lepton asymmetry, as well as more processes which wash it out. The goal of this chapter is to calculate rates of these processes and solve the resulting system of the Boltzmann equations numerically.

The asymmetry is generated in the *CP*–violating decays of the heavy neutrinos and their superpartners, discussed in section 3.1. Technically the *CP* asymmetry arises due to interference of the corresponding tree–level and one–loop–vertex and tree–level and one–loop–self–energy diagrams, discussed in the same section in the limit of strong hierarchy in the Majorana mass matrix.

Scattering processes wash out the asymmetry generated in the decay of the Majorana neutrino. The two–body scattering processes mediated by the right–handed neutrino, which violate lepton number by two units, are considered in section 3.2. We also calculate *CP* asymmetry in the scattering processes and check that after summation over all initial and final states the asymmetry in scattering vanishes, as is required by the unitarity.

Two–body scattering processes with the Majorana neutrino in the initial state, which violate lepton number by one unit, are considered in section 3.3. These processes are to leading order *CP* conserving and contribute to the Boltzmann equation for the lepton number asymmetry only if the latter one differs from zero.

Processes discussed in section 3.4 conserve total lepton number, but reduce the number of the heavy (s)neutrinos and redistribute the lepton asymmetry between the leptons and their superpartners.

In section 3.5 gauge mediated processes transforming leptons into scalar leptons and vice versa are briefly discussed. As strength of these processes is determined by gauge couplings, which are much bigger than the Majorana Yukawa couplings, the gauge mediated scattering processes are in equilibrium and ensure equality of chemical potentials of leptons and their superpartners.

Relations between chemical potentials of various species are considered in section 3.6. These relations differ from those in the Standard Model due to the fact, that the supersymmetric E_6 model contains two Higgs doublets per generation. We also derive relation between the baryon and lepton numbers at temperatures where all Yukawa interactions, apart from the Yukawa interactions of the right–handed neutrinos, are in equilibrium.

Finally in section 3.7 we derive an explicit form of the system of Boltzmann equations and present numerical estimates of the lepton and baryon asymmetries.

3.1 Decay of the heavy neutrino

The *CP* violating and lepton number violating decay of the heavy Majorana neutrino is the source of the lepton asymmetry in the baryogenesis via leptogenesis scenario. Lepton number is violated by two units by the Majorana neutrino mass term, whereas the *CP* violation arises due to complex couplings of the heavy neutrinos to other species in the model.

In the model we consider the heavy neutrino can decay into a lepton+Higgs pair and (if $\lambda_8 \neq 0$) to a pair of quarks. Both processes violate lepton number (recall, that in the model with $\lambda_8 \neq 0$ the exotic state D is a leptoquark) and violate *CP*, thus leading to the generation of lepton and baryon number asymmetries. The fermion Majorana neutrino can decay either into a lepton and a Higgs or into a slepton and a higgsino, whereas its superpartner can decay into a slepton and a Higgs or a lepton and a higgsino (see figure 3.1). The generalization to the case $\lambda_8 \neq 0$ is straightforward.

The decay amplitudes of the heavy neutrino and its superpartner are given at tree–level by

$$T_{\nu_i^c \to L+\tilde{H}^u} = \lambda_a^{ijk}(u_i^\alpha v_\alpha^j), \quad T_{\tilde{\nu}_i^c \to L+H^u} = \lambda_a^{ijk}(v_j^\alpha v_\alpha^k), \quad T_{\tilde{\nu}_i^{c\dagger} \to \tilde{L}+\tilde{H}^u} = M_i \lambda_a^{ijk} \tag{3.1}$$

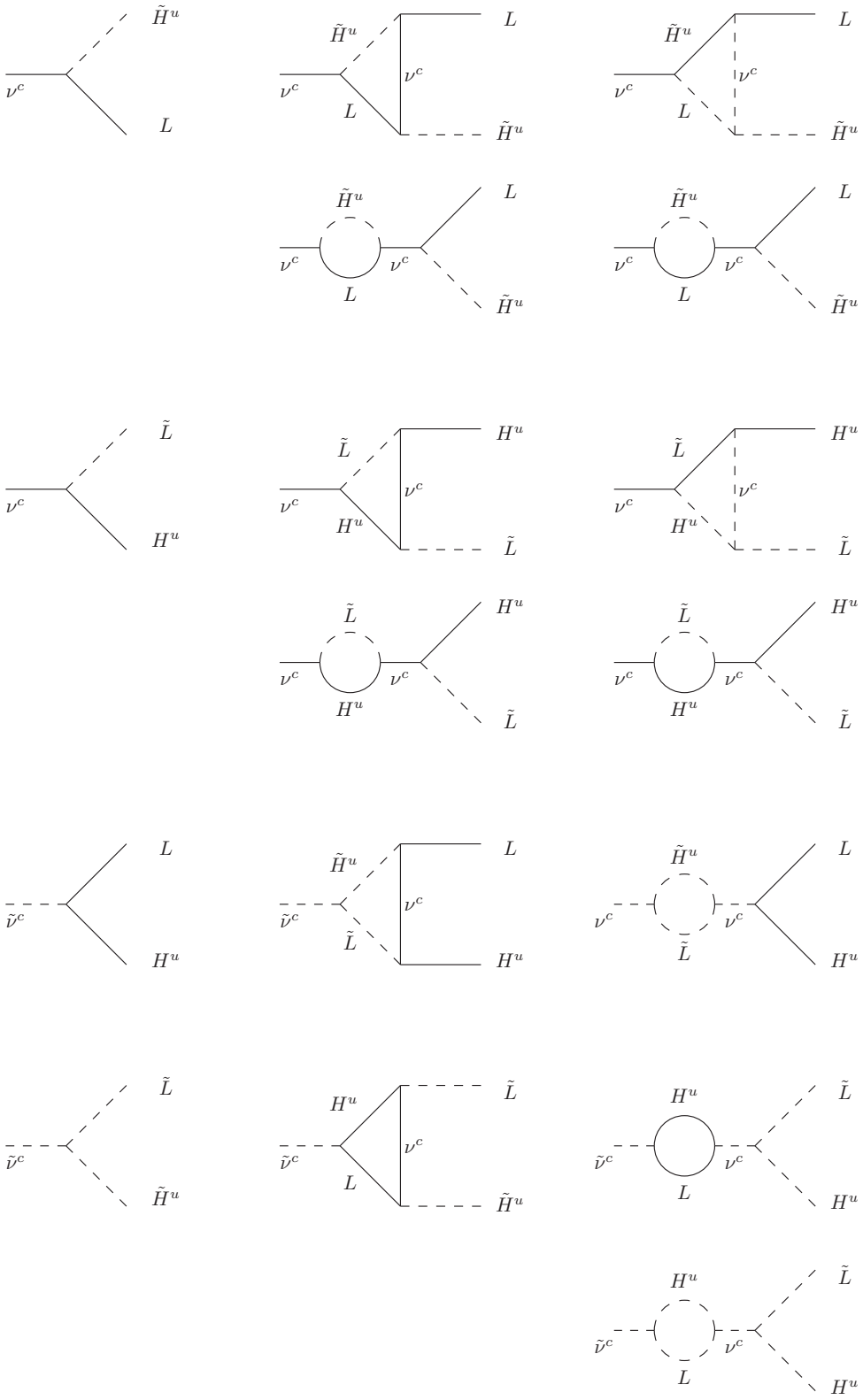

Figure 3.1: Decay of the Majorana neutrinos and their superpartners into leptons at tree and one–loop level. Decays into quarks are not shown.

The corresponding decay widths in the rest–frame of the decaying particle read ($a = 11$)

$$\frac{1}{4}\Gamma_{\nu_i^c} = \Gamma_{\nu_i^c \to L+\tilde{H}^u} = \Gamma_{\nu_i^c \to \bar{L}+\tilde{H}^{u\dagger}} = \Gamma_{\nu_i^c \to \tilde{L}+H^u} = \Gamma_{\nu_i^c \to \tilde{L}^\dagger+\bar{H}^u} = \frac{(\lambda_a\lambda_a^\dagger)_{ii}}{16\pi} M_i \tag{3.2a}$$

$$\frac{1}{2}\Gamma_{\tilde{\nu}_i^c} = \Gamma_{\tilde{\nu}_i^{c\dagger} \to \tilde{L}+\tilde{H}^u} = \Gamma_{\tilde{\nu}_i^c \to \tilde{L}^\dagger+\tilde{H}^{u\dagger}} = \Gamma_{\tilde{\nu}_i^c \to L+H^u} = \Gamma_{\tilde{\nu}_i^{c\dagger} \to \bar{L}+\bar{H}^u} = \frac{(\lambda_a\lambda_a^\dagger)_{ii}}{8\pi} M_i \tag{3.2b}$$

where we have summed over components of the electroweak doublets. In the model with $\lambda_8 \neq 0$ the Majorana neutrino can also decay into a (s)quark pair. The corresponding tree–level decay widths differ from (3.2) in λ_{11} replaced with λ_8 and, since the decay is into the $SU_L(2)$ *singlet* (lepto)*quarks*, by an overall factor of three halves.

The *CP* is violated in all of these processes. That is, the probabilities of a decay into a final state and its charge conjugate are not equal. Technically, the *CP* asymmetry arises due to the interference between the tree–level and the one–loop–vertex [9] and the tree–level and the one–loop–self–energy [10] diagrams shown in figure 3.1. The Majorana neutrino is an unstable particle, and therefore a self–consistent treatment of processes with an intermediate Majorana requires a resummation of all the self–energy diagrams, which leads to a resummed propagator

$$\frac{1}{\hat{q} - M - \Sigma(q)} \tag{3.3}$$

with the self–energy $\Sigma(q)$. The resummation removes the divergence of the transition amplitude in the case that the intermediate Majorana is the same as the initial one (see figure 3.1) and predicts a resonant enhancement of the generated lepton asymmetry in the case of close Majorana masses [72]. We consider only the case of non–resonant leptogenesis, i.e. assume that there is a large hierarchy of the Majorana masses $M_1 \ll M_2 \ll M_3$.

Let us first discuss the $\nu^c \to L + \tilde{H}^u$ and $\nu^c \to \bar{L} + \tilde{H}^{u\dagger}$ decays at one–loop level. The corresponding Feynman graphs are depicted in figure 3.1. Although in many cases the application of Feynman rules can significantly simplify calculations, one should be careful when applying Feynman rules to processes with intermediate Majorana fermions. The reason is that contrary to the case of Dirac particles Majorana fermions have several propagators [73, 74], listed in section B.3. In order to avoid possible confusion, the one–loop amplitudes have been calculated by direct integration of the corresponding elements of the S–matrix. The calculation is to a large extent standard, and the subtleties associated with the Majorana fermions in the initial and intermediate states are easily handled. Using this approach we obtain for amplitude of the one–loop vertex diagram in figure 3.1

$$T_{fi} = -\lambda^{*imn}\lambda^{lmk}\lambda^{ljn}(\bar{v}^i_{\dot{\alpha}} v^j_\beta)\frac{-i}{(2\pi)^4}\int \frac{M_l \delta^\beta_\gamma}{k^2 - M_l^2}\frac{(k-p_3)^\mu \bar{\sigma}_\mu^{\dot{\alpha}\gamma}}{(k-p_3)^2}\frac{1}{(k-p_3+p_1)^2}\, d^4k \tag{3.4}$$

where p_1, p_2 and p_3 are momenta of the initial Majorana neutrino, final lepton and final Higgs respectively, while $\bar{v}^i_{\dot{\alpha}}$ and v^j_β are chiral amplitudes of the initial and final fermions. The first

term under the integral comes from the lepton number violating Majorana propagator (B.20c), the second one is the propagator of a massless lepton, and the third one is the propagator of the (nearly) massless Higgs in the loop. The appearance of the intermediate Majorana neutrino mass M_l is quite natural and expected from general considerations. The reason is that processes with intermediate Weyl fermions are known to conserve lepton number; a good example would be the Standard Model with massless neutrino. Moreover, since in the SM with massless neutrino all the *CP* violating phases can be rotated away, *CP* is also conserved in the leptonic sector. Since a Majorana fermion with vanishing mass is equivalent to a Weyl fermion, the amplitude of the *CP* violating processes should vanish as M_l goes to zero.

The integral over k can be expressed in terms of three–point functions

$$\frac{1}{i\pi^2}\int \frac{1}{k^2-M_l^2}\frac{(k-p_3)^\mu}{(k-p_3)^2}\frac{d^4k}{(k-p_3+p_1)^2} = C_\mu(p_3^2,p_1^2,M_l^2,0,0) - p_3^\mu C_0(p_3^2,p_1^2,M_l^2,0,0) \tag{3.5}$$

As is argued in appendix A, the vector integral can be decomposed into a vector constructed from the external momenta p_1 and p_3. Taking additionally into account that $p_3 = p_1 - p_2$ and that due to the Weyl equation the contribution of the on–shell left–handed neutrino vanishes, we obtain

$$T_{fi} = \lambda^{*imn}\lambda^{lmk}\lambda^{ljn}(\bar{v}_{\dot\alpha}^i\bar\sigma_\mu^{\dot\alpha\beta}p_1^\mu v_\beta^j)\frac{M_l}{16\pi^2}\left[C_0(0,M_i^2,M_l^2,0,0)+C_{12}(0,M_i^2,M_l^2,0,0)\right] \tag{3.6}$$

where a summation over all intermediate states is assumed. One would also expect (for the same reason as above) the mass of the decaying heavy neutrino M_i to appear in the decay amplitude, and this is indeed the case. Using relations (B.23) we find

$$(\bar{v}_{\dot\alpha}^i\bar\sigma_\mu^{\dot\alpha\beta}p_i^\mu v_\beta^j) = -M_i(u_i^\alpha v_\alpha^j) \tag{3.7}$$

which completes the calculation of the amplitude of the one–loop–vertex diagram.

In supersymmetric extensions of the Standard Model, one of which is considered here, there is an additional one–loop vertex diagram with two scalars in the intermediate state, depicted in figure 3.1. Proceeding as above we obtain for the amplitude of this diagram

$$T_{fi} = \lambda^{*imn}\lambda^{lmk}\lambda^{ljn}(u_i^\alpha v_\alpha^j)\frac{M_iM_l}{16\pi^2}C_{12}(0,M_i^2,M_l^2,0,0) \tag{3.8}$$

so that the total contribution of one–loop vertex diagrams in supersymmetric extensions of the Standard Model is given by

$$T_{fi} = -(u_i^\alpha v_\alpha^j)\lambda^{*imn}\lambda^{lmk}\lambda^{ljn}\frac{M_iM_l}{16\pi^2}C_0(0,M_i^2,M_l^2,0,0) \tag{3.9}$$

A similar calculation yields for the total amplitude of the one–loop self–energy diagrams

$$T_{fi} = \lambda^{*imn}\lambda^{lmk}\lambda^{ljn}(u_i^\alpha v_\alpha^j)\frac{M_iM_l}{M_i^2-M_l^2}\frac{C_sC_b}{16\pi^2}B_1(M_i^2,0,0) \tag{3.10}$$

where $b = 8, 11$ and summation over indices of all the intermediate states is assumed. The coefficient $C_s = 2$ takes into account that both particles and their superpartners run in the loop, whereas the coefficient C_b accounts for the number of states of the multiplets in the loop: $C_b = 2$ in the case of a leptonic doublet and $C_b = 3$ in the case of a quark color triplet. The two–point function B_1 (see appendix A) comes from the integration over the momenta of the particles in the loop, whereas the term with the difference of the heavy neutrino masses in the denominator comes from the propagator of the intermediate Majorana neutrino.

Note that the structure of flavor indices of the vertex and self–energy contributions is different due to the presence of three Higgs generations in the model under consideration.

Combining the tree–level and one–loop amplitudes and using relation (A.11) we obtain the one–loop Yukawa coupling h^{ijk} of the Majorana neutrino to the lepton+Higgs pair and the one–loop Yukawa coupling $\bar{h}^{ijk}$ to the antilepton+antiHiggs pair ($a = 11$)

$$\begin{aligned} h_a^{ijk} = \lambda_a^{ijk} &- \lambda_a^{*imn}\lambda_a^{lmk}\lambda_a^{ljn}\frac{M_iM_l}{16\pi^2}C_0(0, M_i^2, M_l^2, 0, 0) \\ &- \lambda_b^{*imn}\lambda_b^{lmn}\lambda_a^{ljk}\frac{M_iM_l}{M_i^2 - M_l^2}\frac{C_b}{16\pi^2}\frac{C_s}{2}B_0(M_i^2, 0, 0) \end{aligned} \tag{3.11a}$$

$$\begin{aligned} \bar{h}_a^{ijk} = \lambda_a^{*ijk} &- \lambda_a^{imn}\lambda_a^{*lmk}\lambda_a^{*ljn}\frac{M_iM_l}{16\pi^2}C_0(0, M_i^2, M_l^2, 0, 0) \\ &- \lambda_b^{*imn}\lambda_b^{lmn}\lambda_a^{ljk}\frac{M_iM_l}{M_i^2 - M_l^2}\frac{C_b}{16\pi^2}\frac{C_s}{2}B_0(M_i^2, 0, 0) \end{aligned} \tag{3.11b}$$

The asymmetry in the decay is defined as

$$\varepsilon_i = \frac{\Gamma_{\nu_i^c \to L + \tilde{H}^u} - \Gamma_{\nu_i^c \to \bar{L} + \tilde{H}^{u\dagger}}}{\Gamma_{\nu_i^c \to L + \tilde{H}^u} + \Gamma_{\nu_i^c \to \bar{L} + \tilde{H}^{u\dagger}}} \tag{3.12}$$

If the two– and three–point functions were real, then, as follows from (3.11), one could obtain (3.11a) from (3.11b) by complex conjugation so that the asymmetry would vanish. Therefore the CP asymmetry in the decay is proportional to the absorptive parts of the two– and three–point functions. Although the terms of third order in λ are small compared to those linear in λ and can safely be neglected in denominator of (3.12), they give the dominant contribution to the numerator. To leading order

$$\varepsilon_i = -\frac{\sum \sqrt{\frac{a_l}{a_i}}\left[\mathrm{Im}(\lambda_a^{*ijk}\lambda_a^{*imn}\lambda_a^{lmk}\lambda_a^{ljn})\ln\left(1 + \frac{a_i}{a_l}\right) + \mathrm{Im}(\lambda_a^{*ijk}\lambda_b^{*imn}\lambda_b^{lmn}\lambda_a^{ljk})\frac{C_sC_b/2}{a_l/a_i - 1}\right]}{8\pi(\lambda_a\lambda_a^\dagger)_{ii}} \tag{3.13}$$

where $a_i \equiv \left(\frac{M_i}{M_1}\right)^2$. To obtain (3.13) we have used the expressions for the imaginary parts of the one–loop integrals (A.6), (A.13) and (A.16). The summation in the first term is over all the intermediate and final states, whereas in the second term $l \neq i$ so as to avoid division of zero by zero. The resummation removes the uncertainty arising in this simplified treatment.

Since supersymmetry is broken only softly, and the masses of all the species are assumed to be much smaller than the masses of the heavy neutrinos, the *CP* asymmetry in the decay into a slepton+higgsino pair is obviously given by (3.13) as well.

The same is true for the *CP* asymmetry in the decay of the heavy sneutrino into two fermions. Moreover, even the amplitudes of the one–loop vertex and one–loop self–energy diagrams coincide with (3.9) and (3.10) respectively (the only difference is that the chiral amplitude of the initial Majorana is replaced by the chiral amplitude of the final higgsino). Although there is only one one–loop vertex diagram in this case, since neither the propagators of the scalar particles in the loop nor the lepton–number violating propagator of the Majorana neutrino are proportional to the loop four–momentum vector k^μ, the resulting amplitude automatically contains only $C_0(0, M_i^2, M_l^2, 0, 0)$ (see definition of the three–point functions in appendix A). Analogously, although there is only one one–loop self–energy diagram, so that the supersymmetry factor $C_s = 2$ does not arise, as both particles in the loop are scalars, the resulting amplitude is proportional to the two–point function B_0 which is twice as big as B_1 arising in the case above. Let us also note, that mass of the decaying sneutrino comes in this case from the triple scalar coupling $M_i \lambda_a^{ijk}$ in (2.44b).

Though the *CP* asymmetry in the decay of the heavy sneutrino into two scalars is given by (3.13), the amplitudes of the one–loop diagrams differ from those above. Since the propagators of the two massless fermions in the one–loop vertex diagram (the second and the third terms under the integral) are proportional to the corresponding four–momenta

$$T = \lambda_a^{*imn} \lambda_a^{ljn} \lambda_a^{lmk} \frac{i}{(2\pi)^4} \int \frac{M_l \delta_{\dot\beta}^{\dot\alpha}}{k^2 - M_l^2} \frac{(k-p_2)_\nu \sigma^\nu_{\alpha\dot\alpha}}{(k-p_2)^2} \frac{(k-p_2+p_1)^\mu \bar\sigma_\mu^{\dot\beta\alpha}}{(k-p_2+p_1)^2} d^4k \tag{3.14}$$

the resulting amplitude is a combination of the two– and three–point functions

$$T = \lambda_a^{*imn} \lambda_a^{ljn} \lambda_a^{lmk} \frac{2M_l}{16\pi^2} \left[B_0(M_i^2, 0, 0) - M_i^2 C_{12}(0, M_i^2, M_l^2, 0, 0) \right.$$
$$\left. + (M_l^2 - M_i^2/2) C_0(0, M_i^2, M_l^2, 0, 0) \right] \tag{3.15}$$

where the overall factor of two comes from convolution of the two σ matrices. The structure of (3.15) differs from that of (3.9). However, since the asymmetry is determined by the imaginary part of this combination, which differs from that of C_0 by only an overall factor $(2M_i^2)^{-1}$, the resulting contribution to the *CP* asymmetry is just the same as in the decay into two fermions.

Analogously, because both lines in the loop are fermionic, the amplitude of the one–loop self–energy diagram (3.16) is a combination of scalar and vector two–point functions.

$$T = -\lambda_b^{*imn} \lambda_b^{lmn} \lambda_a^{ljk} \frac{i}{(2\pi)^4} \frac{C_b}{M_i^2 - M_l^2} \int \frac{q^\mu \bar\sigma_\mu^{\dot\beta\alpha}}{q^2} \frac{(q-p_1)_\nu \sigma^\nu_{\alpha\dot\beta}}{(q-p_1)^2} \tag{3.16}$$

This combination reduces to the scalar two–point function B_0 times $M_i^2/2$. The latter factor one-half is compensated by the factor of two coming from the convolution of the σ matrices.

Note that there is also an additional one–loop self–energy diagram with only scalars in the intermediate state. It contributes to the sneutrino decay width, but does not contribute to the *CP* asymmetry. The reason is that unlike (3.16) the amplitude of this diagram is proportional to the product $\lambda_b^{imn}\lambda_b^{*lmn}\lambda_a^{ljk}$, so that its contribution to the *CP* asymmetry, which is proportional to $\mathrm{Im}[\lambda_a^{ijk}\lambda_b^{*imn}\lambda_b^{lmn}\lambda_a^{*ljk}]$, vanishes after summation over intermediate and final states.

The last process we consider in this section is the decay of the heavy scalar neutrino into three scalars at tree level (see figure 3.2). There is a number of such processes including those

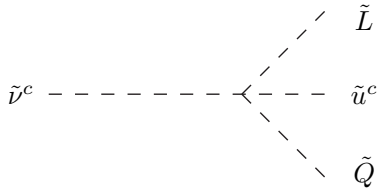

Figure 3.2: Processes determined by quartic scalar couplings.

with the new quarks or the Standard Model singlet S in the final state. The leading contribution, however, is due to the top quark, whose Yukawa coupling is of the order of unity. The partial width of this decay channel is given by

$$\Gamma_{\tilde{\nu}_i^c \to \tilde{L}^\dagger + \tilde{Q} + \tilde{u}^c} = \frac{3\Lambda^i_{(8)11,1}}{64\pi^2} M_i \tag{3.17}$$

where the factor of three is due to three color degrees of freedom and $\Lambda_{(8)}$ is defined in (D.28).

3.2 Processes mediated by the right–handed neutrinos

Lepton number violating two–body scattering processes are responsible for washout of the lepton number asymmetry generated in the decay of the heavy Majorana (s)neutrino. Although of higher order than the tree level decays, these processes have to be taken into account to avoid the generation of an asymmetry in thermal equilibrium [38].

The effects of the *CP* violation in the scattering processes depicted in figure 3.3 can be taken into account by the use of the one–loop couplings (3.11). Since the intermediate heavy neutrinos are off–shell, the Majorana masses are to be replaced by square of the momentum transfer.

Let us first consider processes with one fermion and one scalar in the initial and the final states in the model with $\lambda_8 = 0$. These include the $L + \tilde{H}^u \to \bar{L} + \tilde{H}^{u\dagger}$ scattering process present already in the Standard Model supplemented by three right–handed neutrinos and,

since the model under consideration is supersymmetric, also the processes $\tilde{L} + H^u \to \tilde{L}^\dagger + \bar{H}^u$, $\tilde{L} + H^u \to \bar{L} + \tilde{H}^{u\dagger}$ and $L + \tilde{H}^u \to \tilde{L}^\dagger + \bar{H}^u$. The Feynman diagrams of these processes are depicted in figure 3.3.

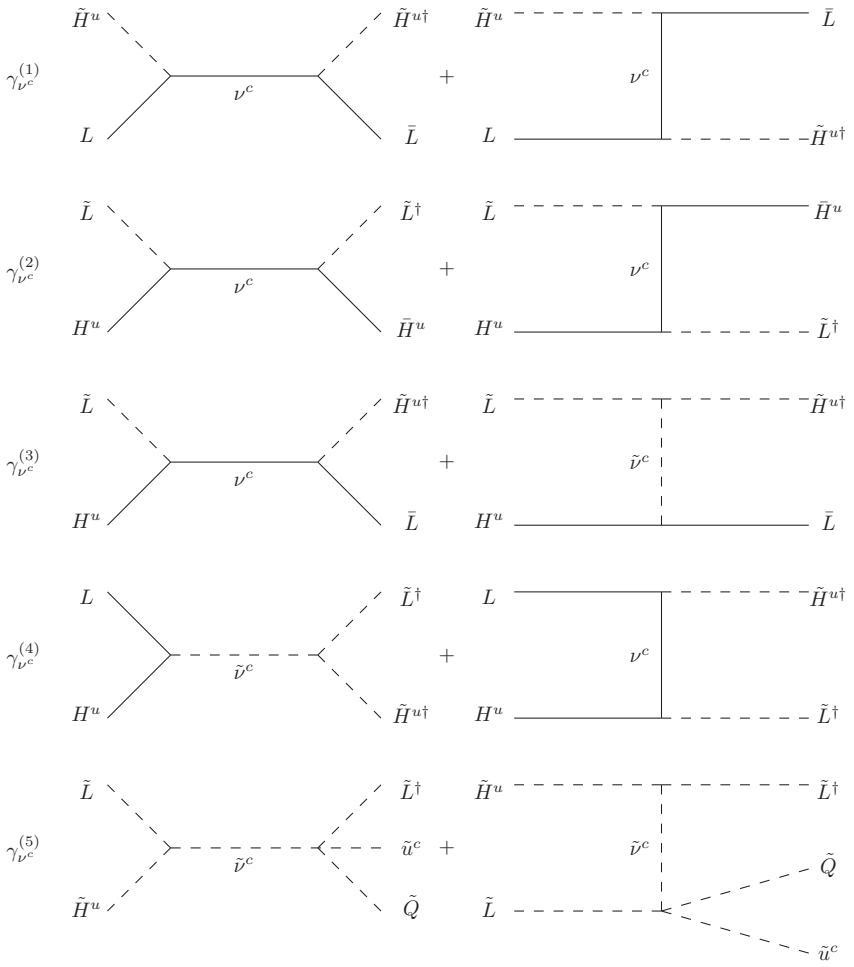

Figure 3.3: Lepton number violating processes mediated by the heavy (s)neutrino.

The amplitude of the s–channel scattering $L_i + \tilde{H}^u_m \to \bar{L}_j + \tilde{H}^{u\dagger}_n$ is given by ($a = 11$)

$$T^{(s)}_{fi} = -(u^\alpha_i v_{\alpha\, j}) \sum_\eta (h^{\eta im}_a h^{\eta jn}_a) \frac{M_\eta}{s - M^2_\eta} \tag{3.18}$$

Keeping only the leading terms (i.e. those of the lowest order in λ_a) and replacing the mass of the intermediate Majorana neutrino M_η by the center of mass energy we obtain

$$T^{(s)}_{fi} = (u^\alpha_i v_{\alpha\, j}) \frac{1}{M_1} \sum_{k,n,p,\eta} \frac{1}{z - a_\eta} [- (\lambda^{\eta im}_a \lambda^{\eta jn}_a) \sqrt{a_\eta} + (\lambda^{\eta im}_a \xi^{\eta jn}_a + \xi^{\eta im}_a \lambda^{\eta jn}_a) + (\lambda^{\eta im}_a \eta^{\eta jn}_a + \eta^{\eta im}_a \lambda^{\eta jn}_a)] \tag{3.19}$$

where $z = s/M_1^2$ and

$$\xi_a^{\eta jn} = \frac{C_s}{16\pi^2} \sum_{l,p,q} \lambda_a^{*\eta pq} \lambda_a^{lpq} \lambda_a^{ljn} \sqrt{a_l} \frac{z}{z - a_l} B_0(s, 0, 0), \tag{3.20a}$$

$$\eta_a^{\eta jn} = \frac{1}{16\pi^2} \sum_{l,p,q} \lambda_a^{*\eta pq} \lambda_a^{lpn} \lambda_a^{ljq} \sqrt{a_l} s C_0(0, s, M_l^2, 0, 0) \tag{3.20b}$$

have been introduced to shorten the notation. Coupling (3.20a) represents the one–loop self–energy contribution, whereas (3.20b) represents the one–loop vertex contribution.

To obtain the amplitude of the charge conjugate process, apart from replacing the chiral amplitudes with the conjugated ones we should also replace $h^{\eta im}$ by $\bar{h}^{\eta im}$ in (3.18). The resulting amplitude, thus, differs from (3.19) by complex conjugation of all the coupling constants (but not the two– and three–point functions) including those in (3.20).

A nonzero *CP* asymmetry is generated only if the corresponding one–loop integrals have nonzero absorptive contributions. Since in the case of t–channel (or u–channel) scattering the square of the momentum transfer is negative, the imaginary parts of the scalar one–loop integrals B_0 and C_0 vanish (see appendix A). Consequently those processes are *CP* conserving to leading order and the one–loop effects can be neglected. The tree–level amplitude of the t–channel process is given by

$$T(t)_{fi} = -(u_i^\alpha v_{\alpha j}) \frac{1}{M_1} \sum_\eta (\lambda_a^{\eta in} \lambda_a^{\eta jm}) \frac{\sqrt{a_\eta}}{y - a_\eta}, \quad y = \frac{t}{M_1^2} \tag{3.21}$$

The amplitudes of the remaining three processes differ from (3.19) and (3.21) only in the chiral amplitudes entering the corresponding expressions: $(u_m^\alpha v_{\alpha n})$, $(u_i^\alpha v_{\alpha n})$ and $(u_m^\alpha v_{\alpha j})$ instead of $(u_i^\alpha v_{\alpha j})$.

Denoting by σ_Σ the sum of the cross sections of all the four processes and by σ_Σ^C the sum of the cross sections of the charge conjugate ones, we define the *CP* asymmetry in scattering as

$$\varepsilon \equiv \frac{\sigma_\Sigma - \sigma_\Sigma^C}{\sigma_\Sigma + \sigma_\Sigma^C} \tag{3.22}$$

Using (3.19) and (3.21) and summing over components of weak isodublets we obtain for the numerator of (3.22)

$$\begin{aligned}
\sigma_\Sigma - \sigma_\Sigma^C \propto \frac{1}{16\pi^3} \sum_{\eta,\bar{\eta}}^{l,p,q} \frac{\sqrt{a_l a_\eta}}{z - a_{\bar{\eta}}} \Bigg\{ & \mathrm{Im} \left[\left(\lambda_a^{*\eta im} \lambda_a^{*\eta jn} \frac{2z}{z - a_\eta} - \lambda_a^{*\eta in} \lambda_a^{*\eta jm} \ln \left(\frac{z + a_\eta}{a_\eta} \right) \right) \right. \\
& \left. \times \left(\lambda_a^{\bar{\eta} im} \lambda_a^{*\bar{\eta} pq} \lambda_a^{lpq} \lambda_a^{ljn} + \lambda_a^{lim} \lambda_a^{lpq} \lambda_a^{*\bar{\eta} pq} \lambda_a^{\bar{\eta} jn} \right) \right] \frac{z}{z - a_l} C_s \mathrm{Im} \left[B_0(s, 0, 0) \right] \\
& + \mathrm{Im} \left[\left(\lambda_a^{*\eta im} \lambda_a^{*\eta jn} \frac{2}{z - a_\eta} - \lambda_a^{*\eta in} \lambda_a^{*\eta jm} \ln \left(\frac{z + a_\eta}{a_\eta} \right) \right) \right. \\
& \left. \times \left(\lambda_a^{\bar{\eta} im} \lambda_a^{*\bar{\eta} pq} \lambda_a^{lpn} \lambda_a^{ljq} + \lambda_a^{liq} \lambda_a^{lpm} \lambda_a^{*\bar{\eta} pq} \lambda_a^{\bar{\eta} jn} \right) \right] \mathrm{Im} \left[s C_0(0, s, M_l^2, 0, 0) \right] \Bigg\}
\end{aligned} \tag{3.23}$$

The imaginary parts of the two– and three–point functions are given by (see appendix A)

$$\mathrm{Im}\left[B_0(s,0,0)\right]=\pi,\quad \mathrm{Im}\left[sC_0(0,s,M_l^2,0,0)\right]=-\pi\ln\left(\frac{z+a_l}{a_l}\right) \tag{3.24}$$

Unitarity requires, that in thermal equilibrium the total *CP* asymmetry be zero [38]. Applied to the case under consideration this means, that summed over all initial and final states σ_Σ should be equal to σ_Σ^C. Using (3.23) we find for the difference of the cross sections

$$\begin{aligned}\sigma_\Sigma-\sigma_\Sigma^C\propto\frac{1}{8\pi^2}\sum_{i,j,n,m}^{\eta,\bar\eta,l,p,q}\frac{\sqrt{a_l a_\eta}}{z-a_{\bar\eta}}\Big\{&\ \mathrm{Im}\left[\lambda_a^{*\eta im}\lambda_a^{\bar\eta im}\lambda_a^{*\eta jn}\lambda_a^{ljn}\lambda_a^{*\bar\eta pq}\lambda_a^{lpq}\right]\frac{2z}{z-a_\eta}\frac{2z}{z-a_l}\\&+\mathrm{Im}\left[\lambda_a^{*\eta in}\lambda_a^{*\eta jm}\lambda_a^{\bar\eta im}\lambda_a^{*\bar\eta pq}\lambda_a^{lpn}\lambda_a^{ljq}\right]\ln\left(\frac{z+a_\eta}{a_\eta}\right)\ln\left(\frac{z+a_l}{a_l}\right)\\&-\mathrm{Im}\left[\lambda_a^{*\eta in}\lambda_a^{*\eta jm}\lambda_a^{\bar\eta im}\lambda_a^{*\bar\eta pq}\lambda_a^{lpq}\lambda_a^{ljn}\right]\frac{2z}{z-a_l}\ln\left(\frac{z+a_\eta}{a_\eta}\right)\\&-\mathrm{Im}\left[\lambda_a^{*\eta im}\lambda_a^{*\eta jn}\lambda_a^{\bar\eta im}\lambda_a^{*\bar\eta pq}\lambda_a^{lpn}\lambda_a^{ljq}\right]\frac{2z}{z-a_\eta}\ln\left(\frac{z+a_l}{a_l}\right)\Big\}\end{aligned} \tag{3.25}$$

It is straightforward to check, that under the permutation $\eta\leftrightarrow l$, $i\leftrightarrow p$, $m\leftrightarrow q$ the imaginary parts of the products of the couplings change their sign, and therefore the whole sum is zero as a convolution of symmetric and antisymmetric matrices, as is required by unitarity. This confirms the consistency of the presented calculation.

If the intermediate Majorana neutrino is on–shell, then the scattering process can be considered as an inverse decay followed by a decay. This implies, that in this case the *CP* asymmetry in the scattering is twice the asymmetry in the decay. If we consider an (almost) on–shell intermediate neutrino, then $\bar\eta=\eta$ (i.e. no summation over the intermediate states) and $z\to a_\eta$ so that the denominator of (3.22) is given approximately by (see the reduced cross section $\sigma_{\nu^c}^{(1)}$, $\sigma_{\nu^c}^{(2)}$ and $\sigma_{\nu^c}^{(3)}$ in appendix D)

$$\sigma_\Sigma+\sigma_\Sigma^C\approx\frac{(\lambda_a\lambda_a^\dagger)_{\eta\eta}^2}{2\pi}\frac{a_\eta^2}{(z-a_\eta)^2} \tag{3.26}$$

For $z\to a_\eta$ the leading terms in (3.25) are the first and the last term. Performing the redefinitions $\eta\to i$, $n\to k$, $p\to m$, $q\to n$ we find for the CP asymmetry ($a=11$)

$$\varepsilon_i=-\frac{\sum\sqrt{\frac{a_l}{a_i}}\left[\mathrm{Im}\left(\lambda_a^{*ijk}\lambda_a^{*imn}\lambda_a^{lmk}\lambda_a^{ljk}\right)\ln\left(1+\frac{a_i}{a_l}\right)+\mathrm{Im}\left(\lambda_a^{*ijk}\lambda_a^{*imn}\lambda_a^{lmn}\lambda_a^{ljk}\right)\frac{2}{a_l/a_i-1}\right]}{4\pi(\lambda_a\lambda_a^\dagger)_{ii}} \tag{3.27}$$

which is twice the asymmetry in the decay (3.12). Note that for the scattering mediated by an on–shell heavy neutrino the parameter of CP violation ε_i, given by (3.12), only arises if we sum over a certain set of diagrams.

Since particles in the thermal bath have non–zero velocities, contribution of the discussed above processes to washout of the lepton asymmetry is obtained by integration over the phase

space of the incoming and outgoing particles. The integration gives the so–called reaction density γ (see appendix C), which can be calculated using reduced cross section $\hat{\sigma}$ of the process. Reduced cross section of a $2 \to 2$ scattering can be calculated by integration of square of absolute value of the process amplitude over the momentum transfer t, see (C.13). Tree–level amplitude of the $L + \tilde{H}^u \to \bar{L} + \tilde{H}^{u\dagger}$ scattering process is given by a sum of (3.18) and (3.21).

$$T_{fi} = -(u_i^\alpha v_{\alpha j}) \frac{1}{M_1} \sum_\eta \left[(\lambda_a^{\eta im} \lambda_a^{\eta jn}) \frac{\sqrt{a_\eta}}{x - a_\eta} + (\lambda_a^{\eta in} \lambda_a^{\eta jm}) \frac{\sqrt{a_\eta}}{y - a_\eta} \right] \tag{3.28}$$

Note that the structure of flavor indices of the s– and t–channel contributions is different due to the presence of the additional Higgses in the model. The contribution of on–shell s–channel intermediate Majorana neutrino has already been taken into account as inverse decay followed by a decay. In order to avoid double counting in the Boltzmann equations one has to subtract the contributions of the real intermediate states (RIS), which is achieved by replacement of the s–channel propagator by the RIS subtracted propagator of the form discussed in [35]. Taking square of absolute value of (3.28), integrating over $y = [-z..0]$ and making use of the RIS subtracted propagator we obtain for the reduced cross section

$$\begin{aligned} \hat{\sigma}_{\nu^c}^{(1)}(z) = \sum_{\eta\bar{\eta}} \frac{\sqrt{a_\eta a_{\bar{\eta}}}}{8\pi z} \Bigg\{ C_a^2 \Lambda_{(1)aa}^{\eta\bar{\eta}} \left[\frac{z^2}{2\mathcal{D}_{\eta\bar{\eta}}(z)} + \frac{z + a_\eta}{a_{\bar{\eta}} - a_\eta} \ln\left(\frac{z + a_\eta}{a_\eta} \right) + \frac{z + a_{\bar{\eta}}}{a_\eta - \bar{\eta}} \ln\left(\frac{z + a_{\bar{\eta}}}{a_{\bar{\eta}}} \right) \right] \\ + 2C_a \mathrm{Re} \left(\frac{\Lambda_{(2)aa}^{\eta\bar{\eta}}}{P_\eta(z)} \right) \left[z - (z + a_{\bar{\eta}}) \ln\left(\frac{z + a_{\bar{\eta}}}{a_{\bar{\eta}}} \right) \right] \Bigg\} \end{aligned} \tag{3.29}$$

where $a = 11$, $C_a = 2$ and $\Lambda_{(1)aa}$ and $\Lambda_{(2)aa}$ are combinations of the Majorana Yukawa couplings:

$$\Lambda_{(1)aa}^{\eta\bar{\eta}} = \sum_{i,m}^{j,n} (\lambda_a^{\eta im} \lambda^{*\bar{\eta} im})(\lambda_a^{\eta jn} \lambda^{*\bar{\eta} jn}), \qquad \Lambda_{(2)aa}^{\eta\bar{\eta}} = \sum_{i,m}^{j,n} (\lambda_a^{\eta im} \lambda^{*\bar{\eta} in})(\lambda_a^{\eta jn} \lambda^{*\bar{\eta} jm}) \tag{3.30}$$

If there is only one generation of the Higgses, then $\Lambda_{(2)aa}^{\eta\bar{\eta}} = \Lambda_{(1)aa}^{\eta\bar{\eta}}$, and the expression for the reduced cross section reduces to that in the Standard Model.

The RIS subtracted propagator $D_{\eta\bar{\eta}}(z)$ is defined as

$$\frac{1}{D_{\eta\bar{\eta}}(z)} = \begin{cases} \dfrac{1}{\mathcal{P}_\eta} - \dfrac{\pi}{\sqrt{a_\eta c_\eta}} \delta(z - a_\eta), & \bar{\eta} = \eta, \\ \dfrac{1}{P_\eta(z) P_{\bar{\eta}}^*(z)}, & \bar{\eta} \neq \eta, \end{cases} \tag{3.31}$$

where $\mathcal{P}_\eta = (z - a_\eta)^2 + a_\eta c_\eta$ is square of absolute value of the inverse Breit–Wigner propagator $P_\eta(z)$

$$\frac{1}{P_\eta(z)} = \frac{1}{z - a_\eta + i\sqrt{a_\eta c_\eta}} \tag{3.32}$$

The reduced cross sections of the remaining diagrams in figure 1.3 are derived analogously and can be found in section D.1. The reduced cross sections of the additional processes present in the model with $\lambda_8 \neq 0$ can be found there as well.

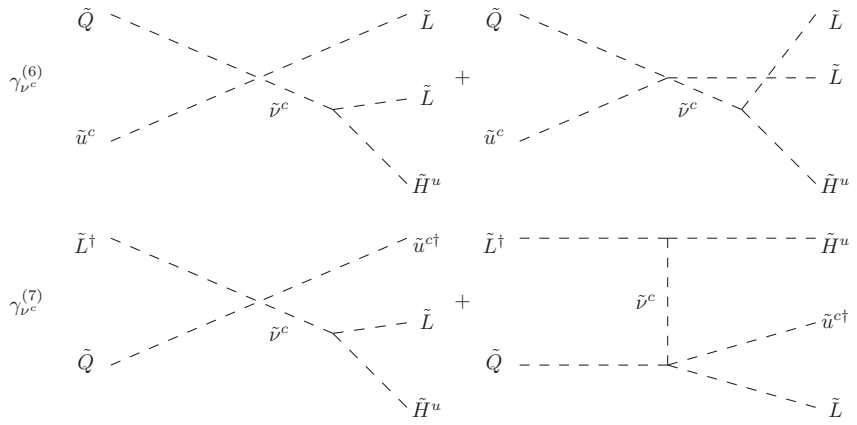

Figure 3.4: Additional processes mediated by the heavy neutrino exchange, which contribute to violation of the lepton number.

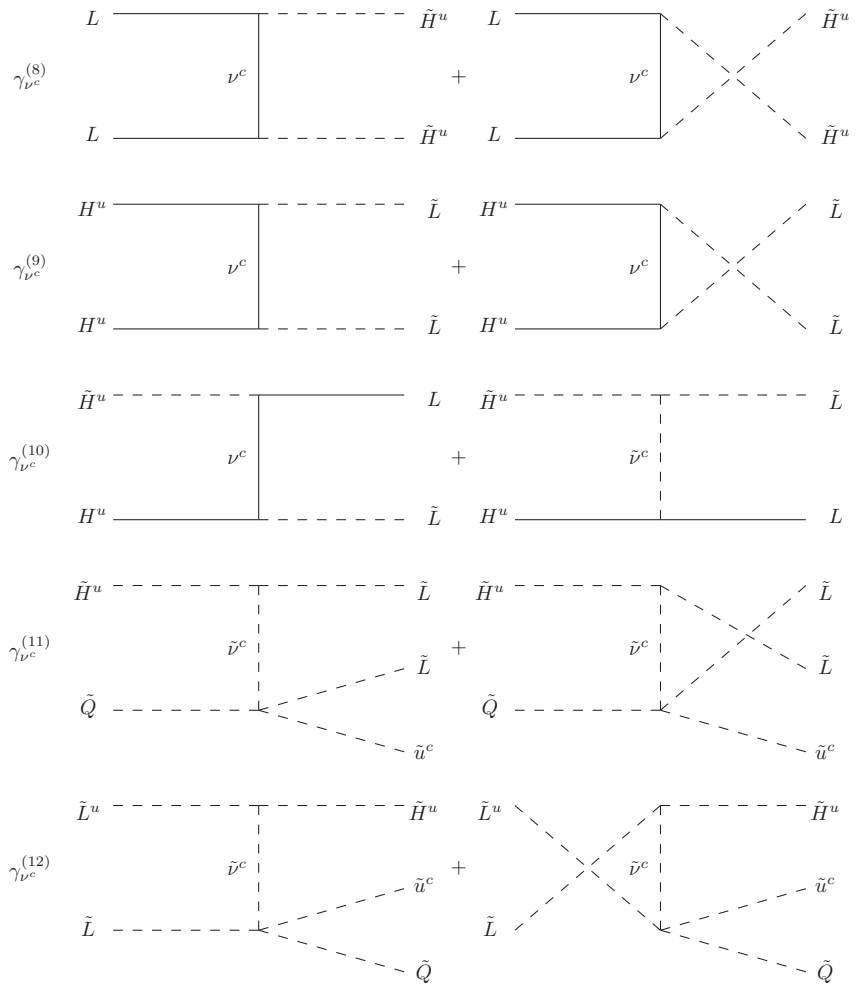

Figure 3.5: Lepton number violating scattering processes mediated by the right–handed neutrino in the t– and u–channels.

The diagrams in figure 3.4 also receive contributions from exchange of the real intermediate right–handed neutrino. As there are three particles in the final state in this case, one should use the formula (C.16) in order to calculate the corresponding reduced cross sections. The RIS subtracted reduced cross sections of these processes can be found in section D.1.

There are also t– and u– channel scattering processes depicted in figure 3.5, which conserve CP to leading order (the square of the corresponding momentum transfer is negative so that the absorptive parts of the two– and three–point functions vanish, see appendix A), but violate lepton number. Consequently, the contribution of these processes to the Boltzmann equation for the lepton asymmetry differs from zero only if the latter one is nonzero.

Let us sketch calculation of the reduced cross section of the first of the processes in figure 3.5, which is present already in the Standard Model. Amplitude of this process reads

$$T_{fi} = -(u_i^{(\alpha)} v_{j(\alpha)}) \frac{1}{M_1} \sum_{\eta} \left[(\lambda_a^{\eta i m} \lambda_a^{\eta j n}) \frac{\sqrt{a_\eta}}{y - a_\eta} + (\lambda_a^{\eta i n} \lambda_a^{\eta j m}) \frac{\sqrt{a_\eta}}{\varsigma - a_\eta} \right], \quad \varsigma \equiv \frac{u}{M_1^2}, \tag{3.33}$$

where u is the standard Mandelstamm variable. Since mass of the incoming and the outgoing particle is zero, $s+t+u=0$. Taking this into account we obtain after integration over $y=[-z..0]$

$$\hat{\sigma}_{\nu^c}^{(8)} = \sum_{\eta\bar{\eta}} \frac{\sqrt{a_\eta a_{\bar{\eta}}}}{8\pi} \left\{ C_a^2 \Lambda_{(1)aa}^{\eta\bar{\eta}} \left[\frac{1}{a_\eta - a_{\bar{\eta}}} \ln\left(\frac{z + a_{\bar{\eta}}}{a_{\bar{\eta}}} \right) + \frac{1}{a_{\bar{\eta}} - a_\eta} \ln\left(\frac{z + a_\eta}{a_\eta} \right) \right] \right.$$
$$\left. + C_a \mathrm{Re}\left(\Lambda_{(2)aa}^{\eta\bar{\eta}} \right) \frac{1}{z + a_\eta + a_{\bar{\eta}}} \left[\ln\left(\frac{z + a_\eta}{a_\eta} \right) + \ln\left(\frac{z + a_{\bar{\eta}}}{a_{\bar{\eta}}} \right) \right] \right\} \tag{3.34}$$

where $a = 11$. Reduced cross sections of the remaining processes in figure 3.5 can be found in section D.1. The processes $\gamma_{\nu^c}^{(8)} - \gamma_{\nu^c}^{(12)}$ are quite important at low temperatures, as they are not suppressed by the Boltzmann factor of the heavy neutrino.

3.3 Scattering off a top or a stop

There are also processes which conserve CP to the leading order but violate lepton number by one unit. The simplest of such processes is the $\tilde{\nu}^c + \tilde{L} \leftrightarrow \tilde{Q} + \tilde{u}^c$ scattering, which is determined by quartic scalar couplings.

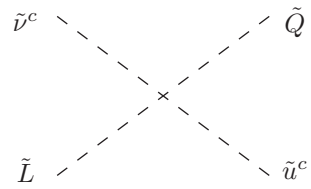

Figure 3.6: Lepton number violating process determined by scalar quartic couplings.

In addition, there are s– and t–channel two–body scattering processes mediated by the Higgs or its superpartner (see figure 3.7), which violate lepton number by one unit. In the model with

$\lambda_8 \neq 0$ there are additional processes of this type which we, however, neglect assuming smallness of the corresponding Yukawa couplings.

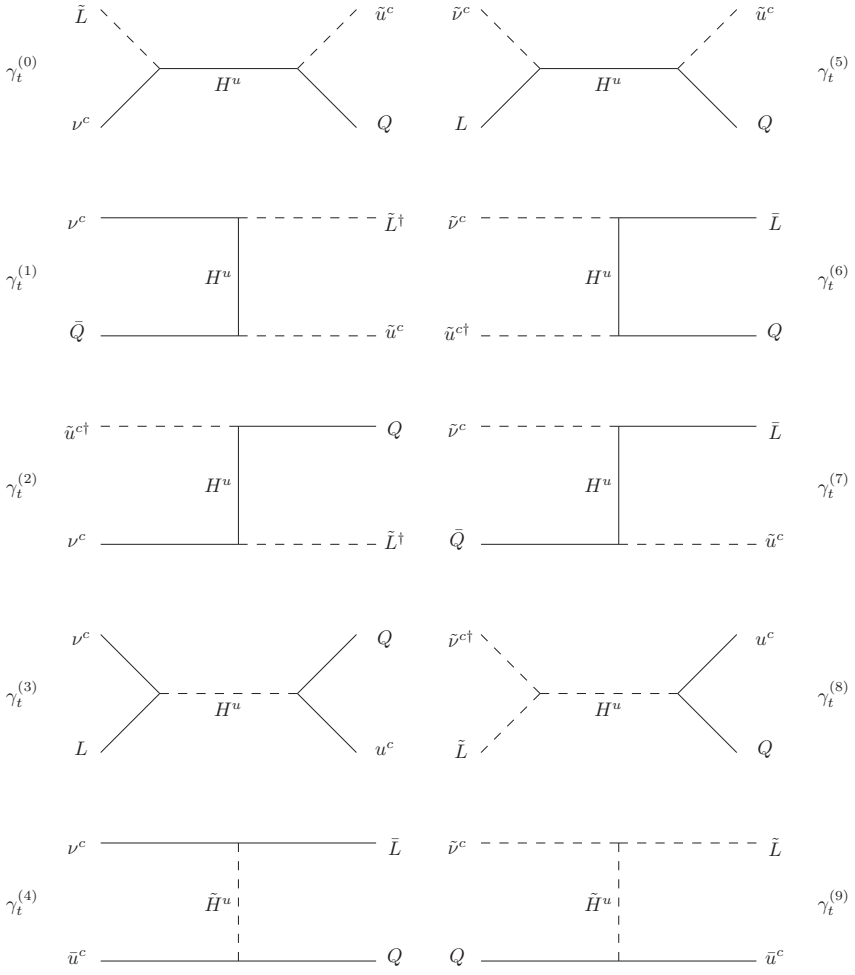

Figure 3.7: Lepton number violating processes mediated by the Higgs and its superpartner.

Consider, for instance, the $\nu^c + L \to Q + u^c$ process, which present already in the Standard Model supplemented by three right–handed neutrinos. Amplitude of this process is given by

$$T_{fi} = \frac{i}{M_1^2} \sum_k (\lambda_a^{\eta ik} \lambda_1^{*knm})(u^{(\alpha)_i} u_{(\alpha)\eta})(\bar{u}_{(\dot{\gamma})n} \bar{u}_m^{(\dot{\gamma})}) \frac{1}{z - a_h}, \quad a_h \equiv \frac{m_h^2}{M_1^2} \tag{3.35}$$

where $a = 11$. After integration over $y = [a_\eta - z..0]$ we obtain for the reduced cross section

$$\hat{\sigma}_t^{(3)} = 3\Lambda^\eta_{(5)11,1} \left(\frac{z - a_\eta}{z - a_h} \right)^2 \tag{3.36}$$

where $\Lambda^\eta_{(5)11,1}$ is a combination of the Yukawa couplings of the right–handed neutrinos and quarks:

$$\Lambda^\eta_{(5)a,b} = \frac{1}{4\pi} \sum_{i,m,n}^{k,\bar{k}} (\lambda_a^{\eta ik} \lambda_a^{*\eta i\bar{k}})(\lambda_b^{*nmk} \lambda_b^{nm\bar{k}}) \tag{3.37}$$

Reduced cross sections of the remaining processes in figure 3.7 can be found in section D.2.

3.4 Annihilation of the right–handed (s)neutrinos

There are also processes which conserve the lepton number but reduce number of the heavy right—handed neutrinos. These include annihilation of two Majorana (s)neutrinos (see figures 3.8 and 3.9) and scattering of the Majorana and its supersymmetric partner (see figure 3.10).

Processes of the fermion right–handed neutrino annihilation, $\gamma^{(2)}_{\nu^c\nu^c}$ and $\gamma^{(3)}_{\nu^c\nu^c}$, are present already in the Standard Model.

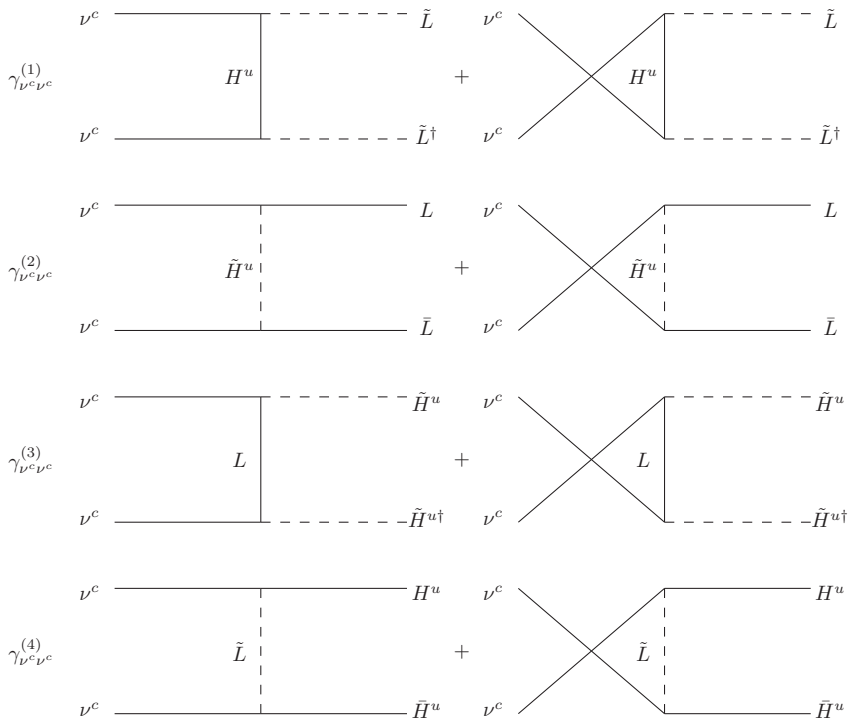

Figure 3.8: Neutrino pair annihilation.

Let us sketch calculation of reduced cross section of $\nu^c_\eta + \nu^c_{\bar{\eta}} \to L_i + \bar{L}_j$ process. Amplitude of this process reads

$$M_{fi} = \frac{1}{M_1^2}\sum_n \left[(\lambda_a^{\eta in}\lambda_a^{*\bar{\eta}jn})(u_\eta^{(\alpha)}v_{i(\alpha)})(u_{\bar{\eta}}^{(\beta)}v_{j(\beta)})\frac{1}{y} - (\lambda_a^{\bar{\eta}in}\lambda_a^{*\eta jn})(u_{\bar{\eta}}^{(\alpha)}v_{i(\alpha)})(u_\eta^{(\beta)}v_{j(\beta)})\frac{1}{\varsigma}\right] \quad (3.38)$$

As the right–handed neutrinos are on–shell, one can use relations (B.24) in order to calculate squared absolute value of the amplitude. Since the annihilating right–handed neutrinos are massive, with masses M_η and $M_{\bar{\eta}}$, the Mandelstamm variables are related by $s+t+u = M_\eta^2+M_{\bar{\eta}}^2$. After integration over y in the range $y = [y_{min}..y_{max}]$, where $y_{min/max} = \frac{a_{\bar{\eta}}+a_\eta}{2} - \frac{x}{2} \mp \sqrt{\lambda_{\eta\bar{\eta}}}$ and $\lambda_{\eta\bar{\eta}} = [x - (\sqrt{a_\eta} - \sqrt{a_{\bar{\eta}}})^2][x - (\sqrt{a_\eta} + \sqrt{a_{\bar{\eta}}})^2]$, we obtain for the reduced cross section:

$$\sigma^{(2)}_{\nu^c\nu^c} = \frac{C_a}{8\pi z}\left\{\Lambda^{\eta\bar{\eta}}_{(6)aa}\left[2\sqrt{\lambda_{\eta\bar{\eta}}} + (a_\eta + a_{\bar{\eta}})L_{\eta\bar{\eta}}\right] - 2\mathrm{Re}\left(\Lambda^{\eta\bar{\eta}}_{(7)aa}\right)\frac{z\sqrt{a_\eta a_{\bar{\eta}}}}{z - a_\eta - a_{\bar{\eta}}}L_{\eta\bar{\eta}}\right\} \quad (3.39)$$

where $L_{\eta\bar{\eta}} = \ln\left(\frac{z-a_\eta-a_{\bar{\eta}}+\sqrt{\lambda_{\eta\bar{\eta}}}}{z-a_\eta-a_{\bar{\eta}}-\sqrt{\lambda_{\eta\bar{\eta}}}}\right)$ and $\Lambda^{\eta\bar{\eta}}_{(6)aa}$ and $\Lambda^{\eta\bar{\eta}}_{(7)aa}$ are combinations of the Yukawa couplings of the right–handed neutrino

$$\Lambda^{\eta\bar{\eta}}_{(6)aa} = \sum_{ij}^{n\bar{n}} (\lambda^{\eta in}_a \lambda^{*\eta i\bar{n}}_a)(\lambda^{*\bar{\eta} jn}_b \lambda^{\bar{\eta} j\bar{n}}_b), \quad \Lambda^{\eta\bar{\eta}}_{(6)aa} = \sum_{ij}^{n\bar{n}} (\lambda^{\eta in}_a \lambda^{\eta j\bar{n}}_a)(\lambda^{*\bar{\eta} jn}_b \lambda^{*\bar{\eta} i\bar{n}}_b) \tag{3.40}$$

Note that the combinations (3.40) differ from $\Lambda^{\eta\bar{\eta}}_{(1)aa}$ and $\Lambda^{\eta\bar{\eta}}_{(2)aa}$ because the summation is over the intermediate Higgses, not over the intermediate Majoranas. Reduced cross sections of the remaining processes in figure 3.8 can be found in section D.3.

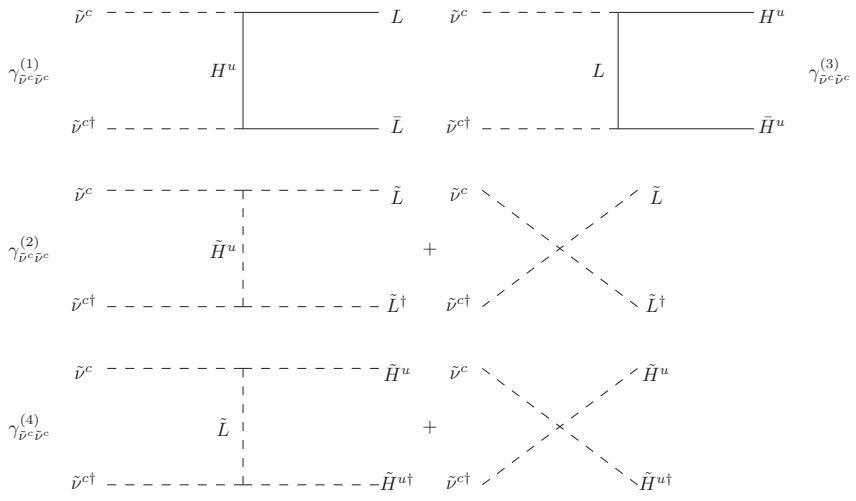

Figure 3.9: Sneutrino pair annihilation.

Calculation of the reduced cross sections of the depicted in figure 3.9 sneutrino pair annihilation processes is to a large extent similar to the calculation above. Reduced cross sections of these processes, as well as reduced cross section of the neutrino–sneutrino scattering processes in figure 3.10, can also be found in section D.3.

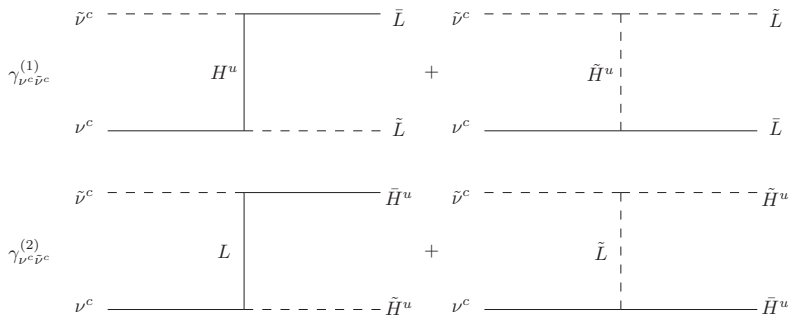

Figure 3.10: Neutrino–sneutrino scattering.

At low temperatures the reaction densities of all of the above processes are strongly suppressed by the Boltzmann factors, and their contribution is rather small.

3.5 Gauge mediated scattering

Apart from the processes discussed above, some of the Majorana mediated processes conserve total lepton number, but redistribute it among leptons and their superpartners. There are also gauge mediated scattering processes transforming leptons into sleptons and vice versa. Let us

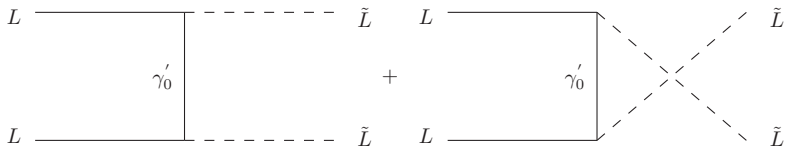

Figure 3.11: A gauge mediated processes redistributing total lepton number among leptons and their superpartners.

consider for instance the process of annihilation of two leptons into two sleptons mediated by the $U_Y(1)$ gauge field[1], which is depicted in figure 3.11. The relevant terms of the superpotential are contained in (2.23).

The intermediate gauge field is a Majorana fermion with mass $m_{\gamma_0'}$ of the order of the soft supersymmetry breaking scale. This process is to a large extent analogous to the Majorana mediated scattering of two leptons considered in section 3.2, and its reduced cross section reads

$$\hat{\sigma}_{\gamma_0'} = \frac{g_{\gamma_0'}^4}{8\pi}\left[\frac{z}{z+a_{\gamma_0'}} + \frac{a_{\gamma_0'}}{z+2a_{\gamma_0'}}\ln\left(\frac{z+a_{\gamma_0'}}{a_{\gamma_0'}}\right)\right], \quad a_{\gamma_0'} = \left(\frac{m_{\gamma_0'}}{M_1}\right)^2 \tag{3.41}$$

At the relevant range of temperatures $x \gg a_{\gamma_0'}$, so that the ratio of the corresponding reaction density to the expansion rate of the Universe is given approximately by

$$\frac{x\hat{\gamma}_{\gamma_0'}}{\mathcal{H}(M_1)} \approx \frac{g_{\gamma_0'}^4}{128\pi^5}\frac{1}{\mathcal{H}(M_1)} \sim 10^3 \gg 1 \tag{3.42}$$

where $\mathcal{H}(M_1)$ and $\hat{\gamma}$ are the dimensionless Hubble parameter and reaction density respectively.

As strength of this processes and the others alike is determined by gauge couplings, which are much bigger than the Majorana Yukawa couplings, the gauge mediated scattering processes are in equilibrium and ensure equality of chemical potentials of leptons and their superpartners.

3.6 Baryon number violation

The asymmetry generated in the decay of the heavy Majorana is immediately redistributed by the sphaleron transitions and fast scattering processes between the Higgses and quarks, inducing

[1]Note that since the $SU_L(2) \otimes U_Y(1)$ symmetry is unbroken at this stage, it would be incorrect to talk about scattering processes mediated by the photino, wino or zino.

nonzero chemical potentials of these species. It is straightforward to generalize the analysis of chemical potentials, performed in section 1.6, to the case of the supersymmetric E_6 model.

In addition to the Standard Model lepton and quark doublets, this model also contains two Higgs doublets, H^u and H^d, per generation, which transform nontrivially under the $SU_L(2)$ group. Since the superfields H^u and H^d also contain fermions, the relation (1.102) is modified as

$$3\mu_Q + \mu_L + \mu_{H^d} + \mu_{H^u} = 0 \tag{3.43}$$

After breaking of the additional $U(1)$ group, which takes place at a scale of the order of 1 TeV, the model under consideration is similar to the Minimal Supersymmetric Standard Model. The $U(1)$ symmetry is broken by a nonzero vacuum expectation value of the Standard Model singlet S. The nonzero VEV of S induces a (presumable strong) mixing of the H^u and H^d states, so that the sum of their chemical potentials turns to zero, just like it is the case in the MSSM. As mass of the lightest right–handed neutrino is many orders of magnitude bigger than 1 TeV, the VEV of the S is zero in the interesting range of temperatures. Consequently, the H^u and H^d are not mixed and the sum of their chemical potentials differs from zero.

As has been argued in the previous section fast gauge mediated scattering processes are in thermal equilibrium and equalize the chemical potentials of the particles and their superpartners, so that we only have to consider reactions determined by the Yukawa interactions. Assuming that all the processes, apart from those involving the heavy (s)neutrino, are in thermal equilibrium, we find the following relations between the chemical potentials in the $\lambda_8 = 0$ model

$$\begin{aligned} &\mu_{u^c} + \mu_Q + \mu_{H^u} = 0, \quad \mu_{d^c} + \mu_Q + \mu_{H^d} = 0, \quad \mu_{e^c} + \mu_L + \mu_{H^d} = 0, \quad \mu_S + \mu_{H^u} + \mu_{H^d} = 0, \\ &\mu_S + \mu_D + \mu_{D^c} = 0, \quad \mu_D + \mu_Q + \mu_Q = 0, \quad \mu_{D^c} + \mu_{u^c} + \mu_{d^c} = 0. \end{aligned} \tag{3.44}$$

The notation is self explanatory. In the $\lambda_8 \neq 0$ model the last two equations are replaced by

$$\mu_{e^c} + \mu_{u^c} + \mu_D = 0, \quad \mu_{D^c} + \mu_Q + \mu_L = 0. \tag{3.45}$$

According to the discussion in chapter 2, after the breaking of the $B - L$ symmetry the residual gauge symmetry is $SU_C(3) \otimes SU_L(2) \otimes U(1) \otimes U(1)$, so that the chemical potentials of the components of electroweak doublets and color triplets are equal, whereas the chemical potentials of the corresponding gauge fields vanish. The $U(1)$ charges of the matter fields can be read off from equation (2.23). The requirement that the total $U(1)$ charges be zero implies

$$\mu_Q - \mu_L - 2\mu_{u^c} + \mu_{d^c} + \mu_{e^c} + \mu_{H^u} - \mu_{H^d} - \mu_D + \mu_{D^c} = 0 \tag{3.46a}$$

$$-6\mu_Q - 3\mu_{u^c} - 6\mu_{d^c} + 9\mu_{D^c} + 6\mu_D + 4\mu_{H^u} + 6\mu_{H^d} - 4\mu_L - \mu_{e^c} - 5\mu_S = 0 \tag{3.46b}$$

where we have assumed, that the chemical potentials of states with the same quantum numbers are equal. Note also, that unlike the Standard Model considered in section 1.6, the E_6 model contains three generations of Higgs doublets, so that the number of generations $N = 3$ appears in (3.46) as an overall factor and can be omitted. In addition, each chiral superfield has the same number of degrees of freedom, and therefore the coefficients in (3.46) are simply the $U(1)$ charges of the corresponding multiplets multiplied by the number of states in the multiplet. Combining equations (3.46), (3.44) and (3.43) we obtain

$$\mu_{e^c} = \mu_Q = \mu_{H^d} = \mu_S = \mu_{u^c} = \mu_{D^c} = -\frac{\mu_L}{2}, \quad \mu_{H^u} = \mu_{d^c} = \mu_D = \mu_L \tag{3.47}$$

It is straightforward to check, that relations (3.47) remain also valid in the model with $\lambda_8 \neq 0$.

Using once again that the chiral superfields have the same number of degrees of freedom, we find, that up to a common overall coefficient the lepton and the baryon numbers are given in the $\lambda_8 = 0$ model by

$$L = N(2\mu_L - \mu_{e^c}), \quad B = N(2\mu_Q - \mu_{u^c} - \mu_{d^c} - 2\mu_D + 2\mu_{D^c}) \tag{3.48}$$

Note, that in the model under consideration the new qarks also contribute to the baryon number. From equations (3.47) and (3.6) it follows, that above the temperature of breaking of the additional $U(1)$ group the baryon and lepton numbers are related by $B = -\frac{9}{5}L$. The scattering processes, which violate lepton number, are frozen long before the breaking of the $U(1)$ symmetry. Since the $B - L$ is conserved by all the other processes, $(B - L)_\infty = -\frac{14}{5}L_\infty$, where L_∞ denotes the lepton asymmetry at $T \ll M_1$, is constant all the way down to zero temperatures.

In the $\lambda_8 \neq 0$ model the new states D and D^c are leptoquarks with baryon and lepton numbers given respectively by $\pm\frac{1}{3}$ and ± 1. We therefore obtain

$$L = N(2\mu_L - \mu_{e^c} + \mu_D - \mu_{D^c}), \quad B = N(2\mu_Q - \mu_{u^c} - \mu_{d^c} + \mu_D - \mu_{D^c}). \tag{3.49}$$

It is interesting to note, that substitution of (3.47) into (3.6) yields $B = 0$, i.e. the baryon asymmetry carried by the leptoquarks is equal in absolute values and opposite in sign to that carried by the Standard Model quarks.

After the breaking of the additional $U(1)$ symmetry, the new (lepto)quarks D and D^c and the Higgs doublets H^u and H^d acquire masses. As has been discussed above, the latter implies, that the relation between the chemical potentials of the leptons and the quarks, implied by the sphaleron transitions, reverts to that in the Standard Model. Provided that masses of the (lepto)quarks are considerably bigger than the temperature of the electroweak symmetry breaking T_C, they decouple, as the temperature drops down to T_C. The same is also true for the superpartners of the SM states. This implies, that at $T \sim T_C$ the system of equations for the chemical potentials (3.46) and (3.47) also reverts to that discussed in section 1.6. The sphaleron

transitions are fast down to the temperature of the electroweak phase transition. Consequently, at the temperature, the sphalerons freeze out, the relation between the B, L and $B-L$ are given by (1.111), where $n = 6$ in the case under consideration.

3.7 Numerical estimates

The lepton number asymmetry is generated in the decay of all three generations of the Majorana (s)neutrino. However, since we consider the scenario of non–resonant leptogenesis here, i.e. the case of large hierarchy in the Majorana mass matrix, the asymmetry generated at the scales $T \sim M_2$ and $T \sim M_3$ will be almost completely washed out by the lepton number violating two–body scattering processes, which are fast at high temperatures. Consequently the asymmetry we observe today has been generated in the decay of the lightest Majorana neutrino. Although the two heavier Majorana (s)neutrinos can be neglected as free particles, they give an important contribution to the lepton number violating processes, and thus have to be taken into account as intermediate states.

Since the fast gauge mediated scattering processes, discussed above, are in thermal equilibrium and equalize the chemical potentials of the particles and their superpartners, lepton numbers carried by the scalar and the fermion leptons are equal. As the temperature drops down, the scalars decay and the scalar lepton number is converted into fermion lepton number. It is therefore sufficient to consider only the total lepton number $n_L \equiv n_{L_f} + n_{L_s}$.

Let us first consider the model with $\lambda_8 = 0$. In this model the Boltzmann equation for the lepton number asymmetry takes the form

$$\begin{aligned}
\frac{dY_L}{dx} = \frac{x}{\mathcal{H}(M_1)} \Bigg\{ & \sum_i \hat{\gamma}_{\nu_i^c} \left[\epsilon_i \left(\frac{Y_{\nu_i^c}}{Y_{\nu_i^c}^{eq}} - 1 \right) - c_1 \frac{Y_L}{Y_L^{eq}} \right] + 2 \sum_i \hat{\gamma}^{(2)}_{\tilde{\nu}_i^c} \left[\epsilon_i \left(\frac{Y_{\tilde{\nu}_i^c}}{Y_{\tilde{\nu}_i^c}^{eq}} - 1 \right) - c_1 \frac{Y_L}{Y_L^{eq}} \right] \\
& - 2(1-c_5) \frac{Y_L}{Y_L^{eq}} \sum_i \left[\hat{\gamma}^{(3)}_{\tilde{\nu}_i^c} + \hat{\gamma}_{22_i} \left(\frac{Y_{\nu_i^c}}{Y_{\nu_i^c}^{eq}} + 2 \right) \right] - 4 \frac{Y_L}{Y_L^{eq}} \Big[2c_1 \left(\hat{\gamma}^{(1)}_{\nu^c} + \hat{\gamma}^{(3)}_{\nu^c} + \hat{\gamma}^{(4)}_{\nu^c} + \hat{\gamma}^{(8)}_{\nu^c} \right. \\
& \left. + \hat{\gamma}^{(10)}_{\nu^c} \right) + c_2 \left(2\hat{\gamma}^{(5)}_{\nu^c} + \hat{\gamma}^{(6)}_{\nu^c} + 4\hat{\gamma}^{(7)}_{\nu^c} + 2\hat{\gamma}^{(11)}_{\nu^c} + \hat{\gamma}^{(12)}_{\nu^c} \right) \Big] - 4 \frac{Y_L}{Y_L^{eq}} \sum_i \left[\frac{Y_{\nu_i^c}}{Y_{\nu_i^c}^{eq}} \left(\hat{\gamma}^{(0)}_{t_i} - c_Q \hat{\gamma}^{(1)}_{t_i} \right. \right. \\
& \left. - c_{u^c} \hat{\gamma}^{(2)}_{t_i} + \frac{1}{2} \hat{\gamma}^{(3)}_{t_i} - c_{u^c} \hat{\gamma}^{(4)}_{t_i} \right) + \frac{Y_{\tilde{\nu}_i^c}}{Y_{\tilde{\nu}_i^c}^{eq}} \left(\hat{\gamma}^{(5)}_{t_i} - c_{u^c} \hat{\gamma}^{(6)}_{t_i} - c_Q \hat{\gamma}^{(7)}_{t_i} + \frac{1}{2} \hat{\gamma}^{(8)}_{t_i} - c_Q \hat{\gamma}^{(9)}_{t_i} \right) \\
& + \left(-c_5 \hat{\gamma}^{(0)}_{t_i} + c_3 \hat{\gamma}^{(1)}_{t_i} + c_4 \hat{\gamma}^{(2)}_{t_i} - \frac{c_5}{2} \hat{\gamma}^{(3)}_{t_i} + c_4 \hat{\gamma}^{(4)}_{t_i} \right) + \left(-c_5 \hat{\gamma}^{(5)}_{t_i} + c_4 \hat{\gamma}^{(6)}_{t_i} + c_3 \hat{\gamma}^{(7)}_{t_i} - \frac{c_5}{2} \hat{\gamma}^{(8)}_{t_i} \right. \\
& \left. \left. + c_3 \hat{\gamma}^{(9)}_{t_i} \right) \right] \Bigg\} \qquad (3.50)
\end{aligned}$$

The first and the second term in the Boltzmann equation for the total lepton number (3.50) represent the contributions of the fermion ($\hat{\gamma}_{\nu_i^c}$) and the scalar ($\hat{\gamma}^{(2)}_{\tilde{\nu}_i^c}$) heavy neutrinos decaying into two–particle final states. The third term represents the contribution of the heavy scalar neutrino

decaying into a three–particle ($\hat{\gamma}^{(3)}_{\tilde{\nu}^c_i}$) final state and the contribution of the two–body scattering process ($\hat{\gamma}_{22,i}$) in figure 3.6. Scattering processes mediated by the Majorana (s)neutrino ($\hat{\gamma}^{(i)}_{\nu^c}$), which violate lepton number by two units, as well as scattering processes mediated by the Higgs ($\hat{\gamma}^{(i)}_{t_j}$), which violate lepton umber by one unit, tend to washout the lepton asymmetry. The coefficients c_Q, c_{u^c} and c_{H^u} are ratios of the corresponding chemical potentials to the chemical potential of the leptons. To shorten the notation we also introduce

$$c_1 = 1 + c_{H^u},\ c_2 = 1 + (c_{H^u} - c_{u^c} - c_Q)/2,\ c_3 = 1 - c_{u^c},\ c_4 = 1 - c_Q,\ c_5 = c_Q + c_{u^c} \quad (3.51)$$

The difference n_{L_f} and the sum $n^{eq}_{L_f}$ of number of fermion leptons and antileptons is given by (1.25). The generalization to the model under consideration, which also contains scalar leptons, obviously reads

$$n_L = n_{L_f} + n_{L_s} = 2C_s N \left(\frac{T^3}{\pi^2}\frac{2\mu_\ell}{T}\right), \quad n^{eq}_L = n^{eq}_{L_f} + n^{eq}_{L_s} = 2C_s N \left(\frac{2T^3}{\pi^2}\right), \quad (3.52)$$

where $C_s = 2$ is the supersymmetry factor.

To derive (3.50) we used, that the chemical potential of the Majorana neutrino is zero, i.e. that number of Majorana neutrinos with right helicity is equal to the number of Majorana neutrinos with left helicity. In a supersymmetric model two polarization states of the fermion Majorana neutrino correspond to two degrees of freedom of the complex scalar Majorana neutrino. To ensure self–consistency of our analysis we should assume, that the chemical potential of the scalar neutrino is zero as well, i.e. that $n_{\tilde{\nu}^c_i} = n_{\tilde{\nu}^{c\dagger}_i}$. Taking this into account, we obtain Boltzmann equations for the number of the Majorana neutrino and its scalar superpartner

$$\begin{aligned}\frac{dY_{\nu^c_i}}{dx} = \frac{x}{\mathcal{H}(M_1)}\Bigg\{&\left(1 - \frac{Y_{\nu^c_i}}{Y^{eq}_{\nu^c_i}}\right)\left(\hat{\gamma}_{\nu^c_i} + 4\hat{\gamma}^{(0)}_{t_i} + 4\hat{\gamma}^{(1)}_{t_i} + 4\hat{\gamma}^{(2)}_{t_i} + 2\hat{\gamma}^{(3)}_{t_i} + 4\hat{\gamma}^{(4)}_{t_i}\right)\\ &+ \sum_j \left(1 - \frac{Y_{\nu^c_i}}{Y^{eq}_{\nu^c_i}}\frac{Y_{\nu^c_j}}{Y^{eq}_{\nu^c_j}}\right)\sum_{k=1}^{4}\hat{\gamma}^{(k)}_{\nu^c_i\nu^c_j} + 2\sum_j\left(1 - \frac{Y_{\nu^c_i}}{Y^{eq}_{\nu^c_i}}\frac{Y_{\tilde{\nu}^c_j}}{Y^{eq}_{\tilde{\nu}^c_j}}\right)\sum_{k=1}^{2}\hat{\gamma}^{(k)}_{\tilde{\nu}^c_j\nu^c_i}\Bigg\}\end{aligned} \quad (3.53)$$

$$\begin{aligned}\frac{dY_{\tilde{\nu}^c_i}}{dx} = \frac{x}{\mathcal{H}(M_1)}\Bigg\{&\left(1 - \frac{Y_{\tilde{\nu}^c_i}}{Y^{eq}_{\tilde{\nu}^c_i}}\right)\left(\hat{\gamma}^{(2)}_{\tilde{\nu}^c_i} + \hat{\gamma}^{(3)}_{\tilde{\nu}^c_i} + 3\hat{\gamma}^{(2)}_{22,i} + 2\hat{\gamma}^{(5)}_{t_i} + 2\hat{\gamma}^{(6)}_{t_i} + 2\hat{\gamma}^{(7)}_{t_i} + \hat{\gamma}^{(8)}_{t_i} + 2\hat{\gamma}^{(9)}_{t_i}\right)\\ &+ 2\sum_j \left(1 - \frac{Y_{\tilde{\nu}^c_i}}{Y^{eq}_{\tilde{\nu}^c_i}}\frac{Y_{\tilde{\nu}^c_j}}{Y^{eq}_{\tilde{\nu}^c_j}}\right)\sum_{k=1}^{2}\hat{\gamma}^{(k)}_{\tilde{\nu}^c_i\tilde{\nu}^c_j} + 2\sum_j\left(1 - \frac{Y_{\tilde{\nu}^c_i}}{Y^{eq}_{\tilde{\nu}^c_i}}\frac{Y_{\nu^c_j}}{Y^{eq}_{\nu^c_j}}\right)\sum_{k=1}^{2}\hat{\gamma}^{(k)}_{\tilde{\nu}^c_i\nu^c_j}\Bigg\}\end{aligned} \quad (3.54)$$

Processes which determine the evolution of the heavy neutrino number density are the Majorana decay, the Higgs mediated scattering and the annihilation of the Majorana (s)neutrinos.

The expansion rate of the Universe is characterized by the dimensionless Hubble parameter

$$\mathcal{H}(M_1) = \left(\frac{4\pi^3 g_*}{45}\right)^{\frac{1}{2}}\frac{M_1}{M_{Pl}}, \quad M_{Pl} = 1.2\cdot 10^{19}\ \text{GeV}, \quad (3.55)$$

which is proportional to square root of the effective number of massless degrees of freedom. At temperatures $T \sim M_1$ all species apart from the Majorana neutrinos can be considered as massless. In the model under consideration there are $\mathbf{8}+\mathbf{3}+\mathbf{1}+\mathbf{1}$ massless gauge fields and $N_f(\mathbf{27}-\mathbf{1})$ massless chiral fields, where $N_f = 3$ is the number of generations. Since both chiral and vector superfields contain two bosonic and two fermionic degrees of freedom, in the interesting range of temperatures the effective number of massless degrees of freedom is given by $g_* = 341.25$. The related to it "equilibrium neutrino mass", which is defined in (1.60), is given in the model under consideration by $m^* \approx 2 \cdot 10^{-3}$ eV. Contribution of the heavy right–handed neutrinos to the energy density, as has been discussed in chapter 1, are relatively small and can be neglected to a first approximation.

As number of the heavy (s)neutrinos falls off rapidly with decrease of the temperature, the processes with Majorana neutrino in the initial or final state (i.e. the neutrino decay and the Higgs–mediated two–body scattering) are only important at high temperatures $T > M_1$. Contribution of the decay processes is proportional to the effective mass $\tilde{m}_1$, which is defined in complete analogy with (1.43)

$$\frac{x}{\mathcal{H}(M_1)}\hat{\gamma}_{\nu_i^c} \propto \tilde{m}_1, \quad \frac{x}{\mathcal{H}(M_1)}\hat{\gamma}^{(2)}_{\tilde{\nu}_i^c} \propto \tilde{m}_1, \quad \frac{x}{\mathcal{H}(M_1)}\hat{\gamma}^{(3)}_{\tilde{\nu}_i^c} \propto \tilde{m}_1. \tag{3.56}$$

Since the only Higgs–mediated two–body scattering processes we consider are those with the lightest Majorana (s)neutrino in the initial state (i.e. $i = 1$), their contributions, as well as contribution of the two–body scattering process determined by quartic couplings, are also proportional to $\tilde{m}_1$

$$\frac{x}{\mathcal{H}(M_1)}\hat{\gamma}_{22_i} \propto \tilde{m}_1, \quad \frac{x}{\mathcal{H}(M_1)}\hat{\gamma}^{(n)}_{t_i} \propto \tilde{m}_1. \tag{3.57}$$

Contrary to the decay and the Higgs–mediated scattering processes, the Majorana–mediated scattering processes are not strongly suppressed at low temperatures and play an important role in washout of the lepton number asymmetry. From the definition of the dimensionless reduced cross section (C.25) it follows, that at low temperatures (i.e. at large x) leading contribution to the corresponding reaction densities comes from the small–z region. As has been argued in [36], in this approximation the contribution of such processes in the case of the Standard Model is determined by the mean square of the physical neutrino masses $3\bar{m}^2 = m_1^2 + m_2^2 + m_3^2$ and the lightest Majorana mass M_1. The model under consideration contains three generations of the Higgses. This implies in particular, that the reduced cross sections depend now on two different combinations of the Yukawa couplings, see for example (D.2) or (D.15). Thus, generally speaking, it is no longer possible to express the contributions of such processes in terms of the mean square of the physical neutrino masses. The masses of the light neutrinos are induced by nonzero VEVs of the scalar Higgses $\tilde{H}_i^u$, which also give masses to the up–quarks. As has been argued in [75],

if quarks of a given charge receive their masses through the coupling to more than one Higgs, strong flavor–changing neutral currents appear. Since experimental observations exclude this possibility, it is natural to assume that the Higgses of the first and the second generations do not acquire VEVs, so that the light neutrino masses are expressed through the Yukawa couplings of the Higgs of the first generation and the right–handed neutrino masses in the same way as in the Standard Model. If, furthermore, the Higgses of the second and the third generations are only weakly coupled to the heavy neutrinos and up–quarks, so that the defined in (D.2) and (D.15) couplings $\Lambda^{\eta\bar{\eta}}_{(i)aa}$ $(i = 1..4)$ are mainly determined by Yukawa couplings of the Higgs of the first generation, then contribution of the scattering processes violating lepton number by two units can again be expressed through the mean square of the physical neutrino masses.

$$\frac{x}{\mathcal{H}(M_1)}\hat{\gamma}^{(i)}_{\nu^c} \propto M_1\bar{m}^2. \tag{3.58}$$

Under these simplifying assumptions also the upper bound on the CP asymmetry in decay of the lightest right–handed neutrino is expressed through mean square of the light neutrino masses and mass of the lightest Majorana in the same way as in the Standard Model:

$$|\varepsilon| \lesssim \frac{3}{8\pi}\frac{M_1(\Delta m^2_{atm})^{\frac{1}{2}}}{v^2} \simeq \frac{3\sqrt{3}}{8\pi}\frac{M_1\bar{m}}{v^2}. \tag{3.59}$$

Note however, that v now stands for vacuum expectation value of $\tilde{H}^u_1$ and, in general, is not equal to expectation value of the Standard Model Higgs.

The lepton asymmetry generated in the decay of the right–handed (s)neutrino reaches an asymptotic value L_∞ long before the spontaneous breaking of the additional $U(1)$ group. As has been argued in the previous section, at this stage $B - L = -\frac{14}{5}L_\infty$. At temperature, the sphalerons freeze out, the baryon asymmetry is related to the $B - L$ by (1.111). We, thus, conclude, that the observed baryon asymmetry of the Universe is related to L_∞ by

$$B = -\frac{8N + 4n}{22N + 13n}\frac{14}{5}L_\infty = -\frac{14}{15}L_\infty \tag{3.60}$$

where we have used $n = 6$ for the evaluation. From the experimental value $Y_B = (6.2-6.9)\cdot 10^{-10}$ we can infer the lepton asymmetry to be generated

$$Y_L = -(6.6 - 7.4)\cdot 10^{-10} \tag{3.61}$$

Typical numerical solutions of the system of Boltzmann equations (3.50), (3.53) and (3.54) corresponding to the choice $\sqrt{3}\bar{m} = 5\cdot 10^{-2}$ eV and $\epsilon_1 = \epsilon_1^{max}$ are presented in figures 3.12–3.14. We consider two values of the effective neutrino mass $\tilde{m}_1 = 10^{-4}$ eV and $\tilde{m}_1 = 10^{-2}$ eV.

As is commonly accepted at present, at the final stage of inflation the inflaton field decayed into lighter particles. The decay of the inflaton field being a strongly out–of–equilibrium process,

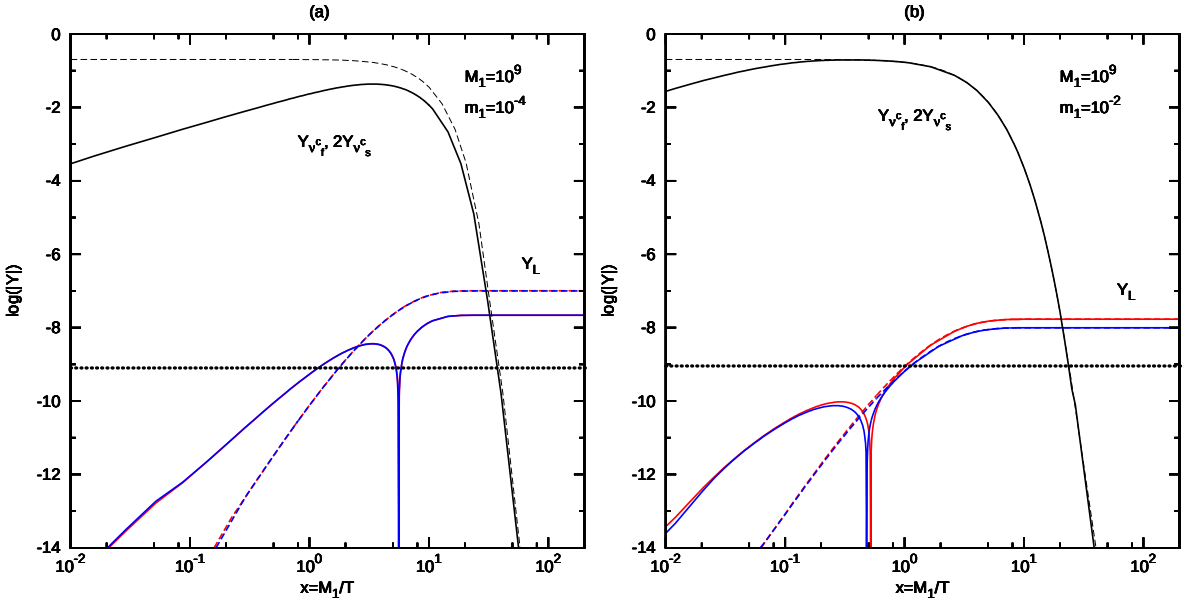

Figure 3.12: Typical numerical solutions of the Boltzmann equations. The red lines are solutions for the lepton number asymmetry with chemical potentials of all the species except for the leptons neglected. The blue lines correspond to the case when chemical potentials of all the species are taken into account. The solid lines correspond to the initial condition $Y_{\nu^c}(x_0) = 0$, while the dashed lines to the initial condition $Y_{\nu^c}(x_0) = Y^{eq}_{\nu^c}(x_0)$. The Majorana mass is given in GeV, whereas the effective neutrino mass is given in eV.

the decay products were distributed non–thermally. As the decay products thermalized, the Universe reheated. If the Majorana neutrinos have been created directly by the inflaton field, then as an initial condition for the Majorana number density one should use the equilibrium one (dashed lines in figure 3.12). On the contrary, if the heavy Majoranas have been created via scattering of the high–energetic light particles (among those are the Higgs–mediated two–body scattering processes discussed in section 3.3), then the initial Majorana number density is zero (solid lines in figure 3.12). The cross sections of the latter processes depend on the Yukawa couplings of the Majorana neutrinos determining also the light neutrino mass matrix. As may be inferred from figure 3.12, for $\tilde{m}_1 = 10^{-4}$ eV the Yukawa interactions are too weak to create a thermal population of the Majorana neutrinos, which results in the smaller upper bound on the lepton asymmetry. Still with $Y^m_L = 2 \cdot 10^{-8}$ it is more than an order of magnitude bigger than the experimental value. For $\tilde{m}_1 = 10^{-2}$ eV the Yukawa interactions are strong enough to bring the heavy Majoranas to equilibrium, so that the resulting upper bound on the lepton asymmetry $Y^m_L = 1 \cdot 10^{-8}$ is independent of the initial conditions. The decrease of Y^m_L is a consequence of stronger lepton asymmetry washout by the inverse decay and the Higgs–mediated scattering processes.

Note also that if the initial number of the heavy Majoranas is zero, then the lepton asymmetry crosses zero (and, thus, changes sign) for both $\tilde{m}_1 = 10^{-4}$ and $\tilde{m}_1 = 10^{-2}$. This effect can easily be understood. The Majorana neutrinos are created by the *CP*–conserving Higgs–mediated scattering and by *CP*–violating inverse decay processes. The latter one obviously leads to a generation of lepton asymmetry of opposite sign. As the temperature drops down, the decaying Majorana neutrinos generate an asymmetry, which compensates the one generated earlier, so that the lepton asymmetry reaches zero, and, after all the Majoranas have decayed, it reaches its asymptotic value.

As has already been mentioned, the lepton asymmetry generated in the decay of the heavy Majorana induces nonzero chemical potentials of the quarks, the Higgses, etc. As a consequence, even the processes conserving *CP* tend to washout the lepton asymmetry. Consequently, the resulting asymmetry is expected to be smaller than in the case if these chemical potentials are neglected. For $\tilde{m}_1 = 10^{-4}$ solutions for the lepton number asymmetry with chemical potentials of all the species except for the leptons neglected (red curves in figure 3.14) and with chemical potentials of all the species taken into account (blue curves in figure 3.14) lie one upon the other, which reflects the minor role of the washout processes. For $\tilde{m}_1 = 10^{-2}$ the washout processes are stronger and the resulting upper bound is (a factor of two) smaller, as one would expect.

In figures 3.13 and 3.14 the development of the lepton asymmetry for the Majorana neutrino masses $M_1 = 10^{10}$ GeV and $M_1 = 10^{11}$ GeV is presented. The increase of the upper bound on Y_L^m is mainly due to the increase of the upper bound on *CP* in the Majorana decay, which, according to equation (1.45), grows linearly with the right–handed neutrino mass.

The development of the lepton asymmetry for $M_1 = 10^9$ GeV and the effective neutrino masses $\tilde{m}_1 = 10^{-3}$ eV and $\tilde{m}_1 = 5 \cdot 10^{-2}$ eV is presented in figure 3.15. As may be inferred from figure 3.15.a, for $\tilde{m}_1 = 10^{-3}$ eV the Yukawa interactions are sufficiently strong to create a thermal population of Majorana neutrinos. The upper bound on the lepton asymmetry is more than an order of magnitude bigger than the experimental value. For $\tilde{m}_1 = 5 \cdot 10^{-2}$ eV on the contrary, the theoretical upper bound is comparable the experimental bound (3.61), which, as follows from equations (3.56) and (3.57), is a consequence of the stronger washout of the lepton asymmetry by the inverse decay and the Higgs–mediated scattering processes.

Finally, let us briefly discuss the role of the additional processes present in the model with $\lambda_8 \neq 0$. Additional decay channels present in this model lead to an increase of the Majorana neutrino decay width and a decrease of deviation from thermal equilibrium, thus leading to a decrease of the efficiency of leptogenesis. The decrease, however, is likely to be compensated by the increase of the *CP* asymmetry in the decay. The reduced cross sections of the scattering processes involving the leptoquarks coincide (up to an overall factor determined by the values

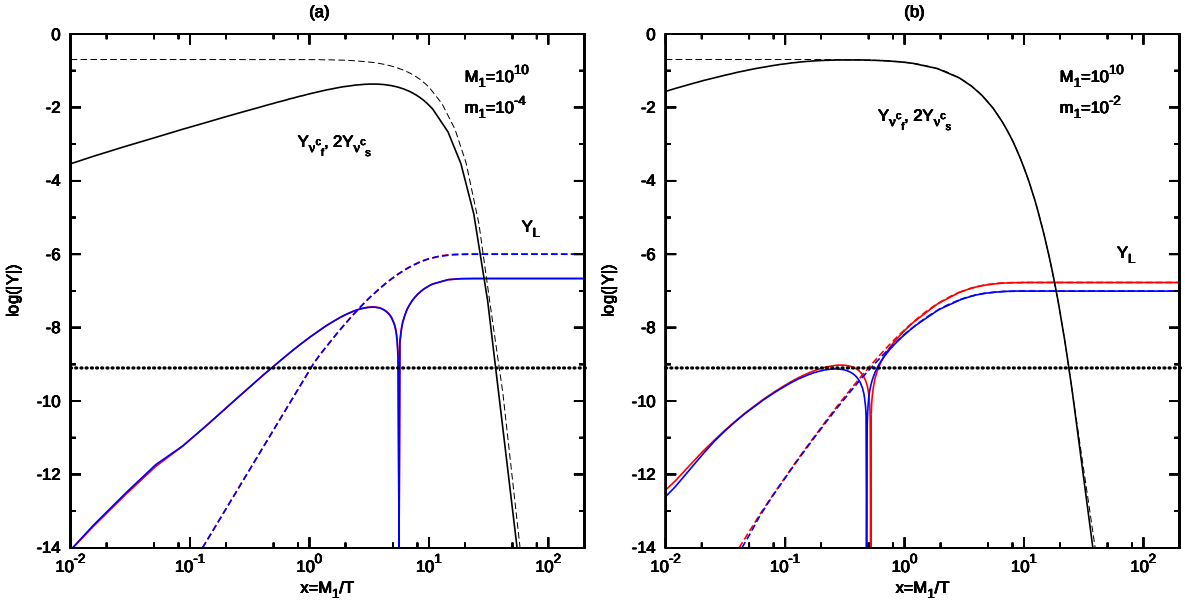

Figure 3.13: Typical numerical solutions of the Boltzmann equations for the lepton number asymmetry for a mass of the lightest Majorana $M_1 = 10^{10}$ GeV. The conventions are the same as in figure 3.12.

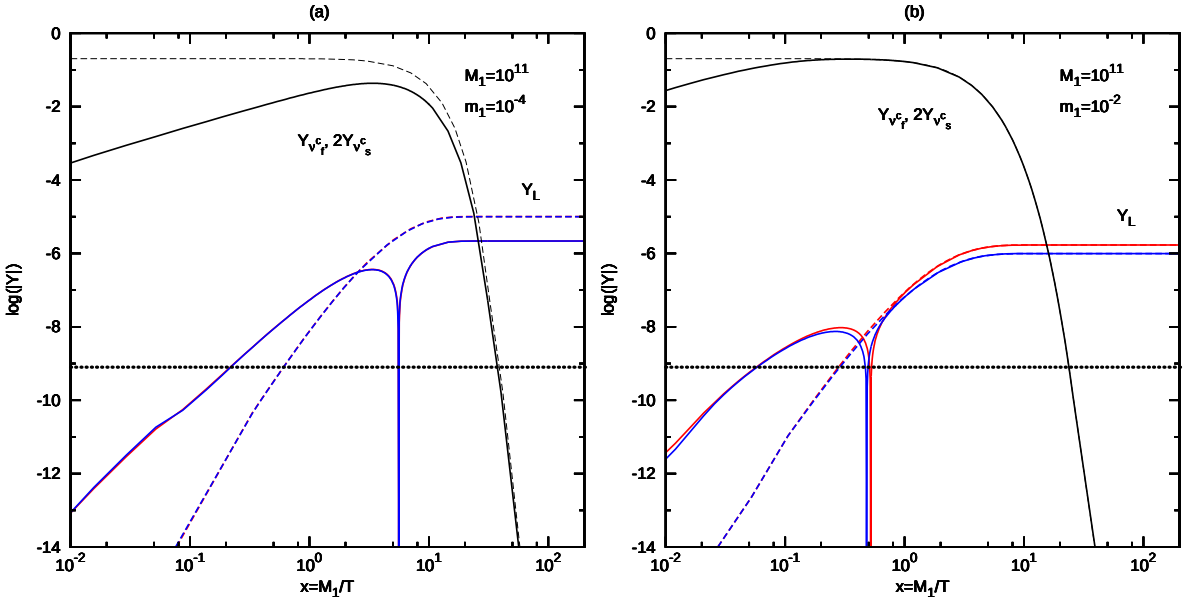

Figure 3.14: Typical numerical solutions of the Boltzmann equations for the lepton number asymmetry for a mass of the lightest Majorana $M_1 = 10^{11}$ GeV. The conventions are the same as in figure 3.12.

of the corresponding coupling constants and the number of states in the multiplets) with those in the model with the Majoranas coupled to the leptons only. Therefore taking these processes into account is equivalent to a modification of parameters in the model with $\lambda_8 = 0$, considered

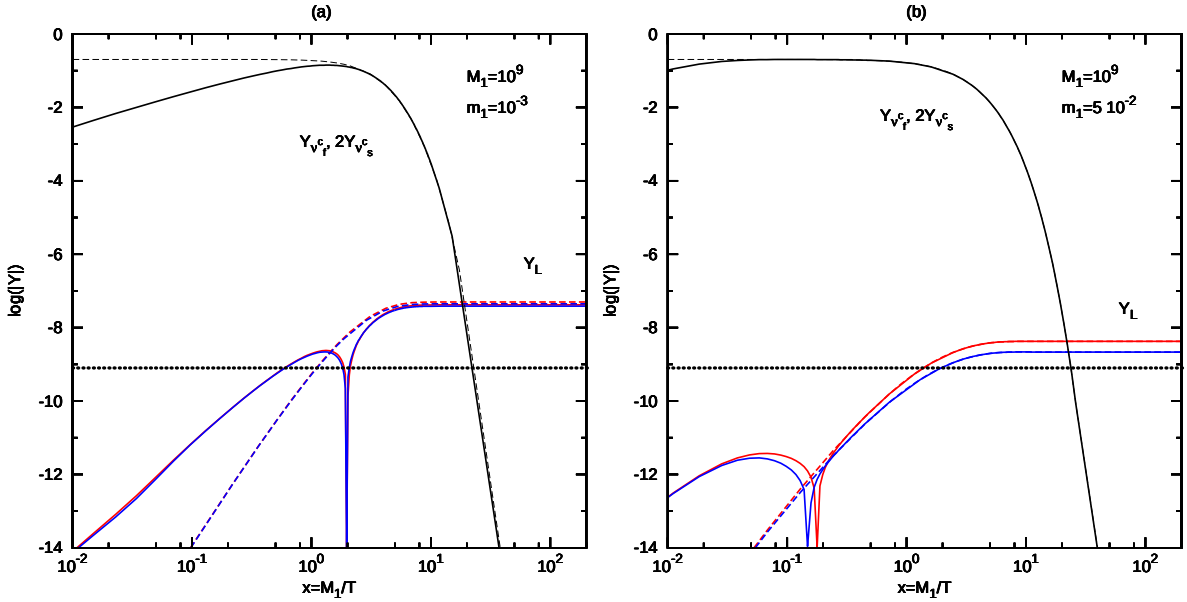

Figure 3.15: Typical numerical solutions of the Boltzmann equations for the lepton number asymmetry for a mass of the lightest Majorana $M_1 = 10^9$ GeV and the effective neutrino masses $\tilde{m}_1 = 10^{-3}$ eV and $\tilde{m}_1 = 5 \cdot 10^{-2}$ eV. The conventions are the same as in figure 3.12.

already. The additional processes involving both the leptons and the quarks lead a to stronger washout of the lepton asymmetry, thus decreasing the efficiency of leptogenesis. Depending on the values of the Yukawa couplings and *CP* violating phases, the interplay of the aforementioned effects may lead to a change of the asymmetry in either direction. If the Yukawa couplings of the leptoquarks are comparable to the Yukawa couplings of the Higgses, one can expect that the asymptotic value of the lepton asymmetry in the model with $\lambda_8 \neq 0$ will not be considerably different from that in the model with $\lambda_8 = 0$.

3.8 Conclusions

In this chapter a numerical analysis of the lepton asymmetry development in the superstring inspired E_6 model has been performed.

The asymmetry is generated in the decay of the heavy Majorana (s)neutrino into a scalar–fermion, scalar–scalar or fermion–fermion pair. As has been shown by an explicit calculation, since the supersymmetry is broken only softly, the associated violation of *CP* is the same in each of the decay channels.

Scattering processes mediated by the Higgs or the Majorana neutrino tend to washout the generated lepton asymmetry. The explicit calculation demonstrates, that the *CP* violation induced by the latter ones vanishes after summation over all initial and final states, as is required

by unitarity.

Scattering processes mediated by the gauge superfields conserve lepton number but redistribute the lepton asymmetry between the fermions and the scalars. Since the corresponding gauge couplings are of the order of unity, the rate of these processes exceeds the expansion rate of the Universe, so that they are in thermal equilibrium. Consequently the fractions of the lepton asymmetry carried by the scalars and the fermions are equal.

Fast Yukawa interactions together with the anomalous processes partially redistribute the asymmetry between all the species in the model, thus inducing nonzero chemical potentials of these species. The numerical analysis demonstrates, that this effect leads to a reduction of the asymptotic value of the asymmetry.

The parameters of the model are relatively weakly constrained by the observables like the light neutrino masses or mixing angles. One of the consequences is that the predicted upper bound for the baryon asymmetry substantially exceeds the observed asymmetry. This is partially explained by the fact, that due to the presence of new states, contributing to the total energy density, the Universe expansion rate (characterized by the Hubble parameter) during the period of leptogenesis is higher than that in the Standard Model; the bigger deviation from thermal equilibrium leads, in turn, to an increase of the efficiency and larger asymptotic value of the asymmetry. The dimensionless Hubble parameter, as well as the upper bound on the *CP* asymmetry in the decay, are proportional to M_1, and therefore with a decrease of the lightest Majorana mass the degree of deviation from thermal equilibrium and the *CP* asymmetry in the decay are expected to decrease along with the asymptotic value of the asymmetry. The theoretical expectations are confirmed by results of the numerical simulations.

For a small ($\tilde{m}_1 \lesssim m_*$) effective mass of the light neutrino the asymptotic lepton asymmetry depends on the initial condition for the Majorana number density, because the Yukawa interactions in this case are too weak to produce a thermal population of the heavy neutrinos. For a large ($\tilde{m}_1 \gtrsim m_*$) effective mass of the light neutrino, on the contrary, the Yukawa interactions are strong and the final lepton asymmetry is independent of the initial conditions.

The numerical analysis shows, that for $\tilde{m}_1 = 5 \cdot 10^{-2}$ eV and $M_1 = 10^9$ the final lepton asymmetry is independent of the initial conditions. The theoretical upper bound on the baryon asymmetry of the Universe is comparable in this case to the observed baryon asymmetry. The difference from the experimental value can accounted for by a smaller value of the *CP* asymmetry in the decay, or by a bigger value of the effective neutrino mass, or by both of these factors.

Chapter 4

Coherent neutrino scattering

An exciting feature of the Fukugita–Yanagida scenario is that it predicts a nonzero mass of the conventional neutrino. Recent K2K and SNO observations confirmed that conventional neutrinos indeed have nonzero masses. High precision measurements of neutrino masses and mixing angles in the forthcoming experiments require a good understanding of the interactions of the neutrino beam with the target material.

A new measurement by the K2K group at an average neutrino energy $E_1 = 1.3$ GeV has set an upper bound on the coherent pion production by neutrinos, which is far below the theoretical expectations [24]. This has raised questions on how accurately the coherent cross section can be calculated in such a low energy region, and whether detail event distributions may be predicted.

Coherent production of pions by neutrinos has been studied by many experimental groups and measurements have been made for neutrino energies ranging from 2 to 80 GeV [76, 77, 78, 79, 80, 81, 82, 83]. The main characteristics of such cross sections is that the energy of the recoiling nucleus and the invariant momentum transfer to it always remain very small. A characteristic signature of these events is a sharp peak in the low $|t|$ region. In addition to this, all experiments have observed that the momentum transfer Q^2 from the leptonic sector also remains very small, sharply peaking at $Q^2 \lesssim 0.2$ GeV^2, while the dependence of the cross section on the neutrino energy appears logarithmic at high energies.

In many models one starts with the Adler relation [25] in the $Q^2 = 0$ limit and extrapolates it to small Q^2 values. In the work of Rein and Sehgal [84] the pole due to the $a_1(1260)$ resonance is introduced together with other assumptions for estimating the pion–nucleus cross section. In several articles, Kopeliovich et al. [85] have claimed that the pion pole term acting on the leptonic current gives a small contribution proportional to the lepton mass, and they are led to argue that the axial current must be dominated by heavy meson fluctuations like $a_1(1260)$ or the $\rho\pi$ branch point.

As is argued in section 4.1, a careful PCAC treatment determines the dominant terms in

a unique way. We first decompose the leptonic current contribution into a spin=0 and spin=1 state with three helicity components. The inner product of the helicity zero polarization vector with the axial hadronic current leads to matrix elements which in the $Q^2 \ll \nu^2$ region are determined by PCAC as $f_\pi T(\pi N \to \pi N)$, with T being the amplitude for the coherent pion–nucleus scattering, which is a smooth function of Q^2, having no pion poles. This way, a Goldberger–Treiman–type relation is obtained, determining the dominant contribution to coherent neutrino–pion production. Contributions arising from the transverse (off shell) vector and axial states, which are estimated phenomenologically here, turn out to be very small.

Since the kinematics for the charged current (CC) cross sections obey $Q^2_{\min} \sim m_\mu^2 \sim m_\pi^2$, all mass terms are retained in the calculation of the density matrix of the leptonic current and the phase space. For the neutral current (NC) reactions, the neutrino masses are of course negligible and they are simplified.

The numerical analysis performed in section 4.2 demonstrates, that for energies of the incident neutrino of the order of a few GeV, the main contribution to the coherent neutrino–pion production is determined by PCAC and the pion–nucleus coherent scattering data. The transverse vector contribution is expressed in terms of the π^0 coherent photoproduction data, and it is thus reliably estimated. Estimating the axial transverse contribution is more difficult, but a Regge analysis indicates that it should be comparable or probably smaller than the transverse vector contribution. Contributions arising from both transverse off–shell vector and axial mesons are very small.

4.1 The formalism

We first consider the coherent π^+ production by neutrino scattering off a heavy nucleus N

$$\nu_\mu(k_1)\ N(p_1) \to \mu^-(k_2)\ \pi^+(p_\pi)\ N(p_2) \tag{4.1}$$

where the momenta are indicated in parentheses (see figure 4.1).

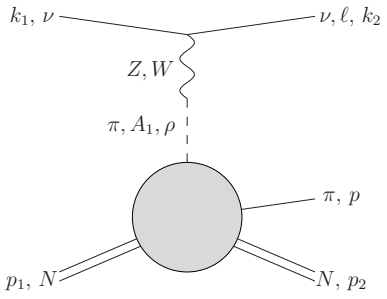

Figure 4.1: Neutrino scattering off a nucleus.

It is convenient to choose Lorentz–invariant quantities as kinematic variables. The commonly used variables are the square of the center of mass energy $s = (k_1 + p_1)^2$, the square of momentum–transfer in the hadronic system $t = (p_2 - p_1)^2$, the invariant mass of the pion–nucleus pair $W^2 = (p + p_1)^2$ and the square of momentum transfer to the final lepton $Q^2 = -q^2$. Here $q = k_1 - k_2$ is the momentum four–vector transferred from the leptonic current to the nucleus N. Its energy–component $\nu = q_0 = E_1 - E_2$ (with E_1 and E_2 being the ν_μ and μ^- laboratory energies respectively) denotes the energy given by the current to the π^+N-pair in the laboratory frame. Kinematic limits on these quantities are given in appendix E. In the coherent scattering regime the nucleus spin is not flipped, and its recoil must be minimal, so that $\nu \simeq E_\pi$, with E_π being the pion energy in the laboratory frame. The existing experimental data also suggest that in the coherence regime $0 \leq Q^2 \lesssim 0.2$ GeV^2, and that the squared momentum–transfer in the hadronic system t is peaked at very small values.

The invariant amplitude for the process (4.1) may then be written as

$$T_W = -\frac{G_F V_{ud}}{\sqrt{2}} \bar{u}(k_2, \mu^-)\gamma^\rho(1 - \gamma_5)u(k_1, \nu_\mu)(\mathcal{V}_\rho^+ - \mathcal{A}_\rho^+) \ , \tag{4.2}$$

where the first factor gives the $(\nu_\mu \to \mu)$ – matrix element of the leptonic current, while

$$\mathcal{V}_\rho^+ = \langle \pi^+ N | V_\rho^1 + i V_\rho^2 | N \rangle \quad , \quad \mathcal{A}_\rho^+ = \langle \pi^+ N | A_\rho^1 + i A_\rho^2 | N \rangle \quad , \tag{4.3}$$

describe (in momentum space) the hadronic matrix elements of the charged vector and axial currents respectively. V_{ud} in (4.2) denotes the appropriate CKM matrix element.

Since the charged leptonic current is not conserved ($m_\mu \neq 0$), it contains spin=0 degrees of freedom described by the vector

$$\epsilon_l^\rho = \frac{q^\rho}{\sqrt{Q^2}} \quad , \tag{4.4}$$

as well as spin=1 degrees of freedom describing off-shell gauge bosons with the helicity polarization vectors

$$\epsilon^\rho(\lambda = \pm 1) = \mp \begin{pmatrix} 0 \\ 1 \\ \pm i \\ 0 \end{pmatrix}^\rho \quad , \quad \epsilon^\rho(\lambda = 0) = \frac{1}{\sqrt{Q^2}} \begin{pmatrix} |\vec{q}| \\ 0 \\ 0 \\ q_0 \end{pmatrix}^\rho \ , \tag{4.5}$$

when $\vec{q}$ is taken along the $\hat{z}$-axis. The $\lambda = \pm 1$ polarizations in (4.5) are often denoted as L(R) respectively, the vanishing helicity vector $\epsilon^\rho(\lambda = 0)$ is identical to ϵ_S^ρ of [86], and $\epsilon^\rho(\lambda) q_\rho = 0$ is of course always satisfied.

Anticipating that we later integrate over all relative angles between the $(\vec{k}_1, \vec{k}_2)$–leptonic plane and the $(\vec{q}, \vec{p}_\pi)$ pion production plane, the only density matrix elements needed for the

above spin=0 and spin=1 states hitting the nucleus N are

$$\frac{(\tilde{L}_{RR}+\tilde{L}_{LL})}{2} = Q^2\left[1+\frac{(2E_1-\nu)^2}{\vec{q}^{\,2}}\right]-\frac{m_\mu^2}{\vec{q}^{\,2}}\left[2\nu(2E_1-\nu)+m_\mu^2\right] \quad , \tag{4.6a}$$

$$\frac{(\tilde{L}_{RR}-\tilde{L}_{LL})}{2} = -\frac{2\left[Q^2(2E_1-\nu)-\nu m_\mu^2\right]}{|\vec{q}|} \quad , \tag{4.6b}$$

$$\tilde{L}_{00} = \frac{2\left[Q^2(2E_1-\nu)-\nu m_\mu^2\right]^2}{Q^2\vec{q}^{\,2}}-2\left(Q^2+m_\mu^2\right) \quad , \tag{4.6c}$$

$$\tilde{L}_{ll} = 2m_\mu^2\left(\frac{m_\mu^2}{Q^2}+1\right) \quad , \tag{4.6d}$$

$$\tilde{L}_{l0} = \frac{2m_\mu^2\left[Q^2(2E_1-\nu)-\nu m_\mu^2\right]}{Q^2|\vec{q}|} \quad . \tag{4.6e}$$

Using these and the hadronic current elements in (4.3), the square of the amplitude in (4.2), summed over all μ^- polarizations, is written as

$$\begin{aligned}\overline{|T_W|^2} = G_F^2|V_{ud}|^2\Bigg\{ & \frac{(\tilde{L}_{RR}+\tilde{L}_{LL})}{2}\sum_{\lambda=L,R}|(\mathcal{V}^+-\mathcal{A}^+)\cdot\epsilon(\lambda)|^2 \\ + & \frac{(\tilde{L}_{RR}-\tilde{L}_{LL})}{2}\left[|(\mathcal{V}^+-\mathcal{A}^+)\cdot\epsilon(R)|^2-|(\mathcal{V}^+-\mathcal{A}^+)\cdot\epsilon(L)|^2\right] \\ + & \tilde{L}_{00}|(\mathcal{V}_\rho^+-\mathcal{A}_\rho^+)\epsilon^\rho(\lambda=0)|^2+\frac{\tilde{L}_{ll}}{Q^2}|(\mathcal{V}_\rho^+-\mathcal{A}_\rho^+)q^\rho|^2 \\ + & \frac{2\tilde{L}_{l0}}{\sqrt{Q^2}}\Re\left([(\mathcal{V}_\rho^+-\mathcal{A}_\rho^+)\epsilon^\rho(0)]\cdot[(\mathcal{V}_\mu^+-\mathcal{A}_\mu^+)q^\mu]^*\right)\Bigg\} \quad ,\end{aligned} \tag{4.7}$$

where the first two terms may be interpreted as giving the contributions from the transverse spin=1 components of the hadronic currents, the third term gives the helicity $\lambda=0$ hadronic contribution, the fourth term arises from the spin=0 component, and finally the last term from the interference of the latter two.

We first concentrate on the axial current matrix elements in the last three terms of (4.7), which turn out to give the most important contributions, for the GeV– scale kinematic region where coherence is relevant. The pion poles contained in these terms induce a singularity at low Q^2, which must be carefully separated, before any approximation is made.

To achieve this we note that the axial hadronic element in (4.3) consists of the pion pole contribution, and the rest, which we call $\mathcal{R}^\rho$, induced by $a_1(1260)$ and any other isovector axial meson that might exist. It is thus written as

$$-i\mathcal{A}_\rho^+ = \frac{f_\pi\sqrt{2}q^\rho}{Q^2+m_\pi^2}T(\pi^+N\to\pi^+N)-\mathcal{R}^\rho \quad , \tag{4.8}$$

where $T(\pi^+N\to\pi^+N)$ is the π-nucleus invariant amplitude, $f_\pi\simeq 92MeV$, and $\mathcal{R}^\rho$ is a very smooth function of Q^2 whose dependence on it may be ignored [1]. The usual PCAC treatment

[1] In principle we could insert here some pole contribution from the $a_1(1260)$ axial vector boson, in order to

then leads to

$$-iq^\rho \mathcal{A}^+_\rho = \langle \pi^+ N|\partial^\rho A^+_\rho|N\rangle = \frac{f_\pi m_\pi^2\sqrt{2}}{Q^2+m_\pi^2}\; T(\pi^+N\to\pi^+N)$$
$$= -\frac{f_\pi Q^2\sqrt{2}}{Q^2+m_\pi^2}\; T(\pi^+N\to\pi^+N) - q_\mu \mathcal{R}^\mu \quad , \tag{4.9}$$

so that

$$q^\mu \mathcal{R}_\mu = -f_\pi\sqrt{2}\; T(\pi^+N\to\pi^+N) \quad . \tag{4.10}$$

Equation (4.10) reminds the classical Goldberger–Treiman treatment, where the pion pole determines not only $\partial^\mu A_\mu$, but in fact also the complete axial current coupling [87].

Using now (4.8), and $\epsilon(0)_\rho q^\rho = 0$ implied by (4.4, 4.5), we conclude that

$$\epsilon(0)^\rho \mathcal{A}^+_\rho = -i\epsilon(0)^\rho \mathcal{R}_\rho \simeq i\frac{f_\pi\sqrt{2}}{\sqrt{Q^2}}\; T(\pi^+N\to\pi^+N) \quad , \tag{4.11}$$

where in the first step the pion pole contribution vanishes identically, while the last step is due to the smoothness of $\mathcal{R}^\rho$ and the restriction to $\nu \gg \sqrt{Q^2}$, which justifies the approximation

$$\epsilon^\rho(0) \simeq \frac{q^\rho}{\sqrt{Q^2}}. \tag{4.12}$$

In order for our treatment to be valid, the kinematics should always be chosen so that this approximation is satisfied. In figure 4.2 we plot kinematic limits on ν considered as a function of Q^2 at the incident neutrino energy $E_1 = 1.3$ GeV for neutrino scattering off Carbon nucleus in the cases of charged and neutral current scattering. According to the condition (4.12) we should integrate only over a relatively small part of phase space lying between the ν_{max} and $\nu = \xi\sqrt{Q^2}$ curves.

$$\max(\xi\sqrt{Q^2}, \nu_{min}) < \nu < \nu_{max} \tag{4.13}$$

For the numerical evaluation we choose $\xi = 3$. As is clear from figure 4.2 this condition automatically restricts Q^2 to small values required by the coherence.

It might be worth emphasizing that it would be incorrect to apply the approximation (4.12) directly on the $\epsilon(0)^\rho \mathcal{A}^+_\rho$ computation using (4.8), because that would replace the identically vanishing expression $\epsilon^\mu(0)q_\mu/(Q^2+m_\pi^2)$ arising there, by the non-vanishing and in fact large quantity $-\sqrt{Q^2}/(Q^2+m_\pi^2)$ [2].

The relations (4.9) and (4.11) fully determine the axial current contribution to the last three terms of (4.7). We also remark that these results are consistent with the Adler theorem in the parallel lepton configuration [25], provided that we set $m_\mu = 0$.

describe a possible Q^2 dependence in $\mathcal{R}^\rho$; but this resonance is so far away from the relevant Q^2 region, that such an effort does not seem useful.

[2] See e. g. also at C. Itzykson and J.-B. Zuber, Quantum Field Theory, McGraw-Hill 1980, p.535, particularly the remark immediately after equation (11-113).

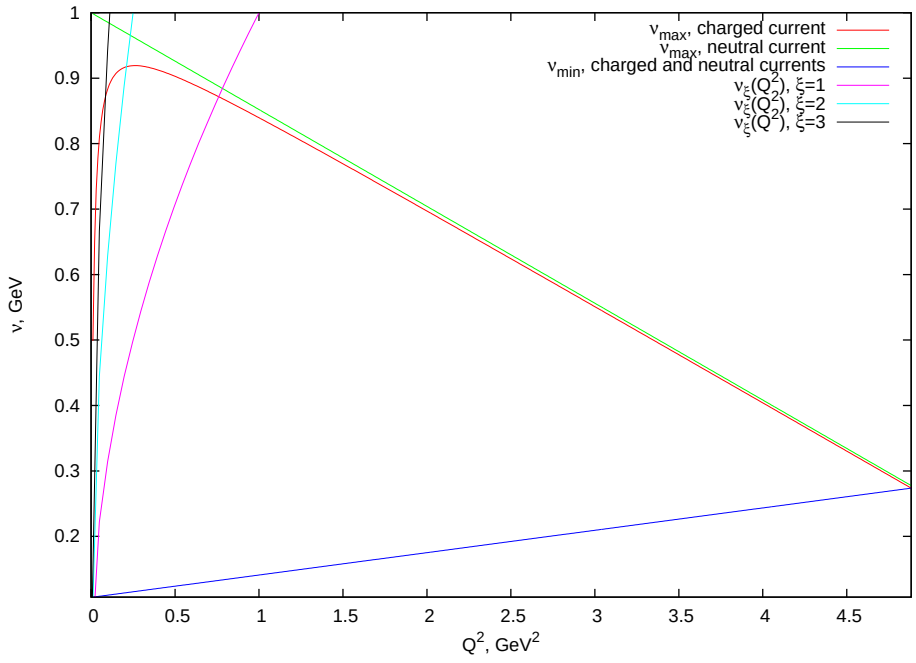

Figure 4.2: ν as a function of Q^2 at $E_1 = 1.3$ GeV for neutrino scattering off Carbon nucleus.

Furthermore, the vector hadronic elements in the last three terms of (4.7) give no contribution, since the vector current is conserved, and the applicability of (4.12) for calculating $\epsilon^\rho(\lambda = 0)\mathcal{V}^+_\rho$ is guaranteed by the absence of any low mass singularity, compare (4.3). Moreover, since in the coherence regime there is no $R - L$ polarization sensitivity to the vector or axial–vector boson cross sections, there will not be any contribution from the second term in (4.7).

Thus, expressed in terms of the leptonic density matrix elements defined in (4.6) the CC neutrino coherent pion production cross section off a nucleus N takes the form

$$\begin{aligned}\frac{d\sigma(\nu N \to \mu^- \pi^+ N)}{dQ^2 d\nu dt} = \frac{G_F^2 |V_{ud}|^2 \nu}{2(2\pi)^2 E_1^2} \Bigg\{ \\ \frac{f_\pi^2}{Q^2}\Big[\tilde{L}_{00} + \tilde{L}_{ll}\Big(\frac{m_\pi^2}{Q^2+m_\pi^2}\Big)^2 + 2\tilde{L}_{l0}\frac{m_\pi^2}{Q^2+m_\pi^2}\Big]\frac{d\sigma(\pi^+ N \to \pi^+ N)}{dt} \\ + \frac{(\tilde{L}_{RR}+\tilde{L}_{LL})}{2}\Big[\frac{1}{2\pi\alpha}\frac{d\sigma(\gamma N \to \pi^0 N)}{dt} + \frac{d\sigma(A_T^+ N \to \pi^+ N)}{dt}\Big]\Bigg\} \ , \end{aligned} \tag{4.14}$$

In deriving this expression we have integrated over all angles between the lepton- and $(\vec{q}, \vec{p}_\pi)$–planes, and ignored any vector–axial interference in (4.7), since it will anyway cancel out after the t–integration we do, before comparing to the experimental data. Notice that in contrast to (4.7), the presentation in (4.14) first gives the numerically most important terms arising from the $\lambda = 0$ and the spin=0 components of the leptonic current, and then the less important contributions from its transverse vector and axial components.

We next turn to the last two terms within the curly brackets in (4.14), which are induced by the transverse components of all off-shell vector and axial vector mesons coupled to the $\mathcal{V}_\nu^+$ and $\mathcal{A}_\nu^+$ matrix elements at very small Q^2; compare (4.3). The vector term is directly related, (after an isospin rotation producing a factor of 2), to π^0 photoproduction for unpolarized photons. In deriving this, it is important to realize that the isoscalar part of the electromagnetic current does not contribute to the coherent π^0 amplitude. This contribution is estimated in the next section, using the experimental data [88].

The transverse axial term within the curly brackets

$$\frac{d\sigma(A_T^+ N \to \pi^+ N)}{dt} = \frac{\sum_{\lambda=L,R} |\mathcal{A}^+ \cdot \epsilon(\lambda)|^2}{128\pi\nu^2 M_N^2} \quad , \tag{4.15}$$

is expressed in terms of the axial matrix element (4.3) and describes the cross section of π^+ – production through "transversely polarized charged axial currents". To calculate it, we would need to know all possible $a_1^+(1260)$ – type mesons that couple to the axial current, their couplings to it, and the corresponding $(a_1^+ N \to \pi^+ N)$ off–shell cross sections, at very small Q^2. We also estimate this in the next section.

A similar procedure may be carried out for the NC coherent π^0-production, for which the result

$$\frac{d\sigma(\nu N \to \nu\pi^0 N)}{dQ^2 d\nu dt} = \frac{G_F^2 \nu}{4(2\pi)^2 E_1^2} \left\{ \frac{f_\pi^2}{Q^2} \tilde{L}_{00} \frac{d\sigma(\pi^+ N \to \pi^+ N)}{dt} \right.$$
$$\left. + \frac{(\tilde{L}_{RR} + \tilde{L}_{LL})}{2} \left[\frac{(1-2s_W^2)^2}{2\pi\alpha} \frac{d\sigma(\gamma N \to \pi^0 N)}{dt} + \frac{d\sigma(A_T^+ N \to \pi^+ N)}{dt} \right] \right\} \tag{4.16}$$

is found, provided the assumption

$$\frac{d\sigma(\pi^+ N \to \pi^+ N)}{dt} \simeq \frac{d\sigma(\pi^0 N \to \pi^0 N)}{dt} \quad , \tag{4.17}$$

is made, which in fact is on the same footing as the isospin rotation we used in writing (4.14) in terms of the π^0 photoproduction data.

In (4.16), the leptonic density matrix elements are given by the same expressions as in (4.6), with the obvious substitution $m_\mu \to 0$. Comparing the NC result (4.16), to the CC in (4.14) we see that there is no CKM factor now, and that the axial contribution to the NC cross section is a factor 2 smaller than the CC one. For the vector contribution though, an extra reduction by a factor $(1-2s_W^2)^2$ appears, which is due to the fact that Z couples not only to the $SU_L(2)$ – current, but also to the isovector part of the electromagnetic current.

4.2 Numerical estimates and results

For numerical estimates we must calculate the three cross sections appearing in equations (4.14) and (4.16). The dominant cross section is $\sigma(\pi^+ N \to \pi^+ N)$ for which we use data on coherent

scattering of pions on nuclei. This being the dominant term, we calculate it precisely and present the results in the figures below. The other two cross sections involve coherent photoproduction of pions and the $a_T^+ N \to \pi^+ N$ process, where the axial vector particles are transversely polarized and give smaller contributions. We have estimated them using available data and showed that they are very small. Thus, assigning to the latter two cross sections an uncertainty even as large as 50%, does not affect our results.

For isoscalar targets, like C^{12}, O^{16}, etc., isospin symmetry implies $d\sigma(\pi^+ N) \simeq d\sigma(\pi^- N) \simeq d\sigma(\pi^0 N)$. In the actual calculation we use the coherent pion–Carbon scattering data [89, 90]. Additional data on other nuclei and other energies are available in [91, 92]. Plots of the differential pion–Carbon cross section at kinetic energies of the incident pion 120, 180 and 260 MeV are presented in figure 4.3. In all cases, the energy transfer ν is identified with the laboratory

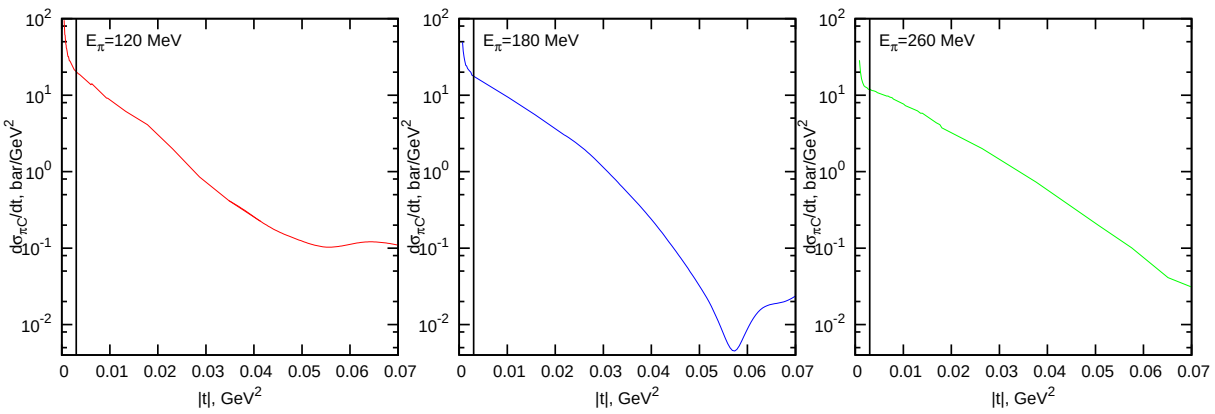

Figure 4.3: Differential cross section of coherent pion–Carbon scattering at kinetic energies of the incident pion 120, 180 and 260 MeV plotted in the logarithmic scale. Only the experimental points right to the vertical lines have been used for computation.

pion energy and the pion–Carbon cross section $\frac{d\sigma}{dt}(\pi^+ C \to \pi^+ C)$ is integrated from the kinematically allowed $|t|_{min}$ given in (E.5), to $|t|_{max} \simeq 0.05$ GeV^2 corresponding to the first dip of the pion–Carbon cross section (see figure 4.3). As can be seen in figure 4.3, at very small $|t|$ the differential pion–Carbon cross section has a sharp peak induced by virtual photon exchange (the Coulomb contribution). As we consider here neutrino scattering mediated by either W or Z boson, the Coulomb contribution should be subtracted. To this end we note that at moderate $|t|$ the differential cross section plotted in logarithmic scale is to a good approximation a linear function of $|t|$ and we extrapolate this dependence to smaller values of $|t|$. The pion–Carbon cross section integrated over t in the range discussed above, considered as a function of ν and the momentum transfer squared Q^2, introduced through the lower limit of the t–integration, is

presented in figure 4.4.

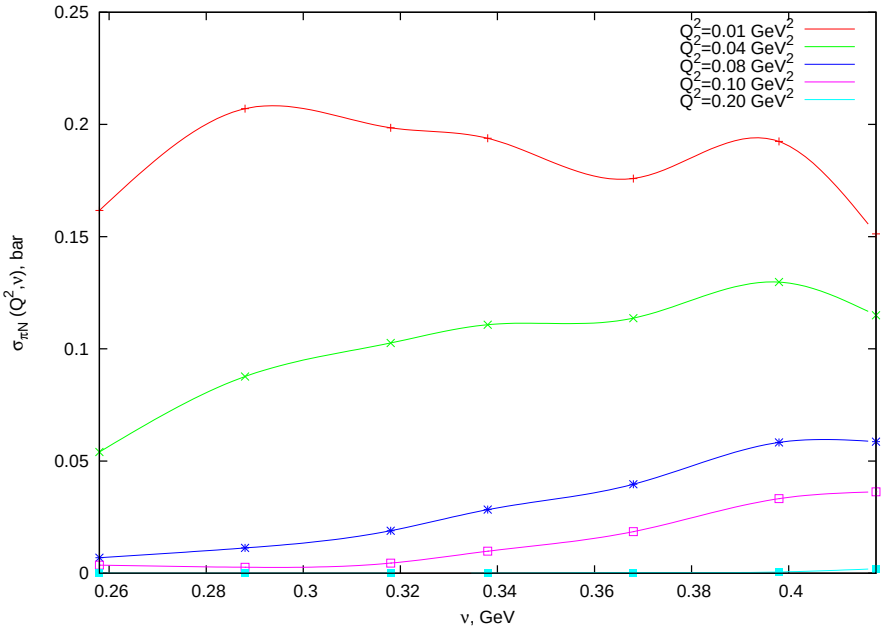

Figure 4.4: Pion-Carbon cross section integrated over t in the range discussed in the text, as a function of ν, at different values of Q^2.

Integrating next (4.14) and (4.16) over ν in the range (4.13), we obtain the differential cross sections $d\sigma(\nu N \to \mu^- \pi^+ N)/dQ^2$ and $d\sigma(\nu N \to \nu \pi^0 N)/dQ^2$ of the CC and NC reactions depicted in figure 4.5. We notice that the shapes of the CC and the NC distributions are different, most notably because of the muon mass effects. The results in figure 4.5 correspond to $\xi = 3$. We also note that such shape differences as indicated in figure 4.5, must be taken into account in the comparison with the Adler parallel configuration.

Finally, integrating over Q^2 in the region (E.2), we obtain the results presented in figures 4.6 and 4.7.

We next turn to the transverse vector and axial contributions supplying the terms proportional to the density matrix elements $\tilde{L}_{RR} + \tilde{L}_{LL}$ in (4.14) and (4.16). For the photon induced reaction, there exist data on the photoproduction of mesons off nuclei [88, 94, 95]. The A-dependence reported in [95] is $A^{2/3}$ which indicates that the same shadowing as in π-nucleus interactions takes place. Using then the data on Pb from figure 9 of [88] at $E_\gamma = 200 - 350$ MeV, and integrating them over the first peak, we obtain

$$\frac{1}{2\pi\alpha} \int_{|t_{\min}|}^{0.01\mathrm{GeV}^2} \frac{d\sigma(\gamma N \to \pi^0 N)}{dt} \left(\frac{12}{207}\right)^{2/3} \simeq 1.40 \text{ mb} \quad , \tag{4.18}$$

where the factor $1/2\pi\alpha$ comes from the elimination of the electromagnetic coupling, and $(12/207)^{2/3}$ from changing the cross section from Lead to Carbon. The numerical value in (4.18) should be

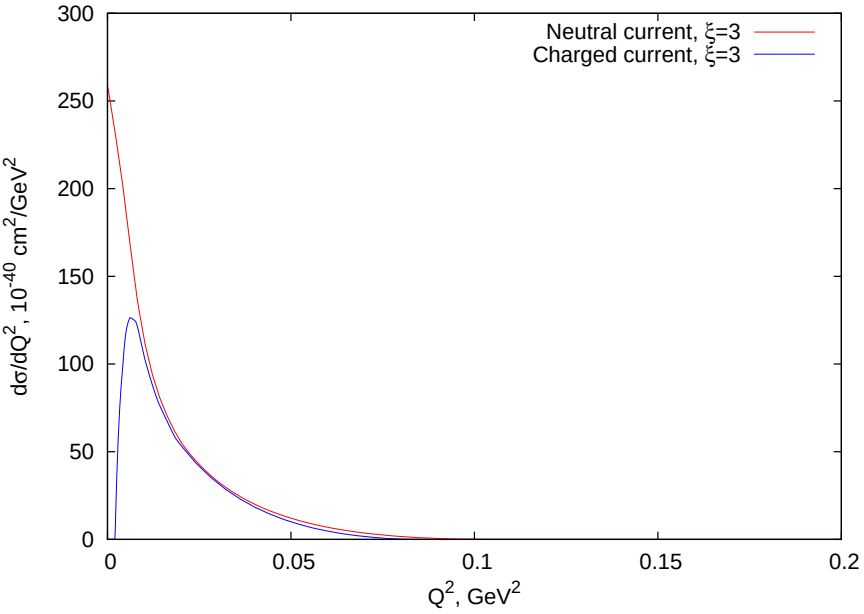

Figure 4.5: Differential cross sections of the coherent pion production by neutrinos $d\sigma(\nu N \to \mu^- \pi^+ N)/dQ^2$ and $d\sigma(\nu N \to \nu \pi^0 N)/dQ^2$. Only contributions of the leading terms have been taken into account. The curves correspond to $\xi = 3$.

compared with the uppermost curve in our figure 4.4. We note that the transverse vector current contribution is approximately 1% of the pion contribution. In addition the ratio of their coefficients in (4.14), $(\tilde{L}_{RR} + \tilde{L}_{LL})/2$ to $f_\pi^2[\tilde{L}_{00} + ...]/Q^2$ in the interesting kinematic region is ~ 0.2. We conclude therefore, that the transverse vector–current contribution to (4.14) and (4.16) is negligible, compared to the pion contribution.

Estimates of the transverse axial current contribution at low energies are more difficult, because of the absence of data. However, as argued below, this contribution to (4.14) and (4.16) should be very small and in fact smaller than the transverse vector one.

A very rough estimate for (4.15) may be obtained by assuming that it receives important contributions from the $a_1^+(1260)$ resonance. We need two kinds of measurements for this. The first one is the partial decay width $\Gamma(\tau^- \to a_1^- \nu_\tau)$, which determines the a_1 coupling to the axial current f_{a_1}, defined through (compare (4.3))

$$\langle 0|A_\rho^1 + iA_\rho^2|a_1^+\rangle = \frac{m_{a_1}^2}{f_{a_1}} \epsilon_\rho(a_1) \quad , \tag{4.19}$$

using

$$\Gamma(\tau^- \to a_1^- \nu_\tau) = \frac{G_F^2 m_{a_1}^2 m_\tau^3}{16\pi f_{a_1}^2} \left(1 - \frac{m_{a_1}^2}{m_\tau^2}\right)^2 \left(1 + \frac{2m_{a_1}^2}{m_\tau^2}\right) \quad , \tag{4.20}$$

where m_{a_1} and $\epsilon_\rho(a_1)$ are the a_1 mass and polarization vector, and m_τ is the τ mass. The a_1

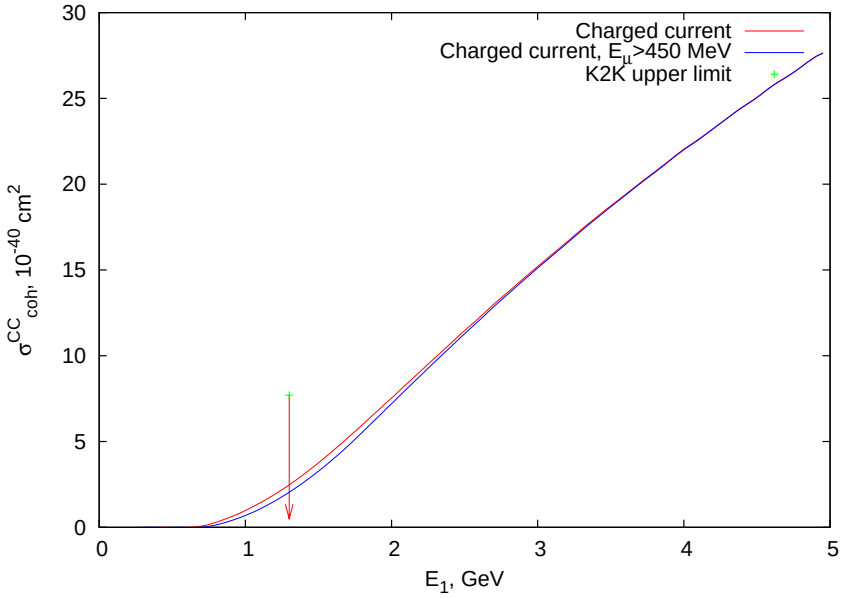

Figure 4.6: Cross section of the charged current coherent pion production by neutrinos per Carbon nucleus. Only contributions of the leading terms have been taken into account. The upper bound is from K2K including one standard deviation. Dotted line represents the integrated cross section with a threshold value for the muon energy $E_\mu > 450$ MeV. The theoretical curves correspond to $\xi = 3$.

subsequently decays into a 3π final state. Unfortunately the data for $\tau^- \to a_1^- \nu_\tau$ do not show a clear 3π resonant state.

Using as an alternative the corresponding coupling of the ρ-meson to the isovector current $f_\rho^2 \simeq 32$, determined from e. g. the $\Gamma(\rho^0 \to e^- e^+)$ data, and taking into account the fact that the a_1–coupling to the axial current could not be stronger [96], we expect

$$f_{a_1}^2 \gtrsim 32 \quad . \tag{4.21}$$

If in addition some data on $d\sigma(\pi^\pm N \to a_{1T}^\pm N)/dt$ for transverse a_1 production were available, we would estimate

$$\frac{d\sigma(A_T^\pm N \to \pi^+ N)}{dt} \sim \frac{2}{f_{a_1}^2} \frac{d\sigma(\pi^+ N \to a_{1T}^+ N)}{dt} \quad , \tag{4.22}$$

where the laboratory energy of the incident pion is again identified with ν.

To get a feeling on the relative magnitude of the transverse axial, versus transverse vector contribution, we compare the integrated $\pi^- p \to a_1^- p$ data at $E_\pi = 16$ GeV of [97], to the $\gamma p \to \pi^0 p$ data at $E_\gamma = 15$ GeV of [98].

The integrated diffractive cross section found in [97] at $E_\pi = 16$ GeV is $\sigma(\pi^- p \to a_1^- p) = 250 \pm 50\ \mu$b. Most of this is of course helicity conserving and refers to the production of a_1 with

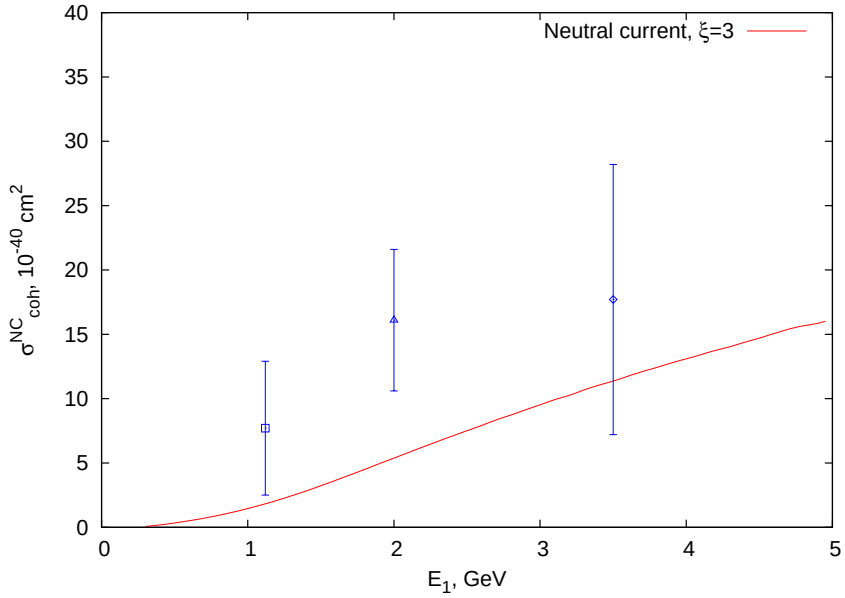

Figure 4.7: Cross section of the neutral current coherent pion production by neutrinos per Carbon nucleus. Only contributions of the leading terms have been taken into account. The experimental points for NC are from: □ MiniBoone [93], △ Aachen-Padova [76], ♢ Gargamelle [78]. The theoretical curve corresponds to $\xi = 3$.

vanishing helicity. According to the authors estimate [97], the transverse helicity part constitutes a fraction of 0.16 ± 0.08 of this. Substituting this in (4.22) and using (4.21) we find

$$\int \frac{d\sigma(A_T^- p \to \pi^- p)}{dt} dt \lesssim 2.5 \pm 1.2 \ \mu\text{b} \ , \tag{4.23}$$

which should be compared with the transverse vector contribution [98, 99]

$$\frac{1}{2\pi\alpha}\sigma(\gamma p \to \pi^0 p) \simeq 5 \ \mu\text{b} \tag{4.24}$$

at E_γ= 6 GeV.

In comparing (4.23) and (4.24) we should remember that the transverse vector and axial processes in (4.14), are both determined by helicity–flip amplitudes. But in contrast to the ω–Regge trajectory which contributes uninhibitedly to the coherent vector amplitude [84], the only established Regge singularity that can contribute to the coherent axial amplitude would had been the Pomeron, provided the associate a_1–particles had helicity zero. Since the currents we consider are transverse though, the only possible contributions to the axial amplitude arises, either from the small s–channel helicity violating component of the Pomeron [100, 101], or the generally unimportant σ–trajectory. On this basis we conclude that (4.23) is very likely an overestimate. The limited amount of data forced us to use proton targets in the estimates of (4.23) and (4.24); for coherent production on a Carbon target, these should be scaled up by a

factor $12^{2/3} \simeq 5.2$, always remaining very small compared to the pion–Carbon coherent cross section (the uppermost curve in the figure 4.4).

To sum up, the limited amount of data forced us to use phenomenological estimates which imply that the transverse contributions are very small in comparison to the pion term. Our results in figures 4.4 – 4.7, based on the pion–nucleus data only, can be considered as lower bounds, with the actual cross sections being a few percent above them.

We next turn to the implications for the oscillation experiments. Figure 4.6 shows our results for the charged current coherent contribution to the neutrino–pion production $\sigma_{\rm coh}^{CC}(E_1)$ for $\nu \geq \xi\sqrt{Q^2}$ with $\xi = 3$. We note that there is a rapid growth of the cross section up to $E_1 \sim 5$ GeV. In fact at $E_1 = 2.0$ GeV the cross section is almost three times bigger than at 1.0 GeV. For $E_1 = 1.3$ GeV and $\xi = 3$ the predicted coherent charged current cross section on a Carbon target with the $E_2 \equiv E_\mu > 450$ MeV cut applied is $\sigma_{\rm coh}^{CC} = 2 \times 10^{-40}$ cm^2. The corresponding experimental upper bound for coherent pion production on Carbon [24] is

$$\sigma_{\rm coh}^{CC} \lesssim (7.7 \pm 1.6\,(\text{stat}) \pm 3.6\,(\text{syst})) \cdot 10^{-40}\ \text{cm}^2 \tag{4.25}$$

which is consistent with our value.

Finally, we apply our work to the coherent production of π^0 in neutral current reactions. This reaction is an important background in oscillation experiments searching for the oscillation of ν_μ's to ν_e's. Several oscillation experiments use two detectors with a long–baseline. The far away detector searches among other channels also for $\nu_e \to e^-$ interactions. The π^0s produced via coherent scattering decay to two photons whose Cherenkov light mimics that of electrons. Furthermore, when the oscillation is to other types of active neutrinos all species contribute equally to coherent scattering, but only ν_e's produce electrons through the charged current. Thus a good understanding of coherent π^0 production is very important.

The neutral current cross section is calculated from (4.16), assuming $\sigma(\pi^0 C \to \pi^0 C) \simeq \sigma(\pi^+ C \to \pi^+ C)$, which follows from isospin symmetry. The neutral current cross section is approximately half as big as the charged current one. The result is shown in figure 4.7 with the solid curve again corresponding to $\xi = 3$. We also plotted results of several experiments carried out at three different energies and targets made of Carbon, Aluminum and Freon, respectively. We use Carbon as our reference nucleus and scale the results for other nuclei by the $A^{\frac{2}{3}}$ rule, as we discussed earlier. Rescaling the Aachen and Gargamelle data we obtain the points in figure 4.7. The three points have large errors and are consistent with the theoretical curves. As in the charged current case, we should mention though that the $\xi = 3$ cut was not imposed in these data. If this was done, the experimental cross sections would had been reduced considerably.

4.3 Conclusions

In this chapter the coherent pion production by neutrino scattering off nuclei has been considered. The main reason for returning to this old topic are the new data from the K2K group [24] that has set an upper bound on the coherent pion production by neutrinos far below the theoretical expectations.

The approach presented here is based on the decomposition of the leptonic tensor into density matrix elements. A careful application of PCAC leads to the formulas (4.14) and (4.16) which should be valid for small values of Q^2 provided that $\nu \gg \sqrt{Q^2}$. Numerical estimates show, that the dominant contribution comes from the zero helicity component of the leptonic tensor. Contributions arising from the transverse (off shell) vector and axial states, which have been estimated phenomenologically, turn out to be very small.

We kept the charged lepton mass in both the matrix element and the phase space of charged current scattering. As is clear from figure 4.5 by neglecting the muon mass the integrated charged current cross section is overestimated by a factor of two.

Finally we computed the total cross sections shown in figures (4.6) and (4.7). It should be stressed that in the analysis presented here we integrate over a relatively small part of the phase space where the approximations we used are applicable. Thus a comparison with experimental data requires similar kinematic cuts on the experimental side. Of course, our results are in agreement with the upper bound for the *total* cross section of coherent neutrino pion production obtained by the K2K group.

Conclusions

At present, the scenario of baryogenesis via leptogenesis suggested by M. Fukugita and T. Yanagida is one of the most attractive explanations of the observed baryon asymmetry of the Universe. The generation of the lepton and baryon asymmetries is a complex phenomenon, which is affected by many factors. In particular, the generation of a nonzero asymmetry requires deviation from thermal equilibrium. In a nonuniform model of the Universe the degree of deviation from thermal equilibrium is a function of space coordinates. We have investigated the influence of the associated effects of general relativity for superhorizon–size perturbations and found, that the generation of the asymmetry has been slightly more efficient in the regions of higher energy density. In other words, even before structure formation began shortly after the onset of the matter–dominated epoch, seeds of the future galaxies and other large scale structures contained a higher–than–average number of baryons and leptons.

The second class of the effects is associated with the fact, that the asymmetry generated in the decay of the right–handed neutrino induces nonzero chemical potentials of quarks and the Higgs. This effect results in a modification of coefficients of individual terms in the Boltzmann equations for the lepton number asymmetry and leads to a decrease of the efficiency of leptogenesis. In addition, the fact that the lepton asymmetry is instantly converted to the baryon asymmetry by the sphaleron processes, which are in equilibrium at this stage of the Universe history, implies, that the Boltzmann equations describe the development of the lepton asymmetry and not the development of the $B - L$ number, as has been tacitly assumed by some researches. As a consequence, the baryon asymmetry is one half, rather than one third of the solution of the Boltzmann equation.

Numerical analysis shows, that theoretical upper bound on the baryon asymmetry of the Universe in the Standard Model is consistent with the experimental observations. However, the Standard Model is very likely to be a part of a more fundamental theory. The exotic interactions, which are strongly suppressed at low energies, will certainly affect the generation of the lepton and baryon asymmetries, which takes place at very high temperatures. Contribution of the new decay and scattering processes constitute the third class of the effects. We have investigated

the generation of the lepton and baryon asymmetries in the superstring inspired E_6 model. The model is likely to be of interest from the point of view of "low–energy" phenomenology and also introduces many new decay and scattering processes, which affect the generation of the asymmetry. The efficiency of leptogenesis turns out to be bigger than in the Standard Model. This is partially explained by the fact, that in this model the Universe expands faster at the temperature where most of the asymmetry is generated. A theoretical upper bound on the baryon asymmetry, consistent with the experimental observations, can easily be obtained for reasonable values of the parameters.

The parameters which determine the lepton and baryon asymmetry of the Universe are related to those measured at low–energy experiments only in a model–dependent way. Nevertheless, any improvement in determination of the masses and mixing angles of the light neutrino brings us closer to the ultimate goal of predicting the baryon asymmetry, instead of estimating the theoretical upper bounds. High precision measurements of neutrino masses and mixing angles in the forthcoming experiments require a good understanding of the interactions of the neutrino beam with the target material. We have considered coherent pion production by neutrino scattering off nuclei using a decomposition of the leptonic tensor into density matrix elements and PCAC. We have computed the total cross section of the charged current scattering keeping the charged lepton mass in both the matrix element and the phase space and the cross section of the neutral current scattering. The numerical results are in agreement with the upper bound for the total cross section of coherent neutrino pion production recently obtained by K2K group.

Appendix A

One–loop integrals

We summarize here some standard formulas for one–loop integrals, useful for the calculation of the *CP* asymmetry in the decay of the heavy right–handed neutrino. We use the notation and conventions adopted in [102] with a flat space–time metric $g_{\mu\nu} = (1, -1, -1, -1)$.

A.1 One–point function

In $n = 4 - 2\epsilon$ dimensions the scalar one–point function reads

$$A_0(m_1) = \frac{\mu^{4-n}}{i\pi^2} \int \frac{d^n k}{D_{m_1}(k)}, \quad D_{m_1}(k) = k^2 - m_1^2 + i\varepsilon \tag{A.1}$$

In the limit $\epsilon \to 0$ it is given by

$$A_0(m_1) = m_1^2 \left[\Delta - \ln\left(\frac{m_1^2}{\mu^2}\right) + 1 \right] + \mathcal{O}(n-4) \tag{A.2}$$

with the UV–divergence contained in

$$\Delta = \frac{1}{\epsilon} - \gamma_{_E} + \ln 4\pi \tag{A.3}$$

where $\gamma_{_E} = 0.577216$ is Euler's constant.

A.2 Two–point functions

The scalar two–point function reads

$$B_0(p_1^2, m_1, m_2) = \frac{\mu^{4-n}}{i\pi^2} \int \frac{d^n k}{D_{m_1}(k) D_{m_2}(k, p_1)}, \quad D_{m_2}(k, p_1) = (k + p_1)^2 - m_2^2 + i\varepsilon \tag{A.4}$$

In the limit $\epsilon \to 0$ it is given by [102, 103]

$$B_0(p_1^2, m_1, m_2) = \Delta - \int_0^1 dx \ln\left(\frac{p_1^2 x^2 - x(p_1^2 - m_1^2 + m_2^2) + m_2^2 - i\varepsilon}{\mu^2} \right) + \mathcal{O}(n-4) \tag{A.5}$$

In particular, in the limit of zero m_1 and m_2 the following identity emerges

$$B_0(p_1^2,0,0) = \Delta + 2 - \ln\left(\frac{|p_1^2|}{\mu^2}\right) + i\pi\theta(p_1^2) \tag{A.6}$$

whereas if p_1^2 and one of the masses are zero, then

$$B_0(0,m,0) = B_0(0,0,m) = \Delta + 1 - \ln\left(\frac{m^2}{\mu^2}\right) = \frac{1}{m^2}A_0(m^2) \tag{A.7}$$

Lorentz covariance of the tensor integrals allows us to decompose them into tensors constructed from the external momenta p_1 and the metric tensor $g_{\mu\nu}$. In the case of the vector integral

$$B_\mu(p_1^2,m_1,m_2) = \frac{\mu^{4-n}}{i\pi^2}\int \frac{k_\mu\, d^n k}{D_{m_1}(k)D_{m_2}(k,p_1)} \tag{A.8}$$

such a decomposition is very simple

$$B_\mu(p_1^2,m_1,m_2) = p_{1,\mu}B_1(p_1^2,m_1,m_2) \tag{A.9}$$

where the coefficient of decomposition B_1 is given by

$$B_1(p_1^2,m_1,m_2) = \frac{1}{2p_1^2}\left[A(m_1) - A(m_2) + (m_2^2 - m_1^2 - p_1^2)B_0(p_1^2,m_1,m_2)\right] \tag{A.10}$$

In the case of vanishing or equal masses

$$B_1(p_1^2,m_1,m_2) = -\frac{1}{2}B_0(p_1^2,m_1,m_2) \tag{A.11}$$

A.3 Three–point functions

The scalar three–point function reads

$$C_0(p_1^2,p_2^2,m_1,m_2,m_3) = \frac{\mu^{4-n}}{i\pi^2}\int \frac{d^n k}{D_{m_1}(k)D_{m_2}(k,p_1)D_{m_3}(k,p_1+p_2)} \tag{A.12}$$

The explicit expression for the scalar three–point function in the limit $\epsilon \to 0$ which can be found in [102] is rather complicated. We will need only the imaginary part of it. In the case two of the masses are zero, it takes the form

$$\mathrm{Im}[C_0(p_1^2,p_2^2,m,0,0)] = -\frac{\pi\theta(p_2^2)}{p_2^2}\ln\left(1+\frac{p_2^2}{m^2}\right) \tag{A.13}$$

Decomposing the vector integral

$$C_\mu(p_1^2,p_2^2,m_1,m_2,m_3) = \frac{\mu^{4-n}}{i\pi^2}\int \frac{k_\mu\, d^n k}{D_{m_1}(k)D_{m_2}(k,p_1)D_{m_3}(k,p_1+p_2)} \tag{A.14}$$

into tensors constructed from the external momenta p_1 and p_2 we obtain

$$C_\mu(p_1^2,p_2^2,m_1,m_2,m_3) = p_{1,\mu}C_{11}(p_1^2,p_2^2,m_1,m_2,m_3) + p_{2,\mu}C_{12}(p_1^2,p_2^2,m_1,m_2,m_3) \tag{A.15}$$

In the case of two vanishing masses and two light–like momenta $p_1^2 = 0$ and $(p_1 + p_2)^2 = 0$ the decomposition coefficients read

$$C_{12}(p_1^2, p_2^2, m, 0, 0) = \frac{1}{2(p_1 p_2)} \left[B_0(0, m, 0) - B_0(p_2^2, 0, 0) - m^2 C_0(p_1, p_2, m, 0, 0) \right] \tag{A.16}$$

$$C_{11}(p_1^2, p_2^2, m, 0, 0) = 2C_{12}(p_1^2, p_2^2, m, 0, 0) \tag{A.17}$$

The imaginary part of C_{12} is given by

$$\mathrm{Im}[C_{12}(p_1^2, p_2^2, m, 0, 0)] = \frac{\pi\theta(p_2^2)}{p_2^2} \left[1 - \frac{m^2}{p_2^2} \ln\left(1 + \frac{p_2^2}{m^2} \right) \right] \tag{A.18}$$

Appendix B

Spinor Notation and Conventions

In this appendix we introduce the notation and summarize some standard formulas of spinor algebra. Greek indices α, β and $\dot{\alpha}$, $\dot{\beta}$ run from one to two and denote the components of Weyl spinors, while all other Greek letters denote Lorentz–indices. We follow here the conventions of [104] with a flat space–time metric $g_{\mu\nu} = (1, -1, -1, -1)$.

B.1 Weyl fermions

Two–component Weyl spinors describe massless fermions with two spin degrees of freedom. Under a Lorentz transformation $M \in \mathrm{SL}(2,\mathbb{C})$ two–component spinors with upper or lower dotted or undotted indices transform as follows:

$$\psi'_\alpha = M_\alpha{}^\beta \psi_\beta, \qquad \bar{\psi}'_{\dot{\alpha}} = M^*{}_{\dot{\alpha}}{}^{\dot{\beta}} \bar{\psi}_{\dot{\beta}} \tag{B.1a}$$

$$\psi'^\alpha = M^{-1}{}_\beta{}^\alpha \psi^\beta, \quad \bar{\psi}'^{\dot{\alpha}} = (M^*)^{-1}{}_{\dot{\beta}}{}^{\dot{\alpha}} \bar{\psi}^{\dot{\beta}} \tag{B.1b}$$

Spinors with dotted indices transform under the $(0, \frac{1}{2})$ representation of the Lorentz group, while those with undotted indices transform under the $(\frac{1}{2}, 0)$ conjugate representation.

The connection between $\mathrm{SL}(2,\mathbb{C})$ and the Lorentz group is established through the Pauli matrices

$$\sigma^0 = \begin{pmatrix} 1 & 0 \\ 0 & 1 \end{pmatrix}, \quad \sigma^1 = \begin{pmatrix} 0 & 1 \\ 1 & 0 \end{pmatrix}, \quad \sigma^2 = \begin{pmatrix} 0 & -i \\ i & 0 \end{pmatrix}, \quad \sigma^3 = \begin{pmatrix} 1 & 0 \\ 0 & -1 \end{pmatrix} \tag{B.2a}$$

The antisymmetric tensors $\varepsilon^{\alpha\beta}$ and $\varepsilon_{\alpha\beta}$

$$\varepsilon_{\alpha\beta} = \begin{pmatrix} 0 & -1 \\ 1 & 0 \end{pmatrix}, \qquad \varepsilon^{\alpha\beta} = \begin{pmatrix} 0 & 1 \\ -1 & 0 \end{pmatrix} \tag{B.3}$$

are invariant under Lorentz transformations. Spinors with upper and lower indices are related through the antisymmetric ε–tensor:

$$\psi^\alpha = \varepsilon^{\alpha\beta}\psi_\beta, \quad \psi_\alpha = \varepsilon_{\alpha\beta}\psi^\beta \tag{B.4}$$

An analogous treatment holds for the ε–tensor with dotted indices. The ε–tensor may also be used to raise the indices of the σ–matrices:

$$\bar{\sigma}^{\mu\dot{\alpha}\alpha} = \varepsilon^{\dot{\alpha}\dot{\beta}}\varepsilon^{\alpha\beta}\sigma^\mu_{\beta\dot{\beta}} \tag{B.5}$$

From the definition of the Pauli matrices it then follows that

$$(\sigma^\mu\bar{\sigma}^\nu + \sigma^\nu\bar{\sigma}^\mu)_\alpha{}^\beta = 2g^{\mu\nu}\delta_\alpha{}^\beta \tag{B.6a}$$

$$(\bar{\sigma}^\mu\sigma^\nu + \bar{\sigma}^\nu\sigma^\mu)^{\dot{\alpha}}{}_{\dot{\beta}} = 2g^{\mu\nu}\delta^{\dot{\alpha}}{}_{\dot{\beta}} \tag{B.6b}$$

$$\mathrm{Tr}(\sigma^\mu\bar{\sigma}^\nu) = 2g^{\mu\nu} \tag{B.6c}$$

$$\sigma^\mu_{\alpha\dot{\alpha}}\bar{\sigma}^{\dot{\beta}\beta}_\mu = 2\delta_\alpha{}^\beta\delta_{\dot{\alpha}}{}^{\dot{\beta}} \tag{B.6d}$$

Since spinors anticommute, the following spinor summation conventions are valid

$$\psi\chi \equiv \psi^\alpha\chi_\alpha = -\psi_\alpha\chi^\alpha = \chi^\alpha\psi_\alpha = \chi\psi \tag{B.7a}$$

$$\bar{\psi}\bar{\chi} \equiv \bar{\psi}_{\dot{\alpha}}\bar{\chi}^{\dot{\alpha}} = -\bar{\psi}^{\dot{\alpha}}\bar{\chi}_{\dot{\alpha}} = \bar{\chi}_{\dot{\alpha}}\bar{\psi}^{\dot{\alpha}} = \bar{\chi}\bar{\psi} \tag{B.7b}$$

$$(\chi\psi)^\dagger = (\chi^\alpha\psi_\alpha)^\dagger = \bar{\psi}_{\dot{\alpha}}\bar{\chi}^{\dot{\alpha}} = \bar{\psi}\bar{\chi} = \bar{\chi}\bar{\psi} \tag{B.7c}$$

We will also need products of Weyl–spinors involving Pauli matrices which read as

$$\chi\sigma^\mu\bar{\psi} = -\bar{\psi}\bar{\sigma}^\mu\chi\,, \tag{B.8a}$$

$$(\chi\sigma^\mu\bar{\psi})^\dagger = \psi\sigma^\mu\bar{\chi}\,, \tag{B.8b}$$

$$\chi\sigma^\mu\bar{\sigma}^\nu\psi = \psi\sigma^\nu\bar{\sigma}^\mu\chi\,, \tag{B.8c}$$

$$(\chi\sigma^\mu\bar{\sigma}^\nu\psi)^\dagger = \bar{\psi}\bar{\sigma}^\nu\sigma^\mu\bar{\chi}\,. \tag{B.8d}$$

B.2 Dirac fermions

Four–component Dirac spinors describe massive fermions with four spin degrees of freedom. A Dirac spinor can be combined of two two–component spinors introduced above.

$$\Psi_D = \begin{pmatrix} \chi_\alpha \\ \bar{\psi}^{\dot{\alpha}} \end{pmatrix} \tag{B.9}$$

In the four–component notation the analogs of the Pauli matrices are the four Dirac matrices γ^μ, which satisfy the following anticommutation relations:

$$\{\gamma^\mu, \gamma^\nu\} = 2g^{\mu\nu} \tag{B.10a}$$

$$\{\gamma^5, \gamma^\nu\} = 0, \quad \gamma^5 = i\gamma^0\gamma^1\gamma^2\gamma^3 \tag{B.10b}$$

$$\gamma^5\gamma^5 = \mathbb{1} \tag{B.10c}$$

The explicit form of the Dirac matrices depends on the choice of representation. In the so–called chiral representation the Dirac matrices take the form

$$\gamma^\mu = \begin{pmatrix} 0 & \sigma^\mu \\ \bar{\sigma}^\mu & 0 \end{pmatrix}, \quad \gamma^5 = \begin{pmatrix} -\mathbb{1} & 0 \\ 0 & \mathbb{1} \end{pmatrix} \tag{B.11}$$

In the case of vanishing mass only two of the four degrees of freedom are independent and the four–component spinors are equivalent to two–component Weyl spinors. Even in this case one can use the four–component notation provided that unphysical degrees of freedom are removed by chiral projectors. In the chiral representations the chiral projectors read

$$P_R = \frac{1+\gamma^5}{2} = \begin{pmatrix} 0 & 0 \\ 0 & \mathbb{1} \end{pmatrix}, \quad P_L = \frac{1-\gamma^5}{2} = \begin{pmatrix} \mathbb{1} & 0 \\ 0 & 0 \end{pmatrix} \tag{B.12}$$

For a Dirac spinor (B.9) and its Dirac conjugate (B.13)

$$\bar{\Psi}_D = \Psi_D^\dagger \gamma^0 = (\psi^\alpha, \bar{\chi}_{\dot{\alpha}}) \tag{B.13}$$

one has

$$P_L\Psi_D = \chi_\alpha\,, \quad P_R\Psi_D = \bar{\psi}^{\dot{\alpha}}, \tag{B.14a}$$

$$\bar{\Psi}_D P_L = \psi^\alpha\,, \quad \bar{\Psi}_D P_R = \bar{\chi}_{\dot{\alpha}} \tag{B.14b}$$

For fermions the operation of charge conjugation is defined as

$$\Psi_D^C \equiv C\bar{\Psi}_D^T \tag{B.15}$$

where the charge conjugation matrix C is given by

$$C = -i\gamma^2\gamma^0 = \begin{pmatrix} \varepsilon_{\alpha\beta} & 0 \\ 0 & \varepsilon^{\dot{\alpha}\dot{\beta}} \end{pmatrix} \tag{B.16}$$

and fulfills the following useful identities

$$C^T = C^\dagger = C^{-1} = -C, \quad C^2 = -1 \tag{B.17}$$

Using (B.13) and the explicit form of the charge conjugation matrix in the spinor representation (B.16) we obtain

$$\Psi_D^C = \begin{pmatrix} \psi_\alpha \\ \bar{\chi}^{\dot{\alpha}} \end{pmatrix} \tag{B.18}$$

B.3 Majorana spinors

Majorana spinors describe massive fermions with two spin degrees of freedom. A Majorana fermion is a truly neutral particle, i.e. it is invariant with respect to charge conjugation. Equations (B.9) and (B.18) imply then

$$\Psi_M = \Psi_M^C = \begin{pmatrix} \psi_\alpha \\ \bar{\psi}^{\dot{\alpha}} \end{pmatrix} \tag{B.19}$$

i.e. a Majorana fermion can be described in terms of one two–component spinor.

Whereas for Weyl and Dirac fermions there is only one propagator, for Majorana neutrinos several propagators can be introduced:

$$\langle \psi_\alpha(x)\bar{\psi}_{\dot{\beta}}(y)\rangle = i\int \frac{d^4k}{(2\pi)^4}\frac{k_\mu \sigma^\mu_{\alpha\dot{\beta}}\, e^{-ik(x-y)}}{k^2 - M^2 + i\epsilon} \tag{B.20a}$$

$$\langle \bar{\psi}^{\dot{\alpha}}(x)\psi^{\beta}(y)\rangle = i\int \frac{d^4k}{(2\pi)^4}\frac{k^\mu \sigma_\mu^{\dot{\alpha}\beta}\, e^{-ik(x-y)}}{k^2 - M^2 + i\epsilon} \tag{B.20b}$$

$$\langle \psi_\alpha(x)\psi^{\beta}(y)\rangle = i\int \frac{d^4k}{(2\pi)^4}\frac{M\delta_\alpha{}^\beta\, e^{-ik(x-y)}}{k^2 - M^2 + i\epsilon} \tag{B.20c}$$

$$\langle \bar{\psi}^{\dot{\alpha}}(x)\bar{\psi}_{\dot{\beta}}(y)\rangle = i\int \frac{d^4k}{(2\pi)^4}\frac{M\delta^{\dot{\alpha}}{}_{\dot{\beta}}\, e^{-ik(x-y)}}{k^2 - M^2 + i\epsilon} \tag{B.20d}$$

Violation of lepton number in scattering processes mediated by Majorana neutrino is described by the propagators (B.20c) and (B.20d) and is associated with chirality flipping. In the limit of vanishing Majorana mass both (B.20c) and (B.20d) vanish, which reflects the fact that for massless particles helicity and the associated lepton number are conserved.

Although in most cases the introduction of Feynman rules leads to a great simplification of analytical calculations, due to the aforementioned complication the direct calculation in terms of helicity amplitudes may turn out to be simpler in the case of Majorana fermions. Using the standard decomposition of spinor fields

$$\psi_\alpha(x) = \sum_{p\sigma}\frac{1}{\sqrt{2\varepsilon_p V}}\left(a_{p\sigma}u_{p\sigma,\alpha}e^{-ipx} + a^+_{p\sigma}v_{p\sigma,\alpha}e^{ipx}\right) \tag{B.21}$$

and the Lagrange equations of motion

$$i\gamma^\mu\partial_\mu\Psi_M - M\Psi_M = 0, \tag{B.22}$$

one can easily derive useful summation relations for on–shell Majorana fermions

$$p_\mu\sigma^\mu_{\alpha\dot{\beta}}\bar{u}^{\dot{\beta}} + Mv_\alpha = 0, \quad p_\mu u^\beta\sigma^\mu_{\beta\dot{\alpha}} + M\bar{v}_{\dot{\alpha}} = 0 \tag{B.23a}$$

$$p_\mu\sigma^\mu_{\alpha\dot{\beta}}\bar{v}^{\dot{\beta}} - Mu_\alpha = 0, \quad p_\mu v^\beta\sigma^\mu_{\beta\dot{\alpha}} - M\bar{u}_{\dot{\alpha}} = 0 \tag{B.23b}$$

$$p^\mu\bar{\sigma}^{\dot{\alpha}\beta}_\mu u_\beta - M\bar{v}^{\dot{\alpha}} = 0, \quad p^\mu\bar{u}_{\dot{\beta}}\bar{\sigma}^{\dot{\beta}\alpha}_\mu - Mv^\alpha = 0 \tag{B.23c}$$

$$p^\mu\bar{\sigma}^{\dot{\alpha}\beta}_\mu v_\beta + M\bar{u}^{\dot{\alpha}} = 0, \quad p^\mu\bar{v}_{\dot{\beta}}\bar{\sigma}^{\dot{\beta}\alpha}_\mu + Mu^\alpha = 0 \tag{B.23d}$$

Analogously for products of chiral amplitudes summed over spin projections we find

$$\sum_\sigma u_{p\sigma,\,\alpha} v^\beta_{p\sigma} = M\delta^\beta_\alpha, \quad \sum_\sigma \bar{v}^{\dot\alpha}_{p\sigma} \bar{u}_{p\sigma,\,\dot\beta} = M\delta^{\dot\alpha}_{\dot\beta} \tag{B.24a}$$

$$\sum_\sigma u_{p\sigma,\,\alpha} \bar{u}_{p\sigma,\,\dot\beta} = p_\mu \sigma^\mu_{\alpha\dot\beta}, \quad \sum_\sigma \bar{v}^{\dot\alpha}_{p\sigma} v^\beta_{p\sigma} = p_\mu \bar\sigma^{\mu\,\dot\alpha\beta} \tag{B.24b}$$

$$\sum_\sigma v_{p\sigma,\,\alpha} u^\beta_{p\sigma} = -M\delta^\beta_\alpha, \quad \sum_\sigma \bar{u}^{\dot\alpha}_{p\sigma} \bar{v}_{p\sigma,\,\dot\beta} = -M\delta^{\dot\alpha}_{\dot\beta} \tag{B.24c}$$

$$\sum_\sigma v_{p\sigma,\,\alpha} \bar{v}_{p\sigma,\,\dot\beta} = p_\mu \sigma^\mu_{\alpha\dot\beta} \quad \sum_\sigma \bar{u}^{\dot\alpha}_{p\sigma} u^\beta_{p\sigma} = p_\mu \bar\sigma^{\mu\,\dot\alpha\beta} \tag{B.24d}$$

B.4 Superfield Products

In the so–called y–basis, where $y^\mu = x^\mu - i\theta\sigma^\mu\bar\theta$, a chiral superfield written in terms of its scalar, fermion and auxiliary components has the form

$$\Phi(y,\theta) = A(y) + \sqrt{2}\theta\Psi(y) + \theta^2 F(y) \tag{B.25}$$

By Taylor expansion in θ and $\bar\theta$ we can write a chiral superfield as a function of x^μ, θ and $\bar\theta$:

$$\begin{aligned}\Phi(x,\theta,\bar\theta) = A(x) - i\theta\sigma^\mu\bar\theta\partial_\mu A(x) - \frac{1}{4}\theta^2\bar\theta^{\,2}\Box A(x) \\ + \sqrt{2}\theta\Psi(x) + \frac{i}{\sqrt{2}}\theta^2\partial_\mu\Psi(x)\sigma^\mu\bar\theta + \theta^2 F(x)\end{aligned} \tag{B.26}$$

Using relations (B.27)

$$\theta^\alpha\theta^\beta = -\frac{1}{2}\varepsilon^{\alpha\beta}\theta^2 \tag{B.27a}$$

$$\theta_\alpha\theta_\beta = \frac{1}{2}\varepsilon_{\alpha\beta}\theta^2 \tag{B.27b}$$

$$\bar\theta^{\dot\alpha}\bar\theta^{\dot\beta} = \frac{1}{2}\varepsilon^{\dot\alpha\dot\beta}\bar\theta^{\,2} \tag{B.27c}$$

$$\bar\theta_{\dot\alpha}\bar\theta_{\dot\beta} = -\frac{1}{2}\varepsilon_{\dot\alpha\dot\beta}\bar\theta^{\,2} \tag{B.27d}$$

$$\theta\sigma^\mu\bar\theta\theta\sigma^\nu\bar\theta = \frac{1}{2}\theta^2\bar\theta^{\,2} g^{\mu\nu} \tag{B.27e}$$

which follow from formulas of section B.1 we obtain products of two and three superfields. Up to a total derivative these read as

$$\Phi_i\Phi_j = A_iA_j + \sqrt{2}\theta(\psi_iA_j + \Psi_jA_i) + \theta^2(A_iF_j + A_jF_i - \Psi_i\Psi_j) \tag{B.28}$$

$$\begin{aligned}\Phi_i\Phi_j\Phi_k = {} & A_iA_jA_k + \sqrt{2}\theta(A_iA_j\Psi_k + A_i\Psi_jA_k + \Psi_iA_jA_k) \\ & - i\theta\sigma^\mu\bar\theta(A_iA_j\partial_\mu A_k + A_iA_k\partial_\mu A_j + A_jA_k\partial_\mu A_i) \\ & + \theta^2(A_iA_jF_k + A_iA_kF_j + A_jA_kF_i - A_i\Psi_j\Psi_k - A_j\Psi_k\Psi_i - A_k\Psi_i\Psi_j)\end{aligned} \tag{B.29}$$

Analogously for the kinetic terms one obtains

$$\begin{aligned}\bar{\Phi}_i\Phi_j = {} & A_i^* A_j + \sqrt{2}(A_i^*\theta\Psi_j + \bar{\Psi}_i\bar{\theta}A_j) + i\theta\sigma^\mu\bar{\theta}(\partial_\mu A_i^* A_j - A_i^*\partial_\mu A_j) \\ & + 2(\bar{\theta}\bar{\Psi})(\theta\Psi) + \frac{i}{\sqrt{2}}\theta^2(\partial_\mu\Psi_j\sigma^\mu\bar{\theta}A_i^* - \Psi_j\sigma^\mu\theta\partial_\mu A_i^* + \sqrt{2}\bar{\Psi}_i\bar{\theta}F_j + A_i^*F_j) \\ & - \frac{i}{\sqrt{2}}\bar{\theta}^2(\theta\sigma^\mu\partial_\mu\bar{\Psi}A_j + \theta\sigma^\mu\bar{\Psi}\partial_\mu A_j - \theta\Psi_i F_j^* + F_i^* A_j) \\ & + \theta^2\bar{\theta}^2(F_i^*F_j + \partial_\mu A_i^*\partial^\mu A_j + \frac{i}{2}\bar{\Psi}_i\bar{\sigma}^\mu\partial_\mu\Psi_j - \frac{i}{2}\partial_\mu\bar{\Psi}_i\bar{\sigma}^\mu\Psi_j)\end{aligned} \tag{B.30}$$

Appendix C

Kinetic theory

This appendix contains useful formulas needed for the calculation of reduced cross sections and reaction densities of the decay as well as the $2 \to 2$ and $2 \to 3$ scattering processes.

C.1 Decay

The quantity that enters the Boltzmann equations is the so–called reaction density of the decay defined as

$$\gamma_D = \int d\Pi_i d\Pi_Y (2\pi)^4 \delta^4(P_Y - P_i) f^a_{eq} |M(i \to Y)|^2 \tag{C.1}$$

where $d\Pi$ is the Lorentz–invariant element of phase space

$$d\Pi = \frac{d^3p}{(2\pi)^3}\frac{g}{2E}, \tag{C.2}$$

and $|M(i \to Y)|^2$ is the decay amplitude. We assume in what follows that f^i_{eq} is given by the Maxwell–Boltzmann distribution

$$f^{eq}_i = \exp(-E_i/T) \tag{C.3}$$

Multiplying and dividing by twice the decaying particle mass $2M_i$ we rewrite the decay reaction density as follows

$$\gamma_D = \int g_i \frac{d^3p}{(2\pi)^3}\frac{M_i}{E} f^i_{eq} \int \frac{1}{2M_i} d\Pi_Y (2\pi)^4 \delta^4(P_Y - P_i) |M(a \to Y)|^2 \tag{C.4}$$

The second integral is the decay width Γ_i, calculated in the rest frame of the decaying particle, which does not depend on the integration variable p. The first integral can then be written as

$$\gamma_D = \frac{g_i}{2\pi^2} x\sqrt{a_i} T^3 \Gamma_i \int \frac{y^2 dy}{\sqrt{a_i x^2 + y^2}} \exp\left(-\sqrt{a_i x^2 + y^2}\right) = \frac{g_i}{2\pi^2} x^2 a_i T^3 \Gamma_i K_1(x\sqrt{a_i}) \tag{C.5}$$

where $x = M_1/T$, $a_i = M_i^2/M_1^2$, and K_1 is a modified Bessel function. Introducing an equilibrium particle number density

$$n_{eq} = \frac{g_i}{(2\pi)^3} \int f^{eq}_i d^3p = \frac{g_i}{2\pi^2} x^2 a_i T^3 K_2(x\sqrt{a_i}) \tag{C.6}$$

we can finally write the thermally averaged decay width in the form

$$\gamma_D(x) = n_{eq}\Gamma_i \frac{K_1(x\sqrt{a_i})}{K_2(x\sqrt{a_i})} \tag{C.7}$$

For the numerical analysis it is also useful to introduce a dimensionless reaction density of the Majorana neutrino decay

$$\hat{\gamma}_D(x) \equiv \frac{\gamma_D}{T^3 M_1} = \frac{\Gamma_i}{M_1}\frac{x^2 a_i}{\pi^2} K_1(x\sqrt{a_i}) \tag{C.8}$$

C.2 Two–body scattering

It is convenient to split the calculation of the thermally averaged cross section of $2 \to 2$ and $2 \to 3$ processes into two steps: calculation of the reduced cross section of the process, which in many cases can be done analytically, and computation of the corresponding reaction density.

C.2.1 Reduced cross section of $2 \to 2$ process

The dimensionless reduced cross section $\hat{\sigma}(s)$ is the amplitude summed over final states

$$\hat{\sigma}(s) = 8\pi\Phi_2(s) \int d\Pi_c d\Pi_d (2\pi)^4 \delta^4(P_f - P_i) \times |M(ab \to cd)| \tag{C.9}$$

where $\Phi_2(s)$ is the two–body phase space for the initial state

$$\Phi_2(s) = \int d\Pi_a d\Pi_b (2\pi)^4 \delta^4(P_f - P_i) = \frac{g_a g_b}{8\pi s} w(s, m_a^2, m_b^2) \tag{C.10}$$

and the triangle function w is defined as

$$w(a,b,c) = \left(a^2 + b^2 + c^2 - 2ab - 2ac - 2bc\right)^{\frac{1}{2}} \tag{C.11}$$

We now multiply and divide (C.9) by the flux factor $I = \frac{1}{2} w(s, m_a^2, m_b^2)$ and, using the expression for the two–body scattering cross section

$$\sigma = \frac{1}{4I} \int d\Pi_c d\Pi_d (2\pi)^4 \delta^4(P_f - P_i) \times |M(ab \to cd)| = \frac{1}{64\pi} \int |M(ab \to cd)| \frac{dt}{I^2}, \tag{C.12}$$

rewrite the reduced cross section in the form convenient for actual calculations [73]

$$\hat{\sigma}(z) = \frac{g_a g_b g_c g_d}{8\pi z} \int |M(ab \to cd)|\, dy\,, \quad z = \frac{s}{M_1^2}, \quad y = \frac{t}{M_1^2} \tag{C.13}$$

C.2.2 Reduced cross section of $2 \to 3$ process

Generalizing equations (C.9) and (C.12) to the case of $2 \to 3$ scattering we obtain

$$\hat{\sigma}(s) = \frac{2w^2(s, m_a^2, m_b^2)}{s} \sigma(ab \to cde) \tag{C.14}$$

where $\sigma(ab \to cde)$ is the cross section summed over all final and initial spin states which can be written in the form

$$\sigma(ab \to cde) = \frac{1}{(4\pi)^5} \int \frac{|M(ab \to cde)|}{I} \frac{d^3p_c}{p_c} \frac{2}{\sqrt{s}} \frac{p_d^2 \, d\Omega_d}{\sqrt{s} - 2p_c} \tag{C.15}$$

At temperatures of the order of the Majorana neutrino mass all other particles can approximately be treated as massless. In this case equation (C.15) can be further simplified and a standard calculation yields

$$\hat{\sigma}(z) = \frac{g_a g_b g_c g_d g_e}{256\pi^3} \frac{M_1^2}{x} \int_0^x \frac{d\xi}{x-\xi} \int_0^{x-\xi} d\eta \int_{\xi-x}^0 dy \, |M(ab \to cde)| \tag{C.16}$$

where the dimensionless variables of integration are defined as

$$\xi = \frac{(p_d + p_e)^2}{M_1^2}, \quad \eta = \frac{(p_c + p_e)^2}{M_1^2}, \quad y = \frac{(p_a - p_c)^2}{M_1^2} \tag{C.17}$$

C.2.3 Reaction density

The quantity that enters the Boltzmann equations is the reaction density, which for $2 \to 2$ scattering is defined as

$$\gamma_S = \int d\Pi_a d\Pi_b d\Pi_c d\Pi_d (2\pi)^4 \delta^4(P_f - P_i) f_a^{eq} f_b^{eq} |M(ab \to cd)|^2 \tag{C.18}$$

Using the definition of the reduced cross section (C.9) we obtain

$$\gamma_S = \int d\Pi_a d\Pi_b f_a^{eq} f_b^{eq} \frac{\hat{\sigma}(s)}{8\pi\Phi_2(s)} \tag{C.19}$$

The remaining integral can be traced back to the two–body phase space (C.10). To this purpose we insert a factor

$$1 = \int_{s_{min}}^\infty ds \int d^4Q \delta(Q - p_a - p_b) \delta_+(Q^2 - s) \tag{C.20}$$

so that the reduced cross section takes the form

$$\begin{aligned} \gamma_S &= \int_{s_{min}}^\infty ds \int \frac{d^4Q}{(2\pi)^4} \delta_+(Q^2 - s) f_a^{eq} f_b^{eq} \frac{\hat{\sigma}(s)}{8\pi\Phi_2(s)} \int d\Pi_a d\Pi_b (2\pi)^4 \delta(Q - p_a - p_b) \\ &= \frac{1}{128\pi^5} \int_{s_{min}}^\infty ds \hat{\sigma}(s) \int d^4Q \delta_+(Q^2 - s) f_a^{eq} f_b^{eq} \end{aligned} \tag{C.21}$$

Assuming Maxwell–Boltzmann statistics for both incoming particles we obtain

$$J \equiv \int d^4Q \delta_+(Q^2 - s) f_a^{eq} f_b^{eq} = \int d^4Q \delta_+(Q^2 - s) e^{-\frac{Q^0}{T}} = \int_0^\infty \frac{d^3Q}{2E_Q} e^{-\frac{E_Q}{T}} \tag{C.22}$$

Integrating over the angles and using $|\vec{Q}| d|\vec{Q}| = E_Q dE_Q$ we obtain

$$J = 2\pi \int_{\sqrt{s}}^\infty |\vec{Q}| e^{-\frac{E_Q}{T}} dE_Q = 2\pi T \sqrt{s} K_1\left(\frac{\sqrt{s}}{T}\right) \tag{C.23}$$

The reaction density takes the form

$$\gamma_S(x) = \frac{T}{64\pi^4} \int_{(m_a+m_b)^2}^{\infty} ds\sqrt{s} K_1\left(\frac{\sqrt{s}}{T}\right) \hat{\sigma}(s) = \frac{TM_1^3}{64\pi^4} \int dz\sqrt{z} K_1\left(\sqrt{z}x\right) \hat{\sigma}(z) \tag{C.24}$$

where again $z = s/M_1^2$ and $x = M_1/T$. It is also useful to introduce a dimensionless reaction density

$$\hat{\gamma}_S(x) \equiv \frac{\gamma_S}{T^3 M_1} = \frac{x^2}{64\pi^4} \int dz\sqrt{z} K_1\left(\sqrt{z}x\right) \hat{\sigma}(z) \tag{C.25}$$

From the derivation of (C.24) it is evident, that the same formula also holds for $2 \to 3$ scattering.

Appendix D

Reduced cross sections

In this appendix we collect the reduced cross sections of the processes discussed in chapter 3. The definition of the reduced cross section along with some useful formulas for the calculation of reduced cross sections of $2 \to 2$ and $2 \to 3$ scattering processes can be found in appendix C.

Supersymmetric leptogenesis has been discussed by a number of authors. In particular, reduced cross sections of various processes in the supersymmetric $SO(10)$ model have been calculated in [16]. Since the model under consideration contains three generations of Higgses, the structure of flavor indices of the one–loop self–energy and one–loop vertex contributions is different, which makes the expressions for the reduced cross sections more complicated. An additional complication comes from the fact, that in the model under consideration the heavy (s)neutrino can decay not only into a lepton and a Higgs, but also into a pair of quarks. Expressions for the reduced cross sections obtained here differ from those in [16] due to the use of a Real Intermediate State subtracted propagator of the form discussed in [35].

D.1 Processes mediated by the right–handed neutrinos

To begin with, let us consider Majorana (s)neutrino mediated processes depicted in figure 3.3 which violate lepton number by two units.

Since supersymmetry is broken only softly, the reduced cross sections of the $L+\tilde{H}^u \leftrightarrow \bar{L}+\tilde{H}^{u\dagger}$ and $\tilde{L} + H^u \leftrightarrow \tilde{L}^\dagger + \bar{H}^u$ processes are equal and given by

$$\hat{\sigma}^{(1a)}_{\nu^c}(z) = \hat{\sigma}^{(2a)}_{\nu^c}(z) = \sum_{\eta\bar{\eta}} \frac{\sqrt{a_\eta a_{\bar{\eta}}}}{8\pi z} \left\{ C_a^2 \Lambda^{\eta\bar{\eta}}_{(1)aa} \left[\frac{z^2}{2P_\eta(z) P^*_{\bar{\eta}}(z)} + \frac{z + a_\eta}{a_{\bar{\eta}} - a_\eta} \ln\left(\frac{z + a_\eta}{a_\eta}\right) \right.\right.$$
$$\left.\left. + \frac{z + a_{\bar{\eta}}}{a_\eta - a_{\bar{\eta}}} \ln\left(\frac{z + a_{\bar{\eta}}}{a_{\bar{\eta}}}\right) \right] + 2C_a \mathrm{Re}\left(\frac{\Lambda^{\eta\bar{\eta}}_{(2)aa}}{P_\eta(z)}\right) \left[z - (z + a_{\bar{\eta}}) \ln\left(\frac{z + a_{\bar{\eta}}}{a_{\bar{\eta}}}\right) \right] \right\} \qquad \text{(D.1)}$$

where $a = 11$ and

$$\Lambda^{\eta\bar{\eta}}_{(1)ab} = \sum_{i,m}^{j,n} (\lambda^{\eta im}_a \lambda^{*\bar{\eta} im}_a)(\lambda^{\eta jn}_b \lambda^{*\bar{\eta} jn}_b) \quad \text{and} \quad \Lambda^{\eta\bar{\eta}}_{(2)ab} = \sum_{i,m}^{j,n} (\lambda^{\eta im}_a \lambda^{*\bar{\eta} in}_a)(\lambda^{\eta jn}_b \lambda^{*\bar{\eta} jm}_b) \tag{D.2}$$

have been introduced. The coefficient $C_{11} = 2$ takes into account that the $SU_L(2)$ doublets L and H^u have two components. From the definition (D.2) it follows that the diagonal components $\Lambda^{\eta\eta}_{(1)aa}$ and $\Lambda^{\eta\eta}_{(2)aa}$ are real. It should also be noted, that if there is only one generation of Higgses then $m = n$ and $\Lambda^{\eta\bar{\eta}}_{(1)aa} = \Lambda^{\eta\bar{\eta}}_{(2)aa}$.

The dimensionless s–channel Breit–Wigner propagator is defined as

$$\frac{1}{P_\eta(z)} = \frac{1}{z - a_\eta + i\sqrt{a_\eta c_\eta}} \tag{D.3}$$

In order to avoid double–counting in the Boltzmann equation, the contributions of an on–shell Majorana neutrinos in the s–channel should be subtracted. This is achieved by the use of the Real Intermediate State (RIS) subtracted propagator [35]

$$|D^{-1}_\eta(z)|^2 = |P^{-1}_\eta(z)|^2 - \frac{\pi}{\sqrt{a_\eta c_\eta}} \delta(z - a_\eta) \tag{D.4}$$

Note that $|D^{-1}_\eta(z)|^2$ only occurs in the squared amplitude pertaining to an s–channel diagram. It is thus convenient to introduce

$$\frac{1}{\mathcal{D}_{\eta\bar{\eta}}(z)} = \begin{cases} \dfrac{1}{\mathcal{P}_\eta} - \dfrac{\pi}{\sqrt{a_\eta c_\eta}} \delta(z - a_\eta), & \bar{\eta} = \eta \\ \dfrac{1}{P_\eta(z) P^*_{\bar{\eta}}(z)}, & \bar{\eta} \neq \eta \end{cases} \tag{D.5}$$

where $\mathcal{P}_\eta = (z - a_\eta)^2 + a_\eta c_\eta$ is the inverse Breit–Wigner propagator modulo squared. The RIS subtracted propagator $\tilde{\mathcal{D}}_{\eta\bar{\eta}}(z)$ and the square of the inverse Breit–Wigner propagator $\tilde{\mathcal{P}}_\eta$ of the scalar neutrino are defined analogously.

The interference terms with $\eta \neq \bar{\eta}$ are always small and can safely be neglected. Subtracting the contribution of the real intermediate states we obtain

$$\begin{aligned} \hat{\sigma}^{(1a)}_{\nu^c}(z) = \hat{\sigma}^{(2a)}_{\nu^c}(z) = \sum_\eta \frac{a_\eta}{8\pi z} \Bigg\{ C^2_a \Lambda^{\eta\eta}_{(1)aa} \left[\frac{z^2}{2\mathcal{P}_\eta(z)} + \frac{z}{a_\eta} - \ln\left(\frac{z + a_\eta}{a_\eta} \right) \right] \\ + 2 C_a \Lambda^{\eta\eta}_{(2)aa} \frac{z - a_\eta}{\mathcal{P}_\eta(z)} \left[z - (z + a_\eta) \ln\left(\frac{z + a_\eta}{a_\eta} \right) \right] \Bigg\} - z \frac{C^2_a}{16} \sum_\eta \Lambda^{\eta\eta}_{(1)aa} \sqrt{\frac{a_\eta}{c_\eta}} \delta(z - a_\eta) \end{aligned} \tag{D.6}$$

In the model with $\lambda_8 \neq 0$ there are two analogous processes $d^c + \tilde{D} \leftrightarrow \bar{d}^c + \tilde{D}^\dagger$ and $\tilde{d}^c + D \leftrightarrow \tilde{d}^{c\dagger} + \bar{D}$ whose reduced cross sections differ from (D.6) in λ_{11} replaced with λ_8 and $C_8 = 3$. There are also s–channel processes $L + \tilde{H}^u \leftrightarrow \bar{d}^c + \tilde{D}^\dagger$, $L + \tilde{H}^u \leftrightarrow \tilde{d}^{c\dagger} + \bar{D}$, $\tilde{L} + H^u \leftrightarrow \bar{d}^c + \tilde{D}^\dagger$ and $\tilde{L} + H^u \leftrightarrow \tilde{d}^{c\dagger} + \bar{D}$ with reduced cross sections given by

$$\hat{\sigma}^{(1b)}_N(z) = \hat{\sigma}^{(2b)}_N(z) = \sum_{\eta\bar{\eta}} \frac{\sqrt{a_\eta a_{\bar{\eta}}}}{16\pi z} C_8 C_{11} \Lambda^{\eta\bar{\eta}}_{(1)11,8} \frac{z^2}{\mathcal{D}_{\eta\bar{\eta}}(z)} \tag{D.7}$$

Reduced cross sections of similar t–channel processes $L+\tilde{d}^c \to \bar{D}+\tilde{H}^{u\dagger}$, $H^u+\tilde{d}^c \leftrightarrow \bar{D}+\tilde{L}^\dagger$, $L+\tilde{D} \leftrightarrow \bar{d}^c+\tilde{H}^{u\dagger}$ and $H^u+D \leftrightarrow \tilde{L}^\dagger+\tilde{d}^{c\dagger}$ are given by

$$\hat{\sigma}_N^{(1c)}(z)=\hat{\sigma}_N^{(2c)}(z)=\sum_{\eta\bar{\eta}}\frac{\sqrt{a_\eta a_{\bar{\eta}}}}{8\pi z}C_8C_{11}\Lambda^{\eta\bar{\eta}}_{(1)11,8}\left\{\frac{z+a_\eta}{a_{\bar{\eta}}-a_\eta}\ln\left(\frac{z+a_\eta}{a_\eta}\right)+\frac{z+a_{\bar{\eta}}}{a_\eta-a_{\bar{\eta}}}\ln\left(\frac{z+a_{\bar{\eta}}}{a_{\bar{\eta}}}\right)\right\} \tag{D.8}$$

The reduced cross section of the $L+\tilde{H}^u \leftrightarrow \bar{H}^u+\tilde{L}^\dagger$ process reads

$$\begin{aligned}\hat{\sigma}_{\nu^c}^{(3a)}(z)=\sum_{\eta\bar{\eta}}\frac{\sqrt{a_\eta a_{\bar{\eta}}}}{8\pi z}\Bigg\{&C_a^2\Lambda^{\eta\bar{\eta}}_{(1)aa}\left[\frac{z^2}{2\mathcal{D}_{\eta\bar{\eta}}(z)}+\frac{a_\eta}{a_\eta-a_{\bar{\eta}}}\ln\left(\frac{z+a_\eta}{a_\eta}\right)+\frac{a_{\bar{\eta}}}{a_{\bar{\eta}}-a_\eta}\ln\left(\frac{z+a_{\bar{\eta}}}{a_{\bar{\eta}}}\right)\right]\\&+2C_a\mathrm{Re}\left(\frac{\Lambda^{\eta\bar{\eta}}_{(2)aa}}{P_\eta(z)}\right)\left[z-a_{\bar{\eta}}\ln\left(\frac{z+a_{\bar{\eta}}}{a_{\bar{\eta}}}\right)\right]\Bigg\}\end{aligned} \tag{D.9}$$

where $a=11$. Apart from the similar process $D+\tilde{d}^c \leftrightarrow \bar{d}^c+\tilde{D}^\dagger$ ($a=8$) there are also t–channel processes $\tilde{L}+D \leftrightarrow \tilde{H}^{u\dagger}+\bar{d}^c$ and $L+\tilde{D} \leftrightarrow \bar{H}^u+\tilde{d}^{c\dagger}$ with reduced cross sections given by

$$\hat{\sigma}_N^{(3b)}(z)=\sum_{\eta\bar{\eta}}\frac{\sqrt{a_\eta a_{\bar{\eta}}}}{8\pi z}C_8C_{11}\Lambda^{\eta\bar{\eta}}_{(1)11,8}\left\{\frac{a_\eta}{a_\eta-a_{\bar{\eta}}}\ln\left(\frac{z+a_\eta}{a_\eta}\right)+\frac{a_{\bar{\eta}}}{a_{\bar{\eta}}-a_\eta}\ln\left(\frac{z+a_{\bar{\eta}}}{a_{\bar{\eta}}}\right)\right\} \tag{D.10}$$

The reduced cross sections of the $L+H^u \leftrightarrow \tilde{L}^\dagger+\tilde{H}^{u\dagger}$ ($a=11$) and $D+d^c \leftrightarrow \tilde{D}^\dagger+\tilde{d}^{c\dagger}$ ($a=8$) processes read

$$\begin{aligned}\hat{\sigma}_{\nu^c}^{(4a)}(z)=\sum_{\eta\bar{\eta}}\frac{\sqrt{a_\eta a_{\bar{\eta}}}}{8\pi}\Bigg\{&C_a^2\Lambda^{\eta\bar{\eta}}_{(1)aa}\left[\frac{z}{\tilde{\mathcal{D}}_{\eta\bar{\eta}}(z)}+\frac{1}{a_{\bar{\eta}}-a_\eta}\ln\left(\frac{z+a_\eta}{a_\eta}\right)+\frac{1}{a_\eta-a_{\bar{\eta}}}\ln\left(\frac{z+a_{\bar{\eta}}}{a_{\bar{\eta}}}\right)\right]\\&+2C_a\mathrm{Re}\left(\frac{\Lambda^{\eta\bar{\eta}}_{(2)aa}}{\tilde{P}_\eta(z)}\right)\ln\left(\frac{z+a_{\bar{\eta}}}{a_{\bar{\eta}}}\right)\Bigg\}\end{aligned} \tag{D.11}$$

For the s–channel processes $L+H^u \leftrightarrow \tilde{D}^\dagger+\tilde{d}^{c\dagger}$ and $D+d^c \leftrightarrow \tilde{L}^\dagger+\tilde{H}^{u\dagger}$ we get

$$\hat{\sigma}_N^{(4b)}(z)=\sum_{\eta\bar{\eta}}\frac{\sqrt{a_\eta a_{\bar{\eta}}}}{8\pi}C_8C_{11}\Lambda^{\eta\bar{\eta}}_{(1)11,8}\frac{z}{\tilde{\mathcal{D}}_{\eta\bar{\eta}}(z)} \tag{D.12}$$

whereas the reduced cross sections of the $L+d^c \leftrightarrow \tilde{H}^{u\dagger}+\tilde{D}^\dagger$, $L+D \leftrightarrow \tilde{H}^{u\dagger}+\tilde{d}^{c\dagger}$, $H^u+d^c \leftrightarrow \tilde{L}^\dagger+\tilde{D}^\dagger$, and $H^u+D \leftrightarrow \tilde{L}^\dagger+\tilde{d}^{c\dagger}$ t–channel processes read

$$\hat{\sigma}_N^{(4c)}(z)=\sum_{\eta\bar{\eta}}\frac{\sqrt{a_\eta a_{\bar{\eta}}}}{8\pi}C_8C_{11}\Lambda^{\eta\bar{\eta}}_{(1)11,8}\left\{\frac{1}{a_{\bar{\eta}}-a_\eta}\ln\left(\frac{z+a_\eta}{a_\eta}\right)+\frac{1}{a_\eta-a_{\bar{\eta}}}\ln\left(\frac{z+a_{\bar{\eta}}}{a_{\bar{\eta}}}\right)\right\} \tag{D.13}$$

Making use of the formula for the reduced cross section of $2\to 3$ scattering (C.16) we obtain for the reduced cross section of the $\tilde{L}+\tilde{H}^u \to \tilde{L}^\dagger+\tilde{u}^c+\tilde{Q}$ process

$$\begin{aligned}\hat{\sigma}_{\nu^c}^{(5)}(z)=\sum_{\eta\bar{\eta}}\frac{3\sqrt{a_\eta a_{\bar{\eta}}}}{32\pi^2 z}\Bigg\{&C_a^2\Lambda^{\eta\bar{\eta}}_{(3)ac}\left[\frac{z^2}{2\tilde{\mathcal{D}}_{\eta\bar{\eta}}(z)}+\frac{z+a_\eta}{a_{\bar{\eta}}-a_\eta}\ln\left(\frac{z+a_\eta}{a_\eta}\right)+\frac{z+a_{\bar{\eta}}}{a_\eta-a_{\bar{\eta}}}\ln\left(\frac{z+a_{\bar{\eta}}}{a_{\bar{\eta}}}\right)\right]\\&+2C_a\left(\frac{\Lambda^{\eta\bar{\eta}}_{(4)ac}}{\tilde{P}_\eta(z)}\right)\left[z-(z+a_{\bar{\eta}})\ln\left(\frac{z+a_{\bar{\eta}}}{a_{\bar{\eta}}}\right)\right]\Bigg\}\end{aligned} \tag{D.14}$$

where $a = 11$, $c = 1$ and

$$\Lambda^{\eta\bar{\eta}}_{(3)ac} = \frac{1}{4\pi} \sum_{i,j,k,m,n}^{q,\bar{q}} (\lambda^{\eta ij}_a \lambda^{*\bar{\eta} ij}_a)(\lambda^{\eta kq}_a \lambda^{*\bar{\eta} k\bar{q}}_a)(\lambda^{*mnq}_c \lambda^{mn\bar{q}}_c), \tag{D.15a}$$

$$\Lambda^{\eta\bar{\eta}}_{(4)ac} = \frac{1}{4\pi} \sum_{i,j,k,m,n}^{q,\bar{q}} (\lambda^{\eta ij}_a \lambda^{*\bar{\eta} kj}_a)(\lambda^{\eta kq}_a \lambda^{*\bar{\eta} i\bar{q}}_a)(\lambda^{*mnq}_c \lambda^{mn\bar{q}}_c) \tag{D.15b}$$

have been introduced to shorten the notation. The leading contribution is due to the stop whose Yukawa coupling is of the order of unity. There are also similar processes like, for instance, $\tilde{D} + \tilde{d}^c \leftrightarrow \tilde{D}^\dagger + \tilde{H}^d + \tilde{Q}$ which we neglect, however, assuming smallness of the corresponding Yukawa couplings.

Let us now consider $2 \to 3$ scattering processes depicted in figure 3.4. For the reduced cross section of the $\tilde{Q} + \tilde{u}^c \to \tilde{L} + \tilde{L} + \tilde{H}^u$ scattering we obtain

$$\begin{aligned}\hat{\sigma}^{(6)}_{\nu^c} = \sum_\eta \frac{3}{64\pi^2}\frac{a_\eta}{z}\Bigg\{ & C_a^2 \Lambda^{\eta\eta}_{(3)11,1}\left[\frac{z-a_\eta}{\sqrt{a_\eta \tilde{c}_\eta}}\left(\arctan\left(\frac{z-a_\eta}{\sqrt{a_\eta\tilde{c}_\eta}}\right) + \arctan\left(\sqrt{\frac{a_\eta}{\tilde{c}_\eta}}\right)\right)\right. \\ & \left. - \frac{1}{2}\ln\left(\frac{(z-a_\eta)^2 + a_\eta\tilde{c}_\eta}{a_\eta(a_\eta+\tilde{c}_\eta)}\right)\right] + C_a \Lambda^{\eta\eta}_{(4)11,1}\int_0^z \frac{d\xi}{\tilde{\mathcal{P}}_\eta(\xi)}\left[\frac{\xi-a_\eta}{2}\ln\left(\frac{(z-\xi-a_\eta)^2+a_\eta\tilde{c}_\eta}{a_\eta(a_\eta+\tilde{c}_\eta)}\right)\right. \\ & \left. + \sqrt{a_\eta\tilde{c}_\eta}\left(\arctan\left(\frac{z-\xi-a_\eta}{\sqrt{a_\eta\tilde{c}_\eta}}\right) - \arctan\left(\sqrt{\frac{a_\eta}{\tilde{c}_\eta}}\right)\right)\right]\Bigg\} - \frac{3C_a^2}{64\pi}\Lambda^{\eta\eta}_{(3)11,1}\sqrt{\frac{a_\eta}{\tilde{c}_\eta}}\frac{\Theta(z-a_\eta)}{z}\end{aligned} \tag{D.16}$$

where $\Theta(z-a_\eta) = z - a_\eta$ if $z - a_\eta$ is positive and zero otherwise. For the process $\tilde{L}^\dagger + \tilde{Q} \to \tilde{L} + \tilde{u}^{c\dagger} + \tilde{H}^u$ we obtain

$$\begin{aligned}\hat{\sigma}^{(7)}_{\nu^c} = \frac{3}{64\pi^2}\sum_\eta \frac{a_\eta}{z}\Bigg\{ & C_a^2\Lambda^{\eta\bar{\eta}}_{(3)11,1}\left[-\frac{1}{2}\ln\left(\frac{(z-a_\eta)^2+a_\eta\tilde{c}_\eta}{a_\eta(a_\eta+\tilde{c}_\eta)}\right) + \frac{z}{a_\eta} - \ln\left(\frac{z+a_\eta}{a_\eta}\right)\right. \\ & \left. + \frac{z-a_\eta}{\sqrt{a_\eta\tilde{c}_\eta}}\left(\arctan\left(\frac{z-a_\eta}{\sqrt{a_\eta\tilde{c}_\eta}}\right) + \arctan\left(\sqrt{\frac{a_\eta}{\tilde{c}_\eta}}\right)\right)\right] + 2C_a\Lambda^{\eta\bar{\eta}}_{(4)11,1}\left[-\frac{1}{2}\mathrm{dilog}\left(\frac{z-a_\eta-i\sqrt{a_\eta\tilde{c}_\eta}}{z-i\sqrt{a_\eta\tilde{c}_\eta}}\right)\right. \\ & - \frac{1}{2}\mathrm{dilog}\left(\frac{z-a_\eta+i\sqrt{a_\eta\tilde{c}_\eta}}{z+i\sqrt{a_\eta\tilde{c}_\eta}}\right) + \frac{1}{2}\mathrm{dilog}\left(\frac{a_\eta+i\sqrt{a_\eta\tilde{c}_\eta}}{-z+i\sqrt{a_\eta\tilde{c}_\eta}}\right) + \frac{1}{2}\mathrm{dilog}\left(\frac{-a_\eta+i\sqrt{a_\eta\tilde{c}_\eta}}{z+i\sqrt{a_\eta\tilde{c}_\eta}}\right) \\ & \left. - \frac{1}{2}\ln\left(\frac{z+a_\eta}{a_\eta}\right)\ln\left(\frac{z^2+a_\eta\tilde{c}_\eta}{a_\eta^2+a_\eta\tilde{c}_\eta}\right)\right]\Bigg\} - \frac{3C_a^2}{64\pi}\Lambda^{\eta\eta}_{(3)11,1}\sqrt{\frac{a_\eta}{\tilde{c}_\eta}}\frac{\Theta(z-a_\eta)}{z}\end{aligned} \tag{D.17, D.18}$$

Let us now consider the t–channel and u–channel lepton number violating processes depicted in figure 3.5.

For the processes $L + L \leftrightarrow \tilde{H}^{u\dagger} + \tilde{H}^{u\dagger}$ and $\tilde{L} + \tilde{L} \leftrightarrow \bar{H}^u + \bar{H}^u$ ($a = 11$) as well as for the similar processes $D + D \leftrightarrow \tilde{d}^{c\dagger} + \tilde{d}^{c\dagger}$ and $\tilde{D} + \tilde{D} \leftrightarrow \bar{d}^c + \bar{d}^c$ ($a = 8$) we get

$$\begin{aligned}\hat{\sigma}^{(8)}_{\nu^c} = \hat{\sigma}^{(9)}_{\nu^c} = \sum_{\eta\bar{\eta}}\frac{\sqrt{a_\eta a_{\bar{\eta}}}}{8\pi}\Bigg\{ & C_a^2\Lambda^{\eta\bar{\eta}}_{(1)aa}\left[\frac{1}{a_\eta - a_{\bar{\eta}}}\ln\left(\frac{z+a_{\bar{\eta}}}{a_{\bar{\eta}}}\right) + \frac{1}{a_{\bar{\eta}}-a_\eta}\ln\left(\frac{z+a_\eta}{a_\eta}\right)\right] \\ & + C_a\mathrm{Re}\left(\Lambda^{\eta\bar{\eta}}_{(2)aa}\right)\frac{1}{z+a_\eta+a_{\bar{\eta}}}\left[\ln\left(\frac{z+a_\eta}{a_\eta}\right) + \ln\left(\frac{z+a_{\bar{\eta}}}{a_{\bar{\eta}}}\right)\right]\Bigg\}\end{aligned} \tag{D.19}$$

The reduced cross sections of the $L+\tilde{L} \leftrightarrow \bar{H}^u + \tilde{H}^{u\dagger}$ ($a=11$) and $D+\tilde{D} \leftrightarrow \bar{d}^c + \tilde{d}^{c\dagger}$ ($a=8$) processes are given by

$$\hat{\sigma}^{(10)}_{\nu^c} = \sum_{\eta\bar{\eta}} \frac{\sqrt{a_\eta a_{\bar{\eta}}}}{8\pi} \left\{ C_a^2 \Lambda^{\eta\bar{\eta}}_{(1)aa} \left[\frac{1}{a_\eta - a_{\bar{\eta}}} \ln\left(\frac{z+a_{\bar{\eta}}}{a_{\bar{\eta}}}\right) + \frac{1}{a_{\bar{\eta}} - a_\eta} \ln\left(\frac{z+a_\eta}{a_\eta}\right) \right] \right.$$
$$\left. - C_a \mathrm{Re}\left(\Lambda^{\eta\bar{\eta}}_{(2)aa}\right) \frac{1}{z+a_\eta+a_{\bar{\eta}}} \left[\ln\left(\frac{z+a_\eta}{a_\eta}\right) + \ln\left(\frac{z+a_{\bar{\eta}}}{a_{\bar{\eta}}}\right) \right] \right\} \tag{D.20}$$

For the reduced cross section of the $\tilde{H}^u + \tilde{Q}^\dagger \to \tilde{L}^\dagger + \tilde{L}^\dagger + \tilde{u}^c$ process we get

$$\hat{\sigma}^{(11)}_{\nu^c} = \sum_{\eta\bar{\eta}} \frac{3}{32\pi^2} \frac{\sqrt{a_\eta a_{\bar{\eta}}}}{z} \left\{ C_a^2 \Lambda^{\eta\bar{\eta}}_{(3)11,1} \left[\frac{z+a_\eta}{a_{\bar{\eta}} - a_\eta} \ln\left(\frac{z+a_\eta}{a_\eta}\right) + \frac{z+a_{\bar{\eta}}}{a_\eta - a_{\bar{\eta}}} \ln\left(\frac{z+a_{\bar{\eta}}}{a_{\bar{\eta}}}\right) \right] \right. \tag{D.21}$$
$$+ \frac{C_a}{2} \mathrm{Re}\left(\Lambda^{\eta\bar{\eta}}_{(4)11,1}\right) \left[\ln\left(\frac{z+a_\eta}{a_\eta}\right) \ln\left(\frac{z+a_\eta+a_{\bar{\eta}}}{a_{\bar{\eta}}}\right) + \ln\left(\frac{z+a_{\bar{\eta}}}{a_{\bar{\eta}}}\right) \ln\left(\frac{z+a_\eta+a_{\bar{\eta}}}{a_\eta}\right) \right.$$
$$\left. \left. - \mathrm{dilog}\left(\frac{a_\eta}{z+a_\eta+a_{\bar{\eta}}}\right) - \mathrm{dilog}\left(\frac{a_{\bar{\eta}}}{z+a_\eta+a_{\bar{\eta}}}\right) + \mathrm{dilog}\left(\frac{z+a_\eta}{z+a_\eta+a_{\bar{\eta}}}\right) + \mathrm{dilog}\left(\frac{z+a_{\bar{\eta}}}{z+a_\eta+a_{\bar{\eta}}}\right) \right] \right\}$$

The $2 \to 3$ process $\tilde{L} + \tilde{L} \to \tilde{H}^{u\dagger} + \tilde{Q} + \tilde{u}^c$ ($a=11$) gives

$$\hat{\sigma}^{(12)}_{\nu^c} = \sum_{\eta\bar{\eta}} \frac{3}{64\pi^2} \frac{\sqrt{a_\eta a_{\bar{\eta}}}}{z} \left\{ C_a^2 \Lambda^{\eta\bar{\eta}}_{(3)11,1} \left[\frac{z+a_\eta}{a_{\bar{\eta}} - a_\eta} \ln\left(\frac{z+a_\eta}{a_\eta}\right) + \frac{z+a_{\bar{\eta}}}{a_\eta - a_{\bar{\eta}}} \ln\left(\frac{z+a_{\bar{\eta}}}{a_{\bar{\eta}}}\right) \right] \right.$$
$$+ 2C_a \mathrm{Re}\left(\Lambda^{\eta\bar{\eta}}_{(4)11,1}\right) \left[\ln\left(\frac{z+a_\eta}{a_\eta}\right) \ln\left(\frac{z+a_\eta+a_{\bar{\eta}}}{a_{\bar{\eta}}}\right) + \ln\left(\frac{z+a_{\bar{\eta}}}{a_{\bar{\eta}}}\right) \ln\left(\frac{z+a_\eta+a_{\bar{\eta}}}{a_\eta}\right) \right.$$
$$\left. \left. + \mathrm{dilog}\left(\frac{z+a_\eta+a_{\bar{\eta}}}{a_{\bar{\eta}}}\right) + \mathrm{dilog}\left(\frac{z+a_\eta+a_{\bar{\eta}}}{a_\eta}\right) + \frac{\pi^2}{6} + \frac{1}{2} \ln\left(\frac{a_\eta}{a_{\bar{\eta}}}\right)^2 \right] \right\} \tag{D.22}$$

D.2 Scattering off (s)top

Scattering processes mediated by the Higgs or its scalar superpartner (see figure 3.7) violate lepton number by one unit and reduce the number of the heavy (s)neutrinos. The corresponding reduced cross sections read

$$\hat{\sigma}^{(0)}_t = \frac{3}{2} \Lambda^\eta_{(5)11,1} \frac{z^2 - a_\eta^2}{(z-a_h)^2} \tag{D.23}$$

$$\hat{\sigma}^{(1)}_t = 3\Lambda^\eta_{(5)11,1} \frac{z-a_\eta}{z} \left[-\frac{2z - a_\eta + 2a_h}{z - a_\eta + a_h} + \frac{z+2a_h}{z-a_\eta} \ln\left(\frac{z-a_\eta+a_h}{a_h}\right) \right] \tag{D.24}$$

$$\hat{\sigma}^{(2)}_t = 3\Lambda^\eta_{(5)11,1} \frac{z-a_\eta}{z} \left[-\frac{z-a_\eta}{z-a_\eta+a_h} + \ln\left(\frac{z-a_\eta+a_h}{a_h}\right) \right] \tag{D.25}$$

$$\hat{\sigma}^{(3)}_t = 3\Lambda^\eta_{(5)11,1} \left(\frac{z-a_\eta}{z-a_h}\right)^2 \tag{D.26}$$

$$\hat{\sigma}^{(4)}_t = 3\Lambda^\eta_{(5)11,1} \frac{z-a_\eta}{z} \left[\frac{z - 2a_\eta + 2a_h}{z-a_\eta+a_h} + \frac{a_\eta - 2a_h}{z-a_\eta} \ln\left(\frac{z-a_\eta+a_h}{a_h}\right) \right] \tag{D.27}$$

where

$$\Lambda^\eta_{(5)a,b} = \frac{1}{4\pi} \sum_{i,m,n}^{k,\bar{k}} (\lambda_a^{\eta ik} \lambda_a^{*\eta i\bar{k}})(\lambda_b^{*nmk} \lambda_b^{nm\bar{k}}) \tag{D.28}$$

To regularize an infrared divergence in the t–channel diagrams an effective Higgs mass was introduced

$$a_h = \left(\frac{\mu}{M_1}\right)^2 \tag{D.29}$$

In the numerical computation the Higgs mass has been set to $\mu = 800$ GeV.

For the reduced cross sections of the similar processes involving a scalar neutrino we obtain

$$\hat{\sigma}_t^{(5)} = \frac{3}{2}\Lambda^{\eta}_{(5)11,1}\left(\frac{z-a_\eta}{z-a_h}\right)^2 \tag{D.30}$$

$$\hat{\sigma}_t^{(6)} = 3\Lambda^{\eta}_{(5)11,1}\frac{z-a_\eta}{z}\left[-2+\frac{z-a_\eta+2a_h}{z-a_\eta}\ln\left(\frac{z-a_\eta+a_h}{a_h}\right)\right] \tag{D.31}$$

$$\hat{\sigma}_t^{(7)} = 3\Lambda^{\eta}_{(5)11,1}\left[-\frac{z-a_\eta}{z-a_\eta+a_h}+\ln\left(\frac{z-a_\eta+a_h}{a_h}\right)\right] \tag{D.32}$$

$$\hat{\sigma}_t^{(8)} = 3\Lambda^{\eta}_{(5)11,1}\frac{a_\eta(z-a_\eta)}{(z-a_h)^2} \tag{D.33}$$

$$\hat{\sigma}_t^{(9)} = 3\Lambda^{\eta}_{(5)11,1}\frac{a_\eta}{z}\left[-\frac{z-a_\eta}{z-a_\eta+a_h}+\ln\left(\frac{z-a_\eta+a_h}{a_h}\right)\right] \tag{D.34}$$

D.3 Neutrino pair creation and annihilation

The reduced cross sections of the processes $\nu^c+\nu^c \leftrightarrow \tilde{L}+\tilde{L}^\dagger$ $(a=11)$ and $\nu^c+\nu^c \leftrightarrow \tilde{d}^c+\tilde{d}^{c\dagger}$ $(a=8)$, depicted in figure 3.8, which conserve lepton and baryon numbers but reduce the number of the heavy neutrinos read

$$\hat{\sigma}^{(1)}_{\nu^c\nu^c} = \frac{C_a}{8\pi z}\left\{\Lambda^{\eta\bar{\eta}}_{(6)aa}\left[-2\sqrt{\lambda_{\eta\bar{\eta}}}+zL_{\eta\bar{\eta}}\right]-2\mathrm{Re}\left(\Lambda^{\eta\bar{\eta}}_{(7)aa}\right)\frac{\sqrt{a_\eta a_{\bar{\eta}}}(a_\eta+a_{\bar{\eta}})}{z-a_\eta-a_{\bar{\eta}}}L_{\eta\bar{\eta}}\right\} \tag{D.35}$$

where

$$\Lambda^{\eta\bar{\eta}}_{(6)ab} = \sum_{ij}^{n\bar{n}}(\lambda^{\eta in}_a\lambda^{*\eta i\bar{n}}_a)(\lambda^{*\bar{\eta}jn}_b\lambda^{\bar{\eta}j\bar{n}}_b), \quad \Lambda^{\eta\bar{\eta}}_{(7)ab} = \sum_{ij}^{n\bar{n}}(\lambda^{\eta in}_a\lambda^{\eta j\bar{n}}_a)(\lambda^{*\bar{\eta}jn}_b\lambda^{*\bar{\eta}i\bar{n}}_b) \tag{D.36}$$

and

$$\lambda_{\eta\bar{\eta}} = [z-(\sqrt{a_\eta}-\sqrt{a_{\bar{\eta}}})^2][z-(\sqrt{a_\eta}+\sqrt{a}_{\bar{\eta}})^2], \quad L_{\eta\bar{\eta}} = \ln\left(\frac{z-a_\eta-a_{\bar{\eta}}+\sqrt{\lambda_{\eta\bar{\eta}}}}{z-a_\eta-a_{\bar{\eta}}-\sqrt{\lambda_{\eta\bar{\eta}}}}\right) \tag{D.37}$$

have been introduced.

The reduced cross sections of the similar processes $\nu^c+\nu^c \leftrightarrow L+\bar{L}$ $(a=11)$ and $\nu^c+\nu^c \leftrightarrow d^c+\bar{d}^c$ $(a=8)$ read

$$\sigma^{(2)}_{\nu^c\nu^c} = \frac{C_a}{8\pi z}\left\{\Lambda^{\eta\bar{\eta}}_{(6)aa}\left[2\sqrt{\lambda_{\eta\bar{\eta}}}+(a_\eta+a_{\bar{\eta}})L_{\eta\bar{\eta}}\right]-2\mathrm{Re}\left(\Lambda^{\eta\bar{\eta}}_{(7)aa}\right)\frac{z\sqrt{a_\eta a_{\bar{\eta}}}}{z-a_\eta-a_{\bar{\eta}}}L_{\eta\bar{\eta}}\right\} \tag{D.38}$$

The reduced cross sections $\sigma^{(3)}_{\nu^c\nu^c}$ and $\sigma^{(4)}_{\nu^c\nu^c}$ of the processes $\nu^c+\nu^c \leftrightarrow \tilde{H}^u+\tilde{H}^{u\dagger}$ and $\nu^c+\nu^c \leftrightarrow \tilde{D}^u+\tilde{D}^\dagger$ and the processes $\nu^c+\nu^c \leftrightarrow H^u+\bar{H}^u$ and $\nu^c+\nu^c \leftrightarrow \tilde{D}^u+\tilde{D}^\dagger$ obviously differ from

(D.35) and (D.38) only in $\Lambda_{(6)}$ replaced by $\Lambda_{(8)}$ and $\Lambda_{(7)}$ replaced by $\Lambda_{(9)}$, where

$$\Lambda^{\eta\bar{\eta}}_{(8)ab} = \sum_{ij}^{n\bar{n}} (\lambda^{\eta ni}_a \lambda^{*\eta\bar{n}i}_a)(\lambda^{*\bar{\eta}nj}_b \lambda^{\bar{\eta}\bar{n}j}_b), \quad \Lambda^{\eta\bar{\eta}}_{(9)ab} = \sum_{ij}^{n\bar{n}} (\lambda^{\eta ni}_a \lambda^{\eta\bar{n}j}_a)(\lambda^{*\bar{\eta}nj}_b \lambda^{*\bar{\eta}\bar{n}i}_b) \tag{D.39}$$

The reduced cross sections of the processes involving one neutrino and one scalar neutrino $\tilde{\nu}^c + \nu^c \leftrightarrow \bar{L} + \tilde{L}$ $(a = 11)$ and $\tilde{\nu}^c + \nu^c \leftrightarrow \bar{d}^c + \tilde{d}^c$ $(a = 8)$ are given by

$$\hat{\sigma}^{(1)}_{\nu^c\tilde{\nu}^c} = \frac{C_a}{8\pi z} \left\{ \Lambda^{\eta\bar{\eta}}_{(6)aa}(z - a_\eta + a_{\bar{\eta}}) L_{\eta\bar{\eta}} - 2\mathrm{Re}\left(\Lambda^{\eta\bar{\eta}}_{(7)aa}\right) \sqrt{a_\eta a_{\bar{\eta}}} \frac{z - a_\eta + a_{\bar{\eta}}}{z - a_\eta - a_{\bar{\eta}}} L_{\eta\bar{\eta}} \right\} \tag{D.40}$$

whereas the reduced cross sections $\hat{\sigma}^{(2)}_{\nu^c\tilde{\nu}^c}$ of the $\tilde{\nu}^{c\dagger} + \nu^c \leftrightarrow \bar{H}^u + \tilde{H}^u$ $(a = 11)$ and $\tilde{\nu}^{c\dagger} + \nu^c \leftrightarrow \bar{D} + \tilde{D}$ $(a = 8)$ processes differ from (D.40) only in $\Lambda_{(6)}$ replaced with $\Lambda_{(8)}$ and $\Lambda_{(7)}$ replaced with $\Lambda_{(9)}$.

For the annihilation of scalar neutrinos into two leptons $\tilde{\nu}^c + \tilde{\nu}^{c\dagger} \leftrightarrow L + \bar{L}$ $(a = 11)$ or quarks $\tilde{\nu}^c + \tilde{\nu}^{c\dagger} \leftrightarrow d^c + \bar{d}^c$ $(a = 8)$ one has

$$\hat{\sigma}^{(1)}_{\tilde{\nu}^c\tilde{\nu}^c} = \frac{C_a}{8\pi z} \Lambda^{\eta\bar{\eta}}_{(6)aa} \left\{ -2\sqrt{\lambda_{\eta\bar{\eta}}} + (z - a_\eta - a_{\bar{\eta}}) L_{\eta\bar{\eta}} \right\} \tag{D.41}$$

whereas the reduced cross sections $\hat{\sigma}^{(3)}_{\tilde{\nu}^c\tilde{\nu}^c}$ of the processes $\tilde{\nu}^c + \tilde{\nu}^c \leftrightarrow H^u + \bar{H}^u$ $(a = 11)$ and $\tilde{\nu}^c + \tilde{\nu}^c \leftrightarrow D + \bar{D}$ $(a = 8)$ differ from (D.41) only in $\Lambda^{\eta\bar{\eta}}_{(6)aa}$ replaced with $\Lambda^{\eta\bar{\eta}}_{(8)aa}$.

Finally there are processes of annihilation of the right–handed scalar neutrinos into two scalar leptons $\tilde{\nu}^c + \tilde{\nu}^{c\dagger} \leftrightarrow \tilde{L} + \tilde{L}^\dagger$ $(a = 11)$ or squarks $\tilde{\nu}^c + \tilde{\nu}^{c\dagger} \leftrightarrow \tilde{d}^c + \tilde{d}^{c\dagger}$ $(a = 8)$, whose reduced cross sections are given by

$$\sigma^{(2)}_{\tilde{\nu}^c\tilde{\nu}^c} = \frac{C_a}{4\pi z} \left\{ \Lambda^{\eta\bar{\eta}}_{(6)aa} \sqrt{\lambda_{\eta\bar{\eta}}} - \mathrm{Re}\left(\Lambda^{\eta\bar{\eta}}_{(7)aa}\right) \sqrt{a_\eta a_{\bar{\eta}}} L_{\eta\bar{\eta}} \right\} \tag{D.42}$$

whereas the reduced cross sections $\hat{\sigma}^{(4)}_{\tilde{\nu}^c\tilde{\nu}^c}$ of the $\tilde{\nu}^c + \tilde{\nu}^{c\dagger} \leftrightarrow \tilde{H}^u + \tilde{H}^{u\dagger}$ $(a = 11)$ and $\tilde{\nu}^c + \tilde{\nu}^{c\dagger} \leftrightarrow \tilde{D} + \tilde{D}^\dagger$ $(a = 8)$ processes differ from (D.42) only in $\Lambda_{(6)}$ replaced with $\Lambda_{(8)}$ and $\Lambda_{(7)}$ replaced with $\Lambda_{(9)}$.

Appendix E

Kinematics of $2 \to 3$ scattering

We consider here the kinematics of the $\nu(k_1) + N(p_1) \to \ell(k_2) + N(p_2) + \pi(p)$ process, where ℓ stands either for the electron e (charged current scattering) or the neutrino ν (neutral current scattering). The latter one can safely be considered as massless here.

The commonly used kinematic variables are the square of the center of mass energy $s = (k_1 + p_1)^2$, the square of the momentum–transfer in the hadronic system $t = (p_2 - p_1)^2$, the square of the momentum transfer to the final lepton $Q^2 = -q^2 = -(k_1 - k_2)^2$ and the invariant mass of the pion–nucleus pair $W^2 = (p + p_1)^2$. The minimal value of the latter one is obviously just a sum of the nucleus and pion masses squared.

$$W^2_{min} = (M_N + m_\pi)^2 \tag{E.1}$$

At a given value of the center of mass energy s momentum transfer square Q^2 varies in the range

$$Q^2_{\rm min/max} = \frac{(s - M_N^2)}{2s}\left[s \mp w\left(s, m_\ell^2, W^2_{min}\right)\right] - \frac{1}{2}\left[W^2_{min} + m_\ell^2 - \frac{M_N^2}{s}(W^2_{min} - m_\ell^2)\right] \tag{E.2}$$

where m_ℓ is the mass of the final lepton. In the rest frame of the initial nucleus the energy transfer to the final lepton $\nu = k_1^0 - k_2^0 \equiv E_1 - E_2$ varies at fixed values of s and Q^2 in the range

$$\nu_{\rm min/max} = \frac{W^2_{\rm min/max}(Q^2) + Q^2 - M_N^2}{2M_N} \tag{E.3}$$

where W^2_{min} is defined in (E.1) whereas $W^2_{max}(Q^2)$ is given by

$$W^2_{max}(Q^2) = \frac{\left(s - M_N^2\right)^2\left(s - m_\ell^2\right)^2 - \left[2sQ^2 - s\left(s - M_N^2\right) + m_\ell^2\left(s + M_N^2\right)\right]^2}{4s\left(s - M_N^2\right)\left(Q^2 + m_\ell^2\right)} \tag{E.4}$$

Finally for fixed values of Q^2 and ν the kinematically allowed range for the square of the momentum transfer in the hadronic system t

$$t_{\rm min/max} = \frac{(Q^2 + m_\pi^2)^2 - \left[w(W^2, -Q^2, M_N^2) \mp w(W^2, m_\pi^2, M_N^2)\right]^2}{4W^2} \tag{E.5}$$

where according to equation (E.3) $W^2 = M_N^2 - Q^2 + 2M_N\nu$.

The other two commonly used variables are $y = \frac{\nu}{E_1}$ and $x = \frac{Q^2}{2M_N\nu}$. The kinematic range for the former one is trivially obtained from (E.3)

$$y_{\mathrm{min/max}} = \frac{W^2_{\mathrm{min/max}}(Q^2) + Q^2 - M_N^2}{s - M_N^2} \tag{E.6}$$

Combining equations (E.1), (E.4) and (E.2) we find for the kinematically allowed range for the latter one

$$x_{min/max} = \frac{Q^2_{min/max}}{Q^2_{min/max} + W^2_{max/min}(Q^2) - M_N^2} \tag{E.7}$$

Bibliography

[1] WMAP, D. N. Spergel *et al.*, Astrophys. J. Suppl. **148**, 175 (2003), [astro-ph/0302209].

[2] A. H. Guth, Phys. Rev. **D23**, 347 (1981).

[3] A. D. Linde, Phys. Lett. **B129**, 177 (1983).

[4] E. W. Kolb and M. S. Turner, Redwood City, USA: Addison-Wesley (1990) 547 p. (Frontiers in physics, 69).

[5] A. D. Sakharov, JETP Letters **5**, 24 (1967).

[6] I. Affleck and M. Dine, Nucl. Phys. **B249**, 361 (1985).

[7] G. 't Hooft, Phys. Rev. Lett. **37**, 8 (1976).

[8] G. 't Hooft, Phys. Rev. **D14**, 3432 (1976).

[9] M. Fukugita and T. Yanagida, Phys. Lett. **B174**, 45 (1986).

[10] M. Flanz, E. A. Paschos and U. Sarkar, Phys. Lett. **B345**, 248 (1995), [hep-ph/9411366].

[11] E. Ma, Phys. Rev. **D36**, 274 (1987).

[12] E. Ma, Phys. Lett. **B380**, 286 (1996), [hep-ph/9507348].

[13] E. A. Paschos, U. Sarkar and H. So, Phys. Rev. **D52**, 1701 (1995), [hep-ph/9504359].

[14] V. D. Barger, N. Deshpande, R. J. N. Phillips and K. Whisnant, Phys. Rev. **D33**, 1912 (1986).

[15] B. A. Campbell, S. Davidson and K. A. Olive, Nucl. Phys. **B399**, 111 (1993), [hep-ph/9302223].

[16] M. Plumacher, Nucl. Phys. **B530**, 207 (1998), [hep-ph/9704231].

[17] G. L. Fogli, E. Lisi, A. Marrone and D. Montanino, Phys. Rev. **D67**, 093006 (2003), [hep-ph/0303064].

[18] K2K, M. H. Ahn *et al.*, Phys. Rev. **D74**, 072003 (2006), [hep-ex/0606032].

[19] SNO, Q. R. Ahmad *et al.*, Phys. Rev. Lett. **89**, 011301 (2002), [nucl-ex/0204008].

[20] SNO, Q. R. Ahmad *et al.*, Phys. Rev. Lett. **89**, 011302 (2002), [nucl-ex/0204009].

[21] J. N. Bahcall, M. C. Gonzalez-Garcia and C. Pena-Garay, JHEP **0108**, 014 (2001), [hep-ph/0106258].

[22] J. N. Bahcall, M. C. Gonzalez-Garcia and C. Pena-Garay, JHEP **0207**, 054 (2002), [hep-ph/0204314].

[23] M. Maltoni, T. Schwetz, M. A. Tortola and J. W. F. Valle, Phys. Rev. **D68**, 113010 (2003), [hep-ph/0309130].

[24] K2K, M. Hasegawa *et al.*, Phys. Rev. Lett. **95**, 252301 (2005), [hep-ex/0506008].

[25] S. L. Adler, Phys. Rev. **135**, B963 (1964).

[26] V. A. Rubakov and M. E. Shaposhnikov, Usp. Fiz. Nauk **166**, 493 (1996), [hep-ph/9603208].

[27] G. Baym and L. Kadanoff, Quantum Statistical Mechanics (Benjamin, New York, 1962).

[28] M. Lindner and M. M. Muller, Phys. Rev. **D73**, 125002 (2006), [hep-ph/0512147].

[29] S. Dodelson, Modern Cosmology (Academic Press, Amsterdam, 2004).

[30] A. Liddle and D. Lyth, Cosmological inflation and large-scale structure (Cambridge University Press, Cambridge, 2000).

[31] M. Landau and E. Lifshitz, The classical theory of fields (Pergamon Press, 1962).

[32] V. F. Mukhanov, H. A. Feldman and R. H. Brandenberger, Phys. Rept. **215**, 203 (1992).

[33] C.-P. Ma and E. Bertschinger, Astrophys. J. **455**, 7 (1995), [astro-ph/9506072].

[34] M. Flanz and E. A. Paschos, Phys. Rev. **D58**, 113009 (1998), [hep-ph/9805427].

[35] A. Pilaftsis and T. E. J. Underwood, Nucl. Phys. **B692**, 303 (2004), [hep-ph/0309342].

[36] W. Buchmuller, P. Di Bari and M. Plumacher, Nucl. Phys. **B643**, 367 (2002), [hep-ph/0205349].

[37] L. Bento and F. C. Santos, Phys. Rev. **D71**, 096001 (2005), [hep-ph/0411023].

[38] E. Roulet, L. Covi and F. Vissani, Phys. Lett. **B424**, 101 (1998), [hep-ph/9712468].

[39] S. Weinberg, Gravitation and Cosmology (Wiley, New York, 1972).

[40] B. Bednarz, Phys. Rev. **D31**, 2674 (1985).

[41] V. Mukhanov, Physical foundations of Cosmology (Cambridge University Press, 2005).

[42] C. G. Callan, R. Dashen and D. J. Gross, Phys. Rev. D **17**, 2717 (1978).

[43] V. A. Kuzmin, V. A. Rubakov and M. E. Shaposhnikov, Phys. Lett. **B155**, 36 (1985).

[44] F. R. Klinkhamer and N. S. Manton, Phys. Rev. **D30**, 2212 (1984).

[45] P. Arnold and L. McLerran, Phys. Rev. D **36**, 581 (1987).

[46] S. Y. Khlebnikov and M. E. Shaposhnikov, Nucl. Phys. **B308**, 885 (1988).

[47] J. A. Harvey and M. S. Turner, Phys. Rev. **D42**, 3344 (1990).

[48] H. K. Dreiner and G. G. Ross, Nucl. Phys. **B410**, 188 (1993), [hep-ph/9207221].

[49] K. Kikkawa, B. Sakita, M. A. Virasoro and S. A. Klein, Phys. Rev. **D1**, 3258 (1970).

[50] S. Fubini, D. Gordon and G. Veneziano, Phys. Lett. **B29**, 679 (1969).

[51] C. S. Hsue, B. Sakita and M. A. Virasoro, Phys. Rev. **D2**, 2857 (1970).

[52] J.-L. Gervais and B. Sakita, Nucl. Phys. **B34**, 632 (1971).

[53] M. Kaku, Introduction to Superstrings and M–theory (Springer, New York, 1999).

[54] E. Witten, Nucl. Phys. **B258**, 75 (1985).

[55] T. Matsuoka and D. Suematsu, Prog. Theor. Phys. **76**, 886 (1986).

[56] R. Slansky, Phys. Rept. **79**, 1 (1981).

[57] J. C. Pati and A. Salam, Two Lectures presented at Int. Neutrino Conf., Aachen, West Germany, Jun 8-12, 1976.

[58] T. Kobayashi, S. Raby and R.-J. Zhang, Nucl. Phys. **B704**, 3 (2005), [hep-ph/0409098].

[59] H. Georgi and S. L. Glashow, Phys. Rev. Lett. **32**, 438 (1974).

[60] D. London and J. L. Rosner, Phys. Rev. **D34**, 1530 (1986).

[61] E. Dynkin, Am. Math. Soc. Trans., Ser. 2 **6**, 245 (1957).

[62] G. W. Anderson and T. Blazek, J. Math. Phys. **41**, 4808 (2000), [hep-ph/9912365].

[63] G. W. Anderson and T. Blazek, hep-ph/0101349.

[64] Y. Hosotani, Phys. Lett. **B126**, 309 (1983).

[65] T. Matsuoka and D. Suematsu, Nucl. Phys. **B274**, 106 (1986).

[66] A. S. Joshipura, E. A. Paschos and W. Rodejohann, Nucl. Phys. **B611**, 227 (2001), [hep-ph/0104228].

[67] M. Plumacher, hep-ph/9807557.

[68] M. Dine, V. Kaplunovsky, M. L. Mangano, C. Nappi and N. Seiberg, Nucl. Phys. **B259**, 549 (1985).

[69] C. A. Lutken and G. G. Ross, Phys. Lett. **B214**, 357 (1988).

[70] T. Hambye, E. Ma, M. Raidal and U. Sarkar, Phys. Lett. **B512**, 373 (2001), [hep-ph/0011197].

[71] E. Ma, Phys. Rev. Lett. **60**, 1363 (1988).

[72] M. Flanz, E. A. Paschos, U. Sarkar and J. Weiss, Phys. Lett. **B389**, 693 (1996), [hep-ph/9607310].

[73] M. A. Luty, Phys. Rev. **D45**, 455 (1992).

[74] E. I. Gates and K. L. Kowalski, Phys. Rev. **D37**, 938 (1988).

[75] E. A. Paschos, Phys. Rev. D **15**, 1966 (1977).

[76] H. Faissner *et al.*, Phys. Lett. **B125**, 230 (1983).

[77] WA59, P. Marage *et al.*, Phys. Lett. **B140**, 137 (1984).

[78] E. Isiksal, D. Rein and J. G. Morfin (Gargamelle), Phys. Rev. Lett. **52**, 1096 (1984).

[79] BEBC WA59, P. Marage *et al.*, Z. Phys. **C31**, 191 (1986).

[80] SKAT, H. J. Grabosch *et al.*, Zeit. Phys. **C31**, 203 (1986).

[81] BEBC WA59, P. P. Allport *et al.*, Z. Phys. **C43**, 523 (1989).

[82] E632, S. Willocq *et al.*, Phys. Rev. **D47**, 2661 (1993).

[83] CHARM-II, P. Vilain *et al.*, Phys. Lett. **B313**, 267 (1993).

[84] D. Rein and L. M. Sehgal, Nucl. Phys. **B223**, 29 (1983).

[85] B. Z. Kopeliovich, Nucl. Phys. Proc. Suppl. **139**, 219 (2005), [hep-ph/0409079].

[86] J. D. Bjorken and E. A. Paschos, Phys. Rev. **D1**, 3151 (1970).

[87] M. L. Goldberger and S. B. Treiman, Phys. Rev. **110**, 1178 (1958).

[88] B. Krusche, Prepared for 32nd International Workshop on Gross Properties of Nuclei and Nuclear Excitation: Probing Nuclei and Nucleons with Electrons and Photons (Hirschegg 2004), Hirschegg, Austria, 11-17 Jan 2004.

[89] CERN-IPN(Orsay), F. Binon *et al.*, Nucl. Phys. **B17**, 168 (1970).

[90] CERN-IPN(Orsay), F. Binon *et al.*, Nucl. Phys. **B33**, 42 (1971).

[91] G. Kahrimanis *et al.*, Phys. Rev. **C55**, 2533 (1997), [nucl-ex/9702003].

[92] M. L. Scott *et al.*, Phys. Rev. Lett. **28**, 1209 (1972).

[93] J. L. Raaf, PhD thesis, (MiniBoone) Fermilab-Thesis-2005-20, 2005, the reported result is preliminary.

[94] CB-ELSA, O. Bartholomy *et al.*, Phys. Rev. Lett. **94**, 012003 (2005), [hep-ex/0407022].

[95] W. T. Meyer *et al.*, Phys. Rev. Lett. **28**, 1344 (1972).

[96] J. Sakurai, *Currents and Mesons* (University of Chicago press, 1969).

[97] J. Ballam *et al.*, Phys. Rev. Lett. **21**, 934 (1968).

[98] M. Guidal, J. M. Laget and M. Vanderhaeghen, Nucl. Phys. **A627**, 645 (1997).

[99] R. Anderson *et al.*, Phys. Rev. D **1**, 27 (1970).

[100] ZEUS, J. Breitweg *et al.*, Eur. Phys. J. **C12**, 393 (2000), [hep-ex/9908026].

[101] ZEUS, S. Chekanov *et al.*, Nucl. Phys. **B718**, 3 (2005), [hep-ex/0504010].

[102] A. Denner, Fortschr. Phys. **41**, 307 (1993).

[103] G. 't Hooft and M. J. G. Veltman, Nucl. Phys. **B153**, 365 (1979).

[104] J. Wess and J. Bagger, Supersymmetry and Supergravity (Princeton University Press, Princeton, New Jersey, 1983).

Acknowledgments

I would like to thank my supervisor, Professor E. A. Paschos, who inspired me to carry out this investigation, for continuous support and a close and fruitful collaboration.

I am grateful to Deutsche Forschungsgemeinschaft for financial support in the framework of the Graduiertenkolleg 841 "Physik der Elementarteilchen an Beschleunigern und im Universum".

Finally, I would like to thank all my colleagues and friends at the University of Dortmund for the pleasant working atmosphere.